UNIVERSITÉ DE LORRAINE

Ecole Doctorale BioSE

Défaillance cardiovasculaire aigue et chronique, Unité INSERM 1116

University of Amsterdam, Amsterdam, The Netherlands

Thèse

Présentée et soutenue publiquement pour l'obtention du titre de

DOCTEUR DE l'UNIVERSITE DE LORRAINE

Mention : SCIENCES DE LA VIE ET DE LA SANTÉ

par **Philippe GUERCI**

Sous la direction de Bruno LEVY

CURRENT AND NEW THERAPIES FOR THE CRITICALLY INJURED MICROCIRCULATION

16 Juin 2020

Membres du jury :

Directeur(s) de thèse :

  Mr Can INCE   Professeur, Docteur, Universiteit van Amsterdam (UvA), Amsterdam, The Netherlands

  Mr Bruno LEVY   Professeur, Docteur, Université de Lorraine, Nancy, France

Co-Directeur de thèse :

  Mme Marie-Reine LOSSER   Professeure, Université de Lorraine, Nancy, France

Rapporteurs :

  Mr Anatole HARROIS   Docteur, Université Paris-Saclay, Paris, France

  Mr Didier PAYEN DE LA GARANDERIE   Professeur, Docteur, Université Paris 7 Denis Diderot, Paris, France

Examinateurs :

Mr A.J. VERHOEVEN	**Professeur, Docteur, Universiteit van Amsterdam (UvA), Amsterdam, The Netherlands**
Mr E.T. van BAVEL	**Professeur, Docteur, Universiteit van Amsterdam (UvA), Amsterdam, The Netherlands**
Mr A.P.J. VLAAR	**Docteur, Universiteit van Amsterdam (UvA), Amsterdam, The Netherlands**
Mr J. BAKKER	**Professeur, Docteur, Erasmus Universiteit Rotterdam, Rotterdam, The Netherlands**
Mr Didier PAYEN DE LA GARANDERIE	**Professeur, Docteur, Université Paris 7 Denis Diderot, Paris, France**

Membres invités :

Mr L. VOGT	**Docteur, Universiteit van Amsterdam (UvA), Amsterdam, The Netherlands**

CURRENT AND NEW THERAPIES FOR THE CRITICALLY INJURED MICROCIRCULATION
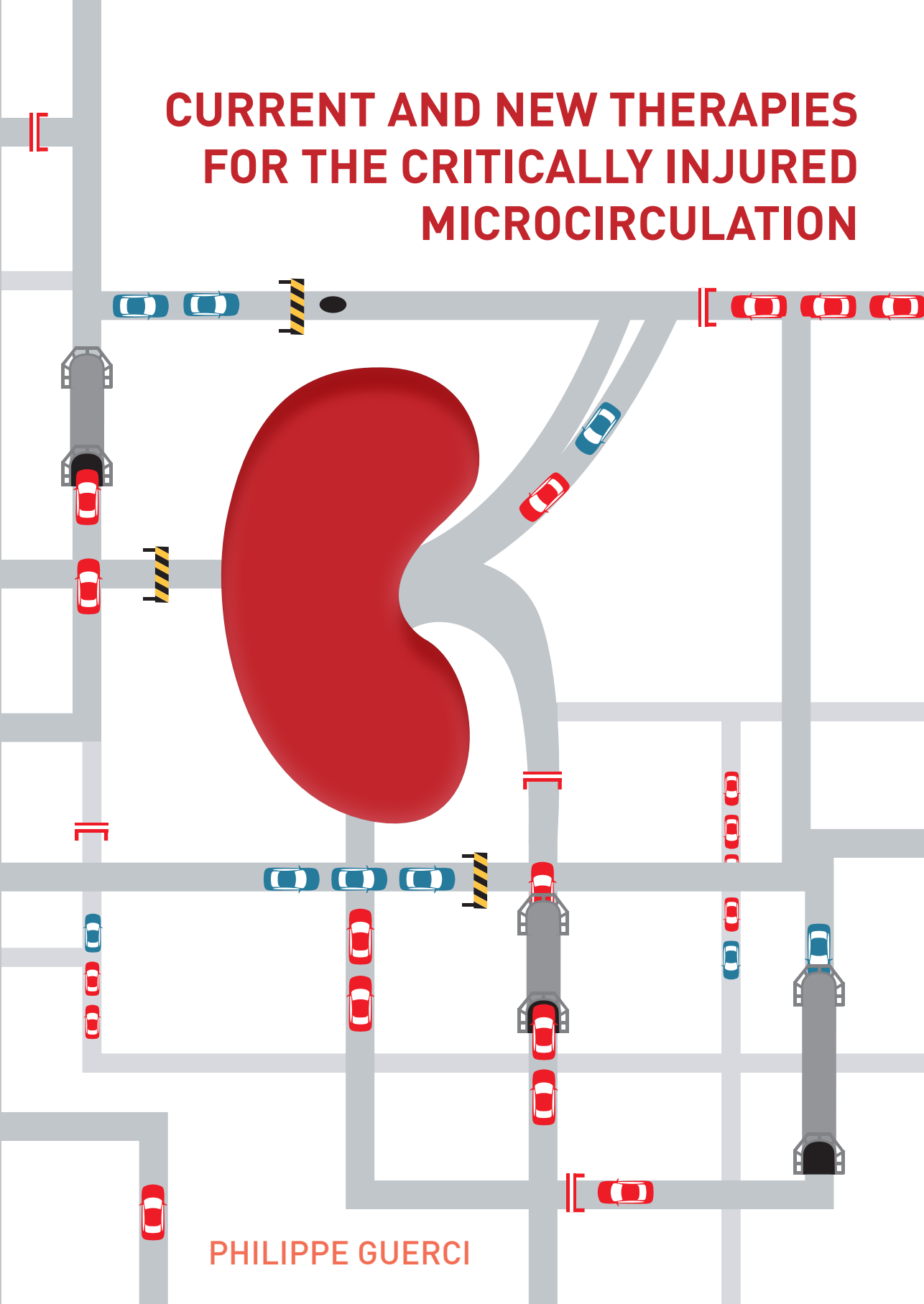
PHILIPPE GUERCI

CURRENT AND NEW THERAPIES FOR THE CRITICALLY INJURED MICROCIRCULATION

Philippe Olivier Guerci

CURRENT AND NEW THERAPIES FOR THE CRITICALLY INJURED MICROCIRCULATION

CURRENT AND NEW THERAPIES FOR THE CRITICALLY INJURED MICROCIRCULATION

ACADEMISCH PROEFSCHRIFT

ter verkrijging van de graad van doctor

aan de Universiteit van Amsterdam

op gezag van de Rector Magnificus

prof. dr. ir. K.I.J. Maex

ten overstaan van een door het College voor Promoties ingestelde commissie,

in het openbaar te verdedigen in de Agnietenkapel

op dinsdag 16 juni 2020, te 14.00 uur

door

Philippe Olivier Guerci

geboren te Nancy

Promotiecommissie

Promotores:	prof. dr. ir. C. Ince	AMC-UvA
	prof. dr. B. Levy	Université de Lorraine
Copromotor:	prof. dr. M.R. Losser	Université de Lorraine
Overige leden:	prof. dr. A.J. Verhoeven	AMC-UvA
	prof. dr. E.T. van Bavel	AMC-UvA
	dr. A.P.J. Vlaar	AMC-UvA
	dr. L. Vogt	AMC-UvA
	prof. dr. D.M. Payen	Université Paris Diderot
	prof. dr. J. Bakker	Erasmus Universiteit Rotterdam

Faculteit der Geneeskunde

Universiteit van Amsterdam en de Université de Lorraine met als doel het behalen van een gezamenlijk doctoraat. Het proefschrift is voorbereid in de Faculteit der Geneeskunde van de Universiteit van Amsterdam en de Faculté de Médecine de Nancy van de Université de Lorraine.

This thesis was prepared within the partnership between the University of Amsterdam and the Université de Lorraine with the purpose of obtaining a joint doctorate degree. The thesis was prepared in the Faculty of Medicine at the University of Amsterdam and in the Faculté de Médecine de Nancy at the Université de Lorraine.

TABLE OF CONTENTS

1

GENERAL INTRODUCTION

The microcirculation is a core element of humans and terrestrial mammals. Microcirculation is a complex and heterogenous network comprising arterioles, capillaries, venules but also lymphatics. The main functions of the microcirculation are to ensure the delivery of oxygen to tissue and cells while providing nutrients and removal of the carbon dioxide produced by the cell metabolism, thus, to meet metabolic demands.

The regulatory mechanisms controlling the microcirculatory flow and perfusion are various, redundant and elaborated. The regulation of flow to and in the microcirculation is determined by: (i) at general level, organ perfusion pressure, cardiac pump output, and (ii) at a microscopic scale by myogenic responses to flow (strain and stress), metabolic demand and acid/base balance (local O_2, CO_2, H^+ and lactate levels) and neurohormonal responses. The microcirculatory blood flow is regulated using autocrine and paracrine interactions to meet the metabolic demand, mainly oxygen requirements of tissue cells. Thus, microcirculatory oxygen level is of critical importance.

From a pragmatic perspective, the structure of the microcirculation comprises three major components: the container defined by the different layers of the vascular wall, the contents representing the flowing plasma and its formed elements and the extraluminal surrounding tissue. In disease, each of these components can be altered separately or simultaneously. The endothelial cells form the interface between the content of the inner lumen of vessels and the surrounding environment. The endothelium is remarkably heterogenous in structure and function and differs from organ to organ. It plays a crucial role in the regulation of macromolecular trafficking, vasomotor tone, hemostasis, immunological functions, and the secretion of molecules by sensing through mechanotransductors, which subsequently initiate transcellular and intra-cellular signaling and activation. Endothelial cells are linked together by transcellular components, including gap junctions for electrical communication for upstream vascular regulation and intercellular tight junctions for maintaining vascular barriers. The glycocalyx is a thin layer lining the luminal membrane and contributes to microvascular permeability of the vascular wall. It is a highly interactive scaffold capable of sensing blood flow and houses many endothelial receptors that interacts with leukocytes and other formed elements. Although, the glycocalyx participates to vascular barrier permeability, its relative contribution to the transcapillary macromolecular and fluid escapes is incompletely elucidated. Regarding the formed elements flowing in the microcirculation, red blood cells and leukocytes are among the most studied, mainly because their size allows readily identification with the help

1

of a handheld intravital microscope. However, the amount of oxygen carried out by red blood cells and released within the microcirculation cannot be assessed by this technique.

In many instances, the microcirculation can be altered or even jeopardized in critical settings. The kidney remains one of the most sensitive organs to injury, especially in case of circulatory shock, or ischemia/reperfusion conditions, leading to acute kidney injury, a leading cause of mortality and morbidity in critically ill patients. Therefore, our research is mainly focused on investigating the renal microcirculation, oxygenation and renal function. The objectives of this thesis were to: (i) provide an overview of the damages of the different components of the microcirculation in various settings such as hemorrhagic shock, sepsis, ischemia/reperfusion injury, (ii) depict the effects of past and current therapies on these constituents and (iii) assess new molecules having capabilities of carrying oxygen and anti-inflammatory actions.

Chapter 2 and *chapter 3* review the structural and functional mechanisms of the renal microcirculation in both states of healthy and sepsis. A comprehensive review of the complex regulatory mechanisms governing the microcirculation are presented.

The alterations of the different structural components considered as having a central role in the regulation microcapillary blood flow and vascular barrier permeability were investigated in the following chapters. Plasma viscosity is among one of the major shear stress-induced modulator of functional capillary density. In *chapter 4*, the impacts of 2 strategies of fluid resuscitation following hemorrhagic shock in pigs, on the plasma viscosity were evaluated. In this study, we demonstrated that plasma viscosity decreased regardless of the strategy used for fluid resuscitation (low volume and hypertonic colloids versus lactated ringer's). Moreover, no differences were found between the groups for other rheological variables, microcirculatory flow or tissue oxygen tension. In *chapter 5* and *chapter 6*, we undertook a physiological integrative assessment of the contributive role of the glycocalyx to vascular barrier permeability in a rodent model following hemorrhagic shock resuscitation and severe hemodilution, respectively. The observed results challenged the contributive importance of glycocalyx to the vascular barrier permeability. Indeed, although the glycocalyx may be damaged in these settings, it did not impair vascular barrier competence but rather caused microcirculatory disturbances and vascular tone alterations probably through diminished mechanotransduction. Considered together these results stress the complexity of vascular barrier permeability regulation in the context of hemorrhagic shock and identify a gradation of vascular injury.

To accurately determine the microcirculatory oxygen pressure within the cortical renal structure, a new LED-based device relying on time-resolved phosphorescence quenching method was developed and presented in **chapter 7**. This device has several advantages over previous flash lamps-based devices, which had a plasma glow that persists for tens of microseconds after the primary discharge. The benefits of using LEDs as a light excitation source are presented.

Various treatments have been considered to treat injured or compromised microcirculation due to a critical condition. Fluid therapy remains cornerstone of the management of shock states. Studies on comparative microcirculatory effects with regards to renal microcirculatory oxygen pressure are limited. In **chapter 8**, we investigated the role of bicarbonate precursors in balanced fluids, used in everyday practice, during hemorrhagic shock with and without compromised liver function A 70% partial liver resection was performed to mimic compromised liver function in a rat model. While the balanced fluids are widely used, no data was available on the fate of anions composing them. Interestingly, acetate-buffered balanced fluids showed superior buffering effects with improve compared with Ringer's lactate or saline, and that gluconate did not contribute to acid–base control.

Antioxidant therapies have been largely evaluated as microcirculatory resuscitation strategies. A large body of evidence is available regarding *N-acetylcysteine* (NAC) use and its antioxidant, vasodilatory and renal protective effects. In **chapter 9**, we studied the effect of NAC administration in conjunction with fluid resuscitation on renal oxygenation and function in a rat model of endotoxemia, hypothesizing that dampening inflammation within the kidney would improve the renal microcirculatory oxygenation and limit the onset of acute kidney injury. We showed that the addition of NAC improved renal oxygenation and attenuated microvascular dysfunction and acute kidney injury. The effects may be partially mediated by a decrease in renal nitric oxide and hyaluronic acid levels.

In the various models investigated, the renal microcirculatory oxygen pressure cannot be fully restored compared to control. Thus, there are still unmet needs regarding the resuscitation of the microcirculation. The so-called concept of "pink fluid resuscitation" emerged based on therapies that should combine a volume expander effect with antioxidant and oxygen carrying capacities. In this idea, new generation of hemoglobin-based oxygen carrier with additional antioxidant properties, such as PEGylated carboxyhemoglobin, is arguably a valuable option to investigate. In **chapter 10**, we investigated the effectiveness of this latter compound on the renal cortical microcirculatory oxygen pressure and the role of its embedded carbon monoxide

1

molecules on the mitigation of acute kidney injury during low volume resuscitation of hemorrhagic shock. Although, it could not compete against blood transfusion in terms of renal cortical oxygenation, the compound limited tubular damage while a lower volume was required to sustain macrocirculation. In *chapter 11*, on the contrary, resuscitation with PEGylated carboxyhemoglobin enhanced renal cortical oxygenation while restoring skeletal muscle microcirculatory flow in previously non-flowing capillaries in an endotoxemia murine model without dampening short term sepsis-induced acute kidney injury.

2

THE MACRO- AND MICROCIRCULATION OF THE KIDNEY

Philippe Guerci,[1,2,3] Bulent Ergin,[3,4] and Can Ince[3,4]

1. Department of Anesthesiology and Critical Care Medicine, University Hospital of Nancy, France
2. INSERM U1116, University of Lorraine, Vandoeuvre-Les-Nancy, France
3. Department of Translational Physiology, Academic Medical Centre, Amsterdam, The Netherlands
4. Department of Intensive Care Medicine, Erasmus MC, University Medical Centre, Rotterdam, The Netherlands

ABSTRACT

Acute kidney injury (AKI) remains one of the main causes of morbidity and mortality in the intensive care medicine today. Its pathophysiology and progress to chronic kidney disease is still under investigation. In addition, the lack of techniques to adequately monitor renal function and microcirculation at the bedside makes its therapeutic resolution challenging. In this article we review current concepts relating to renal hemodynamics compromise as being the event underlying AKI. In doing so, we discuss the physiology of the renal circulation as well as the effects of alterations in systemic hemodynamics leading the way to renal injury specifically in the context of reperfusion injury and sepsis. The ultimate key culprit of AKI leading to failure is the dysfunction of the renal microcirculation. The cellular and subcellular components of the renal microcirculation are discussed and how their injury contribute to AKI.

Keywords: Acute kidney injury, microcirculation, hemodynamic coherence, renal tissue oxygenation, renal blood flow

Introduction

Acute kidney injury (AKI) is among the most common organ failure observed in patients admitted or hospitalized in intensive care units.[1] The AKI morbidity and mortality remains high despite early identification and increasing ability to support organ function.[1,2] As opposed to previously thought, the occurrence of AKI in these patients not only increase their mortality rates, but they will sooner progress towards chronic kidney disease even after apparent fully recovery of the kidney function after the insult.[3,4] The pathophysiological mechanisms behind AKI in critically ill patients is still under investigation but it is now quite clear that it is much more complex than a simple decrease in renal blood flow subsequent to low cardiac output and/or hypotension.[5]

The hallmark feature of AKI is a reduction in glomerular filtration rate (GFR) which implies an underlying impairment in hemodynamic regulation in the kidney. However, this hemodynamic "dysregulation" may occur at both, macro- and microcirculatory levels. In this review, we focus on the role of the macro- and microcirculatory changes in the pathophysiology of AKI. We discuss the respective role of renal blood flow (RBF) and the microcirculation and its interactions with inflammation.

The macrocirculation of the kidney

The kidney is the most vascularized organ of the body. The arteriolar system is rich, tightly regulated and supplies 2 different types of microcirculation in the cortex and in the medulla, each one exerting different functions.[6] The kidneys receive about 20 to 25% of the cardiac output, which in adults is equivalent to 1000 to 1200 ml of blood per minute. Twenty percent of the plasma flow – approximately 120 to 140 ml/minute – is filtered at the glomerulus in the cortex and passes into the Bowman capsule. The remaining 80% (about 480 ml/minute) of plasma flows through the efferent arterioles to the peritubular capillaries in the medulla to ensure solute exchange and water resorption. It is estimated that only 5–15% of total RBF is directed to the medulla, with the outer medulla having higher blood flow (130–340 mL/100 g tissue/min) than the inner medulla (22–69 mL/100 g tissue/min).[7,8]

In the kidney, a local mechanism of autoregulation keeps fairly constant the glomerular perfusion and therefore the GFR over a wide range of arterial pressures between 80 to 180

mmHg. Intravascular volume and mean arterial pressure vary along the day as a result of physiological adaptation to the environment without affecting much the GFR. Pressure in the glomeruli will remain stable by the means of the activation of various regulatory process. The RBF is regulated by intrinsic autoregulatory mechanisms, neural regulation such as the renal sympathetic nerve activation (RSNA), and hormonal regulation such as the renin-angiotensin-aldosterone system (RAAS).

Autoregulation of renal blood flow in physiology

The vascular tone of afferent and efferent arterioles of the glomeruli is able to change to preserve GFR and to prevent fluctuations in systemic arterial pressure from being transmitted to glomerular capillaries, reducing the alterations in solute and water excretion.

Several components are involved in this autoregulatory response in the kidney. The myogenic response is one of the primary and most responsive mechanisms. This mechanism mainly concerns the afferent artery and is driven by the stretch on arteriolar smooth muscle. When arterial pressure increases, the stretch also increases, and the arteriole constricts causing a decrease in glomerular perfusion. Conversely, when the arterial pressure drops, the stretch is less important, and the arteriole relaxes to increase glomerular pressure. It has been shown that the afferent arteriole exhibits a very short delay in activation (200-300 ms) and rapid constriction kinetics when exposed to a sudden elevation of blood pressure and the renal vasculature responds passively to pressure signals presented at rates exceeding the myogenic operating frequency (0.2-0.3 Hz).[9]

The tubuloglomerular feedback (TGF) is the second mechanism involved for keeping GFR constant. Briefly, the macula densa cells in the distal tubule sense the increasing or decreasing amounts of filtered sodium. When the sodium filtration decreases for instance, the macula densa cells drive afferent arteriolar vasodilation in the glomeruli to increase GFR. The vascular tone changes are also themselves under influence of nitric oxide release, adenosine triphosphate and prostaglandin E2 mediators.

Renal Sympathetic Nerve Activation (RSNA)

The diameter of arterioles of the kidney is also regulated by the sympathetic system (adrenergic/noradrenergic fibers). Both afferent and efferent arterioles are richly innervated. The RSNA is mediated through feedback from systemic baroreceptor such as from the carotid

artery or aortic arch. When the baroreflex is activated, a vasoconstriction of the afferent arterioles through activation of α_1-adrenoreceptors occurs. Subsequent decrease in GFR will lead to a decreased water and salt excretion boosting the increase in blood volume. Thus, blood pressure will be increased. Electrical stimulation of the renal nerves has been shown to decrease single nephron GFR.[10,11]

Other physiological or pathophysiological conditions can trigger the RSNA such as exercise or hypoxia. Severe hypoxia, apart from stimulating hypoxia inducible factor and erythropoietin production, mediates the activation of chemoreceptors of the carotid arteries and decreases RBF by means of RSNA.[12]

Renin-Angiotensin-Aldosterone System (RAAS)

The RAAS is a major hormonal regulator of RBF by increasing sodium reabsorption and causing a subsequent rise in arterial blood pressure. The TGF is also activated by the RAAS.[13] Increased levels of angiotensin-2 (Ang-2) leads to a reduction in GFR by causing vasoconstriction of the afferent and efferent arterioles in the glomerulus. The activation of TGF then decreases hydrostatic pressure in the glomerulus and reduces the GFR.

Renin is an enzyme formed and stored in granular cells of the afferent arterioles of the juxta-glomerular apparatus. A decreased blood pressure in the afferent arterioles, a RSNA with stimulation of β-adrenergic receptors on the juxtaglomerular cells, a decreased sodium concentration in the distal convoluted tubule, and a release of prostaglandins are considered triggers for the release of renin. The renin mediates angiotensin-1 (Ang-1) and in the presence of the angiotensin converting enzyme (ACE), Ang-1 converts to Ang-2 to stimulate aldosterone (in the adrenal cortex). Aldosterone causes an increase in sodium reabsorption in the collecting ducts, loop of Henle and in the distal tubules and also stimulates the anti-diuretic hormone.

The renal blood flow and the GFR are tightly regulated parameters with numerous, complex, and redundant physiological systems to ensure a relative independency of the GFR to the local and systemic environment. Of course, these systems can be overwhelmed, leading to a dysregulated TGF and inappropriate secretions and may contribute to the occurrence of AKI.

What happens with the macrocirculation during AKI?

Although we extended the overall understanding of regulation of renal hemodynamics in physiology, little is known of the interactions between systemic, renal and glomerular

hemodynamics and the renal microcirculation during AKI. The reduction in GFR is the hallmark of AKI. It is unclear whether autoregulation mechanisms are still functioning and efficient or if the RBF and GFR become more dependent on the cardiac output.[14–16] In a population of critically ill oliguric patients, although the majority were not cardiac responder to fluid challenge, half of them responded in terms of urine output.[14] Urine sodium concentration was shown to be a poor predictor of fluid responsiveness, translating the variable degree of RAAS activation.[14] Consequently, hemodynamic interventions such as fluid loading or vasopressor infusion aimed at restoring systemic hemodynamics (and RBF) in the hope of limiting insults to the kidney or improving recovery from AKI, is not tailored to the kidney.[15] Traditionally, global renal ischemia secondary to compromised renal perfusion has been advocated to be the common factor leading to development of AKI in ICU patients.

During AKI, the observed changes in macrocirculation of the kidney are largely heterogeneous among experimental models of shock depending on the type of insult (ischemia/reperfusion), the animal considered, the time course of the study and time of analysis, and the design of the study itself. In addition, human clinical studies – in apparent homogeneous population – showed inconsistent results in terms of RBF. To date, the evolution of RBF is largely unpredictable because of the interplay of numerous regulators aforementioned that may or may not be significantly altered.

The techniques of investigation of RBF also differ in experimental, where a transonic Doppler flow probe in easily placed around the renal artery (with adjusted diameter to the artery), and in human clinical practice, where noninvasive surrogates such as ultrasound-based renal blood flow velocity or Contrast Enhanced Ultrasonography (CEUS), are mostly used at bedside.

Numerous experimental studies focused on the evolution of RBF during sepsis (sepsis-associated AKI) or after renal ischemia-reperfusion secondary to surgery or hemorrhage/hypovolemia. Apart from the very typical situations, in some selected ICU patients presenting arterial or venous thrombosis for instance, in which the RBF is totally interrupted (thrombosis for instance), the RBF can be either decreased, unchanged or increased depending on the type of insult and time of observation.

Renal macrocirculation during sepsis-associated AKI

The total RBF during sepsis-associated AKI has been largely studied in both experimental and clinical settings and yielded to inconsistent results. The common accepted theory is that

sepsis causes a decrease in cardiac output and a drop-in blood pressure leading to a decrease in total RBF, with subsequent renal arteriolar vasoconstriction and hypoperfusion. Secondary renal ischemia is believed to occur with acute tubular necrosis and loss of renal function.[17] However, little, if any, human evidence supports this hypothesis because RBF measurement in the septic critically ill patient is scarce.[18] Actually, animal studies have confirmed that sepsis-associated AKI can develop despite no change or even an increase in RBF.[19] The early phase of sepsis is generally "hyperdynamic", meaning that cardiac output is typically increased whereas AKI is already developing or established.[16,20,21] In post-mortem studies, inconsistencies in histopathological findings were noted.[22,23] In a sheep model of septic shock induced by intravenous infusion of *Escherichia coli*, was not associated with changes in RBF, oxygen delivery, nor histological appearance although animals developed AKI.[24] Systematic reviews of experimental and clinical histopathological findings in sepsis-associated AKI revealed mostly nonspecific morphologic changes and acute tubular necrosis was relatively uncommon.[25,26] Therefore, these observations challenge the previous paradigm of global-hypoperfusion secondary to decrease in RBF as the primary cause of sepsis-associated AKI and lead to a new understanding of the pathogenesis of AKI.[27] In this regard, because RBF is preserved while GFR may be lost, the concept of hemodynamic coherence emerged and explains why the microcirculation is disassociated from the macrocirculation.[28]

Large multicenter randomized clinical trials failed to demonstrate a benefit of early goal-directed therapy for reducing mortality and AKI occurrence in patients with septic shock.[29–31] In other words, hemodynamic optimization with aggressive fluid resuscitation and vasopressors administration for early achievement of the recommended targets are of no benefit to prevent or hasten recovery from AKI in this population. A restored RBF – if altered – does not warrant *per se* a recovery of renal function and GFR. On the contrary, fluid resuscitation may promote intrarenal shunting and heterogeneity with a decreased capillary density and enhance intrarenal medullary hypoxia.[27,28,32] Two pitfalls of these large trials should be however considered. First, patients were in established septic shock, in whom AKI was already present. Secondly, the target of mean arterial pressure in not tailored to patient's characteristics, thus, far from the personalized hemodynamic management.[33] A large trial targeting a high versus low blood-pressure in patients with septic shock, resulted in similar mortality at 28 and 90 days.[34] However, a subgroup of patients with chronic hypertension required less renal replacement therapy when treated in high blood-pressure management. This might be the first step of a tailored systemic hemodynamics approach regarding the kidney function.

AKI in hypovolemia or ischemia/reperfusion injury

In the setting of hypovolemia or ischemia/reperfusion injury, it is simpler to count for the changes in RBF. The decrease in RBF follows cardiac output in hypovolemia. During ischemia, the RBF is nearly interrupted, therefore blood and oxygen supply to the kidney is shut down. Changes also occurs in microcirculation after the RBF is re-established, but the magnitude of microcirculatory alterations and related inflammation are dependent on the length of the insult.

The renal microcirculation

The renal microcirculation is complex and plays a major role in the oxygen supply to the kidney and ensures plasma filtration, electrolyte exchange and water reabsorption. Renal microcirculation involves two capillary systems: the glomerular capillary system and peritubular capillary system. The glomerular capillary system is found within the glomerulus that responsible for the glomerular filtration (GFR) which is driven by the filtration pressure (within the Bowman's capsule and hydrostatic pressure). The glomerular capillary system ends with the efferent arteriole. The peritubular capillary bed emerges from this arteriole and surrounds all the tubules. In the medulla, it becomes the vasa recta in order to create the counter-current exchange system along with the parallel positioned Henle loop. The role of counter-current exchange system is to maintain the cortico-medullary osmotic gradient for concentrating the ultrafiltrate (**Figure 1A-B**).[7,35]

A

Interlobar artery

Renal artery

Renal vein

Uretra

Hilus

B

Peritubular Capillaries

Proximal Tubule

Efferent arteriole

Afferent arteriole

Interlobular arteries

Arcuate arteries

Distal tubule

Glomerulus

Vasa recta

Thin descendin limb

Collecting duct

Thin ascending limb

Segmental artery

Intralobar artery
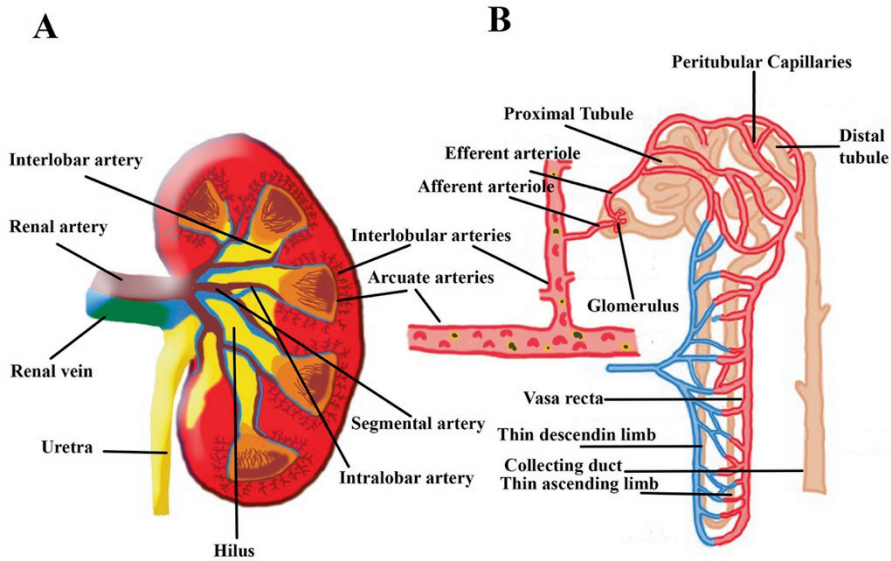
Figure 1: Representative image of the renal preglomerular vessels (Panel A), glomerular vessels and tubules (Panel B).

Renal tissue oxygenation

To achieve all its complex functions, the kidney needs an adequate amount of the oxygen to maintain oxygen-dependent adenosine triphosphate (ATP) production. Both oxygen delivery (DO_2) and consumption (VO_2) determine renal tissue oxygenation, which is not only necessary for cell survival and function but also function of Na/K ATPase pumps. There are two mechanisms to maintain normal renal function in case of renal hypoxia; (i) the increment of DO_2 acts to increase tissue oxygenation, (ii) reduced VO_2 that may protect tissues from hypoxia during moderate to severe arterial hypoxemia. Evans *et al.*, demonstrated that even 55% reduction of arterial oxygen content did not lead to significant impairment of VO_2 because of the adaptive reduction of oxygen demand following the decrease in tubular sodium reabsorption.[8] Thus, prevailing experimental evidence supports the concept that renal VO_2 is relatively stable in the face of hypoxemia unless RBF is also altered.

Under normal conditions, oxygen partial pressure measured by oxygen-dependent phosphorescence quenching methods was found to be 50-80 mmHg and 20-45 mmHg in the rat kidney cortex and medulla respectively.[8,36] Thus, there is a gradient in oxygen concentration in parallel to the countercurrent exchange system. The largest part of renal oxygen consumption is used to drive Na/K ATPase in the proximal tubules and medullary thick ascending limp.[37]

Various clinical conditions may lead to decreased renal oxygenation, such as hemodilution,[38] sepsis induced microcirculatory heterogeneity,[39] mismatch between oxygen consumption and delivery, hypoxemia or severe hypotension.[8,40] A protective mechanism that maintains the global oxygenation homeostasis and functions as an anti-oxidant defense mechanism through arterial-to-venous (AV) oxygen shunting in the renal cortex and shunting of oxygen from descending to ascending vasa recta in the renal medulla exists.[41,42]

The renal endothelium

The endothelium of the kidney is remarkably heterogeneous in structure and function and varies according to the type of microcirculation (glomerular and peritubular).[6,7] Indeed, various endothelial cells arrangements grant different permeability properties. In the glomeruli, the capillaries are lined by fenestrated endothelial cells and covered by specialized epithelial cells known as podocytes. In the cortex, the endothelium is exposed to almost normal oxygen partial pressure (PO_2) and osmolarity whereas the one in the medullar microcirculation functions in an osmolarity of up to 1,200 mosmol.L^{-1} and a PO_2 as low as 20 mmHg. Glomerular endothelial cells are unusually thin; around capillary loops, and present large fenestrated areas constituting 20–50% of the entire endothelial surface. Glomerular microcirculation functions via continuous and fenestrated endothelium with no diaphragm, whereas it is more continuous and nonfenestrated in the descending vasa recta in peritubular microcirculation. Because of their different role in the microcirculation, these endothelial cells are dissimilarly sensitive to injury.

The glycocalyx

Endothelial cells are lined by a gel-like thin layer, the glycocalyx which comprises glycoproteins, glycosylated glycoproteins and proteoglycans. The glycocalyx contributes to vascular barrier permeability however it is not clear to what extent. This highly interactive scaffold is capable of sensing blood flow and facilitating protein interactions with their receptors

or other proteins, and it houses many EC receptors and compounds important for maintaining hemostasis (antithrombotic properties), homeostasis and providing anti-inflammatory defense to the parenchymal cells.

Interplay of the microcirculation with local mediators

Hundreds of mediators interact with the microcirculation in the kidney and it is almost impossible to list their detailed effects in physiology and even more complex in the pathophysiology of AKI. We present here the relevant mediators interacting directly with the vasculature.

Adenosine

Adenosine is an ATP breakdown product causing vasodilatation in most vessels and contributes to the metabolic control of kidney perfusion to provide a balance between the oxygen demand and delivery. It was originally postulated that adenosine is generated in macula densa cells by dephosphorylation of ATP when an increase in transcellular NaCl transport and the cellular energy demand.[43] In the renal vasculature, adenosine can produce vasoconstriction in afferent arteriole, especially arteriolar segment the closest the glomerulus, through A1 adenosine receptor (A1AR) at lower concertation. On the contrary, it accompanies with a renal vasodilator response as a result of A2AR-mediated vasorelaxation in most parts of the renal vasculature, including larger renal arteries, juxtamedullary afferent arterioles, efferent arterioles, and medullary vessels with the plasma concentration above normal.[44] However, because the kidney vasculature is sufficiently heterogeneous, while adenosine causes vasoconstriction in one part of the renal vascular bed and vasodilatation in another, it is difficult to account for the real changes induced by adenosine in the renal vasculature. Recent studies confirmed the biphasic effects of adenosine exerts vasoconstriction via A1 receptors (A1AR) at a lower concentration and vasodilation via A2AR at higher concentration of adenosine. Lately, it has been reported that A1A3 receptor is expressed in the afferent arteriole and activation of this receptor leads to dilate the afferent arteriole.

ATP

Extracellular ATP activates a variety of purinergic receptors – ionotropic P2X receptors and metabotropic G-protein coupled P2Y receptors – since both receptor families are present in renal vascular, glomerular, mesangial and tubular epithelial cells.[45] Intrarenal infusion of α, ß, γ-methylene ATP reduced both cortical and medullary blood flow in rabbit kidneys in vivo,[46] which implicates P2X receptors in the regulation of regional renal blood flow. Intra-arterial infusion of ATP or α, ß-methylene ATP increased perfusion pressure in a dose dependent fashion in isolated rat kidneys and increase in renal vascular resistance.[47]

Endothelin

Endothelin (ET-1,2,3) is one of the most potent renal vasoconstrictors. Endothelin plays an essential role in the regulation of renal blood flow, glomerular filtration, sodium and water transport, and acid-base balance. ET production by the kidney is much higher than any other organ in especially inner medulla.[48] The high ET-1 expression levels in the renal inner medulla suggest a potentially important role for ET-1 in regulating sodium and water balance under physiological conditions and perhaps in regulating medullary blood flow.[49] The physiological or pathophysiological effects of ET are mediated through activation of two ET receptors as ETA and ETB.[48] Moreover, Gellai *et al.* reported that the relative expression of ETA and ETB in the rat kidney was equal in cortex but expression (ratio) of ETB was found much higher in medulla (70:30).[50] ET-1 causes a marked and prolonged renal vasoconstriction manifested by profound reductions in renal blood flow and glomerular filtration rate.[51,52] ET-1 leads to vasoconstriction in both afferent and efferent arterioles, however which segment exhibits the greatest sensitivity to ET-1 remains controversial. In isolated and perfused afferent and efferent arterioles from ETB deficient mice ET-1 induced a greater vasoconstriction of afferent arterioles than efferent arterioles (**Figure 2**).
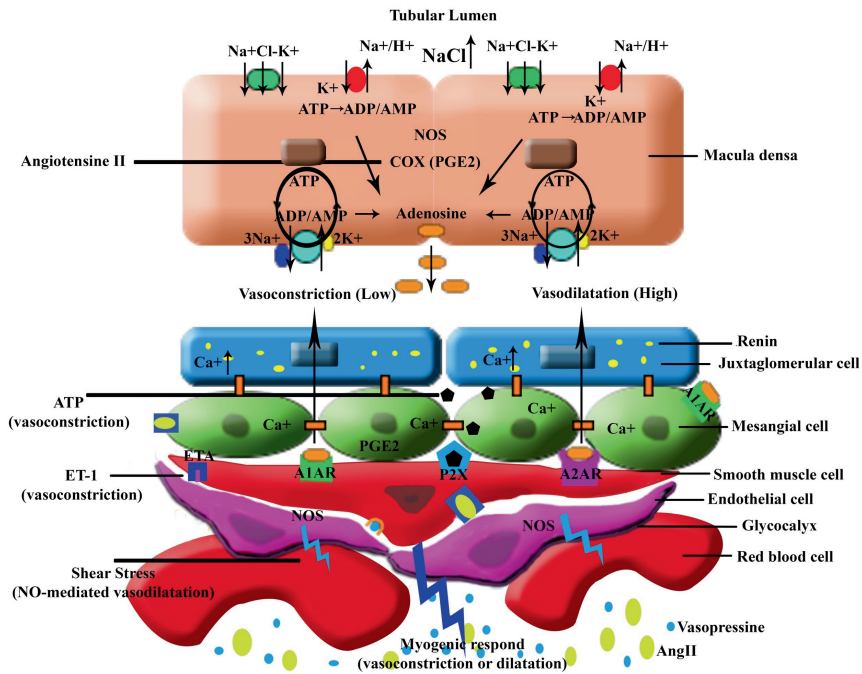
Figure 2: Mechanism of the tubule-glomerular feedback and regulation of glomerular microcirculation through the vasoactive substances.

Ang-II: Angiotensin-II, ATP: adenosine triphosphate, ADP: adenosine diphosphate, AMP: adenosine monophosphate, ET: endothelin, A1AR/A2AR: A1/A2 Adenosine Receptor, COX: cyclo-oxygenase, NO: Nitric oxide, NOS: Nitric Oxide Synthase, P2X: purinergic receptor, PGE 2: Prostaglandin E2

The study also showed that the vasoconstriction caused by ET-1 in the afferent arterioles is due primarily to ETA, while ET-1-mediated vasoconstriction of the efferent arteriole requires both ETA and ETB; the efferent arteriole response is influenced by ETB-mediated release of nitric oxide.[53] In addition, the intense vasoconstriction exhibited by descending vasa recta in response to ET-1 suggests that ET-1 might play an important role in the development of renal injury in conditions where the renal ET system is upregulated, such as ischemia-reperfusion-induced acute kidney injury.[48]

Nitric oxide (NO)

Nitric oxide (NO) is a gas with biological and regulatory properties, produced from arginine by the way of nitric oxide synthase (NOS). It has a very short half-life (few seconds). NO involves extensive metabolic, vascular and cellular effects,[54] with a deep involvement in the renal function. NO exerts its vasodilating effect through activation of the soluble guanylate cyclase and the synthesis of 3',5'-cyclic guanosine monophosphate (cGMP), the final effector of vasodilatation. NO is currently considered an important determinant of vascular integrity through the regulation of many biological effects, such as vascular tone and permeability, leukocytes-endothelial interaction, cell proliferation, maintenance of the antithrombotic properties of the endothelium, neurotransmission, gene transcription, mRNA translation, and posttranslational modifications of proteins.[55] The endothelial NOS (eNOS) isoform is strongly expressed in the renal vascular endothelium and in the tubules.[56] Whereas neuronal NOS (nNOS) is highly expressed in the macula densa. In contrast, inducible NOS (iNOS) is weakly expressed in renal tissues under normal conditions.[56,57] NO dilates both the afferent and the efferent arterioles, increases the glomerular filtration rate (GFR), and affects renal sodium handling in the tubules, from the thick ascending limb to the distal tubule and the collecting duct (**Figure 2**).

The renal microcirculation: a cornerstone in the pathophysiology of AKI

All the mechanisms aforementioned play a crucial role to maintain the regulation of renal microcirculation that finally provides adequate oxygen, nutrient, immune cell, hormones and effective vast removal for renal function. Different type of insults may result in similar mechanisms taking part to subsequent development of AKI.[26,58,59] The two main triggers are: (i) renal tissue hypoxia and (ii) activation of inflammatory pathways. These phenomena are present in either ischemia/reperfusion injury, hypoxemia or septic shock and lead to microcirculatory dysfunction. Different types of microcirculatory dysfunction have been identified.[28,60]

However, the common pattern observed is a decrease in functional capillary density. In sepsis-associated AKI, the microcirculatory dysfunction is characterized by heterogeneous abnormalities, in which some capillaries are under-perfused (sluggish or stopped flow/plugged

vessels) while others have normal or high blood flow (hyperdynamic).[61] In a septic sheep model, while the cortical perfusion and oxygenation were preserved, renal medullary hypoxia caused by intrarenal blood flow redistribution may contribute to the development of septic acute kidney injury.[62] In addition, the authors found that treatment with norepinephrine led to further reduction of the medullary perfusion and oxygenation with a sustained renal and systemic hemodynamics.[62] In dogs, Gullichsen *et al.* also reported that endotoxemia is associated with renal hypoperfusion and hypoxia in the renal cortex despite an increase in venous PO_2.[63] Thus, it has been suggested that oxygen shunts may also contribute to kidney hypoxia during sepsis. Besides the systemic hypotension, the increase in renal vascular resistance in sepsis was associated with global and regional blood flow in kidney impairment and a decrease in renal cortical and medullary microvascular oxygenation.[64,65] Johannes et al. demonstrated that sepsis-induced AKI was associated with renal cortical and medullar perfusion heterogeneity and overexpression of iNOS.[66] Increase in renal vascular resistance which is suggested an important macrohemodynamic factor to induce AKI, can be induced by arteriolar vasoconstriction, microcirculatory disturbances such as a leaky endothelium, tissue edema, leukocyte adhesion and microthrombosis.[67] Finally, in a rat model of endotoxemia, Legrand *et al.* demonstrated that early fluid resuscitation partially improved intrarenal perfusion besides reducing renal inflammation but could not prevent reduced renal microvascular oxygenation.[68]

In sepsis, activation of the RAAS is often part of host response with high levels of Ang II and vasopressin. Although it has been suggested that afferent arteriole dilatation cause a loss of intraglomerular filtration pressure resulting a decrease in GFR,[69] local production of Ang II was found to lead to a reduction in the GFR due to vasoconstriction of the glomerular afferent and efferent arterioles.

Microvascular dysfunction also involves imbalance between the endothelium-dependent vasorelaxation and overresponses to vasoconstrictive agents. NO plays an important role to regulate the vascular tone and is a major contributor to endothelial dysfunction. For instance, lack of the eNOS activity is directly related to the organ perfusion. Indeed, it was shown that while blocking of eNOS activity exacerbate organ ischemia, high eNOS expression may improve sepsis-induced AKI.[70] Moreover, Schwartz *et al.* pointed out that loss of the renal function is due to local inhibition of eNOS by elevated iNOS activation, possibly via NO autoinhibition.[71] Recently, a study found that expression of all NOS subtypes is significantly increased in the renal cortex but decreased in the medulla in a sheep model of sepsis-induced AKI.[26] The authors

hypothesized that overexpression of NOS isoforms in the cortex may induce a shunt from the medulla to the cortex, leading to medullary ischemia.[26]

Sepsis-induced endothelial leukocyte transmigration, together with the activated coagulation system, endothelial swelling, and enhanced vasoconstriction of the arterioles, also results in a compromised renal microcirculation.[72] In this case, the upregulation of endothelial adhesion molecules, production of cytokines, chemokines and NO gives rise to increase in endothelial-leukocyte interactions causing leukocyte transmigration toward renal interstitial area, further enhancing epithelial inflammation and vascular endothelial barrier dysfunction through the production of cytokines, reactive oxygen (ROS) and nitrogen species (RNS). During ischemic AKI, compromise of the endothelial cell–cell junctions and changes in the endothelial glycocalyx increase microvascular permeability and contribute to microcirculatory dysfunction.[73] In case of septic AKI, diabetic nephropathy, or AKI following ischemia/reperfusion injury, the glycocalyx is disrupted, leading to vascular hyperpermeability and albuminuria.[74,75]

Renal microvascular hypoxia during AKI

The occurrence of hypoxia plays also a central role in the development of AKI and is directly linked to microcirculatory alterations. After shock or ischemia/reperfusion injury, persistent oxygen extraction deficit may persist despite the apparent adequate recovery of systemic hemodynamic and oxygen-derived variables.[76] Hypoxic inducible factor (HIF) is widely expressed in renal epithelial cells, endothelial cells, and renal interstitial fibroblast-like cells and plays crucial role in the hypoxic adaptation through the extracellular formation of adenosine.[77] Adenosine signals through binding to 1 of the 4 adenosine receptors of which are expressed by activated immune cells [78] and nephron segments, including the glomerular epithelium, renal vasculature, proximal tubules, and collecting ducts.[79]

Hemodilution or anemia, in addition to their hemorheological effects, cause a reduction in the oxygen carrier capacity of blood and in organ perfusion and oxygenation. Recently, Koning *et al.* investigated the effects of hemodilution with or without cardiopulmonary bypass (CPB) in which they concluded that despite transient impairment of microcirculation after hemodilution alone, hemodilution with CPB may cause a further impairment of renal microcirculation, inflammation and renal injury in rat.[80] Moreover, another study showed that CPB impairs renal oxygenation and perfusion due to renal vasoconstriction, hemodilution and redistribution of

blood flow away from the kidney during and after cardiopulmonary bypass, accompanied by decreased renal oxygen delivery, increased oxygen extraction and release of a tubular injury marker.[81] Results from experimental studies showed that acute normovolemic hemodilution (ANH) led to a reduction of perfused vessel density,[82] increased endothelial activation,[83] renal edema and impaired renal oxygenation.[84] In addition, an increase in hematocrit by red blood cell transfusions during CPB improved microcirculatory perfusion in cardiosurgical patients,[85,86] It has been suggested that the renal oxygen supply of the kidney became critical already in an early stage of ANH causing an increase in intrarenal oxygen shunts that contribute to the development of renal hypoxia.[38]

During the hemorrhagic shock and reperfusion are reported a reduction of systemic perfusion and local perfusion that can lead to multiple-organ failure, including AKI because of ischemia and hypoxia, dysfunction in the microcirculation, release of reactive oxygen species, and endogenous apoptotic pathways associated with mitochondrial disorders.[58,87] In a review Kang *et al.* highlighted the direct correlation between renal hypoxia and the loss of microvasculature with the in stimulation of fibrogenesis and development of glomerular and tubulointestitial scarring.[88] The central role of renal microcirculatory hypoxia to AKI was shown by Zafrani and co-workers in a sepsis model in rats where they demonstrated that blood transfusions was successful in improving kidney microcirculatory oxygen levels and in resolving renal failure in comparison to fluid resuscitation.[89]
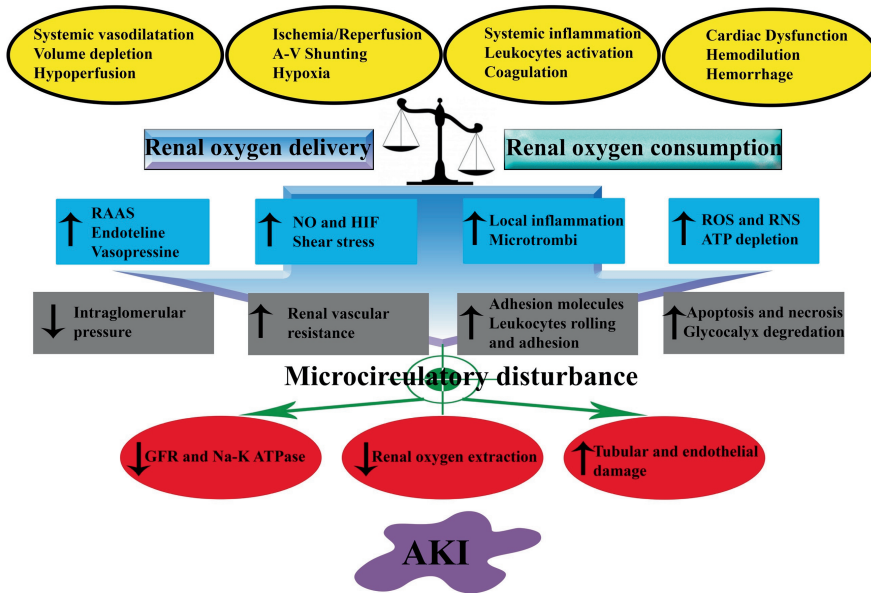
Figure 3: Key mechanisms involved in the development of acute kidney injury (AKI)

GFR: Glomerular Filtration Rate, HIF: Hypoxia Inducible Factor, NO: Nitric oxide, ROS: Reactive Oxygen Species, RAAS: Renin Angiotensin Aldosterone System

Conclusion

The relative contribution of total renal blood flow in the pathophysiology of AKI remains to be determined. A unified theory for the development of sepsis-associated AKI has been recently proposed.[90] Although, the pathophysiological aspects of AKI following ischemia/reperfusion injury are different, it shares common pathways with the sepsis-associated AKI [58] in which the alterations in microcirculation, renal endothelium/inflammation and renal oxygenation are the critical determinants of the severity of AKI (**Figure 3**). Therefore, future targeted therapies aiming at preventing or hastening recovery from injured kidney should take into consideration these 3 main aspects in the resuscitation process.

2

Practice points

- An integrative evaluation of the functional state of the circulation is required to assess the risk for developing AKI and assessing the success of therapy.
- Fluid therapy inappropriately used may contribute to the development of AKI.
- Tissue hypoxia and renal microcirculation compromise should be regards as a key component of the pathogenesis of AKI
- Anemia, either previously present or induced by should be regarded as a major risk factor contributing to AKI.
- Reperfusion injury and sepsis causing renal microcirculatory injury are defining in the pathogenesis of AKI.

Research agenda

- Innovative diagnostic techniques need to be developed to non-invasively monitor renal hemodynamics.
- Sublingual microcirculatory alterations measured by hand-held vital microscopes should be investigated for use as a surrogate for renal microcirculatory dysfunction.
- Contrast enhance ultrasound is a promising technique for non-invasive monitoring of the kidney microcirculation but needs to be further developed taking into account the special properties of compromised renal hemodynamics
- Anti-inflammatory medication as a prophylactic intervention should be considered as a method to protect the kidney at risk for injury.

Improvement of oxygen availability in the injured kidney by blood transfusions or even hemoglobin-based oxygen carriers should be investigated as a new therapeutic strategy to resuscitate the injured kidney.

Conflict of interest

References

1.   Hoste EAJ, Bagshaw SM, Bellomo R, et al. Epidemiology of acute kidney injury in critically ill patients: the multinational AKI-EPI study. *Intensive Care Med*. 2015;41(8):1411-1423.

2.   Rewa O, Bagshaw SM. Acute kidney injury-epidemiology, outcomes and economics. *Nat Rev Nephrol*. 2014;10(4):193-207.

3.   Heung M, Chawla LS. Acute kidney injury: gateway to chronic kidney disease. *Nephron Clin Pract*. 2014;127(1-4):30-34.

4.   Forni LG, Darmon M, Ostermann M, et al. Renal recovery after acute kidney injury. *Intensive Care Med*. 2017;43(6):855-866.

5.   Basile DP, Anderson MD, Sutton TA. Pathophysiology of Acute Kidney Injury. *Compr Physiol*. 2012;2(2):1303-1353.

6.   Pallone TL, Silldorff EP, Turner MR. Intrarenal blood flow: microvascular anatomy and the regulation of medullary perfusion. *Clin Exp Pharmacol Physiol*. 1998;25(6):383-392.

7.   Pallone TL, Edwards A, Mattson DL. Renal medullary circulation. *Compr Physiol*. 2012;2(1):97-140.

8.   Evans RG, Ince C, Joles JA, et al. Haemodynamic influences on kidney oxygenation: clinical implications of integrative physiology. *Clin Exp Pharmacol Physiol*. 2013;40(2):106-122.

9.   Loutzenhiser R, Bidani A, Chilton L. Renal myogenic response: kinetic attributes and physiological role. *Circ Res*. 2002;90(12):1316-1324.

10.   Pelayo JC. Renal adrenergic effector mechanisms: glomerular sites for prostaglandin interaction. *Am J Physiol*. 1988;254(2 Pt 2):F184-190.

11.   Hermansson K, Larson M, Källskog O, Wolgast M. Influence of renal nerve activity on arteriolar resistance, ultrafiltration dynamics and fluid reabsorption. *Pflugers Arch*. 1981;389(2):85-90.

12.   Leonard BL, Malpas SC, Denton KM, Madden AC, Evans RG. Differential control of intrarenal blood flow during reflex increases in sympathetic nerve activity. *Am J Physiol Regul Integr Comp Physiol*. 2001;280(1):R62-68.

13.   Just A. Mechanisms of renal blood flow autoregulation: dynamics and contributions. *Am J Physiol Regul Integr Comp Physiol*. 2007;292(1):R1-17.

14.   Legrand M, Le Cam B, Perbet S, et al. Urine sodium concentration to predict fluid responsiveness in oliguric ICU patients: a prospective multicenter observational study. *Crit Care*. 2016;20(1):165.

15.   Legrand M, Dupuis C, Simon C, et al. Association between systemic hemodynamics and septic acute kidney injury in critically ill patients: a retrospective observational study. *Crit Care*. 2013;17(6):R278.

16.   Langenberg C, Bellomo R, May C, Wan L, Egi M, Morgera S. Renal blood flow in sepsis. *Crit Care*. 2005;9(4):R363-374.

17.   Schrier RW, Wang W. Acute renal failure and sepsis. *N Engl J Med*. 2004;351(2):159-169.

18.   Prowle JR, Ishikawa K, May CN, Bellomo R. Renal blood flow during acute renal failure in man. *Blood Purif*. 2009;28(3):216-225.

19.   Chvojka J, Sykora R, Krouzecky A, et al. Renal haemodynamic, microcirculatory, metabolic and histopathological responses to peritonitis-induced septic shock in pigs. *Crit Care*. 2008;12(6):R164.

20.   Langenberg C, Wan L, Egi M, May CN, Bellomo R. Renal blood flow and function during recovery from experimental septic acute kidney injury. *Intensive Care Med*. 2007;33(9):1614-1618.

21.   Di Giantomasso D, May CN, Bellomo R. Vital organ blood flow during hyperdynamic sepsis. *Chest*. 2003;124(3):1053-1059.

22.   Lerolle N, Nochy D, Guérot E, et al. Histopathology of septic shock induced acute kidney injury: apoptosis and leukocytic infiltration. *Intensive Care Med*. 2010;36(3):471-478.

23.   Takasu O, Gaut JP, Watanabe E, et al. Mechanisms of cardiac and renal dysfunction in patients dying of sepsis. *Am J Respir Crit Care Med*. 2013;187(5):509-517.

24.   Maiden MJ, Otto S, Brealey JK, et al. Structure and Function of the Kidney in Septic Shock. A Prospective Controlled Experimental Study. *Am J Respir Crit Care Med*. 2016;194(6):692-700.

25.   Kosaka J, Lankadeva YR, May CN, Bellomo R. Histopathology of Septic Acute Kidney Injury: A Systematic Review of Experimental Data. *Crit Care Med*. 2016;44(9):e897-903.

26.   Langenberg C, Gobe G, Hood S, May CN, Bellomo R. Renal histopathology during experimental septic acute kidney injury and recovery. *Crit Care Med*. 2014;42(1):e58-67.

27.   Bellomo R, Kellum JA, Ronco C, et al. Acute kidney injury in sepsis. *Intensive Care Med*. 2017;43(6):816-828.

28.   Ince C. Hemodynamic coherence and the rationale for monitoring the microcirculation. *Crit Care*. 2015;19 Suppl 3:S8.

29.   ProCESS Investigators, Yealy DM, Kellum JA, et al. A randomized trial of protocol-based care for early septic shock. *N Engl J Med*. 2014;370(18):1683-1693.

30.   Mouncey PR, Osborn TM, Power GS, et al. Trial of early, goal-directed resuscitation for septic shock. *N Engl J Med*. 2015;372(14):1301-1311.

31.   ARISE Investigators, ANZICS Clinical Trials Group, Peake SL, et al. Goal-directed resuscitation for patients with early septic shock. *N Engl J Med*. 2014;371(16):1496-1506.

32.   Legrand M, Ince C. Intravenous Fluids in AKI: A Mechanistically Guided Approach. *Semin Nephrol*. 2016;36(1):53-61.

33.   Saugel B, Eschermann K, Hoffmann R, et al. Stenotrophomonas maltophilia in the respiratory tract of medical intensive care unit patients. *Eur J Clin Microbiol Infect Dis*. 2012;31(7):1419-1428.

34.   Asfar P, Meziani F, Hamel J-F, et al. High versus low blood-pressure target in patients with septic shock. *N Engl J Med*. 2014;370(17):1583-1593.

35.   Pallone TL, Turner MR, Edwards A, Jamison RL. Countercurrent exchange in the renal medulla. *Am J Physiol Regul Integr Comp Physiol*. 2003;284(5):R1153-1175.

36.   Evans RG, Gardiner BS, Smith DW, O'Connor PM. Intrarenal oxygenation: unique challenges and the biophysical basis of homeostasis. *Am J Physiol Renal Physiol*. 2008;295(5):F1259-1270.

37.   Brezis M, Agmon Y, Epstein FH. Determinants of intrarenal oxygenation. I. Effects of diuretics. *Am J Physiol*. 1994;267(6 Pt 2):F1059-1062.

38.   Johannes T, Mik EG, Nohé B, Unertl KE, Ince C. Acute decrease in renal microvascular PO2 during acute normovolemic hemodilution. *Am J Physiol Renal Physiol*. 2007;292(2):F796-803.

39.   Johannes T, Mik EG, Nohé B, Raat NJH, Unertl KE, Ince C. Influence of fluid resuscitation on renal microvascular PO2 in a normotensive rat model of endotoxemia. *Crit Care*. 2006;10(3):R88.

40.   Evans RG, Goddard D, Eppel GA, O'Connor PM. Factors that render the kidney susceptible to tissue hypoxia in hypoxemia. *Am J Physiol Regul Integr Comp Physiol*. 2011;300(4):R931-940.

41.   O'Connor PM, Anderson WP, Kett MM, Evans RG. Renal preglomerular arterial-venous O2 shunting is a structural anti-oxidant defence mechanism of the renal cortex. *Clin Exp Pharmacol Physiol*. 2006;33(7):637-641.

42.   Zhang W, Edwards A. Oxygen transport across vasa recta in the renal medulla. *Am J Physiol Heart Circ Physiol*. 2002;283(3):H1042-1055.

43.   Ren Y, Garvin JL, Liu R, Carretero OA. Role of macula densa adenosine triphosphate (ATP) in tubuloglomerular feedback. *Kidney Int*. 2004;66(4):1479-1485.

44.   Hansen PB, Schnermann J. Vasoconstrictor and vasodilator effects of adenosine in the kidney. *Am J Physiol Renal Physiol*. 2003;285(4):F590-599.

45.   Bailey MA, Hillman KA, Unwin RJ. P2 receptors in the kidney. *J Auton Nerv Syst*. 2000;81(1-3):264-270.

46.   Eppel GA, Ventura S, Evans RG. Regional vascular responses to ATP and ATP analogues in the rabbit kidney in vivo: roles for adenosine receptors and prostanoids. *Br J Pharmacol*. 2006;149(5):523-531.

47.   Inscho EW. P2 receptors in regulation of renal microvascular function. *Am J Physiol Renal Physiol*. 2001;280(6):F927-944.

48.   Guan Z, VanBeusecum JP, Inscho EW. Endothelin and the renal microcirculation. *Semin Nephrol*. 2015;35(2):145-155.

49.   Kohan DE, Inscho EW, Wesson D, Pollock DM. Physiology of endothelin and the kidney. *Compr Physiol*. 2011;1(2):883-919.

50.   Gellai M, DeWolf R, Pullen M, Nambi P. Distribution and functional role of renal ET receptor subtypes in normotensive and hypertensive rats. *Kidney Int*. 1994;46(5):1287-1294.

51.   Evans RG, Madden AC, Oliver JJ, Lewis TV. Effects of ET(A) - and ET(B)-receptor antagonists on regional kidney blood flow, and responses to intravenous endothelin-1, in anaesthetized rabbits. *J Hypertens*. 2001;19(10):1789-1799.

52.   Pollock DM, Opgenorth TJ. Evidence for endothelin-induced renal vasoconstriction independent of ETA receptor activation. *Am J Physiol*. 1993;264(1 Pt 2):R222-226.

53.   Schildroth J, Rettig-Zimmermann J, Kalk P, et al. Endothelin type A and B receptors in the control of afferent and efferent arterioles in mice. *Nephrol Dial Transplant*. 2011;26(3):779-789.

54.   Moncada S, Higgs A. The L-arginine-nitric oxide pathway. *N Engl J Med*. 1993;329(27):2002-2012.

55.   Majid DS, Navar LG. Nitric oxide in the control of renal hemodynamics and excretory function. *Am J Hypertens*. 2001;14(6 Pt 2):74S-82S.

56. Tessari P. Nitric oxide in the normal kidney and in patients with diabetic nephropathy. *J Nephrol*. 2015;28(3):257-268.

57. Mount PF, Power DA. Nitric oxide in the kidney: functions and regulation of synthesis. *Acta Physiol (Oxf)*. 2006;187(4):433-446.

58. Bonventre JV, Yang L. Cellular pathophysiology of ischemic acute kidney injury. *J Clin Invest*. 2011;121(11):4210-4221.

59. Basile DP. The endothelial cell in ischemic acute kidney injury: implications for acute and chronic function. *Kidney Int*. 2007;72(2):151-156.

60. Arnemann P, Seidel L, Ertmer C. Haemodynamic coherence - The relevance of fluid therapy. *Best Pract Res Clin Anaesthesiol*. 2016;30(4):419-427.

61. Le Dorze M, Legrand M, Payen D, Ince C. The role of the microcirculation in acute kidney injury. *Curr Opin Crit Care*. 2009;15(6):503-508.

62. Lankadeva YR, Kosaka J, Evans RG, Bailey SR, Bellomo R, May CN. Intrarenal and urinary oxygenation during norepinephrine resuscitation in ovine septic acute kidney injury. *Kidney Int*. 2016;90(1):100-108.

63. Gullichsen E, Nelimarkka O, Halkola L, Niinikoski J. Renal oxygenation in endotoxin shock in dogs. *Crit Care Med*. 1989;17(6):547-550.

64. Ergin B, Zafrani L, Kandil A, et al. Fully Balanced Fluids do not Improve Microvascular Oxygenation, Acidosis and Renal Function in a Rat Model of Endotoxemia. *Shock*. 2016;46(1):83-91.

65. Ergin B, Kapucu A, Demirci-Tansel C, Ince C. The renal microcirculation in sepsis. *Nephrol Dial Transplant*. 2015;30(2):169-177.

66. Johannes T, Ince C, Klingel K, Unertl KE, Mik EG. Iloprost preserves renal oxygenation and restores kidney function in endotoxemia-related acute renal failure in the rat. *Crit Care Med*. 2009;37(4):1423-1432.

67. Bouglé A, Duranteau J. Pathophysiology of sepsis-induced acute kidney injury: the role of global renal blood flow and renal vascular resistance. *Contrib Nephrol*. 2011;174:89-97.

68. Legrand M, Bezemer R, Kandil A, Demirci C, Payen D, Ince C. The role of renal hypoperfusion in development of renal microcirculatory dysfunction in endotoxemic rats. *Intensive Care Med*. 2011;37(9):1534-1542.

69. Verma SK, Molitoris BA. Renal endothelial injury and microvascular dysfunction in acute kidney injury. *Semin Nephrol*. 2015;35(1):96-107.

70. Souza ACCP de, Volpini RA, Shimizu MH, et al. Erythropoietin prevents sepsis-related acute kidney injury in rats by inhibiting NF-κB and upregulating endothelial nitric oxide synthase. *Am J Physiol Renal Physiol*. 2012;302(8):F1045-1054.

71. Schwartz D, Mendonca M, Schwartz I, et al. Inhibition of constitutive nitric oxide synthase (NOS) by nitric oxide generated by inducible NOS after lipopolysaccharide administration provokes renal dysfunction in rats. *J Clin Invest*. 1997;100(2):439-448.

72. Ince C. The microcirculation is the motor of sepsis. *Crit Care*. 2005;9 Suppl 4:S13-19.

73. Sutton TA, Mang HE, Campos SB, Sandoval RM, Yoder MC, Molitoris BA. Injury of the renal microvascular endothelium alters barrier function after ischemia. *Am J Physiol Renal Physiol*. 2003;285(2):F191-198.

74.   Adembri C, Sgambati E, Vitali L, et al. Sepsis induces albuminuria and alterations in the glomerular filtration barrier: a morphofunctional study in the rat. *Crit Care*. 2011;15(6):R277.

75.   Singh A, Ramnath RD, Foster RR, et al. Reactive oxygen species modulate the barrier function of the human glomerular endothelial glycocalyx. *PLoS ONE*. 2013;8(2):e55852.

76.   Ince C, Mik EG. Microcirculatory and mitochondrial hypoxia in sepsis, shock, and resuscitation. *J Appl Physiol*. 2016;120(2):226-235.

77.   Heyman SN, Evans RG, Rosen S, Rosenberger C. Cellular adaptive changes in AKI: mitigating renal hypoxic injury. *Nephrol Dial Transplant*. 2012;27(5):1721-1728.

78.   Ramakers BP, Riksen NP, van der Hoeven JG, Smits P, Pickkers P. Modulation of innate immunity by adenosine receptor stimulation. *Shock*. 2011;36(3):208-215.

79.   Vallon V, Mühlbauer B, Osswald H. Adenosine and kidney function. *Physiol Rev*. 2006;86(3):901-940.

80.   Koning NJ, de Lange F, Vonk ABA, et al. Impaired microcirculatory perfusion in a rat model of cardiopulmonary bypass: the role of hemodilution. *Am J Physiol Heart Circ Physiol*. 2016;310(5):H550-558.

81.   Lannemyr L, Bragadottir G, Krumbholz V, Redfors B, Sellgren J, Ricksten S-E. Effects of Cardiopulmonary Bypass on Renal Perfusion, Filtration, and Oxygenation in Patients Undergoing Cardiac Surgery. *Anesthesiology*. 2017;126(2):205-213.

82.   Cabrales P, Tsai AG, Frangos JA, Briceño JC, Intaglietta M. Oxygen delivery and consumption in the microcirculation after extreme hemodilution with perfluorocarbons. *Am J Physiol Heart Circ Physiol*. 2004;287(1):H320-330.

83.   Morariu AM, Maathuis M-HJ, Asgeirsdottir SA, et al. Acute isovolemic hemodilution triggers proinflammatory and procoagulatory endothelial activation in vital organs: role of erythrocyte aggregation. *Microcirculation*. 2006;13(5):397-409.

84.   Ince C. The great fluid debate: when will physiology prevail? *Anesthesiology*. 2013;119(2):248-249.

85.   Yuruk K, Almac E, Bezemer R, Goedhart P, de Mol B, Ince C. Blood transfusions recruit the microcirculation during cardiac surgery. *Transfusion*. 2011;51(5):961-967.

86.   Yuruk K, Bartels SA, Milstein DMJ, Bezemer R, Biemond BJ, Ince C. Red blood cell transfusions and tissue oxygenation in anemic hematology outpatients. *Transfusion*. 2012;52(3):641-646.

87.   Zeng Z, Chen Z, Xu S, et al. Polydatin Protecting Kidneys against Hemorrhagic Shock-Induced Mitochondrial Dysfunction via SIRT1 Activation and p53 Deacetylation. *Oxid Med Cell Longev*. 2016;2016:1737185.

88.   Kang D-H, Kanellis J, Hugo C, et al. Role of the microvascular endothelium in progressive renal disease. *J Am Soc Nephrol*. 2002;13(3):806-816.

89.   Zafrani L, Ergin B, Kapucu A, Ince C. Blood transfusion improves renal oxygenation and renal function in sepsis-induced acute kidney injury in rats. *Crit Care*. 2016;20(1):406.

90.   Gomez H, Ince C, De Backer D, et al. A unified theory of sepsis-induced acute kidney injury: inflammation, microcirculatory dysfunction, bioenergetics, and the tubular cell adaptation to injury. *Shock*. 2014;41(1):3-11.

3

ENDOTHELIAL DYSFUNCTION OF THE KIDNEY IN SEPSIS

Philippe Guerci,[1,2,3] and Can Ince[3,4]

1. Department of Anesthesiology and Critical Care Medicine, University Hospital of Nancy, France
2. INSERM U1116, University of Lorraine, Vandoeuvre-Les-Nancy, France
3. Department of Translational Physiology, Academic Medical Centre, Amsterdam, The Netherlands
4. Department of Intensive Care Medicine, Erasmus MC, University Medical Centre, Rotterdam, The Netherlands

Introduction

Endothelial dysfunction and microcirculation impairment are recognized hallmarks of sepsis-related organ failure.[1-7] Many experimental and clinical studies have emphasized the central role of endothelial cell activation and dysfunction in promoting the coagulation cascade, leukocyte adherence, vascular barrier compromise, hemodynamic collapse and vascular hyporesponsiveness. These processes contribute to organ failure with an increased risk of morbidity and mortality for the patient. Among the organ failures observed in septic patients, acute kidney injury (AKI) is one of the most frequent. Sepsis-induced AKI may be associated with mortality rates above 50%.[8-11] In fact, the kidney exhibits a high sensitivity to microcirculatory alterations, especially heterogeneity, and to tissue hypoxia, two main phenomena that occur during septic shock.[12-15]

This book chapter provides an overview of sepsis-related endothelial dysfunction with a particular focus on the kidney. We discuss the features of healthy and injured septic vascular endothelium of the kidney, the interplay between endothelial cells and blood cells, and interactions among a wide range of molecules. Moreover, we describe how septic insult to endothelium can lead to a loss of kidney function.

The role of renal endothelium in function

The endothelial cells

The endothelial cells (ECs) form the interface between the content of the inner lumen of vessels and the surrounding environment, comprising the vascular smooth muscle cells (VSCMs), the interstitial space and the parenchymal cells that are responsible for organ function.[16] The ECs constitute a monolayer lining the interior of all blood vessels. This surface is estimated to comprise approximately 10^{13} cells, covering 4000 to 7000 m^2. ECs generally have a thickness of approximately 0.5 μm and are 100 μm long by 10 μm wide.

The endothelium is remarkably heterogeneous in structure and function. The arrangement of ECs may significantly differ from one organ to the next, from juxtaposed arrangements to overlapping arrangements. This heterogeneous distribution may also vary within the same organ; in the kidney, for instance, various ECs arrangements grant different permeability properties. The EC lining contains pores and fenestrations to ensure partial permeability and to

transport molecules to the underlying cells and basal membrane. The kidney and intestines exhibit the highest permeability. ECs are linked together by transcellular components, including gap junctions for electrical communication for upstream vascular regulation and intercellular tight junctions for maintaining vascular barriers.[6,17] Previously considered a passive barrier, it is now apparent that ECs play a crucial role in the regulation of vasomotor tone, hemostasis, immunological functions, and the secretion of molecules by sensing through mechanotransductors, which subsequently initiate transcellular and intra-cellular signaling and activation.

3

The glomerular and peritubular endothelium

Glomerular endothelial cells are unusually thin; around capillary loops, they have a cell thickness of approximately 50–150 nm, whereas in other locations, this thickness is approximately 500 nm.[18] ECs in the glomerulus present large fenestrated areas constituting 20–50% of the entire endothelial surface.[19] These fenestrations are typically 60–70 nm in diameter but, unlike renal peritubular ECs, do not seem to possess a thin (3–5 nm) diaphragm.[20,21] In general, these fenestrations act as a sieving barrier to control the production of urine in the glomerulus, filtering plasma due to hydrostatic pressure.[22] The kidney has one of the richest and most diverse EC populations found within any organ. The microcirculation of the kidney presents two specialized capillary beds connected in series: the glomerular capillary bed in the cortex for plasma filtration and the peritubular capillary bed, which forms the vasa recta responsible for electrolyte reabsorption in the outer and inner medulla. Thus, the arrangement of ECs and the permeability of the endothelium differ for these 2 microcirculations. Glomerular microcirculation functions via continuous and fenestrated endothelium with no diaphragm, whereas it is more continuous and nonfenestrated in the descending vasa recta in peritubular microcirculation.[23,24]

The endothelium must face and resist extreme physiological conditions, such as large changes in oxygenation and osmolality. Indeed, ECs in the cortex are exposed to almost normal oxygen partial pressure and osmolality, whereas those in medullar microcirculation function in an osmolality of up to 1,200 mosmol.L^{-1} and a PO_2 as low as 20 mm Hg.[23,25,26] The microvascular arrangement has a specialized structure in the medulla. The vasa recta, connected in series with the juxtaglomerular microvasculature, surround the peritubular cells in the outer and inner medulla and are responsible for solute exchange. The ECs of these microvessels are exposed

to countercurrent oxygen exchange resulting in a gradient of decreasing oxygen tension (to ~10 mmHg).[26,27] Thus, their functions differ considerably along the tubule. In addition, ECs are affected and injured by ischemia injury differently.[28]

Interplay of endothelium and leukocytes

The inner lumen of ECs is exposed to blood flow, consisting of red blood cells, leukocytes and plasma. In the physiological state, endothelium–leukocyte interactions are limited. Five steps generally describe the interactions between ECs and leukocytes during inflammation, beginning with limited contact, then more prolonged contact, leukocyte rolling, strong adhesion, and finally transendothelial migration, a process referred to as diapedesis.[29] ECs regulate leukocyte trafficking between circulating blood and the surrounding tissue. When activated, the endothelium exhibits enhanced endothelium–leukocyte interactions that are secondary to increased expressions of cell adhesion molecules (CAMs), such as intercellular adhesion molecule selectins (E-selectin and L-selectin), ICAM-1, ICAM-2, vascular adhesion molecule (VCAM), and platelet endothelial cell adhesion molecule (PECAM).[6,30] The up-regulation of CAMs promotes increased adhesion, rolling, and transmigration of circulating leukocytes. Many integrins are also involved in the adhesion of polymorphonuclear leukocytes and monocytes in the proximal tubule and serve as transcellular mechanotransducers.[31]

Regulation of vascular tone

An essential mechanism involved in the vasomotor tone underlying renal autoregulation is endothelium-dependent relaxation. Various physiologic stimuli, including myogenic, metabolic and neurohormonal factors, lead to endothelium-mediated vascular smooth muscle (VSM) relaxation or constriction. Myogenic activation is mediated by shear stress induced by blood flow and translated into biochemical signals through mechanotransductors, inducing vasorelaxation by vasoactive compounds such as nitric oxide (NO).[4,5,17,30,32] ECs synthetize and release various enzymes or molecules (EDHF: endothelium-derived hyperpolarizing factor, NOS: nitric oxide synthase, SOD: superoxide dismutase, COX: cyclo-oxygenase, and CSE: cystathionine γ-lyase) that also produce various relaxing factors (NO, PGI$_2$, and H$_2$S). These factors then diffuse towards VSM cells to produce relaxation. Endothelial NO synthase (eNOS)-derived NO prevents vascular dysfunction via a direct vasodilatory effect, inhibiting platelet aggregation and leukocyte activation.[4]

Under physiological conditions, the glomerular filtration rate (GFR) is tightly regulated by the renin angiotensin aldosterone system (RASS). The RASS system is activated by tubuloglomerular feedback (TGF) that acts as a negative feedback control mechanism driven by distal tubular fluid flow and sodium and chloride reabsorption.[25] TGF modulates the renal blood flow entering the glomerulus, subsequently controlling the hydrostatic pressure within Bowman's capsule by varying the tone of afferent and efferent arterioles via the aforementioned regulators.[26]

3

The endothelial surface layer: the role of the glycocalyx

Among the essential components constituting of vascular barrier, the glycocalyx, a thin layer lining of the luminal membrane of ECs, protects the endothelium and regulates cellular and macromolecular traffic.[33-35] The glycocalyx contributes to the microvascular barrier permeability.[34] The glycocalyx is a 0.2- to 0.5-µm-thick negatively charged gel-like surface structure of proteoglycans with bound polysaccharide chains called glycosaminoglycans (GAGs), glycoproteins and glycolipids.[33-35] It is thought to represent 20% of the intravascular volume.[33,36] This highly interactive scaffold is capable of sensing blood flow and facilitating protein interactions with their receptors or other proteins, and it houses many EC receptors and compounds important for maintaining hemostasis, homeostasis and providing anti-inflammatory defense to the parenchymal cells.[31,34,35] The glycocalyx also exhibits anticoagulant properties[33] by means of negatively charged components.[34]

The morphology and composition of the glycocalyx layer vary from organ to organ and contribute to the heterogeneity observed in EC functions. Significant differences among vascular beds[37] and between fenestral and interfenestral regions of glomerular ECs were revealed in an analysis of the composition of the ECs in the glycocalyx.[38] For instance, the glycocalyx in the fenestrae region presents a higher ratio of heparan sulfates and hyaluronic acid to sialoproteins. The particular composition of the glycocalyx in the fenestrae is likely crucial for its sieving and permeability properties.[33]

Endothelium and hemostasis

The interactions between ECs and the coagulation system are very complex. These interactions not only regulate pro- and anticoagulant patterns involving ECs, plasma soluble factors, platelets and leukocytes, but also direct platelets and fibrin clotting to injured areas of

the endothelium. ECs are like minifactories that synthetize and express molecules necessary to regulate hemostasis, with either anticoagulant or procoagulant activities. Thrombomodulin, endothelial protein C receptor (EPCR), heparan, tissue-type plasminogen activator (t-PA), tissue factor pathway inhibitor (TFPI), endothelial nitric oxide synthase (eNOS), and CD39 are the main anticoagulant factors. Procoagulant factors include tissue factor (TF), von Willebrand factor (VWF), factor VIII, and plasminogen activator inhibitor type 1 (PAI-1). TF creates complexes with factor VIIa and then activates factors IX and X. Importantly, each of these molecules is differentially expressed across the vascular tree, arteries, capillaries or veins. For every procoagulant response, there is a natural anticoagulant reaction, resulting in the finely tuned balance that is needed to control hemostasis.

Under physiological conditions, ECs inhibit blood coagulation via the activation of protein C, the expression of thrombomodulin and specific proteoglycans, and the release of TPA. TFPI controls the extrinsic pathway and regulates TF,[39] antithrombin III (ATIII)–heparan counterbalances the serine proteases in the cascade,[40] the thrombomodulin (TM)/protein C/protein S mechanism inactivates cofactors Va and VIIIa, and plasmin degrades preformed fibrin.[30] Plasma VWF binds and aggregates platelets by bridging platelet receptor platelet glycoprotein (GPIb-IX) to denudated endothelium. The cleaving of VWF is regulated by a disintegrin and metalloproteinase with thrombospondin motifs, also known as ADAMTS-13. Various components of the coagulation system directly signal within endothelium via protease-activated receptors (PAR-1). This complex cascade and interplay among leukocytes, endothelium and hemostasis is severely disturbed in sepsis and contributes to the pathogenesis of sepsis-induced organ failure.

Endothelial cells and the pathophysiology of sepsis

The host response to pathogens primarily determines how severe its inflammatory activation is promoted, contributing to endothelial injury. This sequence of events leads to microcirculation derangement, resulting in plugged microvessels, functional microcirculation shunting contributing to reduced O_2 extraction, and renal tissue hypoxemia. This heterogeneous flow generates microareas of ischemia, leading to functional failure of the kidney. The next step is characterized by organ dysfunction, which affects patient outcome. Therefore, septic kidneys can become compromised due to several pathogenic events, including

(i) endothelial function directly affecting peritubular epithelial cells causing AKI,[41] (ii) glycocalyx shedding that alters the venal vascular barrier,[33] and (iii) microcirculation heterogeneity and renal tissue hypoxia.[15]

Endothelial cell activation causes important structural changes in the glomerular and peritubular capillaries. The damage- or pathogen-associated molecular patterns (DAMPs/PAMPs) are key signals that trigger systemic reactions by priming, signaling, alerting, and guiding the immune system to fight pathogens.[42,43] The etiology of endothelium impairment during sepsis has not been clearly established. DAMPs/PAMPs involved in EC dysfunction can also be recognized by several cellular types, causing indirect deleterious effects on EC functions. Thus, ECs, leukocytes, platelets and the endothelium surface simultaneously trigger cascades of mediators, causing massive physiological changes. However, leukocyte–EC interactions are considered of specific importance. The cross-talk between ECs and leukocytes is mediated by CAMs, as described above, which enables leukocytes to adhere the endothelium. Because these molecules are embedded in the EC glycocalyx layer, such activation is presumably preceded by glycocalyx shedding due to inflammatory mediators, e.g., cytokines, reactive oxygen species, and nitrosatives species.[6,13,17,33,44,45] An illustrative clinical setting that puts into perspective the contributing effect of each component in sepsis-induced endothelium dysfunction is the context of agranulocytosis/neutropenia or bone marrow-suppressed patients. These patients exhibit the most severe pattern of septic shock, although no leukocyte–EC interactions are present because no leukocytes exist. Moreover, many studies have analyzed endothelium dysfunction via perfusion with various fluids and molecules without the addition of leukocytes. Eliminating leukocytes could be considered a weakness of such studies or could emphasize the fact that leukocyte–EC interactions may not be a fundamental element contributing to endothelial dysfunction in renal dysfunction.

TNF-α exerts deleterious effects on renal ECs and plays a key role in AKI.[46] In the light of these findings, Xu *et al.* observed in TNF receptor 1 (TNFR1) knocked-out mice submitted to endotoxin challenge that the glomerular endothelial surface layer, endothelial cell fenestrae, GFR, and albuminuria were diminished. These results suggest that sepsis-induced endothelial dysfunction may be mediated by TNF-α activation of TNFR1.[46,47] In addition, Wu *et al.* demonstrated that mice lacking expression of ICAM-1 exhibited reduced AKI, leukocyte infiltration and mortality in response to endotoxin.[48] ICAM-1 may not solely be crucial for leukocyte–EC interactions, although it may play a pivotal role in endotoxin-induced AKI. Mice lacking expressions of the 2 principal ligands for ICAM-1, ß1 integrin LFA-1 (CD11a/CD18) and

Mac-1 (CD11b/ CD18), present on circulating leukocytes, were not protected against neutrophil infiltration nor endotoxin-induced AKI.[48] These findings suggest that sepsis involves multiples pathways leading to endothelial dysfunction and AKI.

Shedding or damaged glycocalyx expose CAMs, previously embedded in the glycocalyx and shielded from the leukocyte interaction. Under such conditions, many EC functions mediated by the glycocalyx are jeopardized.[17,33,44,49] Glycocalyx degradation contributes to an increase in vascular barrier permeability with subsequent albuminuria.[17,50-53] An up-regulation of P-selectin, ICAM-1 and VCAM-1 has also been observed in the peritubular capillaries during sepsis.[48,54] Inflammatory mediators and reactive oxygen species released by leukocytes and ECs and upregulated to destroy pathogens may themselves harm the endothelium as an unwanted side effect. Clinical studies have demonstrated that increased excretion of glycocalyx degradation products in urine was associated with microalbuminuria.[51,52] This finding indicates that the glomerular basal membrane is damaged during sepsis as the result of the endothelial vascular barrier injury. At the tissue level, damage to the glycocalyx correlates with increased interstitial fluid and tissue edema.

Plasma leakage is a result of altered vascular barrier permeability. In addition to CAMs and cell-cell junction molecules, vascular endothelial growth factor (VEGF) and angiopoietin–Tie2 systems are critically involved in vascular barrier permeability compromise during sepsis.[55-60] High levels of VEGF have been shown in septic patients.[58-63] However, low VEGF concentrations were preferentially associated with more severe renal dysfunction.[63] Whereas VEGF and angiopoietin-2 promote microvascular permeability, angiopoeitin-1 (Ang1) acts as an anti-permeability molecule and may protect against plasma leakage during sepsis.[64,65] In fact, Kim *et al.* showed that the administration of a variant of Ang-1 (COMP-Ang1) in mice subjected to endotoxin mitigated renal EC dysfunction and protected against AKI.[66]

The systemic inflammatory response associated with sepsis leads to activation of coagulation and disrupts hemostasis, promoting procoagulant and anti-fibrinolytic states.[67,68] Increasing evidence points to an extensive cross-talk between coagulation and inflammation during sepsis. After injury, EC express tissue factor and initiate coagulation cascades that activate thrombin and deposit fibrin.[40,68] Tissue factor expression triggers the activation of coagulation. In sepsis, TF upregulation is insufficiently counteracted by TF inhibitors. In addition, the fibrinolytic pathway is altered with increased PAI-1 activity, resulting in an inhibition of fibrin removal.[67] The level of activated protein C is decreased, contributing to the formation of micro-clots/plugs in the microcirculation.[5] If uncorrected, this procoagulant state may cause thrombi

3

formation and/or severe bleeding or hematomas as part of disseminated intravascular coagulation (DIC) syndrome. Bleeding is caused by the consumption and subsequent exhaustion of coagulation proteins and platelets due to the ongoing activation of the coagulation system.[67] Additionally, platelets may also attach to ECs and are involved in EC activation by several mechanisms. The engagement of platelet GPIIbIIIa upregulates CD40 ligand expression on the platelet membrane, stimulating endothelial cells to express adhesion molecules and TF.[69] Platelet P-selectin, not endothelial P-selectin, is key in the development of ischemic AKI.[70] Platelet consumption may also play an important role in patients with sepsis due to the ongoing generation of thrombin.[71] Platelets contribute to microvascular dysfunction and play a pivotal role in organ failure.[72,73] Finally, neutrophil extracellular traps (NETs) also contribute to microvascular impairment.[68] NETs are networks of chromatin filaments composed of histones and DNA strands, decorated with proteins and lysosomal enzymes. They are released by neutrophils upon contact with infectious agents, inflammatory cytokines or ROS.[68]

A common end product of microvascular injury and the combined degradation arising from the glycocalyx, ECs, leukocytes, red blood cells and platelets is the generation of microparticles (MPs).[74] MPs are cell membrane–derived particles which are 0.2–2 μm in diameter, that promote coagulation and inflammation and that contribute to multiple-organ injury, including AKI.[75] MPs remotely promote widespread endothelial dysfunction.[76] Zafrani *et al.* showed a direct role of MPs in sepsis induced-AKI by using calpastatin, a calpain-specific inhibitor (calpain is essential in MPs release).[77] Several procoagulants (TF and phosphatidylserine) are included in the outer leaflet of MPs perpetuating the prothrombotic state of sepsis.

The above described events generate oxidative and nitrosative stress. Due to tissue hypoxia caused by microvascular dysfunction during sepsis, parenchymal and endothelial cells can switch from aerobic to anaerobic respiration, producing toxic byproducts, such as ROS. Reactive nitrogen species (RNS) derived from NO and ROS, such as superoxide (O_2^-), are produced in large amounts during sepsis. The upregulated production of superoxide arises from (i) the reactions catalyzed by NAPDH oxidase present in leukocytes and endothelial cells, (ii) the conversion of xanthine dehydrogenase to xanthine oxidase, and (iii) the uncoupling of NOS in conditions of tetrahydrobiopterin deficiency.[78] In an anaerobic state, ROS are aggressively produced by the mitochondria, resulting in more cell damage and endothelial cell dysfunction. Both RNS and ROS alter EC functions and cause lipid peroxidation, in addition to exerting anti-microbiotic action. Noiri *et al.* demonstrated that L-N^6-(1-iminoethyl)lysine hydrochloride (L-Nil) administration, an inhibitor of inducible NO synthase (iNOS), resulted in

amelioration of renal dysfunction and reduced nitrotyrosine formation, lipid peroxidation, and DNA damage. This suggests that peroxynitrite, rather than superoxide anions, is responsible for renal cell damage.[79] In a model of renal ischemia/reperfusion (I/R) injury, L-Nil also prevented ischemic-induced renal microvascular hypoxia, indicating that renal I/R induced early iNOS-dependent microvascular hypoxia by disrupting the balance between the microvascular oxygen supply and consumption.[80] Conversely, *N*-nitro-L-arginine methyl ester (L-NAME), an NO blocker, has been shown to aggravate the course of AKI following I/R injury.[81]

In contrast to many other organs, iNOS is constitutively expressed in both mouse and human renal tubule cells[82] and may contribute to changes in renal hemodynamics and a reduction in the GFR. The generation of iNOS results in two pathogenic actions: (i) the inhibition of eNOS-derived NO generation and (ii) the contribution of ROS to the formation of peroxynitrite. Depletion of essential cofactors necessary for eNOS activity, such as tetrahydrobiopterin, uncouples eNOS and results in the generation of superoxide anion and reduced NO production, a process referred to eNOS uncoupling. Langenberg *et al.* demonstrated in a sheep model of sepsis-induced AKI, that all subtypes of NOS were highly expressed in the renal cortex but not in the renal medulla.[83] They hypothesized that overexpression of NOS isoforms in the cortex may lead to intrarenal shunting. This may induce a lack of blood flow in the medulla, promoting medullar hypoxia. Vascular hyporesponsiveness is one of the final pathogenic effects in EC injury and further contributes to microcirculation disorders.[4] However, vasodilation, microcirculation alterations and tissue hypoxia are heterogeneous during septic shock, and the kidney is no exception.[1,15]
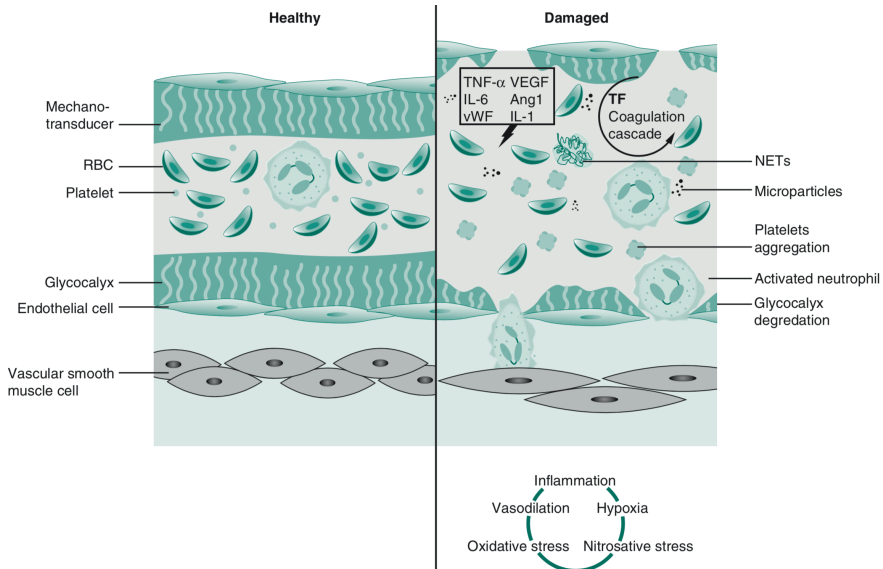
Figure 1. General overview of endothelium dysfunction occurring during sepsis

The region of interest is focused on arterioles where vascular smooth muscle cells are present.

RBC: Red Blood Cells, VEGF: Vascular Endothelium Growth Factor, IL-: Interleukin, vWF: von Willebrand Factor, Ang-1: angiopoietin 1, TF: Tissue Factor, NETs: Neutrophil Extracellular Traps

How does endothelium damage translate into a loss of kidney function?

As described above, endothelial dysfunction is a consequence of a series of simultaneous or consecutive pathogenic events mediated by toxic compounds produced in large quantities, including IL-6, IL-8, TNF-alpha, VWF fragments, plasma free hemoglobin, MPs, ROS and RNS (figure 1). It was previously thought that histologic damages were present in critically ill patients suffering from AKI. Lerolle *et al.* revealed fibrin deposition in the glomeruli and signs of acute tubular injury and leukocyte activation, primarily monocytes, in kidney biopsies taken from 19 patients with AKI within 30 minutes postmortem.[84] However, these results need to be interpreted with caution, as the patients were enrolled after having AKI for 2 days with severe hypoperfusion, which could be responsible for the observed renal alterations and not related

solely to AKI (causing irreversible damages). Indeed, in experimental studies, no cellular changes have been found, which could account for the marked reduction in glomerular filtration as observed in AKI, supporting the notion that early septic acute kidney injury represents a functional disturbance within the kidney.[85,86] This concept is in line with the need to identify physiological biomarkers of AKI instead of pharmacological markers of cellular damage.[87] These results suggest that AKI may be prevented or at least controlled via pharmacologic treatments because the insult does not induce irremediable histologic damages.

Because different microcirculations coexist in the kidney, sepsis-induced disturbances of the microvascular bed may take different forms. Thus, albuminuria may be more related to glomerular microcirculation EC glycocalyx degradation, inadequate Na^+ reabsorption, and ineffective tubulo-glomerular feedback (TGF) due to the peritubular microcirculation. All of these contribute to decreases in the GFR. Rodent models of sepsis-induced AKI suggest that cortical peritubular microvasculature is among the first structures injured.[88-91]

The interactions among various factors contributing to the development of renal failure implicates inflammatory activation characterized by leukocyte-EC interactions. These interactions paired with the dysbalance of O_2 homeostasis, involving the delicate balance among O_2, NO and ROS, and inflammation causes renal microcirculatory dysfunction. These events represent the mechanism of renal function failure.

The role of kidney hypoxia

The final common pathway of the pathophysiological response to sepsis, as discussed above, leads to tissue hypoxia.[15] EC damage is associated with microcirculation impairment followed by tissue hypoperfusion and hypoxia. Lack of oxygen to parenchymal cells directly causes loss of organ function, especially in tubular cells of the kidney.[15] Increasing evidence has demonstrated that a loss of renal oxygenation in heterogeneous areas occurs during sepsis and resuscitation.[92-94] Therefore, the role of hypoxia may have been previously overlooked, assuming that RBF is increased during the early phase of sepsis such that oxygen delivery is maintained or even increased. However, a thorough literature review emphasized the high heterogeneity of RBF changes during sepsis that depends on the time of insult, the model of sepsis-induced AKI, and the monitoring tools and analyses used in the experiments.[95] Alterations in the microvascular perfusion distribution and a mismatch between kidney tissue oxygen demand

and delivery occur, especially in the kidney cortex during the early phase of insult. Functional shunting of O_2 transport occurs, resulting in small areas of hypoxia.[96,97]

Oxygen consumption by the kidney has predominantly and directly related to Na reabsorption (~80%).[98-101] Indeed, the oxygen requirement of the kidney is mainly determined by the ATP production needed for Na/K pump function on the basal side of thick ascending limb cells. Microcirculatory dysfunction can severely limit the ability of circulation to provide adequate oxygen for fueling oxidative phosphorylation for the production of ATP and can directly impair the function of the Na/K ATPase pump.[102] Numerous studies have demonstrated oxygen impairments in the kidney even during the early phase of sepsis.[94,103,104] The unique arrangement of the renal microvasculature, serially organized, with vasa recta emerging from the efferent arterioles of the juxtamedullary glomeruli, makes the maintenance of the medullary perfusion highly depend on adequate cortical perfusion. O_2 shunting occurs between the descending and ascending vasa recta and contributes to the high sensitivities of the medulla and corticomedullary junction to decreased O_2 supply.[23,26,27,92,105] Thus, decreased O_2 availability reduces solute and electrolyte exchange, leading to further activation of the TGF to maintain DGF constant. Johannes *et al.* showed in an endotoxemia rat model that cortical microcirculatory PO_2 was preserved despite hypotension and a drop in renal arterial flow. Interestingly, despite fluid resuscitation in this model, which corrected the mean arterial pressure and increased RBF, the renal cortical microvascular oxygenation paradoxically worsened and VO_2/T_{Na+} increased.[94] Evans *et al.* suggested that arterio-venous shunts may represent an adaptive mechanism for preventing hyperoxia and the overproduction of ROS due to the high renal perfusion needed to sustain the glomerular filtration rate (GFR) and for limiting oxygen debt in the entire kidney.[27]

The role of hypoxia-induced factor α (HIFα) activation and regulation in the kidney during sepsis is a subject of intense investigation.[83,92,106-108] HIFα may play a crucial role in protecting the kidney during I/R injury.[28] Studies have shown that the expressions of HIFα genes and mRNA is upregulated during sepsis-induced AKI in both caecal ligation puncture and endotoxemia models of insult.[83,107] HIFα is an O_2-sensitive transcription factor that accumulates and binds to the key sequence of the erythropoietin (EPO) gene, the hypoxia-responsive element (HRE), and activates transcription of EPO when oxygen tensions decrease. HIFα possesses two isoforms, HIF-1α and HIF-2α, which are expressed in a cell-type fashion: HIF-1α is expressed in tubular cells, and HIF-2α is expressed in interstitial and endothelial cells.[109] In a multi-insult rat model of AKI, Rosenberger *et al.* showed that HIF-1α was more expressed in collecting ducts than in the

medullary thick ascending limb of the loop of Henle (mTAL).[109] The limited activation of HIF-1α in the mTAL may explain the susceptibility of these cells to injury.

The activation of TGF via the renin-angiotensin aldosterone system (RASS) is part of the response to sepsis insult. Increased levels of angiotensin II (Ang II) leads to a reduction in GFR by causing vasoconstriction of both the afferent and efferent arterioles in the glomerulus. The activation of TGF then decreases hydrostatic pressure in the glomerulus and reduces the GFR.[43] Regional reductions in microcirculatory flow cause heterogeneous regional micro-ischemia, resulting in impaired cortical and medullar μPO_2 and contributing to the recruitment of shunts and a reduction in renal oxygen extraction.[92]

Renal tissue edema

The primary cause of renal edema is thought to be initiated by the degradation of the EC glycocalyx. The actors involved in glycocalyx shedding are thought to be reactive oxygen species (ROS), such as hydroxyl anions, hydrogen peroxide, peroxynitrite, and superoxide, or other molecules/enzymes, including heparanase or tumor necrosis factor-α (TNF-α).[6,110,111] Indeed, anti-oxidant enzyme treatments (catalase or superoxide dismutase) experimentally dampened the shedding products of the endothelium and maintained vascular barrier integrity.[45] The final result of loss-of-barrier function is interstitial edema. Edema and, more generally, fluid overload following fluid resuscitation of septic patients, is a well-recognized contributor to organ dysfunction. The use of fluids to treat AKI is a controversial topic, as the amount[112-114] and type of fluid are currently under debate. The kidney is contained in a non-compliant capsule, increasing the harmfulness of increased interstitial renal pressure secondary to fluid overload.[114] Due to glycocalyx degradation and EC disjunction, increases in vascular barrier permeability in both the glomerular and peritubular microcirculations occur.[86,112,115] Subsequent fluid accumulation in renal tissue causes a rise interstitial pressure, increases the pressure gradient across the glomerular capillary, and may result in microcirculatory flow impairment and capillary collapse. In a large cohort of critically ill septic patients presenting AKI, fluid overload was a major contributor of AKI.[116] During renal I/R in a murine model, intra-subcapsular pressure increased due to tissue edema, possibly increasing renal vein pressure, and was correlated with considerably reduced tubular excretion rates and renal perfusion.[117] These considerations suggest that fluid resuscitation during sepsis must be carefully guided to avoid fluid overload

and further impairment of renal microcirculation.[112,114] Vascular congestion has also been noted as a cause of AKI.[118]

Therapies targeting renal ECs in sepsis-induced AKI

Targeting endothelial cells

More than 100 randomized clinical trials have tested the hypothesis of modulating the host response to sepsis, many dedicated to studying target receptors on or in ECs or blocking/modulating molecules known to promote EC injury.[119] Unfortunately, most studies failed to demonstrate any benefits on outcome. Matejovic *et al.* analyzed all ongoing experimental and clinical studies, aiming to improve renal microcirculation hemodynamics during sepsis, either in the glomerular or in the peritubular microvascular bed, with promising results that require confirmation.[120] There is a growing body of evidence suggesting benefits of using corticosteroids during septic shock.[121] However, the specific action of glucocorticoids on ECs in the kidney is incompletely addressed. Selective iNOS inhibition for the treatment of sepsis-induced AKI has also been suggested as a potential EC-targeted therapeutic strategy, outlining the importance of this enzyme as a therapeutic target.[122] To date, however, specific iNOS inhibitors are not currently in use in clinical practice, although anti-inflammatory drugs such as steroids are potent inhibitors of iNOS. Holthoff *et al.* investigated the effects of rolipram, a selective phosphodiesterase 4 inhibitor, and resveratrol, a polyphenol vasodilator that is also capable of scavenging reactive nitrogen species, in a rodent model of sepsis-induced AKI induced by CLP.[90,123] Both treatments improved renal microcirculation, reduced vascular permeability, and improved renal function. In a retrospective clinical study, the administration of ulinastatin, a urinary trypsin inhibitor that possesses a variety of anti-inflammatory effects was found to be associated with a lower incidence of AKI after cardiopulmonary bypass surgery.[124] The authors concluded that the favorable outcome observed may be related to less EC-damaging cytokines that are often present in AKI. Another recent review listed the novel repair targets in endothelial cells during AKI.[125] However, these therapies often focused on one target, whereas cellular and tissue repair are more complex processes involving hundreds of pathways.

New and interesting approaches incorporate cell-based therapies, such as mesenchymal stem cells[126-128] and endothelial progenitor cells (EPCs),[129,130] which may be more efficient given the complex mechanisms of injury. Cellular therapies aim to utilize cells that are capable of

modulating the global inflammatory response by secreting large quantities of pro- and anti-inflammatory agents and other types of molecules. The many molecules that can be secreted cells can target a variety of receptors, better preventing/limiting sepsis-induced organ damage, restoring microcirculation and promoting parenchymal function than a single drug may do. These cell-based therapies are also believed to speed the recovery of renal function and healing. This approach is the object of intense research and several ongoing projects.[126,129] Several authors have demonstrated potential interest of cell-based therapies for treatment of acute renal ischemia/reperfusion injury in rats using EPCs derived from either bone marrow or Wharton's jelly of human umbilical cords.[127,130,131] However, it should be emphasized that the reported data regarding EPCs during sepsis are inconsistent. Some authors found that an increased number of EPCs in critically ill patients was positively associated with better outcomes,[132,133] suggesting a positive effect, whereas others reported the opposite.[134]

Impact of fluid resuscitation on ECs

Fluid resuscitation is the cornerstone of the management of sepsis-induced AKI. The choice of fluid used during the resuscitation process has been largely debated. Briefly, current evidence suggests that fluid resuscitation should not further harm ECs or aggravate tissue edema, with the goal to not further worsen kidney function.[112,114] However, the optimal fluid and optimal dose that should be administered to a specific patient remains a source of debate, and to what extent fluid therapy promotes microcirculatory flow and preserves EC functions in the kidney is unknown.[135]

Data regarding the specific action of fluids on ECs in the kidney are scarce. To date, although there is a growing body of evidence regarding the importance of the glycocalyx in vascular barrier permeability, it is not clear if restoring or preserving the glycocalyx layer from shedding influences renal outcome or decreases the occurrence of sepsis-induced AKI.

Conclusion

ECs play a key role in the protection of the kidney from injury and functional failure. New monitoring techniques that aim to directly providing information regarding renal ECs and microcirculatory function may facilitate goal-directed strategies for identifying and treating AKI.

References

1.   Ince C. The microcirculation is the motor of sepsis. *Crit Care*. 2005;9 Suppl 4(Suppl 4):S13–9.

2.   Vincent J-L, De Backer D. Circulatory shock. *N Engl J Med*. 2014;370(6):583–583.

3.   Boisrame-Helms J, Kremer H, Schini-Kerth V, Meziani F. Endothelial dysfunction in sepsis. *Curr Vasc Pharmacol*. 2013;11(2):150–160.

4.   Levy B, Collin S, Sennoun N, et al. Vascular hyporesponsiveness to vasopressors in septic shock: from bench to bedside. *Intensive Care Med*. 2010;36(12):2019–2029.

5.   Ait-Oufella H, Maury E, Lehoux S, Guidet B, Offenstadt G. The endothelium: physiological functions and role in microcirculatory failure during severe sepsis. *Intensive Care Med*. 2010;36(8):1286–1298.

6.   Ince C, Mayeux PR, Nguyen T, et al. The endothelium in sepsis. *Shock*. 2016;45(3):259–270.

7.   Levi M, van der Poll T. Endothelial injury in sepsis. *Intensive Care Med*. 2013;39(10):1839–1842.

8.   Alobaidi R, Basu RK, Goldstein SL, Bagshaw SM. Sepsis-associated acute kidney injury. *Semin Nephrol*. 2015;35(1):2–11.

9.   Zarbock A, Gomez H, Kellum JA. Sepsis-induced acute kidney injury revisited: pathophysiology, prevention and future therapies. *Curr Opin Crit Care*. 2014;20(6):588–595.

10.   Mandelbaum T, Scott DJ, Lee J, et al. Outcome of critically ill patients with acute kidney injury using the Acute Kidney Injury Network criteria. *Crit Care Med*. 2011;39(12):2659–2664.

11.   Uchino S, Kellum JA, Bellomo R, et al. Acute renal failure in critically ill patients: a multinational, multicenter study. *JAMA*. 2005;294(7):813–818.

12.   Ergin B, Kapucu A, Demirci-Tansel C, Ince C. The renal microcirculation in sepsis. *Nephrol Dial Transplant*. 2015;30(2):169–177.

13.   Zafrani L, Payen D, Azoulay E, Ince C. The microcirculation of the septic kidney. *Semin Nephrol*. 2015;35(1):75–84.

14.   Le Dorze M, Legrand M, Payen D, Ince C. The role of the microcirculation in acute kidney injury. *Curr Opin Crit Care*. 2009;15(6):503–508.

15.   Ince C, Mik EG. Microcirculatory and mitochondrial hypoxia in sepsis, shock, and resuscitation. *J Appl Physiol*. 2016;120(2):226–235.

16.   Vita JA. Endothelial function. *Circulation*. 2011;124(25):e906–12.

17.   Salmon AHJ, Satchell SC. Endothelial glycocalyx dysfunction in disease: albuminuria and increased microvascular permeability. *J Pathol*. 2012;226(4):562–574.

18.   Haraldsson BS. The endothelium as part of the integrative glomerular barrier complex. *Kidney Int*. 2014;85(1):8–11.

19.   Bulger RE, Eknoyan G, Purcell DJ, Dobyan DC. Endothelial characteristics of glomerular capillaries in normal, mercuric chloride-induced, and gentamicin-induced acute renal failure in the rat. *J Clin Invest*. 1983;72(1):128–141.

20.   Satchell SC, Braet F. Glomerular endothelial cell fenestrations: an integral component of the glomerular filtration barrier. *Am J Physiol Renal Physiol*. 2009;296(5):F947–56.

3

21.   Ichimura K, Stan RV, Kurihara H, Sakai T. Glomerular endothelial cells form diaphragms during development and pathologic conditions. *J Am Soc Nephrol*. 2008;19(8):1463–1471.

22.   Haraldsson B, Nyström J, Deen WM. Properties of the glomerular barrier and mechanisms of proteinuria. *Physiol Rev*. 2008;88(2):451–487.

23.   Pallone TL, Turner MR, Edwards A, Jamison RL. Countercurrent exchange in the renal medulla. *Am J Physiol Regul Integr Comp Physiol*. 2003;284(5):R1153–75.

24.   Verma SK, Molitoris BA. Renal endothelial injury and microvascular dysfunction in acute kidney injury. *Semin Nephrol*. 2015;35(1):96–107.

25.   Pallone TL, Silldorff EP, Turner MR. Intrarenal blood flow: microvascular anatomy and the regulation of medullary perfusion. *Clin Exp Pharmacol Physiol*. 1998;25(6):383–392.

26.   Pallone TL, Edwards A, Mattson DL. Renal medullary circulation. *Compr Physiol*. 2012;2(1):97–140.

27.   Evans RG, Gardiner BS, Smith DW, O'Connor PM. Intrarenal oxygenation: unique challenges and the biophysical basis of homeostasis. *Am J Physiol Renal Physiol*. 2008;295(5):F1259–70.

28.   Bonventre JV, Yang L. Cellular pathophysiology of ischemic acute kidney injury. *J Clin Invest*. 2011;121(11):4210–4221.

29.   Springer TA. Traffic signals on endothelium for lymphocyte recirculation and leukocyte emigration. *Annu Rev Physiol*. 1995;57(1):827–872.

30.   Aird WC. The role of the endothelium in severe sepsis and multiple organ dysfunction syndrome. *Blood*. 2003;101(10):3765–3777.

31.   Raghavan V, Weisz OA. Discerning the role of mechanosensors in regulating proximal tubule function. *Am J Physiol Renal Physiol*. 2016;310(1):F1–5.

32.   Kang D-H, Kanellis J, Hugo C, et al. Role of the microvascular endothelium in progressive renal disease. *J Am Soc Nephrol*. 2002;13(3):806–816.

33.   Dane MJC, van den Berg BM, Lee DH, et al. A microscopic view on the renal endothelial glycocalyx. *Am J Physiol Renal Physiol*. 2015;308(9):F956–66.

34.   Curry FE, Adamson RH. Endothelial glycocalyx: permeability barrier and mechanosensor. *Ann Biomed Eng*. 2012;40(4):828–839.

35.   Weinbaum S, Tarbell JM, Damiano ER. The structure and function of the endothelial glycocalyx layer. *Annu Rev Biomed Eng*. 2007;9(1):121–167.

36.   Reitsma S, Slaaf DW, Vink H, van Zandvoort MAMJ, oude Egbrink MGA. The endothelial glycocalyx: composition, functions, and visualization. *Pflugers Arch*. 2007;454(3):345–359.

37.   Bankston PW, Milici AJ. A survey of the binding of polycationic ferritin in several fenestrated capillary beds: indication of heterogeneity in the luminal glycocalyx of fenestral diaphragms. *Microvasc Res*. 1983;26(1):36–48.

38.   Avasthi PS, Koshy V. The anionic matrix at the rat glomerular endothelial surface. *Anat Rec*. 1988;220(3):258–266.

39.   Ellery PER, Adams MJ. Tissue factor pathway inhibitor: then and now. *Semin Thromb Hemost*. 2014;40(8):881–886.

40.   Levy JH, Sniecinski RM, Welsby IJ, Levi M. Antithrombin: anti-inflammatory properties and clinical applications. *Thromb Haemost*. 2015;115(4).

41.   Molitoris BA. Therapeutic translation in acute kidney injury: the epithelial/endothelial axis. *J Clin Invest*. 2014;124(6):2355–2363.

42.   Timmermans K, Kox M, Scheffer GJ, Pickkers P. Danger in the Intensive Care Unit: Damps in Critically Ill Patients. *Shock*. 2016;45(2):108–116.

43.   Gomez H, Ince C, De Backer D, et al. A unified theory of sepsis-induced acute kidney injury: inflammation, microcirculatory dysfunction, bioenergetics, and the tubular cell adaptation to injury. *Shock*. 2014;41(1):3–11.

44.   Satchell S. The role of the glomerular endothelium in albumin handling. *Nat Rev Nephrol*. 2013;9(12):717–725.

45.   Singh A, Ramnath RD, Foster RR, et al. Reactive oxygen species modulate the barrier function of the human glomerular endothelial glycocalyx. Guerrot D, ed. *PLoS ONE*. 2013;8(2):e55852.

46.   Xu C, Chang A, Hack BK, Eadon MT, Alper SL, Cunningham PN. TNF-mediated damage to glomerular endothelium is an important determinant of acute kidney injury in sepsis. *Kidney Int*. 2014;85(1):72–81.

47.   Cunningham PN, Dyanov HM, Park P, Wang J, Newell KA, Quigg RJ. Acute renal failure in endotoxemia is caused by TNF acting directly on TNF receptor-1 in kidney. *J Immunol*. 2002;168(11):5817–5823.

48.   Wu X, Guo R, Wang Y, Cunningham PN. The role of ICAM-1 in endotoxin-induced acute renal failure. *Am J Physiol Renal Physiol*. 2007;293(4):F1262–71.

49.   Chelazzi C, Villa G, Mancinelli P, De Gaudio AR, Adembri C. Glycocalyx and sepsis-induced alterations in vascular permeability. *Crit Care*. 2015;19(1):26.

50.   Rabelink TJ, de Zeeuw D. The glycocalyx--linking albuminuria with renal and cardiovascular disease. *Nat Rev Nephrol*. 2015;11(11):667–676.

51.   De Gaudio AR, Adembri C, Grechi S, Novelli GP. Microalbuminuria as an early index of impairment of glomerular permeability in postoperative septic patients. *Intensive Care Med*. 2000;26(9):1364–1368.

52.   Adembri C, Sgambati E, Vitali L, et al. Sepsis induces albuminuria and alterations in the glomerular filtration barrier: a morphofunctional study in the rat. *Crit Care*. 2011;15(6):R277.

53.   Huxley VH, Williams DA. Role of a glycocalyx on coronary arteriole permeability to proteins: evidence from enzyme treatments. *Am J Physiol Heart Circ Physiol*. 2000;278(4):H1177–85.

54.   Peters K, Unger RE, Brunner J, Kirkpatrick CJ. Molecular basis of endothelial dysfunction in sepsis. *Cardiovasc Res*. 2003;60(1):49–57.

55.   Augustin HG, Koh GY, Thurston G, Alitalo K. Control of vascular morphogenesis and homeostasis through the angiopoietin-Tie system. *Nat Rev Mol Cell Biol*. 2009;10(3):165–177.

56.   Yano K, Liaw PC, Mullington JM, et al. Vascular endothelial growth factor is an important determinant of sepsis morbidity and mortality. *J Exp Med*. 2006;203(6):1447–1458.

57.   Doi K, Leelahavanichkul A, Hu X, et al. Pre-existing renal disease promotes sepsis-induced acute kidney injury and worsens outcome. *Kidney Int*. 2008;74(8):1017–1025.

58.   Siner JM, Bhandari V, Engle KM, Elias JA, Siegel MD. Elevated serum angiopoietin 2 levels are associated with increased mortality in sepsis. *Shock*. 2009;31(4):348–353.

59.   Orfanos SE, Kotanidou A, Glynos C, et al. Angiopoietin-2 is increased in severe sepsis: correlation with inflammatory mediators. *Crit Care Med*. 2007;35(1):199–206.

60.   van der Flier M, van Leeuwen HJ, van Kessel KP, Kimpen JL, Hoepelman AI, Geelen SP. Plasma vascular endothelial growth factor in severe sepsis. *Shock*. 2005;23(1):35–38.

61.   Shapiro NI, Aird WC. Sepsis and the broken endothelium. 2011;15(2):135–2.

62.   Yang K-Y, Liu K-T, Chen Y-C, et al. Plasma soluble vascular endothelial growth factor receptor-1 levels predict outcomes of pneumonia-related septic shock patients: a prospective observational study. *Crit Care*. 2011;15(1):R11.

63.   Karlsson S, Pettilä V, Tenhunen J, et al. Vascular endothelial growth factor in severe sepsis and septic shock. *Anesth Analg*. 2008;106(6):1820–1826.

64.   Thurston G, Rudge JS, Ioffe E, et al. Angiopoietin-1 protects the adult vasculature against plasma leakage. *Nat Med*. 2000;6(4):460–463.

65.   David S, Kümpers P, van Slyke P, Parikh SM. Mending leaky blood vessels: the angiopoietin-Tie2 pathway in sepsis. *J Pharmacol Exp Ther*. 2013;345(1):2–6.

66.   Kim DH, Jung YJ, Lee AS, et al. COMP-angiopoietin-1 decreases lipopolysaccharide-induced acute kidney injury. *Kidney Int*. 2009;76(11):1180–1191.

67.   Levi M, Poll TVD. Coagulation in patients with severe sepsis. *Semin Thromb Hemost*. 2015;41(1):9–15.

68.   Semeraro N, Ammollo CT, Semeraro F, Colucci M. Coagulopathy of Acute Sepsis. *Semin Thromb Hemost*. 2015;41(6):650–658.

69.   de Stoppelaar SF, van 't Veer C, van der Poll T. The role of platelets in sepsis. *Thromb Haemost*. 2014;112(4):666–677.

70.   Singbartl K, Forlow SB, Ley K. Platelet, but not endothelial, P-selectin is critical for neutrophil-mediated acute postischemic renal failure. *FASEB J*. 2001;15(13):2337–2344.

71.   Levi M. Platelets in Critical Illness. *Semin Thromb Hemost*. 2016;42(3):252–257.

72.   Woth G, Varga A, Ghosh S, et al. Platelet aggregation in severe sepsis. *J Thromb Thrombolysis*. 2011;31(1):6–12.

73.   Russwurm S, Vickers J, Meier-Hellmann A, et al. Platelet and leukocyte activation correlate with the severity of septic organ dysfunction. *Shock*. 2002;17(4):263–268.

74.   Meziani F, Delabranche X, Asfar P, Toti F. Bench-to-bedside review: circulating microparticles--a new player in sepsis? *Crit Care*. 2010;14(5):236.

75.   Piccin A, Murphy WG, Smith OP. Circulating microparticles: pathophysiology and clinical implications. *Blood Rev*. 2007;21(3):157–171.

76.   Souza ACP, Yuen PST, Star RA. Microparticles: markers and mediators of sepsis-induced microvascular dysfunction, immunosuppression, and AKI. *Kidney Int*. 2015;87(6):1100–1108.

77.   Zafrani L, Gerotziafas G, Byrnes C, et al. Calpastatin controls polymicrobial sepsis by limiting procoagulant microparticle release. *Am J Respir Crit Care Med*. 2012;185(7):744–755.

78.   Pacher P, Beckman JS, Liaudet L. Nitric oxide and peroxynitrite in health and disease. *Physiol Rev*. 2007;87(1):315–424.

79.   Noiri E, Nakao A, Uchida K, et al. Oxidative and nitrosative stress in acute renal ischemia. *Am J Physiol Renal Physiol*. 2001;281(5):F948–57.

80.   Legrand M, Almac E, Mik EG, et al. L-NIL prevents renal microvascular hypoxia and increase of renal oxygen consumption after ischemia-reperfusion in rats. *Am J Physiol Renal Physiol*. 2009;296(5):F1109–17.

81.   Mashiach E, Sela S, Winaver J, Shasha SM, Kristal B. Renal ischemia-reperfusion injury: contribution of nitric oxide and renal blood flow. *Nephron*. 1998;80(4):458–467.

82.   Kone BC. Nitric oxide in renal health and disease. *Am J Kidney Dis*. 1997;30(3):311–333.

83.   Langenberg C, Gobe G, Hood S, May CN, Bellomo R. Renal histopathology during experimental septic acute kidney injury and recovery. *Crit Care Med*. 2014;42(1):e58–67.

84.   Lerolle N, Nochy D, Guérot E, et al. Histopathology of septic shock induced acute kidney injury: apoptosis and leukocytic infiltration. *Intensive Care Med*. 2010;36(3):471–478.

85.   Maiden MJ, Otto S, Brealey JK, et al. Structure and Function of the Kidney in Septic Shock: A Prospective Controlled Experimental Study. *Am J Respir Crit Care Med*. 2016;194(6):rccm.201511–2285OC–700.

86.   Stenzel T, Weidgang C, Wagner K, et al. Association of Kidney Tissue Barrier Disrupture and Renal Dysfunction in Resuscitated Murine Septic Shock. *Shock*. February 2016:1.

87.   Okusa MD, Jaber BL, Doran P, et al. Physiological biomarkers of acute kidney injury: a conceptual approach to improving outcomes. In: Vol 182. Basel: S. KARGER AG; 2013:65–81.

88.   Wu L, Gokden N, Mayeux PR. Evidence for the role of reactive nitrogen species in polymicrobial sepsis-induced renal peritubular capillary dysfunction and tubular injury. *J Am Soc Nephrol*. 2007;18(6):1807–1815.

89.   Wu L, Tiwari MM, Messer KJ, et al. Peritubular capillary dysfunction and renal tubular epithelial cell stress following lipopolysaccharide administration in mice. *Am J Physiol Renal Physiol*. 2007;292(1):F261–8.

90.   Holthoff JH, Wang Z, Seely KA, Gokden N, Mayeux PR. Resveratrol improves renal microcirculation, protects the tubular epithelium, and prolongs survival in a mouse model of sepsis-induced acute kidney injury. *Kidney Int*. 2012;81(4):370–378.

91.   Tiwari MM, Brock RW, Megyesi JK, Kaushal GP, Mayeux PR. Disruption of renal peritubular blood flow in lipopolysaccharide-induced renal failure: role of nitric oxide and caspases. *Am J Physiol Renal Physiol*. 2005;289(6):F1324–32.

92.   Evans RG, Ince C, Joles JA, et al. Haemodynamic influences on kidney oxygenation: clinical implications of integrative physiology. *Clin Exp Pharmacol Physiol*. 2013;40(2):106–122.

93.   Johannes T, Mik EG, Nohé B, Unertl KE, Ince C. Acute decrease in renal microvascular PO2 during acute normovolemic hemodilution. *Am J Physiol Renal Physiol*. 2007;292(2):F796–803.

94.   Johannes T, Mik EG, Nohé B, Raat NJH, Unertl KE, Ince C. Influence of fluid resuscitation on renal microvascular PO2 in a normotensive rat model of endotoxemia. *Crit Care*. 2006;10(3):R88.

95.   Langenberg C, Bellomo R, May C, Wan L, Egi M, Morgera S. Renal blood flow in sepsis. *Crit Care*. 2005;9(4):R363–74.

96.   Casellas D, Mimran A. Shunting in renal microvasculature of the rat: a scanning electron microscopic study of corrosion casts. *Anat Rec*. 1981;201(2):237–248.

97.   Mafeld S, Stenberg B, Elliott S. Intrarenal arteriovenous shunts in kidney transplants demonstrated by contrast-enhanced ultrasound. *Clin Imaging*. 2015;39(1):144–151.

3

98.   Thurau K. Renal Na-reabsorption and O2-uptake in dogs during hypoxia and hydrochlorothiazide infusion. *Proc Soc Exp Biol Med*. 1961;106:714–717.

99.   Deetjen P, Kramer K. [The relation of O2 consumption by the kidney to Na re-resorption]. *Pflugers Arch Gesamte Physiol Menschen Tiere*. 1961;273:636–650.

100.   Welch WJ. Intrarenal oxygen and hypertension. *Clin Exp Pharmacol Physiol*. 2006;33(10):1002–1005.

101.   Wilcox CS, Palm F, Welch WJ. Renal oxygenation and function of the rat kidney: effects of inspired oxygen and preglomerular oxygen shunting. *Adv Exp Med Biol*. 2013;765(Chapter 46):329–334.

102.   Blantz RC, Deng A, Miracle CM, Thomson SC. Regulation of kidney function and metabolism: a question of supply and demand. *Trans Am Clin Climatol Assoc*. 2007;118:23–43.

103.   Legrand M, Bezemer R, Kandil A, Demirci C, Payen D, Ince C. The role of renal hypoperfusion in development of renal microcirculatory dysfunction in endotoxemic rats. *Intensive Care Med*. 2011;37(9):1534–1542.

104.   Johannes T, Ince C, Klingel K, Unertl KE, Mik EG. Iloprost preserves renal oxygenation and restores kidney function in endotoxemia-related acute renal failure in the rat. *Crit Care Med*. 2009;37(4):1423–1432.

105.   Legrand M, Mik EG, Johannes T, Payen D, Ince C. Renal hypoxia and dysoxia after reperfusion of the ischemic kidney. *Mol Med*. 2008;14(7-8):502–516.

106.   Haase VH. Mechanisms of hypoxia responses in renal tissue. *J Am Soc Nephrol*. 2013;24(4):537–541.

107.   Castoldi A, Braga TT, Correa-Costa M, et al. TLR2, TLR4 and the MYD88 signaling pathway are crucial for neutrophil migration in acute kidney injury induced by sepsis. *PLoS ONE*. 2012;7(5):e37584.

108.   Nangaku M, Eckardt K-U. Hypoxia and the HIF system in kidney disease. *J Mol Med*. 2007;85(12):1325–1330.

109.   Rosenberger C, Heyman SN, Rosen S, et al. Up-regulation of HIF in experimental acute renal failure: evidence for a protective transcriptional response to hypoxia. *Kidney Int*. 2005;67(2):531–542.

110.   Jeansson M, Haraldsson B. Glomerular size and charge selectivity in the mouse after exposure to glucosaminoglycan-degrading enzymes. *J Am Soc Nephrol*. 2003;14(7):1756–1765.

111.   Jeansson M, Haraldsson B. Morphological and functional evidence for an important role of the endothelial cell glycocalyx in the glomerular barrier. *Am J Physiol Renal Physiol*. 2006;290(1):F111–6.

112.   Legrand M, Ince C. Intravenous Fluids in AKI: A Mechanistically Guided Approach. *Semin Nephrol*. 2016;36(1):53–61.

113.   Prowle JR, Bellomo R. Sepsis-associated acute kidney injury: macrohemodynamic and microhemodynamic alterations in the renal circulation. *Semin Nephrol*. 2015;35(1):64–74.

114.   Prowle JR, Kirwan CJ, Bellomo R. Fluid management for the prevention and attenuation of acute kidney injury. *Nat Rev Nephrol*. 2014;10(1):37–47.

115.   Lee WL, Slutsky AS. Sepsis and endothelial permeability. *N Engl J Med*. 2010;363(7):689–691.

116.   Wang N, Jiang L, Zhu B, Wen Y, Xi X-M, Beijing Acute Kidney Injury Trial (BAKIT) Workgroup. Fluid balance and mortality in critically ill patients with acute kidney injury: a multicenter prospective epidemiological study. *Crit Care*. 2015;19(1):371.

117.   Herrler T, Tischer A, Meyer A, et al. The intrinsic renal compartment syndrome: new perspectives in kidney transplantation. *Transplantation*. 2010;89(1):40–46.

118.   Legrand M, Dupuis C, Simon C, et al. Association between systemic hemodynamics and septic acute kidney injury in critically ill patients: a retrospective observational study. *Crit Care*. 2013;17(6):R278.

119.   Marshall JC. Why have clinical trials in sepsis failed? *Trends Mol Med*. 2014;20(4):195–203.

120.   Matejovic M, Ince C, Chawla LS, et al. Renal Hemodynamics in AKI: In Search of New Treatment Targets. *J Am Soc Nephrol*. 2016;27(1):49–58.

121.   Annane D, Bellissant E, Bollaert P-E, Briegel J, Keh D, Kupfer Y. Corticosteroids for treating sepsis. Annane D, ed. *Cochrane Database Syst Rev*. 2015;12(12):CD002243.

122.   Heemskerk S, Masereeuw R, Russel FGM, Pickkers P. Selective iNOS inhibition for the treatment of sepsis-induced acute kidney injury. *Nat Rev Nephrol*. 2009;5(11):629–640.

123.   Holthoff JH, Wang Z, Patil NK, Gokden N, Mayeux PR. Rolipram improves renal perfusion and function during sepsis in the mouse. *J Pharmacol Exp Ther*. 2013;347(2):357–364.

124.   Wan X, Xie X, Gendoo Y, Chen X, Ji X, Cao C. Ulinastatin administration is associated with a lower incidence of acute kidney injury after cardiac surgery: a propensity score matched study. *Crit Care*. 2016;20(1):42.

125.   Humphreys BD, Cantaluppi V, Portilla D, et al. Targeting Endogenous Repair Pathways after AKI. *J Am Soc Nephrol*. 2016;27(4):990–998.

126.   Monsel A, Zhu Y-G, Gennai S, Hao Q, Liu J, Lee JW. Cell-based Therapy for Acute Organ Injury: Preclinical Evidence and Ongoing Clinical Trials Using Mesenchymal Stem Cells. *Anesthesiology*. 2014;121(5):1099–1121.

127.   Morigi M, De Coppi P. Cell therapy for kidney injury: different options and mechanisms--mesenchymal and amniotic fluid stem cells. *Nephron Exp Nephrol*. 2014;126(2):59–63.

128.   Tögel FE, Westenfelder C. Mesenchymal stem cells: a new therapeutic tool for AKI. *Nat Rev Nephrol*. 2010;6(3):179–183.

129.   Becherucci F, Mazzinghi B, Ronconi E, et al. The role of endothelial progenitor cells in acute kidney injury. *Blood Purif*. 2009;27(3):261–270.

130.   Liang C-J, Shen W-C, Chang F-B, et al. Endothelial Progenitor Cells Derived From Wharton's Jelly of Human Umbilical Cord Attenuate Ischemic Acute Kidney Injury by Increasing Vascularization and Decreasing Apoptosis, Inflammation, and Fibrosis. *Cell Transplant*. 2015;24(7):1363–1377.

131.   Brodsky SV, Yamamoto T, Tada T, et al. Endothelial dysfunction in ischemic acute renal failure: rescue by transplanted endothelial cells. *Am J Physiol Renal Physiol*. 2002;282(6):F1140–9.

132.   Cribbs SK, Sutcliffe DJ, Taylor WR, et al. Circulating endothelial progenitor cells inversely associate with organ dysfunction in sepsis. *Intensive Care Med*. 2012;38(3):429–436.

133.   Rafat N, Hanusch C, Brinkkoetter PT, et al. Increased circulating endothelial progenitor cells in septic patients: correlation with survival. *Crit Care Med*. 2007;35(7):1677–1684.

3

134.   Patschan SA, Patschan D, Temme J, et al. Endothelial progenitor cells (EPC) in sepsis with acute renal dysfunction (ARD). *Crit Care*. 2011;15(2):R94.

135.   Ince C. The rationale for microcirculatory guided fluid therapy. *Curr Opin Crit Care*. 2014;20(3):301–308.

4

Impact of fluid resuscitation with hypertonic-hydroxyethyl starch versus lactated Ringer on hemorheology and microcirculation in hemorrhagic shock

Philippe Guerci,[1,2] Nguyen Tran,[2] Patrick Menu,[3]

Marie-Reine Losser,[1] Claude Meistelman,[1] Dan Longrois [5,6]

1. Department of Anesthesiology and Intensive Care Medicine, University Hospital of Nancy-Brabois, Vandoeuvre-Les-Nancy, France
2. School of Surgery, Faculty of Medicine, University of Lorraine, Vandoeuvre-Les-Nancy, France
3. Chief of School of Surgery, UHP-INSERM U684, Faculty of Medicine, Vandoeuvre-Les-Nancy, France
4. Group of Bioengineering, UMR CNRS 7561, UHP-Nancy 1, Faculty of Medicine, Vandoeuvre-Les-Nancy, France
5. Department of Anesthesiology and Intensive Care Assistance Publique-Hopitaux de Paris, Hopital Bichat-Claude Bernard, Paris, France
6. University Paris 7 Denis Diderot, INSERM U698, Paris, France

Abstract

The choice of volume expander for fluid resuscitation in hemorrhagic shock is still debated. Changes in plasma viscosity (PV) are barely investigated while PV modulates functional capillary density, microcirculation and organ function. The present study evaluated the impact of 2 strategies of fluid resuscitation in hemorrhagic shock in pigs.

Ten pigs were subjected to hemorrhagic shock and randomly assigned to a low viscosity fluid regimen (Lactated Ringer's, LR) group or a high viscosity regimen (hypertonic-hydroxyethyl starch, HES) for volume resuscitation. Sublingual microcirculatory flow and tissue oxygen tension were assessed together with macro- and microcirculatory, biochemical and rheological variables at baseline, 30 minutes after hemorrhagic shock, immediately after reaching resuscitation endpoints (R-0), and 60 minutes after resuscitation (R-60).

PV decreased similarly in both groups following resuscitation (from 1.36 [1.32-1.38] to 1.21 [1.21-1.23] for LR, and from 1.32 [1.31-1.32] to 1.20 [1.17-1.21] mPa.s for HES). No differences were found between the groups for other rheological variables, microcirculatory flow or tissue oxygen tension at R-0 and R-60.

Despite a 6-fold difference in the volumes required to achieve blood flow endpoints, commercially available volume expanders had similar effects on rheological and microcirculatory variables, irrespective of their viscosity. Our findings are consistent with the absence of clinically relevant differences between crystalloid and colloid resuscitation of hemorrhagic shock.

Keywords*: hemorrhagic shock, volume expander, plasma viscosity, microcirculation, pigs, functional capillary density

Introduction

There is persistent controversy concerning the choice of a volume expander in hemorrhagic shock. Most of the published articles have not demonstrated any beneficial effect on survival associated with either crystalloid or colloid.[1,2] One of the most neglected areas in the literature [3] concerns the impact of fluid administration on blood rheology, which among other factors exerts a certain influence on oxygen delivery to tissue, especially in the microvessels.[4] For instance, changes in plasma viscosity (PV) have barely been investigated.

According to Poiseuille's equation, vascular resistance is related to blood viscosity. Although this relationship is frequently used for calculation, it applies for rigid and straight tubes, Newtonian fluids, steady laminar flow and a fully developed parabolic velocity profile, conditions which are not met *in vivo*.[5,6] This model does not consider the variable geometry of the vascular network [7] (autoregulatory processes), since vasomotor tone alters vessel radius and hence has a direct influence on vascular resistance. Recent studies have shown that if blood viscosity is severely decreased by hemodilution, microvascular function is impaired and tissue survival is jeopardized due to maldistribution of blood flow in the microcirculation, rather than because of decreased systemic oxygen delivery.[8]

In capillaries, hematocrit is lower than in the systemic circulation due to a skimming effect;[5,9] as the capillary diameter decreases, the number of red blood cells is lower, and apparent whole blood viscosity (WBV) decreases. Thus, PV remains the major regulatory factor of wall shear stress and capillary perfusion. Functional capillary density (FCD) determines functional perfusion.[10] It has been demonstrated that FCD is independent of oxygen carrying capacity and tissue pO_2.[11] These findings suggest that a threshold of PV is required to maintain FCD and is crucial for improving survival in hemorrhagic shock.

In a porcine model of hemorrhagic shock, goal-directed fluid resuscitation titrated on SvO_2 and stroke volume was made in one group with Lactated Ringer's (LR) (lowest viscosity) and, in a second group, named HES group, with hypertonic saline hydroxyethyl starch (HHES) plus normal saline hydroxyethyl starch (HES) (highest viscosity). We hypothesized that the most viscous colloid commercially available would significantly increase PV compared with crystalloid, and would result in better microcirculatory parameters within the same blood flow endpoints during resuscitation (restoration of SvO_2 and stroke volume index to baseline values). Therefore, we investigated the influence of two fluid regimens (colloids versus crystalloids, with viscosities and physico-chemical properties at extremes of the spectrum), on the macrohemodynamic

variables and sublingual tissue oxygen tension ($PtiO_2$) and laser Doppler flow (LDF) and hemorheological (WBV, PV) parameters.

Materials and Methods

These experiments were approved by the Bureau for Animal Protection of the French Ministry for Fishing, Agriculture and Food, and were conducted in accordance with the Guiding Principles for Research Involving Animals and ethical guidelines for publication in Clinical Hemorheology and Microcirculation.

Physicochemical properties of volume expanders

We measured the intrinsic viscosity of the 5 most commonly used, commercially available, volume expanders in France, with a Couette-type coaxial viscometer (Low Shear 30, Contraves LS 30, Zurich, Switzerland).[12] Volume expanders and plasma are Newtonian fluids, as their viscosity does not vary with shear rate. Viscosities of the plasma expanders were determined at 20°C (temperature of storage) and at 37°C (body temperature) at a shear rate of $128s^{-1}$.

We chose two clinically-used solutions with physicochemical properties at the extremes of the spectrum: one with the lowest viscosity (0.82 mPa.s at 37°C) and plasma-expanding effect, i.e, Lactated Ringer's solution (B-Braun Medical, Melsungen Germany) and the other with the highest viscosity (2.50 mPa.s at 37°C) and plasma-expanding effect, i.e, HHES (HES 6% 200/0.5+NaCl 7.2% HyperHES, Fresenius Kabi, Graz, Austria) (Table 1). On account of the current limitations on clinical use of HHES (a maximum of 4 ml/kg) due to its hyperosmolarity, we decided to complement fluid resuscitation in the HES group using the 2nd most viscous plasma expander available on the market (1.91 mPa.s at 37°C): HES (HES 6% 130/0.42, Voluven, Fresenius Kabi, Graz, Austria) (Table 1).

Table 1. Physico-chemical properties of clinically-used volume expanders

Plasma Expander	Electrolytes (mmol. L^{-1})	pH	Osmolarity (mOsmol.L^{-1})	MMW (Daltons) / MS	Colloid content (g.L^{-1})	Time estimated of volume effect (H)	Viscosity at 20°C (mPa.s)	Viscosity at 37°C (mPa.s)
Lactated Ringer's	Na$^+$ 130.30 Ca^{2+} 1.40 K$^+$ 4.00 Cl$^-$ 108.00 Lactate 27.70	~6.7	~253	-	-	0.5-1	1.04	0.82
HES (Voluven®)	Na$^+$ 154 Cl$^-$ 154	4.0-5.5	308	130 000 / 0.38-0.45	60	4-6	2.53	1.91
NaCl 7.2%+HES (HyperHES®)	Na$^+$ 1232 Cl$^-$ 1232	3.5-6.0	2464	200 000 / 0.43-0.55	60	8-12	3.47	2.50

MMW, Molecular Mass Weight; MS, Molecular Substitution

Animal model and anesthesia

Ten domestic pigs (Landrace) weighing from 23 to 40 kg were fasted overnight with free access to water until the morning of the experiment. Each pig was premedicated with intramuscular ketamine (10-15 mg/kg) and midazolam (0.1 mg/kg). General anesthesia was induced by intravenous administration of thiopentone (10-15 mg/kg bolus) and maintained by continuous infusion (7-10 mg/kg/h). To provide analgesia, sufentanil was injected as a bolus (0.5 μg/kg) for intubation and during surgical preparation (0.25 μg/kg) before the start of the experiment when an increase in heart rate or arterial pressure was observed. Animals were intubated and mechanically ventilated with zero end-expiratory pressure in supine position. Tidal volume (10-12 ml/kg) and respiratory rate were adjusted to maintain end-tidal carbon dioxide between 35 and 45 mmHg (Horus, Taema, Antony, France) and the fractional inspired oxygen (FiO$_2$) concentration was set at 0.4. Pancuronium bromide (0.2-0.3 mg/kg i.v.) was injected to provide muscular relaxation. Body temperature was maintained constant with warming blankets. The baseline fluid requirements were substituted with glucose 5%, infused at 1 ml/kg/H until the beginning of hemorrhage and prophylactic cefamandole (1.5 g) was administered.

Catheterization and monitoring

A 16-Gauge catheter (Introcan Safety, B-Braun Medical, Melsungen Germany) was placed in the left external jugular vein for volume infusion at a rate between 30 and 50 mL/min. The left

carotid was cannulated for collection of blood samples (arterial blood gas, fibrinogen, plasma protein, lactate), and continuous arterial pressure monitoring. A 7.5 Fr tip-balloon-catheter with continuous thermodilution cardiac output and venous mixed saturation (Swan-Ganz CCOmbo Pulmonary Artery Catheter, Edwards Lifesciences, Irvine, CA, USA) was inserted in the right internal jugular vein into the pulmonary artery, guided by classical waveforms. Cardiac output and SvO_2 were continuously obtained through a cardiac monitor (Vigilance, Edwards Lifesciences, Irvine, CA, USA). The zero-reference point for pressure measurements was the midpoint between the anterior and posterior chest walls.

Heart rate (HR; bpm), systolic (SAP; mm Hg), diastolic (DAP; mm Hg), and mean arterial pressure (MAP; mm Hg), core temperature (°C), and pulse oxygen saturation of hemoglobin (SpO2; %) were monitored continuously from a multiparameter monitor (SpaceLabs 90369, SpaceLabs, Issaquah, WA, USA). Cardiac output (CO; L/min), mixed venous saturation (SvO_2; %), pulmonary artery pressure (PAP; mmHg), pulmonary capillary wedge pressure (PCWP; mmHg) and central venous pressure (CVP; mmHg) were obtained through the pulmonary artery catheter.

Formulas

Body surface area (BSA) was calculated according to Kelley's formula [13] (734 x body weight$^{0.656}$), and applied to the calculations of cardiac index (CI), stroke volume index (SVI), systemic vascular resistance index (SVRI), pulmonary vascular resistance index (PVRI), oxygen delivery index (DO_2I) and oxygen consumption (VO_2). Finally, O_2 extraction index was determined by $EIO_2= (SaO_2-SvO_2)/SaO_2$ (%).

Sublingual microcirculatory assessment

Since it shares a similar embryologic origin with the digestive mucosa, the assessment of sublingual microcirculation provides an easy and reliable overview of the splanchnic mucosa, which is known to be impaired in shock state.[14] Two probes were placed in sublingual mucosa. A laser Doppler flowmetry (LDF) probe (MNP110XP, OxyFlo, Oxford Optronix, Oxford, United Kingdom) measured blood flow velocity in a tissue sample, called Blood Perfusion Unit (BPU, arbitrary units).[15] Tissue oxygen tension ($PtiO_2$) was determined by a fiber optic probe (quenching of fluorescence, LAS-8/O/E, OxyLite, Oxford Optronix, Oxford, United Kingdom).[16] Laser Doppler blood flow and $PtiO_2$ as well as SvO_2 and CO were continuously recorded during

the experiment by a data acquisition system (PowerLab 4/30 + Chart 5.2, ADInstruments, Colorado Springs, CO, USA).

Measurements

To avoid preanalytical errors (hemodilution), 7 mL of arterial blood were withdrawn before other samples were taken.

Arterial blood gas, lactate, hemoglobin, hematocrit, plasma protein and fibrinogen levels

Serial arterial blood samples were used to determine pH, PaO_2 (mmHg), $PaCO_2$ (mmHg), HCO_3^- (mmol/L), base excess (mmol/L; ABL 505, Radiometer, Copenhagen, Denmark), serum lactate (mmol/L; Lactate Pro, ARKRAY, ARKRAY Group, Tokyo, Japan; normal values 0.8-1.2 mmol/L), plasma protein (g/L; AU5400 Chemistry System, Beckman Coulter, Nyon, Switzerland; normal values 52-62 g/L), and fibrinogen (g/L; ACL TOP, Instrumentation Laboratory, Lexington, ILL, USA; normal values 1.4-2.2 g/L). Hemoglobin concentration and hematocrit were assessed by an automated hematology analyzer (ABX Micros 60, Horiba ABX S.A.S, Montpellier, France). Osmolarity (mOsmol/L) was determined using freezing point osmometry (Micro-Osmometer, Löser, Berlin, Germany).

Rheological measurements

Blood samples were collected in EDTA tubes. Whole blood viscosity (WBV; mPa.s) was measured at 37°C and at shear rates from 0.5 to $128s^{-1}$ using the same viscometer described above. Whole blood is considered as a non-Newtonian fluid; therefore its viscosity is dependent on the shear rate. Given that plasma is a Newtonian fluid, its viscosity is independent of shear rate. Therefore plasma viscosity was determined only at $128s^{-1}$.

Measurements of WBV were performed after correction of hematocrit to 35% by the addition or subtraction (centrifugation and resuspension in a smaller volume) of autologous plasma. All hemorheological values were obtained at each time point. As systemic vascular resistance is not relevant to the effect of vascular geometry on flow, another rheological

parameter, vascular hindrance, was used.[17] Vascular hindrance is calculated as the ratio between systemic vascular resistance and WBV (at a shear rate of $128s^{-1}$).

Nitric oxide production

Plasma nitrate (NO_2^-) and nitrite (NO_3^-) measurement was used as a surrogate of nitric oxide (NO) production.[18] Endothelial NO production should be elevated in case of increased endothelial shear stress, e.g., infusion of high viscosity plasma expanders.[19] The NO_x levels (range 6.25 to 200μmol/L) were quantified by colorimetric assays based on the Griess reaction; techniques have already been described elsewhere.[20,21] The intra-assay and inter-assay coefficients of variation (CVs) were 2.5% and 4.6% respectively.

Experimental design

Animals were randomly allocated, by opening a sealed envelope, to a low viscosity fluid resuscitated group (n=5; LR), or a high viscosity fluid group (n=5; HHES+HES called HES group). The animals were allowed to stabilize after induction of anesthesia and insertion of catheters and probes. Before the beginning of hemorrhage, baseline measurements (BL) of systemic and microcirculatory hemodynamics, arterial blood gas, arterial lactate, hemoglobin, hematocrit, plasma protein, fibrinogen and hemorheologic variables were performed.

Blood loss from the carotid artery at a rate of 8-10mL/kg/10 min was induced for 30 minutes. Shock state was reached when 30 ml/kg were withdrawn representing 40% of total blood volume. It resulted in a decrease in MAP of 45-50 mmHg. The pigs were allowed to recover for 30 minutes without additional blood removal or administration of fluid until resuscitation was started. Study design was summarized in Fig. 1. We opted for a goal-directed therapy, primarily to restore SvO_2 and SVI to baseline values. In the HES group, HHES was administered up to the maximal dose allowed (4ml/kg) and then HES was used for fluid resuscitation in order to achieve blood flow endpoints.
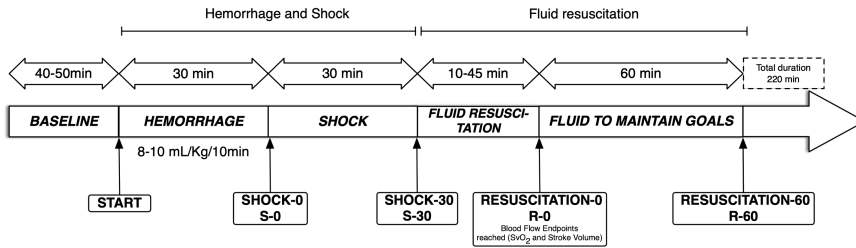
Figure 1. Design of the experimental study

Values were collected at the different time points of the experiment. Animal preparation (general anesthesia, catheterization, insertion of probes and rest) took 40 to 50 minutes. The macro-, microcirculatory variables were collected before the start of hemorrhage (Baseline; BL), at shock (S-0), 30 minutes after shock (S-30), immediately after macrocirculatory endpoints were reached following fluid resuscitation (R-0), and 60 minutes after R-0. Blood samples were withdrawn at each time point.

Fluid administration was continued for 60 minutes (R-60), as required to maintain SvO_2 and SVI close to baseline. Systemic hemodynamic and microcirculatory variables were obtained and recorded at each time point (Fig. 1). Hemorheological parameters, DO_2, VO_2, arterial blood gas, arterial lactate, osmolarity and plasma nitrite/nitrate levels were obtained at each time point except S-0. Plasma protein and fibrinogen were only assessed at baseline, state of shock and at the end of resuscitation. After completion of the experiment, the animals were sacrificed by an intravenous injection of potassium chloride.

Statistical analysis

All computations were performed with the SigmaStat 3.5 statistical software (SigmaStat, Aspire Software International, Ashburn, VA, USA). We hypothesized that therapy with 2 regimens of volume expanders with physico-chemical properties at the extremes of the spectrum would result in a higher than 10 % difference in PV between the two groups at the end of the resuscitation period (R-60). Preliminary data showed that PV in pigs was 1.34 mPa.s with a standard deviation of 0.04. Power analysis was conducted as follows: assuming a difference of 0.1 mPa.s of the nadir value in PV between the 2 treatment groups at R-0, five pigs in each group provided a 90% power to detect a significant difference between 2 groups for alpha=0.05. Data in text, tables, and figures are presented as median [25th–75th percentiles], if not otherwise stated. Non-parametric two-way (time and group) analysis of variance was performed to determine differences caused by time and among groups. Holm-Sidak's post hoc test was used

to determine significant differences ($p <0.05$) for paired comparisons. Correlation between continuous variables was investigated by Pearson correlation coefficient.

Results

All 10 pigs survived until the end of the experiment. The median weight of pigs (31 [28 - 33] kg) was not significantly different between groups. The total blood loss was similar in the two groups (HES group: 26.5 [26.4 – 27.3] mL/kg versus LR: 27.9 [26.6 – 28.4] mL/kg). As expected, at R-60, animals in the LR group received a significantly higher volume expansion ($p<0.001$): 60.0 [59.4 – 61.5] mL/kg versus a total of 9.0 [6.3 – 14.8] ml/kg in HES group. Total dose of sufentanil was not different (38 [32-45] vs 39 [36-40] mcg/kg).

Macrocirculatory hemodynamics

Baseline values were similar in the two groups. Hemorrhage caused significant changes in systemic hemodynamic parameters. Data are summarized in Table 2. During hemorrhagic shock, blood pressure, cardiac output, left and right filling pressures and SvO_2 decreased significantly in both groups as compared with baseline values. Conversely, HR, O_2EI, SVRI, PVRI and VH increased significantly in both groups, with no difference between groups. Oxygen delivery and VO_2 were significantly lower at shock state when compared to baseline.

After resuscitation, the majority of variables returned to baseline values, and endpoints (SvO_2 and SVI) were achieved with no significant differences between groups, as per protocol. Despite ongoing fluid resuscitation, endpoints were only partially met at the end of resuscitation, indicating no fluid responsiveness; SVI was significantly lower in both groups compared with baseline. Only HR, MPAP and CI were significantly higher in the LR group compared with baseline ($p<0.05$).

Table 2. Systemic hemodynamic variables

Parameter	Baseline	Shock-0	Shock-30	Resuscitation-0	Resuscitation-60
Temperature (°C)					
HES	37.4 [37.1 – 40.3]	38 [37.6 – 40.0]	38.1 [38.0 – 40.0]	37.6 [37.6 – 39.0]	37.8 [37.8 - 38.6]
LR	37.7 [37.5 - 38.5]	38.4 [37.8 - 38.6]	38.6 [37.8 - 38.7]	37.2 [36.2 - 38]	37.1 [36.5 – 38.0]
HR (beat.min^{-1})					
HES	112 [111 - 122]	177 [152 - 184] ^{c}	168 [167 - 190] ^{c}	136 [128 - 157]	135 [121 - 142]
LR	94 [91 - 95]	145 [132 - 175] ^{c}	166 [144 - 167] ^{c}	131 [120 - 133] ^{c}	119 [110 - 142] ^{b}
MAP (mmHg)					
HES	103 [85 - 110]	49 [48 - 49] ^{c}	63 [59 - 63] ^{c}	89 [88 - 100]	90 [90 - 92]
LR	89 [78 - 93]	51 [46 - 53] ^{c}	66 [65 - 66] ^{c}	98 [93 - 98]	98 [97 - 98]
MPAP (mmHg)					
HES	18 [14 - 19]	10 [9 - 11] ^{c}	11 [11 - 15] ^{b}	15 [14 - 17] ^{d}	13 [11 - 17] ^{d}
LR	18 [18 - 19]	13 [13 - 13] ^{c}	14 [14 - 14] ^{b}	24 [24 - 24] ^{c}	20 [16 - 24]
PCWP (mmHg)					
HES	2 [2 - 5]	1 [1 - 1] ^{b}	0 [0 - 1] ^{b}	2 [2 - 2]	3 [2 - 3]
LR	6 [5 - 6]	2 [1 - 3] ^{c}	3 [0 - 4] ^{b}	7 [6 - 7]	6 [6 - 6]
CVP (mmHg)					
HES	3 [3 - 4]	2 [2 - 3] ^{b}	3 [3 - 3] ^{a}	4 [4 - 4]	3 [3 - 4]
LR	7 [7 - 8]	3 [2 - 6] ^{c}	4 [3 - 5] ^{c}	9 [8 - 10] ^{a}	7 [7 - 8]
CI (L.min^{-1}.m^{-2})					
HES	6.8 [6.4 - 6.9]	2.5 [2 - 3.7] ^{c}	2.9 [2.8 – 3.0] ^{c}	6.9 [6.8 - 7.3] ^{b}	7.1 [6.1 - 7.6]
LR	5.6 [5.1 - 6.1]	2.4 [2.3 - 2.9] ^{c}	2.7 [2.3 - 3] ^{c}	7.5 [7.4 - 7.7] $^{c.d}$	6.9 [6 - 6.9]
SVI (mL.beat^{-1}.m^{-2})					
HES	56.8 [52.9 - 58.4]	13.5 [11.3 - 20.7] ^{c}	16.7 [15.4 – 20.0] ^{c}	50.9 [48.1 - 56.9]	50.4 [47.6 - 52.5] ^{a}
LR	60.1 [58.8 - 63.2]	16.4 [16.1 - 17.4] ^{c}	16.1 [13.4 - 19.1] ^{c}	56.8 [55.1 - 62.5]	50.4 [50.3 - 54.3] ^{a}
SVRI (dynes.s.cm^{-5}.m^{-2})					
HES	1143 [963 - 1315]	1329 [1267 - 1898] ^{a}	1575 [1336 - 1605] ^{a}	961 [925 - 1002]	1026 [980 - 1144]
LR	1097 [1045 - 1170]	1395 [1328 - 1413] ^{a}	1599 [1550 - 2157] ^{c}	938 [901 - 959]	1058 [1008 - 1249]
PVRI (dynes.s.cm^{-5}.m^{-2})					
HES	138 [137 - 166]	269 [262 - 323] ^{b}	289 [288 - 323] ^{c}	138 [135 - 164]	136 [113 - 142]
LR	196 [161 - 198]	307 [279 - 388] ^{b}	431 [320 - 499] ^{c}	179 [123 - 195]	167 [138 - 197]
VO$_2$ (mL O$_2$/dL m^{-2})					
HES	236 [212 - 302]	N.D	202 [184 - 256] ^{a}	231 [186 - 240] ^{a}	204 [203 - 227] ^{a}
LR	243 [209 - 250]	N.D	191 [184 - 208] ^{a}	224 [208 - 236]	190 [185 - 211]
DO$_2$ (mL O$_2$/dL m^{-2})					
HES	873 [850 - 944]	N.D	352 [337 - 396] ^{c}	683 [630 - 712] ^{b}	634 [565 - 718] ^{c}
LR	687 [639 - 762]	N.D	347 [311 - 348] ^{c}	601 [590 - 759]	559 [537 - 679] ^{a}
SvO$_2$ (%)					
HES	73 [70 - 78]	37 [28 - 50] ^{c}	43 [39 - 46] ^{c}	72 [66 - 77]	70 [70 - 72]
LR	70 [69 - 71]	34 [29 - 44] ^{c}	45 [40 - 47] ^{c}	68 [66 - 70]	68 [62 - 69]
EIO$_2$ (%)					
HES	26 [22 - 30]	63 [50 - 72] ^{c}	57 [54 - 61] ^{c}	28 [23 - 33]	30 [28 - 30]
LR	30 [29 - 31]	66 [56 - 71] ^{c}	55 [53 - 60] ^{c}	32 [30 - 34]	32 [31 - 38]
VH (dynes.cm^{-5}.mPa^{-1})					
HES	500 [459 - 577]	N.D	754 [704 - 755] ^{b}	636 [569 - 681]	712 [551 - 739] ^{a}
LR	512 [417 - 566]	N.D	843 [630 - 928] ^{c}	586 [531 - 691]	601 [589 - 731] ^{a}

Significant difference from baseline value: ^{a} (p<0.05), ^{b} (p<0.01), ^{c} (p<0.001). Significant difference from LR group: ^{d} (p<0.05). HR, Heart Rate; MAP, Mean Arterial Pressure; MPAP, Mean Pulmonary Arterial Pressure; PCWP, Pulmonary Capillary Wedge Pressure; CVP, Central Venous Pressure; C.I, Cardiac Index; SVI, Stroke Volume Index; SVRI/PVRI, Systemic/Pulmonary Vascular Resistance Index; VH, Vascular Hindrance; EIO$_2$, Extraction Index O$_2$; SvO$_2$, Mixed Venous Oxygen Saturation, N.D; Not Documented. Values are Median [IQR]

Overview of microcirculation

Sublingual LDF and PtiO$_2$

Baseline LDF values were 352 [218 - 478] and 350 [192 - 1501] BPU in HES and LR animals respectively. Because of the scattering of BPU values, variations from baseline values were expressed as percentage of change (Fig. 2). Hemorrhage resulted in a significantly impaired microcirculation (decreased PtiO$_2$ and BPU) when compared to baseline. Baseline and shock values were not significantly different between the two groups. Fluid resuscitation restored PtiO$_2$ and tissue blood flow velocity in both groups but BPU was significantly higher at R-0 with LR compared to baseline and HES treated group. This result is correlated with an increased cardiac index at R-0 in LR group. Neither LR, nor HHES+HES could maintain sublingual LDF or PtiO$_2$ above baseline values at R-60, despite the continuation of fluid resuscitation.

In addition, we found a significant correlation (r^2=0.83 for LR and r^2=0.85 for HES) between SVI and PtiO$_2$ (Fig. 3), suggesting the relationship of macro- and microcirculation. The lowest PtiO2 values were observed for the lowest SVI.
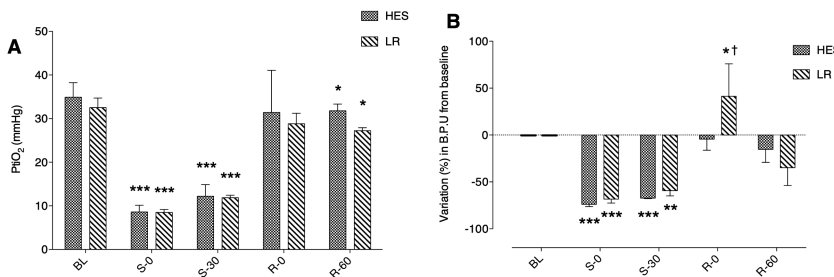
Figure 2. Changes in sublingual PtiO2 (A) and microcirculatory blood flow (B) during hemorrhagic shock and after fluid resuscitation, assessed by quenching of fluorescence probe and laser Doppler flowmetry.

*BL, Baseline; S-0, Shock state; S-30, 30 minutes after shock state; R-0, Achieved endpoints following fluid resuscitation; R-60, 1 hour after R-0. Significant difference from baseline value: * (p<0.05), ** (p<0.01), *** (p<0.001). Significant difference from HES group: † (p<0.05)*

Nitrates/nitrites level

Baseline values for serum NOx were similar (134µmol [114–141] in HES vs 122µmol [90–148] in LR). Hemorrhagic shock did not lead to a significant modification in serum NO_x concentrations over time. Fluid resuscitation did not increase NO_x serum concentrations. The choice of the plasma expander did not impact NO_x concentration.
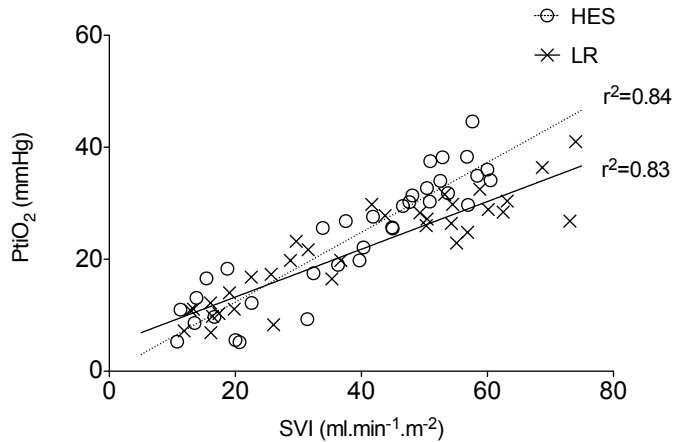

Figure 3. Linear regression between stroke volume index and tissue oxygen tension

SVI, Stroke Volume Index.

Hemorheological characteristics

Whole blood and plasma viscosity

Hemorrhage did not produce a significant decrease in WBV (whatever the shear rate) or PV (Table 3). At corrected hematocrit (35%) and shear rate 128s^{-1}, WBV decreased significantly only in the LR group at R-0 (*p<0.05*). After completion of fluid resuscitation, WBV decreased similarly in both groups. At shear rate 0.5s^{-1}, WBV was significantly lower after resuscitation (R-0 and R-60) with no difference between the groups. Interestingly, although variations in PV were very low compared to WBV, PV decreased significantly in both groups after resuscitation (*p<0.001*), despite viscosities of volume expanders at the extremes of the spectrum (Fig. 4). PV had a stronger correlation with plasma protein concentration (r^2=0.70, *p<0.01*) than with fibrinogen (r^2=0.48; *p<0.01*).

Table 3. Hemorheological variables

Hemorhreological variable	BL	S-30	R-0	R-60
PV (mPa.s)				
HES	1.32 [1.31 - 1.32]	1.30 [1.29 - 1.34]	1.21 [1.19 - 1.21] [c]	1.20 [1.17 - 1.21] [c]
LR	1.36 [1.32 - 1.38]	1.30 [1.28 - 1.31]	1.20 [1.19 - 1.22] [c]	1.21 [1.21 - 1.23] [c]
WBV 128 s^{-1} (original Hct)				
HES	3.26 [3.14 - 3.33]	3.22 [2.92 - 3.40]	2.48 [2.38 - 2.49] [c]	2.28 [2.23 - 2.56] [c]
LR	3.38 [2.88 - 3.50]	3.42 [3.13 - 3.51]	2.37 [2.20 - 2.43] [c]	2.45 [2.42 - 2.62] [c]
WBV 0.5 s^{-1} (original Hct)				
HES	9.35 [6.84 - 11.61]	7.27 [4.77 - 12.29]	4.17 [3.94 - 4.74] [b]	4.29 [4.17 - 4.31] [b]
LR	10.21 [6.86 - 15.36]	9.87 [9.39 - 13.31]	3.78 [3.47 - 3.97] [c]	5.34 [4.77 - 6.70] [b]
WBV 128 s^{-1} (Hct 35%)				
HES	4.07 [4.02 - 4.43]	4.02 [3.99 - 4.03]	3.83 [3.81 - 3.97]	3.81 [3.75 - 3.87] [a]
LR	4.13 [3.97 - 4.15]	4.06 [4.00 - 4.17]	3.53 [3.25 - 3.89] [a]	3.56 [3.42 - 3.60] [a]
WBV 0.5 s^{-1} (Hct 35%)				
HES	22.53 [16.5 - 22.99]	19.8 [16.5 - 20.03]	10.15 [9.74 - 12.18] [c]	11.13 [10.19 - 11.72] [c]
LR	20.36 [18.17 - 20.70]	20.3 [19.12 - 21.05]	10.65 [9.58 - 12.86] [c]	10.26 [9.65 - 11.61] [c]
Hematocrit (%)				
HES	31 [30 - 32]	27 [26.5 - 32]	22 [21 - 22] [c]	22 [21 - 22] [c]
LR	33 [32 - 35]	31 [30 - 33]	24 [23 - 25] [c]	24 [22 - 26] [c]
Plasma protein (g.L^{-1})				
HES	56 [55 - 58]	49 [49 - 50] [c]	N.D	42 [42 - 43] [c]
LR	57 [56 - 59]	50 [49 - 51] [c]	N.D	41 [39 - 42] [c]
Fibrinogen (g.L^{-1})				
HES	1.36 [1.32 - 1.63]	1.28 [1.28 - 1.42]	N.D	1.08 [1.01 - 1.18] [c]
LR	1.54 [1.47 - 1.67]	1.37 [1.20 - 1.42] [a]	N.D	1.08 [1.01 - 1.14] [c]

Significant difference from baseline value: [a] (p<0.05), [b] (p<0.01), [c] (p<0.001). There is no difference between groups. Values are Median [IQR]. N.D. Not Documented
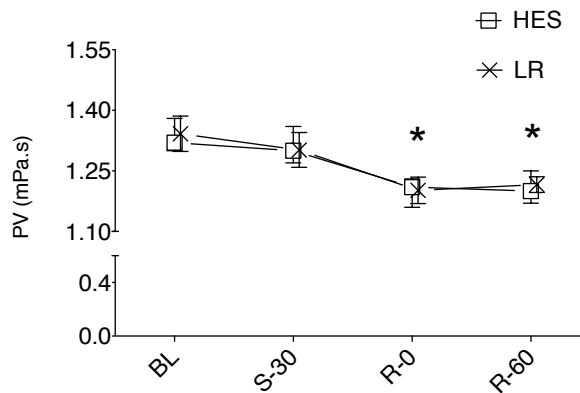

Figure 4. Plasma viscosity measured at each time point of the experiment

*Significant difference from baseline value: * (p<0.001). There were no differences between groups.*

Biochemistry and hematologic variables

A significant increase in plasma lactate concentrations was observed during hemorrhage (*p<0.001*) (Table 4). After initial volume expansion, lactate concentrations were still elevated compared to baseline, in both groups (*p<0.05*). At the end of the experiment, arterial lactate, pH and HCO_3^- returned to baseline values in both groups. Plasma protein concentration was significantly lower at S-30 (*p<0.001*) whereas hematocrit, hemoglobin and fibrinogen concentrations were not affected by hemorrhagic shock (Table 3). Whatever the volume expander used for fluid resuscitation, significant decreases in hematocrit, plasma protein and fibrinogen concentrations occurred compared with baseline (*p<0.001*), with no difference between the groups. Osmolarity was significantly increased in the HES group compared with baseline and LR group (Table 4, *p<0.001*).

Table 4. Arterial blood gas (ABG). lactate and plasma osmolarity values.

ABG variable	BL	S-30	R-0	R-60
pH				
HES	7.49 [7.47 - 7.53]	7.46 [7.42 - 7.46]	7.44 [7.41 - 7.50]	7.50 [7.45 - 7.51]
LR	7.51 [7.49 - 7.53]	7.47 [7.46 - 7.48]	7.50 [7.44 - 7.52]	7.49 [7.44 - 7.54]
$PaCO_2$ (mmHg)				
HES	35 [33 - 39]	39 [39 - 41]	38 [36 - 46]	41 [37 - 41]
LR	36 [35 - 36]	38 [36 - 39]	39 [35 - 40]	36 [33 - 40]
HCO_3^- (mmol.L^{-1})				
HES	29.5 [25.1 - 29.9]	26.8 [24.3 - 27.1] *a*	27.9 [24.8 - 28.1]	28.7 [26.7 - 30.3]
LR	27.9 [26.9 - 28.5]	27.2 [25.3 - 27.3]	27.6 [25.7 - 27.9]	28.2 [27.3 - 28.2]
SaO_2 (%)				
HES	99 [99 - 100]	99 [99 - 100]	99 [98 - 100]	99 [98 - 100]
LR	99 [99 - 100]	99 [99 - 100]	99 [98 - 99]	99 [98 - 99]
Lactate (mmol.L^{-1})				
HES	0.8 [0.8 – 0.8]	3.3 [3.1 - 3.8] *c*	2.0 [1.8 - 2.5] *c*	0.8 [0.8 - 0.9]
LR	0.8 [0.8 - 0.8]	3.1 [3 - 3.4] *c*	1.3 [1.2 - 1.7] *b*	0.8 [0.8 - 0.8]
Osmolarity (mOsmol.L^{-1})				
HES	298 [297 - 299]	308 [305 - 308]	322 [316 - 324] c	318 [316 - 320] c
LR	297 [292 - 300]	307 [302 - 307]	299 [298 - 304] †	303 [301 - 303] †

Significant difference from baseline value: [a] (p<0.05), [b] (p<0.01), [c] (p<0.001). Significant difference from HES group: † (p<0.001). Values are Median [IQR].

Discussion

Considering plasma viscosity as a major determinant of microcirculation,[8] it could become a potential target for resuscitation of hemorrhagic shock. Hence, we investigated the effects of two strategies of fluid resuscitation on hemorheology. In these experiments, we hypothesized

that a goal-directed therapy of hemorrhagic shock titrated on SvO_2 and stroke volume with two regimens of volume expanders could result in significant differences in PV. There were no significant differences in the measured macrocirculatory or microcirculatory variables between the two groups after fluid resuscitation, when blood flow endpoints were reached. As $PtiO_2$ was correlated with SVI, it supports the concept that tissue oxygenation variables could be used as a surrogate of cardiac output.[22]

Hemodilution induced by volume expansion changed hemorheological variables with a decrease in WBV and PV in both groups. Despite the fact that the two strategies of fluid replacement have very different physicochemical properties and a 6-fold difference in cumulative volumes, the modifications induced in hemorheological variables were very similar in both groups.

Volume expansion with LR has been used for decades in the pre-hospital setting and in operating rooms for resuscitation of hemorrhagic shock. Its rheological properties are similar to those of water, especially its viscosity (≈ 0.9 mPa.s). Therefore, when infused in large volumes, LR is expected to decrease WBV and PV because its viscosity is lower than plasma. The volume expanding effect of LR lasts approximately 30 minutes, because it is poorly retained in the vascular compartment and is quickly excreted by the kidney. After LR infusion is interrupted, PV will rise gradually as LR diffuses to the interstitial space.

Changes in PV are more difficult to account for in the use of colloids. Although they have much greater viscosity than crystalloids, two phenomena can lead to a decrease in PV. First, NaCl 7.2%, being a hypertonic fluid that causes a rapid shift of free water from the interstitial to the intravascular compartment, contributes to the decrease in WBV and PV through hemodilution. It is an important but short-term effect as it promptly restores macrohemodynamic variables. The additional use of HES in our experiment was intended to sustain the volume expanding effect initiated by hypertonic saline. However, even high viscosity HES used in this experiment can barely compensate for the steep decrease in PV. Secondly, the chemical and physical characteristics of HES preparations are defined by mean molecular weight, the molar substitution (MS) and the C2/C6 ratio. This confers different properties to HES and makes their basal viscosity vary. We report viscosities of 1.91 and 2.50 mPa.s at 37°C respectively for HES 130/0.4 and HES 200/0.5, which is consistent with earlier investigations.[23,24] However, the expected increase in PV after HES resuscitation did not occur. The *in vivo* behavior of HES is different from what could be expected by its *in vitro* properties. *In vivo* mean molecular weight of HES may vary over time because HES molecules are hydrolyzed by plasma amylase.

The speed of enzymatic breakdown is inversely related to the degree of MS and the C2/C6 ratio.[25] Cleavage products are then cleared from the intravascular space, by continuous renal excretion, thus decreasing the concentration of HES in plasma.[26] It would result in a global decrease of PV. Nevertheless, within the time frame of our experiments, it is unlikely that significant hydrolysis occurred. Our results are in agreement with other studies performed in humans showing a decrease or no change in PV after large infusion of HES 130/0.4, up to 70 ml/kg.[24,27] Several studies using HES 200/0.5 have shown a slight increase in PV.[23,27,28] These studies were however performed under conditions of normovolemic hemodilution and their results cannot be extrapolated to hemorrhagic shock. Under isovolemic conditions, microcirculation seems not to be jeopardized above a hematocrit of 10%.[29] In our study, the combination of HHES and HES was unable to increase PV. Despite its high viscosity, HES could not counteract the decrease in PV induced by hypertonic saline.

It can be concluded from these experiments that the cumulative volumes of colloids (approximately 15 % of the estimated blood volume) and their relatively low viscosity (2-3 mPa.s) are insufficient to increase PV. In two previously published articles in animals, volume expansion with a 6% dextran 500 (a high viscosity solution; 5.92±0.7 mPa.s) at 4 % of the estimated blood volume resulted in the doubling of PV.[30,31] Studies performed by Audibert *et al.* [28] and Freyburger *et al.* [23] in humans confirmed that neither albumin, nor gelatin, nor dextran 40 or 60 were able to significantly increase PV *in vivo* during preoperative normovolemic hemodilution.

In a canine model of hemorrhagic shock, hyperviscous fluid resuscitation was unable to improve microcirculatory parameters,[32] but it induced a systemic vasodilatation. Krieter and Chen have already shown that colloid resuscitation with viscosities and volumes higher than those used in our experiments and in clinical practice resulted in significantly increased PV.[30,31] The consequence of the increased PV was vasodilatation occurring in vital organs (heart, brain, liver). Our data demonstrated that with modern colloids and current limitations on cumulative volumes, it is impossible to achieve a clinically relevant increase in PV. In the absence of PV increase in our model, shear stress-mediated release of NO was not observed, as plasma NO_x remained unchanged over the experiment.

Limits of the study

In this experiment, we worked on a small number of animals in each group. The hypothesis that was used to make the power calculations was a 0.1 mPa.s decrease in PV. We did observe

such a decrease (Table 3) which was related to the resuscitation process rather than to the type of volume expander. In our model, the blood loss was substantial (40% of total blood volume) but the consequences in these young and healthy animals were moderate (MAP 50mmHg, hyperlactatemia 3mmol/l). Supine position was used in these experiments but may alter the venous blood return. We used a pig model, because of its rheological similarities with the human species.[33] Unlike others studies, fluid therapy was titrated on mixed SvO_2 and stroke volume in our model, rather than an empirical target of volume replacement or a blood pressure level to achieve.

Systemic hemodynamics, especially cardiac output were monitored through a continuous thermodilution catheter, which is unable to quantify beat-to-beat CO. Basically, it requires at least 60 seconds (up to 180 seconds) for analyzing and determining CO. This latency could explain the "overshoot" (increase in cardiac index) observed in the LR group at R-0.

Microcirculation was assessed by indirect indicators such as $PtiO_2$ and tissue blood flow, whereas other investigators used intravital videomicroscopy (IVM). Indeed, IVM provides a visual analysis of microcirculatory flow that is usually discontinuous. Nevertheless, measurement sites were the same over the whole experiment allowing valid comparisons over time.

We monitored the hemorheological effects for 60 minutes because we assumed the impact of fluid therapy on hemorheology would be major in the first hour of resuscitation. We overlooked late effects of fluid resuscitation. After massive bleeding and fluid resuscitation, inflammatory effects occur. This inflammatory response is unpredictable and could interfere with hemorheology. It has been shown that infusion of large volumes of LR may have pro-inflammatory effects [34-36] whereas hypertonic saline did not.[37] This would be due mainly to the use of D-lactate. This model focused on circulatory variables and did not examine the inflammatory response or lung injury and tissue edema.

Conclusion

It can be concluded that within the limits of the study design, the commercially available plasma expanders have similar effects on rheological and microcirculatory variables despite a 6-fold difference in the volumes required to restore blood flow endpoints. Our findings are consistent with the absence of clinically relevant differences between crystalloid and colloid resuscitation of hemorrhagic shock.[1,2] At this time, in clinical practice, plasma viscosity cannot

be increased during resuscitation solely with colloids. Given that plasma viscosity is known to modulate capillary perfusion and finally organ oxygen delivery and function, it appears necessary to restore hemorheological homeostasis. The design of volume expanders, especially their rheological properties, should be reconsidered independently of oxygen-carrying capacity.

Conflict of interest statement

Ethical adherence

These experiments were approved by the Animal Protection Bureau of the French Ministry for Fishing, Agriculture and Food, and were conducted in accordance with the Guiding Principles for Research Involving Animals.

Acknowledgements

References

1.   Bunn F, Trivedi D. Colloid solutions for fluid resuscitation. *Cochrane Database Syst Rev.* 2012;7:CD001319.

2.   Perel P, Roberts I, Ker K. Colloids versus crystalloids for fluid resuscitation in critically ill patients. *Cochrane Database Syst Rev.* 2013;2:CD000567.

3.   Niemi T, Miyashita R, Yamakage M. Colloid solutions: a clinical update. *J Anesth.* 2010;24(6):913-925.

4.   Intaglietta M, Cabrales P, Tsai AG. Microvascular perspective of oxygen-carrying and -noncarrying blood substitutes. *Annu Rev Biomed Eng.* 2006;8:289-321.

5.   Baskurt OK, Meiselman HJ. Blood rheology and hemodynamics. *Semin Thromb Hemost.* 2003;29(5):435-450.

6.   Thurston GB. Rheological parameters for the viscosity viscoelasticity and thixotropy of blood. *Biorheology.* 1979;16(3):149-162.

7.   Ando J, Yamamoto K. Vascular mechanobiology: endothelial cell responses to fluid shear stress. *Circ J.* 2009;73(11):1983-1992.

8.   Tsai AG, Friesenecker B, McCarthy M, Sakai H, Intaglietta M. Plasma viscosity regulates capillary perfusion during extreme hemodilution in hamster skinfold model. *Am J Physiol.* 1998;275(6 Pt 2):2170-2180.

9.   Barbee J, Cokelet G. The Fahraeus effect. *Microvasc Res.* 1971;3(1):6-16.

10.   Tsai AG, Friesenecker B, Intaglietta M. Capillary flow impairment and functional capillary density. *Int J Microcirc Clin Exp.* 1995;15(5):238-243.

11.   Cabrales P, Tsai AG, Intaglietta M. Is resuscitation from hemorrhagic shock limited by blood oxygen-carrying capacity or blood viscosity? *Shock.* 2007;27(4):380-389.

12.   Heuser G, Opitz R. A Couette viscometer for short time shearing of blood. *Biorheology.* 1980;17(1-2):17-24.

13.   Kelley KW, Curtis SE, Marzan GT, Karara HM, Anderson CR. Body surface area of female swine. *J Anim Sci.* 1973;36(5):927-930.

14.   Nakagawa Y, Weil M, Tang W, et al. Sublingual capnometry for diagnosis and quantitation of circulatory shock. *Am J Respir Crit Care Med.* 1998;157(6 Pt 1):1838-1843.

15.   Dryden C, Gray W, Asbury A. Oxford Optronix MPM 3S: a clinical assessment of a microvascular perfusion monitor. *J Med Eng Technol.* 1992;16(4):159-162.

16.   Griffiths J, Robinson S. The OxyLite: a fibre-optic oxygen sensor. *Br J Radiol.* 1999;72(859):627-630.

17.   Baskurt OK, Yalcin O, Meiselman HJ. Hemorheology and vascular control mechanisms. *Clin Hemorheol Microcirc.* 2004;30(3-4):169-178.

18.   Grau M, Hendgen-Cotta U, Brouzos P, et al. Recent methodological advances in the analysis of nitrite in the human circulation: nitrite as a biochemical parameter of the L-arginine/NO pathway. *J Chromatogr B Analyt Technol Biomed Life Sci.* 2007;851(1-2):106-123.

19.   Salazar Vazquez B, Martini J, Chavez Negrete A, et al. Cardiovascular benefits in moderate increases of blood and plasma viscosity surpass those associated with lowering viscosity: Experimental and clinical evidence. *Clin Hemorheol Microcirc.* 2010;44(2):75-85.

20.   Giustarini D, Rossi R, Milzani A, Dalle-Donne I. Nitrite and nitrate measurement by Griess reagent in human plasma: evaluation of interferences and standardization. *Meth Enzymol.* 2008;440:361-380.

21.   Tsikas D. Analysis of nitrite and nitrate in biological fluids by assays based on the Griess reaction: appraisal of the Griess reaction in the L-arginine/nitric oxide area of research. *J Chromatogr B Analyt Technol Biomed Life Sci.* 2007;851(1-2):51-70.

22.   Bartels S, Bezemer R, de Vries F, et al. Multi-site and multi-depth near-infrared spectroscopy in a model of simulated (central) hypovolemia: lower body negative pressure. *Intensive Care Med.* 2011;37(4):671-677.

23.   Freyburger G, Dubreuil M, Boisseau MR, Janvier G. Rheological properties of commonly used plasma substitutes during preoperative normovolaemic acute haemodilution. *Br J Anaesth.* 1996;76(4):519-525.

24.   Neff T, Fischler L, Mark M, Stocker R, Reinhart W. The influence of two different hydroxyethyl starch solutions (6% HES 130/0.4 and 200/0.5) on blood viscosity. *Anesth Analg.* 2005;100(6):1773-1780.

25.   Treib J, Haass A, Pindur G, et al. HES 200/0.5 is not HES 200/0.5. Influence of the C2/C6 hydroxyethylation ratio of hydroxyethyl starch (HES) on hemorheology, coagulation and elimination kinetics. *Thromb Haemost.* 1995;74(6):1452-1456.

26.   Jung F, Koscielny J, Mrowietz C, et al. Elimination kinetics of different hydroxyethyl starches and effects on blood fluidity. *Clinical hemorheology.* 1994;14:189-202.

27.   Standl T, Burmeister M, Schroeder F, et al. Hydroxyethyl starch (HES) 130/0.4 provides larger and faster increases in tissue oxygen tension in comparison with prehemodilution values than HES 70/0.5 or HES 200/0.5 in volunteers undergoing acute normovolemic hemodilution. *Anesth Analg.* 2003;96(4):936-943.

28.   Audibert G, Donner M, Lefèvre JC, Stoltz JF, Laxenaire MC. Rheologic effects of plasma substitutes used for preoperative hemodilution. *Anesth Analg.* 1994;78(4):740-745.

29.   Hiebl B, Mrowietz C, Ploetze K, Matschke K, Jung F. Critical hematocrit and oxygen partial pressure in the beating heart of pigs. *Microvasc Res.* 2010;80(3):389-393.

30.   Chen RY, Carlin RD, Simchon S, Jan KM, Chien S. Effects of dextran-induced hyperviscosity on regional blood flow and hemodynamics in dogs. *Am J Physiol.* 1989;256(3 Pt 2):898-905.

31.   Krieter H, Brückner UB, Kefalianakis F, Messmer K. Does colloid-induced plasma hyperviscosity in haemodilution jeopardize perfusion and oxygenation of vital organs? *Acta Anaesthesiol Scand.* 1995;39(2):236-244.

32.   Cooper ES, Bateman SW, Muir WW. Evaluation of hyperviscous fluid resuscitation in a canine model of hemorrhagic shock: a randomized, controlled study. *J Trauma.* 2009;66(5):1365-1373.

33.   Windberger U, Bartholovitsch A, Plasenzotti R, Korak KJ, Heinze G. Whole blood viscosity, plasma viscosity and erythrocyte aggregation in nine mammalian species: reference values and comparison of data. *Exp Physiol.* 2003;88(3):431-440.

34.   Ayuste E, Chen H, Koustova E, et al. Hepatic and pulmonary apoptosis after hemorrhagic shock in swine can be reduced through modifications of conventional Ringer's solution. *J Trauma.* 2006;60(1):52-63.

35.   Jaskille A, Alam H, Rhee P, Hanes W, Kirkpatrick J, Koustova E. D-lactate increases pulmonary apoptosis by restricting phosphorylation of bad and eNOS in a rat model of hemorrhagic shock. *J Trauma.* 2004;57(2):262-269.

36.   Koustova E, Stanton K, Gushchin V, Alam H, Stegalkina S, Rhee P. Effects of lactated Ringer's solutions on human leukocytes. *J Trauma.* 2002;52(5):872-878.

37.   Gushchin V, Alam H, Rhee P, Kirkpatrick J, Koustova E. cDNA profiling in leukocytes exposed to hypertonic resuscitation fluids. *J Am Coll Surg.* 2003;197(3):426-432.

4

5

Glycocalyx degradation is independent of vascular barrier permeability increase in non-traumatic hemorrhagic shock in rats

Philippe Guerci,[1,2,3] Bulent Ergin,[1,4] Zuhre Uz,[1] Yasin Ince,[1] Martin Westphal,[5] Michal Heger,[6] Can Ince,[1,4]

1. Department of Translational Physiology, Academic Medical Center, University of Amsterdam, Amsterdam, The Netherlands
2. INSERM U1116, University of Lorraine, Vandoeuvre-Les-Nancy, France
3. Department of Anesthesiology and Critical Care Medicine, University Hospital of Nancy, France
4. Department of Intensive Care Medicine, Erasmus MC, University Medical Center, Rotterdam, Rotterdam, The Netherlands
5. Fresenius Kabi Deutschland GmbH, Bad Homburg, Germany
6. Department of Experimental Surgery, Academic Medical Center, University of Amsterdam, Amsterdam, The Netherlands

Abstract

Background: Glycocalyx shedding following traumatic hemorrhagic or septic shock as well as different resuscitation fluids has been causally linked to increased vascular barrier permeability (VBP) resulting in tissue edema. In non-traumatic hemorrhagic shock (NTHS), it remains questionable whether glycocalyx degradation in itself results in an alteration of VBP. The composition of fluids can also have modulatory effect on glycocalyx shedding and VBP. We hypothesized that the shedding of the glycocalyx during NTHS has little effect on VBP and that the composition of fluids can modulate these effects.

Methods: Fully instrumented Wistar-albino rats were subjected to a pressure-controlled NTHS (mean arterial pressure of 30 mmHg) for 60 min. Animals were fluid resuscitated with either Ringer's acetate, balanced hydroxyethyl starch (HES) solution or 0.9% NaCl to a MAP of 80 mmHg and compared with shams or non-resuscitated NTHS. Glycocalyx shed products were determined at baseline and 60 min after fluid resuscitation. Skeletal muscle microcirculation was visualized using hand-held vital microscopy. VBP changes were assessed using: plasma decay of 3 fluorescent dyes (40 and 500-kDa Dextran and 70-kDa Albumin), Evans blue dye exclusion, intravital fluorescence microscopy, and determination of tissue edema (wet/dry weight ratio).

Results: All glycocalyx shedding products were upgraded as a result of NTHS. Syndecan-1 significantly increased in NTHS (mean diff. -1668, 95%CI [-2336 to -1001], *P<0.0001*), balanced crystalloid (mean diff. -964.2, 95% CI[-1492 to -436.4], *P=0.0001*) and HES (mean diff. -1030, 95% CI[-1594 to -465.8], *P=0.0001*) groups at the end of the experiment compared to baseline. Hyaluronan levels were higher at the end of the experiment in non-resuscitated NTHS (-923.1, 95%CI [-1216 to -630], *P=0.0001*) and balanced crystalloid (-1039, 95% CI[-1332 to -745.5], *P=0.0001*) or HES (-394.2, 95% CI[-670.1 to -118.3], *P=0.0027*) groups compared to controls. Glycocalyx shedding resulted in microcirculation alterations as observed by HVM. Total vessel density was altered in the normal saline (mean diff. 4.092, 95%CI [0.6195-7.564], *P=0.016*) and hemorrhagic shock (mean diff. 5.022, 95%CI [1.55-8.495], *P=0.0024*) groups compared to the control group, as well as the perfused vessel density and mean flow index. Despite degradation of endothelial glycocalyx, VBP as determined by four independent assays remained intact and continued to be so following fluid resuscitation.

Conclusions: NTHS induced glycocalyx shedding and microcirculation alterations, without altering VBP. Fluid resuscitation partially restored the microcirculation without altering VBP. These results challenge the concept that the glycocalyx barrier is a significant contributor to VBP.

Keywords: glycocalyx, hemorrhagic shock, vascular barrier permeability, microcirculation, fluid resuscitation

Key points Summary

- **Question:** Is glycocalyx degradation occurring during non-traumatic hemorrhage followed by fluid resuscitation of different composition associated with a degradation of the vascular barrier?
- **Finding:** Glycocalyx degradation occurs during non-traumatic hemorrhagic shock but without affecting vascular barrier permeability and is not prevented by fluids of different composition.
- **Meaning:** Increase in vascular barrier permeability seen in states of perioperative and critical illness requires compromise of other barrier constituents such as cell to cell junctions than solely glycocalyx shedding.

Introduction

The vascular barrier is mainly composed of the glycocalyx, endothelial cells, and cell-to-cell junctions.[1-3] The main functions of the glycocalyx are to protect the endothelium, facilitate numerous physiological processes, and regulate cellular and macromolecular traffic.[4] Degradation of the glycocalyx has been associated as a key step in the pathogenesis of a large number of cardiovascular diseases such as shock,[5,6] sepsis,[7,8] diabetes,[9] atherosclerosis,[10] heart failure and volume overload.[11]

One of the main implicit assumption in the literature, has been that the glycocalyx barrier is the key vascular component defining vascular barrier permeability (VBP),[3] and that its disruption is the primary cause of vascular leakage causing tissue edema. However, the causal relationship between glycocalyx degradation and vascular barrier breakdown has not been clearly demonstrated. Studies that have demonstrated glycocalyx shedding in various experimental and clinical settings have not demonstrated that glycocalyx shedding in itself produces an increase in vascular barrier permeability (VBP).[12-15] Other experimental studies carried out on glycocalyx degradation have used interventions, such as enzymatic degradation,[16-19] not often seen in clinical conditions, which besides the glycocalyx, could also disrupt other components associated with VBP such as endothelial cell integrity and endothelial cell-to-cell junctions leading to capillary leakage.

This uncertainty has led us to formulate the hypothesis that in non-traumatic hemorrhagic shock (NTHS) such as can occur during the perioperative phase, glycocalyx degradation can indeed occur but without the negative consequences of VBP alterations and that this degradation might not be the primary component responsible for VBP alterations associated with edema. In extension to this hypothesis, we assumed that fluid resuscitation may influence components of the glycocalyx but may not result in deleterious effects on VBP indicating fluid therapy is a safe and effective therapy during NTHS.

In the present study we proposed to induce NTHS and investigate these issues. To demonstrate that the intervention of glycocalyx shedding has been achieved, we intended to measure the presence of shedding products of the glycocalyx in plasma and to use direct imaging of the microcirculation using hand-held vital microscope to analyze microcirculatory disturbances known to be associated with the endothelial glycocalyx degradation.[9,20]

In doing so we proposed to investigate whether the NTHS-induced glycocalyx shedding in the rat model resulted in an alteration in VBP. To this end, we used 4 independent assays for

the measurement of VBP. (i) analysis of plasma decay of fluorescence dyes of different molecular sizes, ii) extravasation of Evan's blue dye in organs, iii) observation of fluorescent dye extravasation in microvessels by intravital fluorescence microscopy and (iv) edema formation in organs measured by water content (wet/dry weight ratio). The reason we chose these four independent methodologies to measure VBP was to provide solid base of evidence as to the presence or absence of vascular leakage in our model. Using this approach, we propose to provide comprehensive evidence as to the effects of glycocalyx degradation on VBP and its possible modulation by use of fluid resuscitation of different composition.

Methods

Animals

This study was approved by the Animal Research Committee of the Academic Medical Center of the University of Amsterdam (DFL 190AA). Care and handling of the animals were in accordance with the guidelines from the Institutional Animal Care and Use Committees. This manuscript adheres to the applicable ARRIVES guidelines. Experiments were performed on male Wistar albino rats (Charles River Laboratories, The Netherlands), aged 10±2 weeks, with a mean±SD body weight (B.W.) of 334±24 g.

Surgical preparation

The rats (n=59) were anesthetized with an intraperitoneal injection of 100 mg.kg^{-1} ketamine (Nimatek®; Eurovet, The Netherlands), 0.5 mg.kg^{-1} medetomidine (Domitor; Pfizer, USA) and 0.05 mg.kg^{-1} atropine-sulfate (Centrafarm, The Netherlands). Anesthesia was maintained with 50 mg.kg.h^{-1} ketamine. Fluid maintenance consisted in Ringer's acetate (Baxter, Utrecht, The Netherlands) at a rate of 10 ml kg^{-1} hour^{-1}. After a tracheostomy, the animals were connected to a ventilator (Babylog 8000, Dräger, Nederland) and ventilated with tidal volumes of 6 ml.kg^{-1} with a positive end-expiratory pressure of 3 cmH$_2$O and an FiO$_2$ of 0.4. A heating pad under the animal allowed the body temperature to be controlled and maintained at 37±0.5°C. The end-tidal PCO$_2$ was maintained between 30 and 35 mmHg (CapnoMac, Datex-Ohmeda, USA).

The right carotid (pressure) and left femoral (for blood shedding and samples) arteries and jugular (anesthesia and fluid maintenance) and femoral (fluid resuscitation) veins were

cannulated with polyethylene catheters (outer diameter = 0.9 mm; Braun, Germany). The right biceps femoris was exposed, and the femoral artery blood flow (FABF) was monitored with a transonic flowmeter probe (0.5 mm, T206; Transonic Systems Inc). To prevent muscle desiccation, the exposed area was protected with a humidified gauze with warm 0.9% NaCl. The bladder was catheterized via a mini-midline incision with a polyethylene tube (outer diameter = 1.2 mm) and a homemade tip to prevents spontaneous displacement and traumatic lesions. The urine output was quantified.

Experimental protocol (*Supplemental figure 1*)

Animals were randomized according to a unique code generated by an internet website (https://www.sealedenvelope.com). On the day of experiment, a technician prepared the resuscitation fluid according to the generated code.
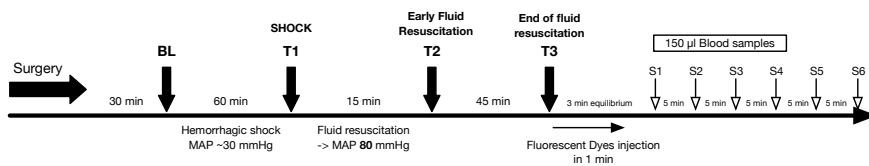
Supplemental Figure 1. Time course of the experiment

BL: baseline, T1: 1 hour after initiation of hemorrhagic shock, T2: 30 min after starting fluid resuscitation, T3: end of fluid resuscitation, time point before fluorescent dye injection

After a 30-min stabilization period, baseline (BL) values were recorded, and arterial blood gas was assessed (ABLFlex 80, Radiometer, Denmark). Hemorrhagic shock was induced by withdrawing blood at a rate of 0.5 ml min^{-1} using a syringe pump (Harvard Apparatus, USA) until a MAP of 30 mmHg, maintained for 1 hour (T1) by re-infusing or withdrawing blood. After this period, animals were left unresuscitated (hemorrhagic shock group) or resuscitated with either balanced crystalloid (Ringer's acetate), normal saline (0.9% NaCl) or balanced HydroxyEthyl Starch (Volulyte® HES 130/0.4, all solutions from Fresenius Kabi, Germany) was started (T2 at 15 min) to maintain the MAP at 80 mmHg for 1 hour (T3). Control-instrumented animals (sham) underwent surgical preparation of the limb but were neither hemorrhaged nor resuscitated. A non-resuscitated group was We deliberately chose a target of 80 mmHg because baseline MAP was higher in healthy rats than in healthy humans.

Biomarkers of glycocalyx shedding

Syndecan-1, heparan sulfate and hyaluronan were used as indirect makers of glycocalyx degradation. Plasma samples were stored at -20°C and were thawed and analyzed using commercial enzyme-linked immunoabsorbent assay (ELISA) kits according to the manufacturer's instructions: DuoSet® Hyaluronan (DY3614, R&D Systems, Minneapolis, USA), Syndecan-1/CD138(SCD1) ELISA kit (Cusabio Biotech Co., Ltd., Wuhan, China) and heparan sulfate proteoglycan 2 (HSPG2) ELISA Kit (Cusabio Biotech Co., Ltd., Wuhan, China).

Skeletal muscle microcirculatory measurements

Glycocalyx degradation results in alterations in microcirculatory perfusion which can be observed using hand-held videomicroscopy (HVM).[9] Incident dark-field (IDF) based HVM CytoCam™ (Braedius Scientific, Huizen, The Netherlands) was placed on the surface of the exposed biceps femoris.[21] Briefly, the IDF-imaging technique uses green polarized light that is produced from a ring of circumferential LEDs that is transmitted to the tissue and absorbed by hemoglobin, thus appearing dark on images. The imaging results in sharp contour visualization of the microcirculation, showing flowing erythrocytes and leukocytes. Continuous monitoring of the same microcirculatory spot was performed with the help of a micromanipulator. One hundred frames clips (100 sec) were recorded at every time point. All clips obtained were randomly anonymized and analyzed in a blinded fashion (group and time point). The analysis of the microvasculature was performed at baseline and T3 with AVA 3.2 (Microvision Medical, Amsterdam, The Netherlands) for total vessel density (TVD), perfused vessel density (PVD) and the mean flow index (MFI) by 2 trained and independent operators (Z. U. and Y. I.) as described elsewhere.[22]

Assessment of vascular barrier permeability

Fluorescent tracers

The time dependent plasma concentration of different size fluorescent tracer molecules in plasma can be used to measure the permeability of vascular barrier since smaller molecules will decay faster than larger tracer molecules.[9] Degradation of the vascular barrier will lead to enlargement of the protein sieving, that translates in a faster plasma decay (transendothelial

escape) of larger molecules. At the end of the experiment, fluid resuscitation and maintenance were stopped. Three fluorescent dyes conjugated with different sizes of molecules and dissolved in saline were thoroughly mixed together and injected intravenously by hand over 1 minute: Texas Red-40 kDa dextran (10 mg/ml, D1829, Molecular Probes, ThermoFischer Scientific, Breda, the Netherlands), Albumin-Alexa 680 (5 mg/ml, A34787, Molecular Probes, ThermoFischer Scientific, Breda, the Netherlands), and fluorescein isothiocyanate (FITC)-500 kDa dextran (10 mg/ml, MFCD00131092, Sigma-Aldrich, Zwijndrecht, the Netherlands) (100 μl each). Blood samples (200 μl) were withdrawn at 2, 5, 10, 15, 20, 25 and 30 minutes to obtain the decay in plasma concentration of the dyes as we had researched previously.[9] Plasma concentrations were measured for each dye in a 96-well plate fluorometer (ClarioStar, BMG LabTech, Ortenberg, Germany) in accordance with the excitation/emission wavelengths of each dye and after obtaining a standard calibration curve: 580±20 nm/625±20 nm for FITC, 480±15 nm/530±25 nm for TexasRed and 675±10 nm/740±40 nm for Alexa 680. The concentration-time curves of all dyes were fitted for each experiment separately with a monoexponential function. A retention ratio (RR) of the dye was calculated as follows: RR = final concentration at 30 min / initial concentration at 2 min.

For total intravascular blood volume (TBV) determination, the concentration of Albumin-Alexa 680 was determined at time = 2 min after bolus injection according to the following calculation: TBV (ml) = ([Albumin-Alexa syringe] x 0.1) / [Albumin Alexa plasma].

Evans blue dye technique

Evans blue is a fluorescent dye that readily binds to albumin once introduced intravascularly. The strong binding property of Evans Blue dye to serum albumin makes its escape from the vasculature to the tissue cells a well-established method for assessment of VBP.[23] A separate series of experiment (n=12) was performed to determine albumin-bound Evans blue dye (EBD) extravasation in the lung, heart, liver and kidney in control, crystalloid and colloid resuscitated groups. At the end of experiment, 1 ml/kg B.W. EBD 4% (Fluka, Sigma Aldrich, Zwijndrecht, the Netherlands) was injected intravenously. Thirty minutes after injection, the inferior vena cava was incised for exsanguination and evacuation of the dye, and the animal's body was flushed thoroughly with 0.9% NaCl containing heparin (100U/ml) via the femoral artery and jugular vein, until the fluid leaving was clear. At least 100 ml was required. Each harvested organ was cut in small pieces, rinsed, weighed and placed in 1:1 weight (mg):volume (μl) ratios

of 0.9% NaCl. Samples were homogenized for 5 min using a handheld homogenizer (Polytron 1200 E, Kinematica, Luzern, Switzerland). Trichloroacetic acid (TCA) 50% (Sigma Aldrich, Zwijndrecht, the Netherlands) was added in a 3:1 ratio (volume (µl):weight (mg)). The TCA/homogenates were centrifuged at 10,000 x g for 20 min to remove precipitates and tissue debris, and the supernatants were added to a 96-well plate (30 µl per well, each plate supplemented with 90 µl of 95% ethanol and thoroughly mixed by pipetting) for fluorescence spectroscopy (620 nm/680 nm).[24] EBD was extracted from the tissue, expressed as µg per g of tissue and determined against a calibration curve fitted with a five-parameter logistic equation (5PL).

Intravital fluorescence microscopy

A direct method for the measurement of vascular barrier permeability is by intravital fluorescent microscopy based on the quantitative visualization of large fluorescent tracers (>70kDa) escaping from the microvasculature through the endothelial barrier into the interstitium.[25] After injection of this fluorescent dye the time dependent fluorescence intensity change in the vessel and in the surrounding tissue can be used to quantify VBP. In a second set of animals (n=17), intravital fluorescence microscopy was used as described elsewhere[26] to measure extravasation of fluorescently labeled dextran (FITC-70 kDa dextran 10 mg/ml, 46945, Sigma-Aldrich, Zwijndrecht, The Netherlands) as a model for macromolecular leakage and to determine extravascular accumulation. The setup of the experiment was exactly the same (NTHS, method of dye injection, muscle exposure) except that the handheld microscope was replaced by a fluorescence microscope. The microscopy setup consisted of a stereo fluorescence microscope (model M165 FC, Leica Microsystems, Wetzlar, Germany) equipped with a Peltier-cooled DFC420C color camera, a Planapo 1.0× objective lens, a 0.5× video objective (C-mount), 0.73× optical zoom, filter sets for bright field (420 nm cut on filter) and fluorescence microscopy (λ_{ex} = 470 ± 20 nm, λ_{em} = 515 nm long pass), and a Leica EL6000 light source. The adjustable settings for fluorescence imaging were camera exposure time: 10 s; camera gain: 10; saturation: 1.0; gamma: 0.78; and light source setting: 5 (maximum). The camera was white balanced before every experimental session, and the hardware settings were kept constant throughout the entire experiment.

Before infusion of FITC-dextran, a bright field image was made of the region of interest as well as a baseline fluorescence image. Following a 100 µl infusion over 1 min, fluorescence images were acquired at 2, 5, 10, 15, 20, 25, and 30 min.

Images were analyzed in ImageJ software (National Institutes of Health, Bethesda, MD) for FITC fluorescence intensity as a measure of leakage and extravascular accumulation of dextran. Images were split into RGB images, and the integrated density was calculated in the green channel. The fluorescence intensity was normalized to baseline fluorescence and plotted as a fold-increase for every post-infusion time point.

Tissue edema

Edema formation may occur following accumulation of water as a result of vascular barrier compromise. At the end of the experiment, the heart, brain, kidney, lung and liver were harvested to determine their water content using the wet/dry weighing technique (held at 100°C for 24 h) and were calculated as follows: wet tissue weight/dry tissue weight ratio. This technique allows the measurement of water content in the organ.

Statistical analysis

Values are expressed as mean±SD when normally distributed (Kolmogorov-Smirnov test), or as median [IQR] otherwise. Repeated measures 2-way analysis of variance (ANOVA) (2 factors: time as a related within-animal factor and group as a between-animal factor) with *post hoc* Bonferroni's correction test for multiple analysis were used to determine intergroup and/or intragroup differences of hemodynamic, microcirculation, biochemical data, glycocalyx degradation biomarkers, and intravital fluorescence microscopy. When significant interaction was observed between time and group, we reported simple main effects of group (type of fluid) compared to the control group at each timepoint and the simple main effect of time versus baseline within the same group. Ordinary one-way ANOVA with Bonferroni's correction was used for the analysis of total intravascular blood volume, tissue edema (organ by organ), urine output, and fluorescent tracers retention ratios. The decays in plasma concentration of fluorescent dyes at each timepoint were fitted with an exponential one phase decay using the least squares methods. Because of their non-gaussian distribution, the analyses of power of exponential decay times fitting curves of each fluorescent dye and Evans Blue dye concentrations within

organs were performed using a Kruskal-Wallis test with Dunn's correction test. Statistical analysis was performed using GraphPad Prism version 7.0a for Mac (GraphPad Software, La Jolla, USA). The overall significance level for each hypothesis was 0.05. Adjusted P-values were reported throughout the manuscript in *post hoc* tests.

Based on a previous study by Bansch *et al.*,[27] we postulated that fluid resuscitation with crystalloids after hemorrhage will increase the plasma volume by approximately 25% to target a mean arterial pressure of at least 80 mmHg. Sample size was calculated by nQuery Advisor. A sample size of 6 in each group will have 80% power to detect a difference in means of -9.40 ml/kg (36.1 ml/kg versus 45.5 ml/kg) assuming that the hemorrhagic shock group standard deviation, $\sigma 1$, is 2.700 and the balanced crystalloid group standard deviation, $\sigma 2$, is 6.200 (ratio of Group 2 to Group 1 standard deviation is 2.296) using a two group Satterthwaite t-test with a 0.050 two-sided significance level.

Results

A total of 59 animals were included in this study, 30 rats for the predefined study, 17 rats for the second set of experiments and 12 rats for the study with EBD. No animals died during the experiment. Hemodynamic parameters are presented in **Table 1**. MAP and FABF significantly decreased during hemorrhagic shock. Shock induced metabolic acidosis associated with hyperlactatemia (>5 mmol.l^{-1}), compared to controls (F (4, 25) = 11.52, *P<0.0001*). The mean blood withdrawal was 5.7±0.6 ml (17.1±2 ml.kg^{-1} B.W.), corresponding to 27.5±3.2% of total blood volume (BV) of the rats when calculated according to the following formula: BV (ml) = 0.06 x B.W. + 0.77.[28]

The total fluid resuscitation volumes were 63 [48 – 70] ml, 41.5 [36 – 45.2] ml and 6.5 [5.7 – 12.2] ml for the 0.9% NaCl, balanced crystalloid and colloid groups, respectively (F (2, 16) = 64.85, *P<0.0001*). Fluid resuscitation induced a significant decrease in hemoglobin levels (**Supplemental Table 1**). The associated urine output during the hour following fluid resuscitation was significantly higher in balanced crystalloid and 0.9% NaCl groups compared to controls, 0.067 [0.056 – 0.094] ml.g^{-1}.h^{-1} (mean diff. -0.0587, 95%CI [-0.0986 to -0.0187], adjusted *P=0.0038*) and 0.088 [0.058 – 0.14] ml.g^{-1}.h^{-1} (mean diff. -0.0871, 95%CI [-0.1257 to -0.0484], adjusted *P=0.0001*) versus 0.031 [0.019 – 0.044] ml.g^{-1}.h^{-1}, respectively (**Supplemental Figure 2**). No urine was produced in the hemorrhagic shock group. The MAP was significantly lower in the

fluid resuscitated groups compared to the control group at the end of the experiment. Strategies of fluid resuscitation with balanced crystalloid or colloid were both efficient in correcting pH and plasma lactate levels (**Supplemental Table 1**) compared to normal saline.

Table 1. Hemodynamic parameters and lactate for animals resuscitated with either balanced crystalloid, balanced HES or normal saline

	BL	T1	T2	T3
MAP (mmHg)				
Control	91±7	99±7[$]	105±6[$]	115±6[$]
Hemorrhagic shock	97±9	32±2[*$]	31±2[*$]	25±4[*$]
Balanced crystalloid	100±8	32±2[*$]	85±6[*$]	81±3[*$]
Balanced HES	97±8	33±2[*$]	101±13	88±11[*$]
0.9% NaCl	90±6	33±2[*$]	76±4[*$]	77±7[*$]
CVP (mmHg)				
Control	5±1	5±1	5±1	5±1
Hemorrhagic shock	5±1	5±2	4±2	5±2
Balanced crystalloid	5±1	5±1	7±1	7±1
Balanced HES	6±1	6±1	8±1[*$]	8±1[*$]
0.9% NaCl	5±2	6±2	8±2[*$]	8±3[*$]
FABF (ml min^{-1})				
Control	2.4±0.1	1.8±0.1	2.3±0.3	2.5±0.2
Hemorrhagic shock	2.8±0.3	1.6±0.5[$]	1.2±0.4[*$]	1.1±0.6[*$]
Balanced crystalloid	2.3±0.5	0.8±0.4[*$]	2.7±0.7	3±1.4
Balanced HES	2.5±0.3	1.2±0.8[$]	3±0.6	3.7±1
0.9% NaCl	2.2±0.5	1.1±0.4[$]	2.4±0.7	2.3±0.3
Lactate (mmol L^{-1})				
Control	1.2±0.1	1.7±0.1	1.7±0.2	1.7±0.1
Hemorrhagic shock	1.2±0.4	4.5±1[*$]	4.6±1.3[*$]	5.9±1[*$]
Balanced crystalloid	1.4±0.3	5.1±0.9[*$]	3.6±0.7[*$]	2.2±0.7
Balanced HES	1.4±0.2	5.2±1.2[*$]	2.9±0.8[*$]	1.6±0.5
0.9% NaCl	1.4±0.4	5.7±1.7[*$]	3±0.8[*$]	1.3±0.2

BL= baseline, MAP= Mean arterial pressure, CVP= Central venous pressure, FABF= Femoral artery blood flow, HES = Hydroxyethyl Starch. Differences between groups at the different time points were evaluated using the repeated measures two-way ANOVA with Bonferroni's correction to adjust for multiple comparisons. * adjusted P<0.05 vs. Control group, $ P<0.05 vs. baseline value within the same group. Values are represented as means±SD, n=6 per group.

Supplementary Table 1. Arterial Blood Gases and Hematological and Biochemical Parameters

	BL	T1	T2	T3
pH				
Control	7.42±0.03	7.38±0.02	7.38±0.02	7.41±0.03
Hemorrhagic shock	7.46±0.03	7.32±0.03*$	7.27±0.02*$	7.25±0.1*$
Balanced crystalloid	7.44±0.03	7.33±0.03$	7.33±0.03$	7.45±0.04
Balanced HES	7.44±0.01	7.34±0.05$	7.33±0.04$	7.42±0.06
0.9% NaCl	7.46±0.04	7.30±0.04*$	7.23±0.05*$	7.26±0.05*$
$PaCO_2$ (kPa)				
Control	4.4±0.3	4.6±0.3	4.4±0.6	4.3±0.4
Hemorrhagic shock	4±0.5	4±0.2*	4.3±0.6	3.9±0.7
Balanced crystalloid	4.1±0.4	3.1±0.5*$	4.6±0.6	4.1±0.6
Balanced HES	4.1±0.4	3.7±0.8	4.8±0.5	4.7±1
0.9% NaCl	3.8±0.5	4±0.4	4.4±0.4	4.5±0.5
BE (mmol L^{-1})				
Control	-3.5±1.9	-3.7±1	-4.6±1.6	-3.3±0.8
Hemorrhagic shock	-1.2±1.9	-9.6±1.9*$	-11.7±1.6*$	-14.7±2.1*$
Balanced crystalloid	-2.6±2.1	-12.2±1.3*$	-7.3±0.8$	-2.4±1
Balanced HES	-1.9±1.1	-10.1±2.7*$	-6.4±2.1$	-2.1±1
0.9% NaCl	-2.1±2.1	-13.5±3.4*$	-12.5±2*$	-10.1±1.4*$
HCO^-_3 (mmol L^{-1})				
Control	20.2±1	20.1±1.2	19±1.8	19.9±0.7
Hemorrhagic shock	21.2±2.2	15±1.5*$	14.3±2*$	11.9±1.3*$
Balanced crystalloid	20.1±2.1	12.1±1.4*$	17.4±1.1$	20.8±1.4
Balanced HES	20.7±1.4	14±2.2*$	18.4±1.9$	21.6±1.5
0.9% NaCl	19.9±2.3	12.5±2.5*$	13.5±1.5*$	15.2±1.2*$
Anion Gap (mmol L^{-1})				
Control	17.5±0.9	17.8±0.8	18.9±1.2	18.2±0.5
Hemorrhagic shock	15.2±1.7	20.6±1.6*$	21.9±1.3*$	24.4±2.1*$
Balanced crystalloid	16.2±1.9	23±2*$	19.6±1.3$	16.5±1.3
Balanced HES	15.7±1.7	21.5±2.8*$	18.3±2.1$	15.3±0.7*
0.9% NaCl	16.1±1.5	25.1±2.8*$	20.1±1.9$	17.8±1.2$
Hb (g dL^{-1})				
Control	14.5±1.1	14.6±0.4	13.5±0.9	13.6±0.4
Hemorrhagic shock	14.1±1.1	10.8±0.8*$	10.6±0.6*$	9.8±1.1*$
Balanced crystalloid	13.1±1.3	9.3±1.4*$	6.6±1*$	5.8±1.6*$
Balanced HES	14.2±0.9	10.8±0.9*$	7.6±0.9*$	7.2±0.9*$
0.9% NaCl	13.8±1	9.9±1*$	6±0.8*$	4.9±1.6*$

BE= base excess, HCO_3= bicarbonate level, $PaCO_2$= Arterial carbon dioxide pressure. Differences between groups at the different time points were evaluated using the repeated measures two-way ANOVA with Bonferroni's correction to adjust for multiple comparisons. * adjusted P<0.05 vs. Control group, $ P<0.05 vs. baseline value within the same group. Values are represented as mean±SD, n=6 per group

5
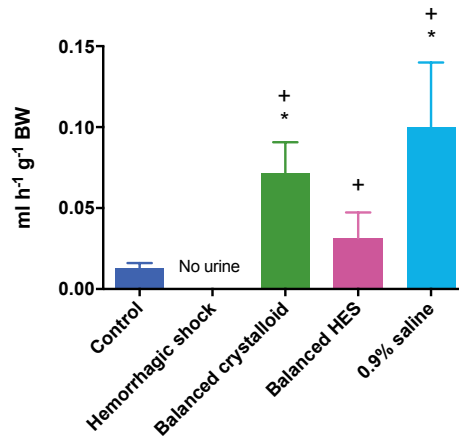
Supplemental Figure 2. Urine output at the end of the experiment

* adjusted P<0.05 vs control, \$ adjusted P<0.001 vs hemorrhagic shock. Ordinary one-way ANOVA test was used with Bonferroni's correction to adjust for multiple comparisons (n=6/group).

Shedding products of glycocalyx constituents
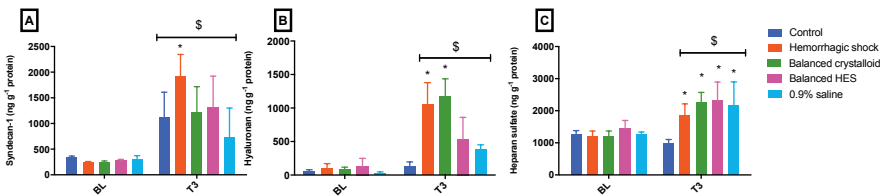
Figure 1. Plasma levels of syndecan-1 (panel A), hyaluronan (panel B) and heparan sulfate (panel C) during the experiment

Increased glycocalyx shedding persists after fluid resuscitation except for the hyaluronan component, which is decreased with balanced HES resuscitation. Repeated measures 2-way ANOVA test used with Bonferroni's correction to adjust for multiple comparisons. * adjusted P<0.01 vs. Control group at the same time point, \$ P<0.05 vs. baseline value within the same group. (n=6-8/group)

Glycocalyx shed products (hyaluronan, syndecan-1, heparan) were all upregulated as a result of NTHS. Syndecan-1 levels (**Figure 1A**) were significantly increased in controls (mean diff.

-788.7, 95%CI [-1456 to -121.1], adjusted P=0.015), non-resuscitated hemorrhagic shock (mean diff. -1668, 95%CI [-2336 to -1001], adjusted P<0.0001), balanced crystalloid (mean diff. -964.2, 95% CI [-1492 to -436.4], adjusted P=0.0001) and HES (mean diff. -1030, 95% CI [-1594 to -465.8], adjusted P=0.0001) groups at the end of the experiment (T3) compared to baseline (BL) values.

No changes in syndecan-1 were observed in the 0.9% NaCl group. Fluid resuscitation with either balanced crystalloid (mean diff. 704, 95%CI [163.8 to 1244], adjusted P=0.0067), balanced HES (mean diff. 604.2, 95%CI [49.43 to 1159], adjusted P=0.029) solutions or normal saline (mean diff. 1178, 95%CI [623.7 to 1733], adjusted P=0.0001) significantly reduced levels of syndecan-1 at the end of the experiment compared to the non-resuscitated hemorrhagic shock group. Hyaluronan levels (**Figure 1B**) were significantly higher at the end of the experiment in the non-resuscitated hemorrhage (mean diff. -923.1, 95%CI [-1216 to -630], adjusted P=0.0001) and balanced crystalloid (mean diff. -1039, 95% CI[-1332 to -745.5], adjusted P=0.0001) or HES (mean diff. -394.2, 95% CI[-670.1 to -118.3], adjusted P=0.0027) groups compared to controls. The increase in glycocalyx shedding products was persistent after fluid resuscitation except for the hyaluronan component, which was decreased following balanced HES and normal saline administration. Heparan sulfate levels remained higher regardless of the resuscitation regimen or the absence of fluid resuscitation (P<0.001), when compared to the controls (**Figure 1C**).

Microcirculatory changes in muscle

The microcirculatory parameters in the biceps femoris are represented in **figure 2**. While TVD, MFI and PVD were not different after fluid resuscitation with either balanced crystalloid or colloid (*P>0.05*). TVD was significantly altered in the normal saline (mean diff. 4.092, 95%CI [0.6195 to 7.564], adjusted *P=0.016*) and hemorrhagic shock (mean diff. 5.022, 95%CI [1.55 to 8.495], adjusted *P=0.0024*) groups when compared to the control group, as PVD and MFI were. The same parameters of these 2 latter groups were also significantly decreased compared to their baseline values (*P<0.05*).
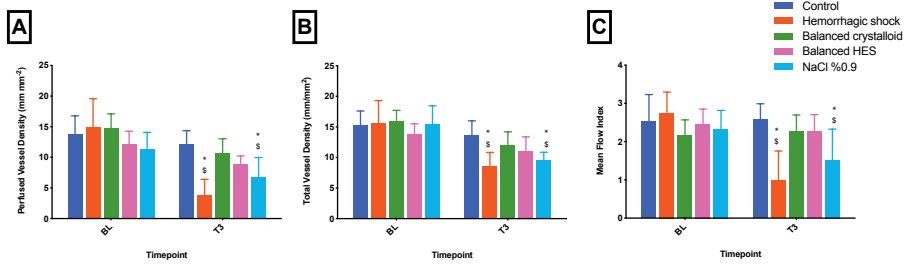
Figure 2. Microcirculatory parameters assessed at a single spot of the biceps femoris with handheld intravital microscopy.

*Despite normal MAP, the microcirculation is not fully restored after fluid resuscitation when considering the total vessel density. Repeated measures 2-way ANOVA test used with Bonferroni's correction to adjust for multiple comparisons. * adjusted* $P<0.05$ *vs. Control group at the same time point, $ * $P<0.05$ *vs. baseline value within the same group. (n=8/group)*

Vascular barrier permeability

Fluorescent tracer decays and retention ratios

The decay-times of fluorescent tracers are presented in **supplemental Figure 3**. The rate of disappearance can be given by the power of the exponential fit of the tracer curves provided for different groups. No significant alteration in this power was observed among the different groups. When considering the decrease in normalized concentrations at each time point per group of fluid resuscitation (**Supplemental Figure 4**), a significant difference was present between FITC 500 kDa and Texas Red 40 kDa dextrans (*P<0.05*), suggesting a different escape rate from the vascular system according to molecular size. Albumin Alexa 680 and FITC 500 kDa showed similar decays regardless of the group, proving that these dyes did not cross the vascular barrier.
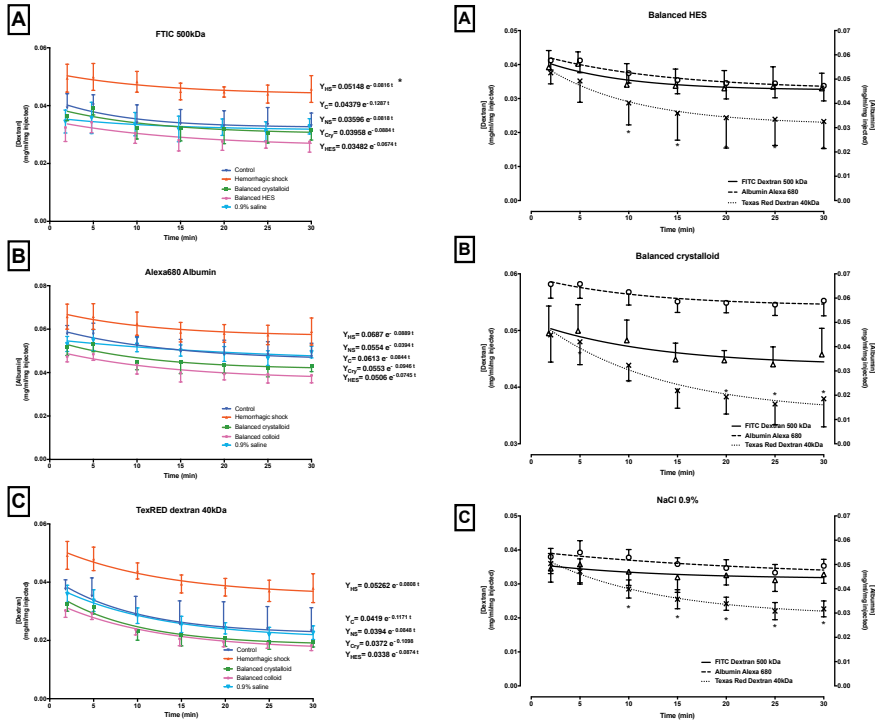
Supplemental Figure 3 & 4. Decay-time of fluorescent tracer concentrations according to their molecular size and their associated exponential decays in different groups (*left*), and time course of concentration decays of fluorescent dyes in each fluid resuscitation group of the study (*right*)

Left*: (A) FITC Dextran 500 kDa, (B) Albumin Alexa 680, (C) TexasRed Dextran 40 kDa. * adjusted* $P<0.05$ *vs control group according to exponential decay with Bonferroni's correction to adjust for multiple comparisons (n=6/group)*

Right: All concentrations were normalized for comparison in $mg.ml^{-1}.mg^{-1}$ of dye injected. (A) Balanced HES group, (B) balanced crystalloid, and (C) normal saline. ✱ P<0.05 versus FITC 500 kDa dextran dye (n=6/group)

The retention ratio of different dyes bound to different molecular size is presented in **figure 3**. No significant differences were noted.
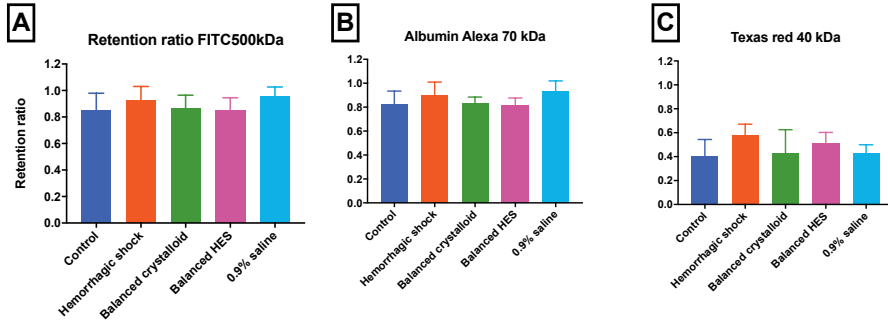
Figure 3. Retention ratio of the different tracers expressed as the ratio between the final (at 30 min) and initial concentrations (at 2 min) of the dye

One-way ANOVA test used for each fluorescent dye with Bonferroni's correction to adjust for multiple comparisons (n=6/group).
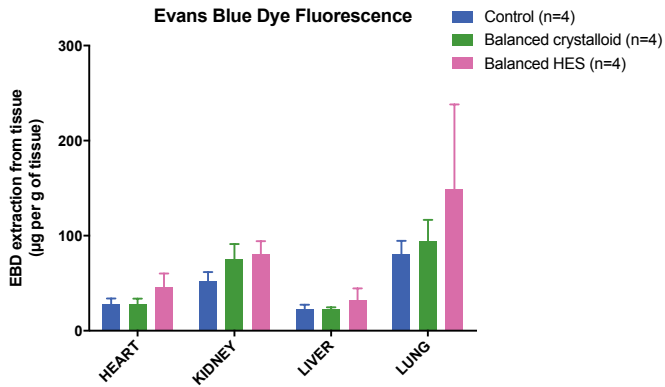
Supplemental Figure 5. Fluorescence of Evans blue dye extraction from different tissues

Only balanced starch and crystalloid groups were included in this study

Evans Blue dye technique

The Evans blue dye extraction from tissues is presented in **Supplemental figure 5** (n = 4 per group, excluding non-resuscitated NTHS and normal saline groups). A broad variability in the pulmonary EBD concentration was observed. No differences were noted in the other organs between control and resuscitated animals regardless of the fluid chosen.

Fluorescence intravital microscopy

Figure 4A is an example of the time course of fluorescence escaping through the microvasculature obtained with intravital fluorescence microscopy in animals undergoing NTHS resuscitation with different fluids or the control. The fluorescence levels did not significantly differ from the control group. As a damage positive control for vascular barrier disruption, hyperthermia (T >42°C) was induced in a rat. The time course of the relative increase in fluorescence is displayed in **figure 4B**. We did not include a non-resuscitated hemorrhagic shock group in this setting as we did not see any significant leakage after fluid resuscitation of hemorrhagic shock in the other groups. Leakage was unlikely to happen, and the experiment was considered futile and not in accordance with the local animal ethic committee.
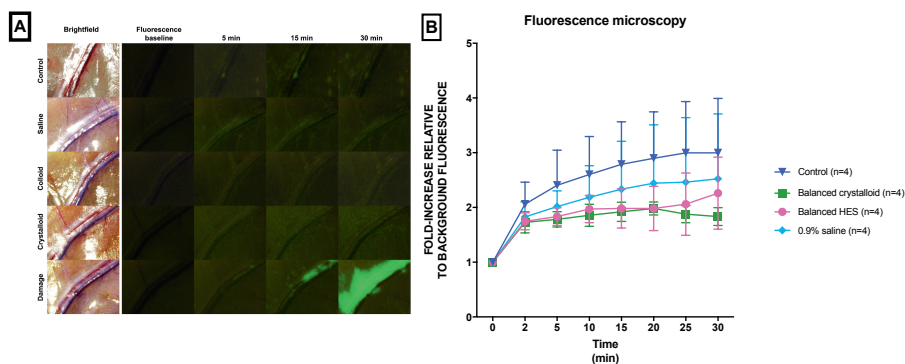
Figure 4. Fluorescence microscopy of the microcirculation of the right biceps femoris. (A) Time course of fluorescence imaging at different time points after dye infusion. (B) Increase in fluorescence relative to background during the 30 minutes after injection

Infusion of 100 µl FITC-70 kDa dextran (10 mg/ml) and subsequent fluorescence images at 2, 5 10, 15, 20, 25 and 30 minutes. For the sake of clarity, only baseline, 5-, 15- and 30-min time points are shown. The hemorrhagic shock group was not determined. Repeated measures 2-way ANOVA test used with Bonferroni's correction to adjust for multiple comparisons.

Tissue edema

The quantification of tissue edema in different organs (lung, brain, liver, kidney and heart) is presented in **Supplemental Figure 6**. Although the wet/dry ratio may be different among organs, no significant tissue edema was present after fluid resuscitation compared to the control group. Non-resuscitated hemorrhagic shock animals exhibited a significantly smaller wet-to-dry weight ratio in the liver compared to control (mean diff. 0.373, 95%CI [0.03158 to 0.7151], adjusted *P=0.029*). In addition, no difference was noted between balanced crystalloid and colloid fluid resuscitation with regard to tissue edema.
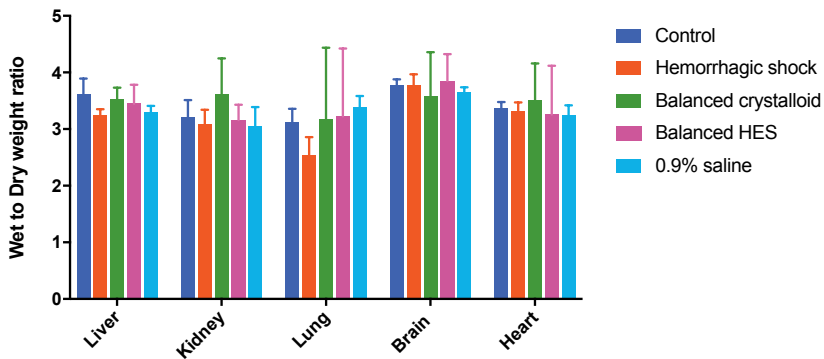
Supplemental Figure 6. Tissue edema in the liver, kidney, lung, brain and heart expressed as the wet to dry weight ratio

Ordinary one-way ANOVA test was used with Bonferroni's correction to adjust for multiple comparisons (n=8/group).

Total intravascular blood volume

The TBV was reduced in the non-resuscitated hemorrhagic shock group (15.2±1.3 ml) compared to the control group (17.5±1.3 ml) (mean diff. 2.3, 95%CI [0.20 to 4.5], *P=0.027*) (**Figure 5**). Fluid resuscitation increased TBV significantly in the balanced crystalloid group (21.1±1.1 ml) compared to the control and hemorrhagic shock groups, mean diff. -3.6, 95%CI [-5.7 to -1.5], adjusted *P<0.0001* and -5.9, 95%CI [-8.07 to -3.9], adjusted *P<0.0001* respectively.
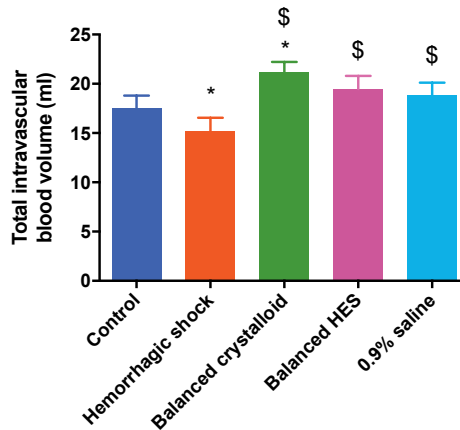
Figure 5. Total intravascular blood volume at the end of the experiment as determined by Albumin Alexa 680 fluorimetry.

* adjusted P<0.05 vs control, $ adjusted P<0.001 vs hemorrhagic shock. One-way ANOVA test used with Bonferroni's correction to adjust for multiple comparisons (n=6/group).

Discussion

The main result of our study has been the demonstration that in NTHS, glycocalyx degradation occurs but is not associated with an increased vascular barrier permeability. Furthermore, our results show that glycocalyx degradation and microcirculatory alterations persists following fluid resuscitation independent of its composition. However, fluid resuscitation alone does not result in a change in VBP and in its extension tissue edema. These results on changes in VBP were demonstrated using four independent techniques. However, some differences remain regarding the nature of glycocalyx shedding products, as indicated by the biomarkers profile differing between resuscitation fluids. Normal saline was found to be the less suitable fluid, as it did neither restore the microcirculatory alterations nor the acid-base balance. These results stress the complexity of VBP regulation in the context of hemorrhagic shock and identify a gradation of vascular injury. A partial shedding of the glycocalyx either NTHS-induced or following fluid resuscitation, did not impair vascular barrier competence. This result challenges the role of the glycocalyx as a major contributor of the VBP.

It is assumed that glycocalyx shedding is a direct cause of an increase in VBP. Glycocalyx shedding products are often considered as surrogate markers of vascular permeability. Most of the data regarding the relationship between glycocalyx shedding and increased VBP come from *ex vivo* isolated organs experiments or *in vivo* enzymatic degradation treatments. However, these models have serious shortcomings and ignore a large part of the pathophysiological pathways occurring in response to shock.[19,29] Thus, the results of these experiments may not be relevant to physiological situations. Rehm *et al.,* in an isolated heart model, first introduced the concept of a "double-barrier" where the glycocalyx can be enzymatically erased while the endothelial cells remain untouched, without causing significant effects on coronary permeability.[19] Our results support these findings, although we observed microcirculatory alterations related to hemorrhagic shock. These microcirculatory disturbances are usually a marker of endothelial cell dysfunction. In an hamster window chamber model, Landsverk *et al.* observed a significant decrease in functional capillary density after hyaluronidase injection without associated vascular leakage.[30] The authors reported a 50-100 fold increase in plasma levels of hyaluronan, suggesting an efficient glycocalyx degradation. In another study, Bansh *et al.* did not observe any leak of radio-labelled albumin in an acute model of hemorrhage 4 h after resuscitation with either Ringer's acetate or 5% albumin, suggesting an intact microvascular barrier, bearing out our results.[27]

Similarly to other authors, we demonstrated that NTHS did injure the different endothelial glycocalyx components and fluid resuscitation following hemorrhage may alter glycocalyx components' in different ways.[6,13,14,31] However, the level of injury may vary according to the model used, the duration of shock or the vascular bed under observation. In a rodent model of hemorrhagic shock, Kozar *et al.* showed that lung injury was markedly increased with decreased cell surface syndecan-1 expression in pulmonary alveolar cells following lactated ringer's resuscitation.[13] On the contrary, fresh frozen plasma (FFP) restored in part the shed glycocalyx. Direct assessment of vascular barrier permeability was however not performed in this experiment nor tissue edema measurements (wet/dry ratio). Torres Filho *et al.* published several experimental studies of NTHS in rats, where microvascular permeability in the cremaster muscle was increased in association with glycocalyx degradation after fluid resuscitation with crystalloids compared to FFP or whole blood.[6,14,15] In these studies, vascular barrier permeability was assessed in one vascular bed (cremaster) which had been surgically prepared and may have induced local inflammation. Besides this difference, animals were subjected to a fixed relative volume hemorrhage (40% of total blood volume) and were fluid-resuscitated with empirical

amounts not matching clinical practice which usually targets a macrocirculatory endpoint. These authors showed a positive correlation between changes in microvascular permeability and in glycocalyx shedding products (plasma syndecan-1 and heparan sulfate).[15] The discrepancies with other studies may lie in the fact that we undertook a multifaceted approach of the VBP. We did not focus on a specific vascular bed that might be more sensitive to hyper-permeability but rather took into consideration the whole cardiovascular system and different organs. Besides, the glycocalyx has a remarkable heterogeneous distribution within organs. Finally, compared to other authors the duration of our hemorrhagic shock and fluid resuscitation observation time periods were shorter, 60 min versus 90 min and 1 hour versus 3 hours respectively.[13,32]

An intact glycocalyx is a prerequisite for normal vascular physiology, and each component exhibits a unique function. Many of its components are essential for homeostasis,[33,34] mechanosensors for flow-mediated shear stress and autoregulation,[1,33] and leukocyte-endothelial cell interactions.[35] Glycocalyx shedding could be an essential and normal response to injury and could be appropriate or even beneficial. Could preventing glycocalyx shedding even be harmful?[36] Its degradation occurs in a wide range of conditions such as diabetes/hyperglycemia,[9] atherosclerosis and hypertension,[4] sepsis,[8,37] reperfusion injury,[38] or smoking.[39] Whether glycocalyx shedding alone causes tissue edema or capillary leakage remains controversial. We suggest that although the glycocalyx is essential from a functional point of view, it is not a key component of the permeability of the vascular barrier. The traditional Starling's law has been revised several times, taking into account not only the glycocalyx but also most significant components such as the endothelial cell junctions, the basement membrane and pericytes.[3,40,41]

In the light of the literature and our data, a hierarchy of vascular injury can be proposed, initiated by glycocalyx shedding followed by microcirculatory alterations, and ultimately if injury persists or induces major inflammation, by a loss of VPB and tissue edema. This concept of graded injury although intuitive would need further investigation in different models and vascular beds. Only the most severe models, using degradative enzymes or sustained sepsis such as cecal ligation and puncture where other components of the vascular barrier (e.g., adherens junctions/cadherins) become compromised have shown vascular leakage and tissue edema.[16,17,41,42] In the present model, this level of vascular injury was not achieved.

Due to the large amounts of crystalloids used for fluid resuscitation, one was expecting to observe fluid accumulation within various organs. Although crystalloids inevitably accumulate in tissues when given in large amounts, such findings do not necessarily imply VBP alterations.[43] In

our experiment, balanced crystalloid or normal saline markedly increased urine output. Between a third and a half of the resuscitation volume administered was promptly excreted (<1h). Few experimental studies have focused on urine output during fluid resuscitation in hemorrhagic shock, and the results were consistent with ours.[44] While we did not observe an overall increase in VBP nor tissue edema in the lung, brain, liver, kidney or heart, it might be possible that fluid in excess tends to accumulate in the intestinal mucosae and mesentery, muscles, or skin.

In our study, balanced HES solution administered after NTHS markedly decreased the level of hyaluronan compared to balanced crystalloid. However, Nelson *et al.* noted that a decrease in glycocalyx shedding biomarkers may be related to a dilutional effect induced by the volume expander effect of colloids or FFP.[31] Torres *et al.* did not notice any beneficial effect of high molecular weight starch on plasma syndecan-1 levels or *in vivo* glycocalyx thickness after fluid resuscitated hemorrhagic shock.[15,45] To date, there is no evidence that restoring the glycocalyx in the context of jeopardized VBP would be beneficial or would help reduce capillary leakage when already present.

Limitations of the study

Due to a limited number of animals per group, the reproducibility of certain techniques may be questioned; however, the results were consistent in each group among different techniques that analyzed the VBP. In such a heavily instrumented model, it is difficult to control all of the factors that may induce glycocalyx shedding. Surgery and fluid maintenance, similar in all groups, may have induced some glycocalyx degradation, as indeed observed in the control group. NTHS could have been prolonged for several hours but would have been at variance with clinical practice in operating or emergency rooms. We did not investigate the mechanisms behind glycocalyx shedding, such as oxidative stress and inflammation. Our technique of microcirculation measurements did not allow leukocyte-endothelium interaction analyses because of the high velocity of these cells due to hemodilution.

Conclusion

This study is the first to provide an integrative assessment of the VBP, including macro and microhemodynamic monitoring, glycocalyx shedding and vascular leakage, in a clinically relevant model of NTHS. NTHS induced glycocalyx shedding and microcirculatory modifications, but these were not associated with increased VBP after fluid resuscitation. These results challenge the concept of glycocalyx as a key determinant of vascular permeability. The endothelial cell junctions may be a more important contributor to the VBP.[41]

Financial disclosures & funding

Conflicts of interest

Dr Can Ince runs an Internet site microcirculationacademy.org which offers services (e.g., training, courses, analysis) related to clinical microcirculation and, has received honoraria and independent research grants from Fresenius-Kabi, Baxter Health Care, and AM-Pharma; has developed SDF imaging; is listed as an inventor on related patents commercialized by MicroVision Medical under a license from the Academic Medical Center; and has been a consultant for MicroVision Medical in the past but has not been involved with this company for more than 5 years. The company that developed the CytoCam-IDF imaging system, Braedius Medical, is owned by a relative of Dr Ince. Dr Ince has no financial relationship with Braedius Medical (i.e., never owned shares or received consultancy or speaker fees). Dr Martin Westphal is the Chief Medical Officer of Fresenius Kabi AG. The remaining authors declare no conflicts of interest.

5

Authors contribution

Philippe Guerci and Bulent Ergin contributed equally to this manuscript.

Philippe Guerci: this author helped in study design, carrying out experiments, data analysis, writing of the first draft and of the final version, and review of the manuscript.

Bulent Ergin: this author helped in study design, carrying out experiments, data analysis, writing of the first draft and of the final version, and review of the manuscript.

Michal Heger: this author helped in carrying out experiments, data analysis, writing of the first draft, and review of the manuscript.

Zuhre Uz: this author helped in data analysis (microcirculation clips), and review of the manuscript.

Yasin Ince: this author helped in data analysis (microcirculation clips), and review of the manuscript.

Martin Westphal: this author helped in data analysis (microcirculation clips) and review of the manuscript.

Can Ince: this author helped in study design, data analysis, writing of the final version, and review of the manuscript.

References

1.   Weinbaum S, Tarbell JM, Damiano ER. The structure and function of the endothelial glycocalyx layer. *Annu Rev Biomed Eng* 2007;9:121–67.

2.   Curry FE, Adamson RH. Endothelial glycocalyx: permeability barrier and mechanosensor. *Ann Biomed Eng* 2012;40:828–39.

3.   Woodcock TE, Woodcock TM. Revised Starling equation and the glycocalyx model of transvascular fluid exchange: an improved paradigm for prescribing intravenous fluid therapy. *Br J Anaesth* 2012;108:384–94.

4.   Tarbell JM, Cancel LM. The glycocalyx and its significance in human medicine. *J Intern Med* 2016;280:97–113.

5.   Chignalia AZ, Yetimakman F, Christiaans SC, et al. The glycocalyx and trauma: a review. *Shock* 2016;45:338–48.

6.   Torres Filho I, Torres LN, Sondeen JL, Polykratis IA, Dubick MA. In vivo evaluation of venular glycocalyx during hemorrhagic shock in rats using intravital microscopy. *Microvasc Res* 2013;85:128–33.

7.   Ince C, Mayeux PR, Nguyen T, et al. The endothelium in sepsis. *Shock* 2016;45:259–70.

8.   Chelazzi C, Villa G, Mancinelli P, De Gaudio AR, Adembri C. Glycocalyx and sepsis-induced alterations in vascular permeability. *Crit Care* 2015;19:26.

9.   Zuurbier CJ, Demirci C, Koeman A, Vink H, Ince C. Short-term hyperglycemia increases endothelial glycocalyx permeability and acutely decreases lineal density of capillaries with flowing red blood cells. *J Appl Physiol* 2005;99:1471–6.

10.   Miranda CH, de Carvalho Borges M, Schmidt A, Marin-Neto JA, Pazin-Filho A. Evaluation of the endothelial glycocalyx damage in patients with acute coronary syndrome. *Atherosclerosis* 2016;247:184–8.

11.   Chappell D, Bruegger D, Potzel J, et al. Hypervolemia increases release of atrial natriuretic peptide and shedding of the endothelial glycocalyx. *Crit Care* 2014;18:538.

12.   Kataoka H, Ushiyama A, Akimoto Y, et al. Structural Behavior of the Endothelial Glycocalyx Is Associated With Pathophysiologic Status in Septic Mice: An Integrated Approach to Analyzing the Behavior and Function of the Glycocalyx Using Both Electron and Fluorescence Intravital Microscopy. *Anesth Analg* 2017;125:874–83.

13.   Kozar RA, Peng Z, Zhang R, et al. Plasma restoration of endothelial glycocalyx in a rodent model of hemorrhagic shock. *Anesth Analg* 2011;112:1289–95.

14.   Torres LN, Chung KK, Salgado CL, Dubick MA, Torres Filho IP. Low-volume resuscitation with normal saline is associated with microvascular endothelial dysfunction after hemorrhage in rats, compared to colloids and balanced crystalloids. *Crit Care* 2017;21:160.

15.   Torres Filho IP, Torres LN, Salgado C, Dubick MA. Plasma syndecan-1 and heparan sulfate correlate with microvascular glycocalyx degradation in hemorrhaged rats after different resuscitation fluids. *Am J Physiol Heart Circ Physiol* 2016;310:H1468–78.

16.   VanTeeffelen JWGE, Brands J, Janssen BJA, Vink H. Effect of acute hyaluronidase treatment of the glycocalyx on tracer-based whole body vascular volume estimates in mice. *J Appl Physiol* 2013;114:1132–40.

17.   Gao L, Lipowsky HH. Composition of the endothelial glycocalyx and its relation to its thickness and diffusion of small solutes. *Microvasc Res* 2010;80:394–401.

18.   Cabrales P, Vázquez BYS, Tsai AG, Intaglietta M. Microvascular and capillary perfusion following glycocalyx degradation. *J Appl Physiol* 2007;102:2251–9.

19.   Rehm M, Zahler S, Lötsch M, et al. Endothelial glycocalyx as an additional barrier determining extravasation of 6% hydroxyethyl starch or 5% albumin solutions in the coronary vascular bed. *Anesthesiology* 2004;100:1211–23.

20.   Donati A, Damiani E, Domizi R, et al. Alteration of the sublingual microvascular glycocalyx in critically ill patients. *Microvasc Res* 2013;90:86–9.

21.   Aykut G, Veenstra G, Scorcella C, Ince C, Boerma C. Cytocam-IDF (incident dark field illumination) imaging for bedside monitoring of the microcirculation. *Intensive Care Med Exp* 2015;3:40.

22.   Massey MJ, Shapiro NI. A guide to human in vivo microcirculatory flow image analysis. *Crit Care* 2015;20:35–5.

23.   Cooksey CJ. Quirks of dye nomenclature. 1. Evans blue. *Biotech Histochem* 2014;89:111–3.

24.   Wang H-L, Lai TW. Optimization of Evans blue quantitation in limited rat tissue samples. *Sci Rep* 2014;4:6588.

25.   Kenne E, Lindbom L. Imaging inflammatory plasma leakage in vivo. *Thromb Haemost* 2011;105:783–9.

26.   Olthof PB, van Golen RF, Meijer B, et al. Warm ischemia time-dependent variation in liver damage, inflammation, and function in hepatic ischemia/reperfusion injury. *Biochim Biophys Acta* 2017;1863:375–85.

27.   Bansch P, Statkevicius S, Bentzer P. Plasma volume expansion with 5% albumin compared to Ringer's acetate during normal and increased microvascular permeability in the rat. *Anesthesiology* 2014;121:817–24.

28.   Lee HB, Blaufox MD. Blood volume in the rat. *Journal of Nuclear Medicine* 1985.

29.   Bruegger D, Rehm M, Jacob M, et al. Exogenous nitric oxide requires an endothelial glycocalyx to prevent postischemic coronary vascular leak in guinea pig hearts. *Crit Care* 2008;12:R73.

30.   Landsverk SA, Tsai AG, Cabrales P, Intaglietta M. Impact of enzymatic degradation of the endothelial glycocalyx on vascular permeability in an awake hamster model. *Crit Care Res Pract* 2012;2012:842545–8.

31.   Nelson A, Statkevicius S, Schött U, Johansson PI, Bentzer P. Effects of fresh frozen plasma, Ringer's acetate and albumin on plasma volume and on circulating glycocalyx components following haemorrhagic shock in rats. *Intensive Care Med Exp* 2016;4:6.

32.   Pati S, Peng Z, Wataha K, et al. Lyophilized plasma attenuates vascular permeability, inflammation and lung injury in hemorrhagic shock. *PLoS ONE* 2018;13:e0192363.

33.   Reitsma S, Slaaf DW, Vink H, van Zandvoort MAMJ, oude Egbrink MGA. The endothelial glycocalyx: composition, functions, and visualization. *Pflugers Arch* 2007;454:345–59.

34.   Chappell D, Brettner F, Doerfler N, et al. Protection of glycocalyx decreases platelet adhesion after ischaemia/reperfusion: an animal study. *Eur J Anaesthesiol* 2014;31:474–81.

35. Constantinescu AA, Vink H, Spaan JAE. Endothelial cell glycocalyx modulates immobilization of leukocytes at the endothelial surface. *Arterioscler Thromb Vasc Biol* 2003;23:1541–7.

36. Hayashida K, Parks WC, Park PW. Syndecan-1 shedding facilitates the resolution of neutrophilic inflammation by removing sequestered CXC chemokines. *Blood* 2009;114:3033–43.

37. Schmidt EP, Yang Y, Janssen WJ, et al. The pulmonary endothelial glycocalyx regulates neutrophil adhesion and lung injury during experimental sepsis. *Nat Med* 2012;18:1217–23.

38. van Golen RF, Reiniers MJ, Vrisekoop N, et al. The mechanisms and physiological relevance of glycocalyx degradation in hepatic ischemia/reperfusion injury. *Antioxid Redox Signal* 2014;21:1098–118.

39. Ikonomidis I, Marinou M, Vlastos D, et al. Effects of varenicline and nicotine replacement therapy on arterial elasticity, endothelial glycocalyx and oxidative stress during a 3-month smoking cessation program. *Atherosclerosis* 2017;262:123–30.

40. Kottke MA, Walters TJ. Where's the Leak in Vascular Barriers? A Review. *Shock* 2016;46:20–36.

41. Goldenberg NM, Steinberg BE, Slutsky AS, Lee WL. Broken barriers: a new take on sepsis pathogenesis. *Sci Transl Med* 2011;3:88ps25–5.

42. Chappell D, Jacob M. Role of the glycocalyx in fluid management: Small things matter. *Best Pract Res Clin Anaesthesiol* 2014;28:227–34.

43. Chawla LS, Ince C, Chappell D, et al. Vascular content, tone, integrity, and haemodynamics for guiding fluid therapy: a conceptual approach. *Br J Anaesth* 2014;113:748–55.

44. Todd SR, Malinoski D, Muller PJ, Schreiber MA. Lactated Ringer's is superior to normal saline in the resuscitation of uncontrolled hemorrhagic shock. *J Trauma* 2007;62:636–9.

45. Torres LN, Sondeen JL, Ji L, Dubick MA, Torres Filho I. Evaluation of resuscitation fluids on endothelial glycocalyx, venular blood flow, and coagulation function after hemorrhagic shock in rats. *J Trauma Acute Care Surg* 2013;75:759–66.

5

6

GLYCOCALYX SHEDDING DURING STEPWISE HEMODILUTION AND MICROVASCULAR PERMEABILITY

Bulent Ergin,[1,4] Philippe Guerci,[1,2,3] Zuhre Uz,[1] Martin Westphal,[5]

Yasin Ince,[1] Matthias Hilty,[1] Can Ince[1,4]

1. Department of Translational Physiology, Academic Medical Center, University of Amsterdam, Amsterdam, The Netherlands
2. INSERM U1116, University of Lorraine, Vandoeuvre-Les-Nancy, France
3. Department of Anesthesiology and Critical Care Medicine, University Hospital of Nancy, France
4. Department of Intensive Care Medicine, Erasmus MC, University Medical Center, Rotterdam, Rotterdam, The Netherlands
5. Fresenius Kabi Deutschland GmbH, Bad Homburg, Germany

Bulent Ergin and Philippe Guerci contributed equally to this manuscript.

Abstract

Background: Acute normovolemic hemodilution (ANH) may develop as a consequence of fluid loading in the perioperative period. The consequences of ANH on the different components of the glycocalyx and on the vascular barrier permeability have been barely investigated. We hypothesized that ANH with balanced HES would result in lesser damage to the glycocalyx without affecting vascular barrier permeability (VBP).

Methods: 24 male Wistar albinos rats were anesthetized ,ventilated and subjected to a stepwise ANH at hematocrit levels of 35%, 25%, 20% and 15%, induced by stepwise exchange of blood with either balanced hydroxyethyl starch (HES) (ratio 1:1), balanced crystalloid or normal saline 0.9% (ratios 1:3). Glycocalyx shed products were measured in the plasma during different levels of hemodilution. VBP was assessed with (i) plasma decays of fluorescence dyes of different molecular sizes and their retention ratios in the plasma, and ii) edema formation in organs measured by water content. Skeletal muscle microcirculation was monitored at a single spot using a hand-held intravital microscope.

Results: ANH was associated with a significant decrease in mean arterial pressure in all groups compared to control, that was maximal at Htc 15% ($F_{(4, 20)}$=113.7, P<0.0001). NaCl 0.9% degraded heparan sulfate and hyaluronan components compared to control group (mean diff. -1213, 95%CI[-2070 to -356], P=0.003, and -66, 95%CI[-115 to -18], P=0.004 respectively). Syndecan-1 increased over time ($F_{(3, 60)}$=23.88, P<0.0001) irrespective of the group. No increase in VBP nor tissue edema was observed regardless of the fluid used. Total and perfused vessel densities of skeletal muscle microcirculation were decreased at Hct 15% in the balanced crystalloid and normal saline groups, mean diff. 3.1, 95%CI[0.32-5.9], P=0.02 and 4.7, 95%CI[1.9-7.5], P=0.0003 respectively compared to baseline.

Conclusions: Balanced HES better preserved glycocalyx during ANH. No increase in VBP was demonstrated even at Hct 15% irrespective of the fluid administered. Normal saline was the fluid having the more deleterious effects during ANH.

Keywords: microcirculation, acute normovolemic hemodilution, hydroxyethyl starch, vascular barrier permeability, handheld intravital microscopy, hyperresponsiveness

Introduction

The perioperative fluid choice has been largely debated in the literature over the past 40 years.[1,2] In this setting, acute normovolemic hemodilution (ANH) may develop as a consequence of fluid loading,[3,4] especially if a goal directed protocol is applied to increase stroke volume.

The glycocalyx consists of highly negatively charged glycosaminoglycans lining the endothelial cells, that provides a protective layer and serves as a regulator of leukocyte to endothelial cells adhesion processes and macromolecular traffic.[5,6] It has been suggested in a human clinical setting that ANH does not jeopardize the glycocalyx constituents as opposed to hypervolemia by the mediated release of atrial natriuretic peptide.[7] The disruption of glycocalyx is reportedly being the primary cause of increase in vascular barrier permeability (VBP) leading to secondary tissue edema, which result in unfavorable outcomes.[8] However, the role of glycocalyx in VBP has been recently challenged.[9]

The type of fluid chosen for expanding blood volume or compensate for intraoperative blood loss (leading to ANH) may alter glycocalyx components inconsistently. Colloidal solutions may preserve glycocalyx components, by maintaining the shear stress on endothelial due to a higher viscosity,[10] osmotic pressure and also to the presence of macromolecules. However, the degree to which glycocalyx shedding occurs in response to a stepwise ANH using different types of fluid is not well described. In addition, the consequences of severe ANH on the VBP are unknown.

The aims of the present study were: (i) to investigate which of the different component of the glycocalyx were shed according to the type of fluid used for stepwise ANH and (ii) their consequences on microcirculatory parameters and vascular barrier permeability. We hypothesized that ANH with balanced HES would result in lesser damage to the glycocalyx without affecting vascular barrier permeability (VBP).

Materials and methods

Animals

This study was approved by the Animal Research Committee of the Academic Medical Center of the University of Amsterdam (DFL 190AA). Care and handling of the animals were in accordance with the guidelines from the Institutional Animal Care and Use Committees. This manuscript adheres to the applicable ARRIVES guidelines. Experiments were performed at 8:30 am in the Department of experimental surgery (Academic Medical Center, Amsterdam, The Netherlands) on male Wistar albino rats (Charles River Laboratories, The Netherlands), aged 10±3 weeks, with a mean±SD body weight (B.W.) of 309±17 g.

Surgical preparation

Anesthesia was induced with an intraperitoneal injection of 100 mg.kg^{-1} ketamine (Nimatek®; Eurovet, The Netherlands), 0.5 mg.kg^{-1} medetomidine (Domitor; Pfizer, USA) and 0.05 mg.kg^{-1} atropine-sulfate (Centrafarm, The Netherlands) and was maintained with 50 mg.kg.h^{-1} ketamine. Fluid maintenance consisted in Ringer's acetate (Baxter, Utrecht, The Netherlands) at a rate of 10 ml.kg^{-1}.h^{-1}. After a tracheostomy, the animals were connected to a ventilator (Babylog 8000, Dräger, Nederland) and ventilated with tidal volumes of 6 ml.kg^{-1} with a positive end-expiratory pressure of 3 cmH$_2$O and an FiO$_2$ of 0.4. A heating pad under the animal allowed the body temperature to be controlled and maintained at 37±0.5°C. The end-tidal CO$_2$ was maintained between 30 and 35 mmHg (CapnoMac, Datex-Ohmeda, USA).

The right carotid (pressure) and left femoral (for blood shedding and samples) arteries and jugular (anesthesia and fluid maintenance) and femoral (fluid resuscitation) veins were cannulated with polyethylene catheters (outer diameter = 0.9 mm; Braun, Germany). The right biceps femoris was exposed, and the femoral artery blood flow (FABF) was monitored with a transonic flowmeter probe (0.5 mm, T206; Transonic Systems Inc). To prevent muscle desiccation, the exposed area was protected with a humidified gauze with warm 0.9% NaCl. The bladder was catheterized via a mini-midline incision with a polyethylene tube (outer diameter = 1.2 mm) and a homemade tip to prevents spontaneous displacement and traumatic lesions. The urine output was quantified.

Experimental protocol

Animals were randomized according to a unique code generated by an internet website. On the day of experiment, a technician prepared the fluid used for the hemodilution protocol according to the generated code. After a 30-min stabilization period, baseline (BL) values were recorded, and arterial blood gas was assessed (ABLFlex 80, Radiometer, Denmark).

Acute normovolemic hemodilution (ANH) was induced by stepwise exchange of blood (withdrawn at a rate of 0.5 ml min^{-1} using a syringe pump (Harvard Apparatus, USA)) and exchanged with one of the following plasma expanders according to the following ratios; 1:1 for balanced hydroxyethyl starch (Volulyte® HES 130/0.4, in Ringer's acetate), 1:3 for balanced crystalloid or normal saline 0.9%, until targeted hematocrit (Hct) levels were reached. All solutions were purchased from Fresenius Kabi, Germany. Each stepwise hemodilution targeted 4 different levels of Hct: 35%, 25%, 20% and 15%. Each step was reached in 15-20 minutes and stabilized for 15 minutes before taking measurements or blood samples. The Hct levels were checked before blood sampling with the help of capillary tubes and a microhematocrit tube reader (EZ Reader, LW Scientific, Atlanta, GA, USA). The time course of the experiment is presented in **Supplementary Figure 1**.
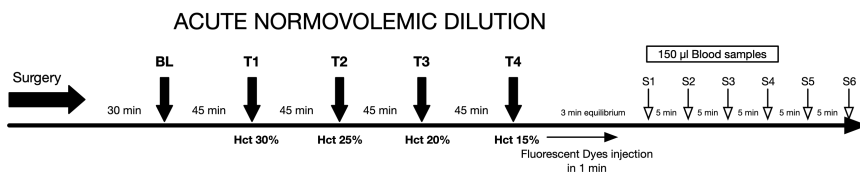
Supplementary Figure 1. Time course of the acute normovolemic hemodilution

Biomarkers of glycocalyx shedding

Circulating plasma syndecan-1, heparan sulfate and hyaluronan considered as surrogates of glycocalyx degradation were measured. Plasma samples were taken at each timepoint and stored at -20°C. Then, plasma samples were thawed and analyzed using commercial enzyme-linked immunoabsorbent assay (ELISA) kits according to the manufacturer's instructions: DuoSet® Hyaluronan (DY3614, R&D Systems, Minneapolis, USA), Syndecan-1/CD138(SCD1) ELISA kit (Cusabio Biotech Co., Ltd., Wuhan, China) and heparan sulfate proteoglycan 2 (HSPG2) ELISA Kit (Cusabio Biotech Co., Ltd., Wuhan, China).

Skeletal microcirculatory measurements

A hand-held in vivo microscope using incident dark-field (IDF) imaging, CytoCam™ (Braedius Scientific, Huizen, The Netherlands) was placed on the surface of the exposed biceps femoris to continuously monitor the same microcirculatory spot with the help of a micromanipulator.[11] One hundred frames clips (100 sec) were recorded at every time point (each Hct level). All clips obtained were randomly anonymized and the analysis of the microvasculature was performed in a blinded fashion (group and time point) at baseline and at each timepoint of hemodilution with AVA 3.2 (Microvision Medical, Amsterdam, The Netherlands) for total vessel density (TVD), perfused vessel density (PVD), proportion of perfused vessels (PPV) and the mean flow index (MFI) by 2 trained and independent operators (Z. U. and Y. I.) and reviewed by 2 other experts (P.G and M. H.) as described elsewhere.[12]

Assessment of vascular barrier permeability

Tissue edema

At the end of the experiment, different organs (heart, brain, kidney, lung and liver) were harvested to determine their water content. The organs were placed in the oven, held at 100°C for 24 h. The wet-to-dry weight ratio were calculated as follows: wet tissue weight/dry tissue weight ratio.

Fluorescent tracers

The analysis of VBP using fluorescent has been described elsewhere.[9] At the end of the experiment, fluid maintenance was stopped. Three fluorescent dyes conjugated with different sizes of molecules and dissolved in saline were thoroughly mixed together and injected intravenously by hand over 1 minute: Texas Red-40 kDa dextran (10 mg/ml, D1829, Molecular Probes, ThermoFischer Scientific, Breda, the Netherlands), Albumin-Alexa 680 (5 mg/ml, A34787, Molecular Probes, ThermoFischer Scientific, Breda, the Netherlands), and fluorescein isothiocyanate (FITC)-500 kDa dextran (10 mg/ml, MFCD00131092, Sigma-Aldrich, Zwijndrecht, the Netherlands) (100 μl each). Blood samples (200 μl) were withdrawn at 2, 5, 10, 15, 20, 25 and 30 minutes to obtain the decay in plasma concentration of the dyes as we had researched previously. Plasma concentrations were measured for each dye in a 96-well plate fluorometer

(ClarioStar, BMG LabTech, Ortenberg, Germany) in accordance with the excitation/emission wavelengths of each dye and after obtaining a standard calibration curve: 580±20 nm/625±20 nm for FITC, 480±15 nm/530±25 nm for TexasRed and 675±10 nm/740±40 nm for Alexa 680. The concentration-time curves of all dyes were fitted for each experiment separately with a monoexponential function. A retention ratio (RR) of the dye was calculated as follows: RR = final concentration at 30 min / initial concentration at 2 min.

For total intravascular volume (TIV) and plasma volume (PV) determinations, the concentration of Albumin-Alexa 680 was determined at time = 2 min after bolus injection according to the following calculation: TIV (ml) = ([Albumin-Alexa syringe] x 0.1) / [Albumin Alexa plasma]) and PV (ml) = ([Albumin-Alexa syringe] x 0.1) / [Albumin Alexa plasma]) x (1-Hematocrit (%)).

Statistical analysis

Values are expressed as mean±standard deviation (SD) when normally distributed (Kolmogorov-Smirnov test), or as median [IQR] otherwise. Repeated measures 2-way analysis of variance (RM-ANOVA) (2 factors: time as a related within-animal factor and group as a between-animal factor) with *post hoc* Bonferroni's correction test for multiple analysis were used to determine intergroup and/or intragroup differences of hemodynamic, microcirculatory parameters, biochemistry, and glycocalyx degradation biomarkers. When significant interaction was observed between time and group, we reported simple main effects of group (type of fluid) compared to the control and to the balanced HES groups at each timepoint and the simple main effect of time versus baseline within the same group. Ordinary one-way ANOVA with Bonferroni's correction was used for the retention ratios. Because of their non-gaussian distribution, Kurskal-Wallis test was used Dunn's posttest. The decays in plasma concentration of fluorescent dyes at each timepoint were fitted with an exponential one phase decay using the least squares methods. Statistical analysis was performed using GraphPad Prism version 7.0a for Mac (GraphPad Software, La Jolla, USA).

For comparison of microcirculatory parameters between baseline, and hemodilution time-points, two-way linear mixed effects model analysis was used (R environment for statistical computing, version 3.4.1, using the R library *lme4*, version 1.1.13). P values for individual fixed effects were obtained by Satterthwaite approximation. For subgroups where a statistically significant effect was detected a one-way linear mixed effect model was applied for subgroup

analysis. The overall significance level for each hypothesis was 0.05. Adjusted P-values were reported throughout the manuscript in post hoc tests. We did not perform any *a priori* power analysis.

Results

All rats (n=24) survived the stepwise ANH. However, ANH was associated with a significant decrease in mean arterial pressure (MAP) in all groups compared to control, that was maximal at Htc 15% (F (4, 20) = 113.7, *P<0.0001*). The hemodynamic data is summarized in **Table 1**. Stepwise ANH with NaCl 0.9% induced progressive metabolic acidosis (F (3, 15) = 16.89, *P<0.0001*) compared to control (mean diff. 0.12, 95%CI [0.09 to 0.15], *P<0.0001*) and baseline (mean diff. 0.165, 95%CI [0.13 to 0.2], *P<0.0001*) accompanied by changes in pH and bicarbonate levels (**Table 1**). At Hct level of 15%, ANH was significantly associated with hyperlactatemia compared to control irrespective of the fluid administered (mean diff. -1.27, 95%CI [-1.81 to -0.72] for balanced colloid, -0.95, 95%CI [-1.49 to -0.41] for balanced crystalloid, and -0.85, 95%CI [-1.39 to -0.31] for normal saline, *P<0.001*).

The urine output was markedly decreased along with the level of Hct in all groups compared to baseline values (F (4, 20) = 15.35, *P<0.0001*) (**Figure 1**). However, at Hct level of 15%, only the ANH with NaCl 0.9% group exhibited a significantly lower urine output compared to control group (mean diff. 0.60, 95%CI [0.11 to 1.1], *P=0.013*).
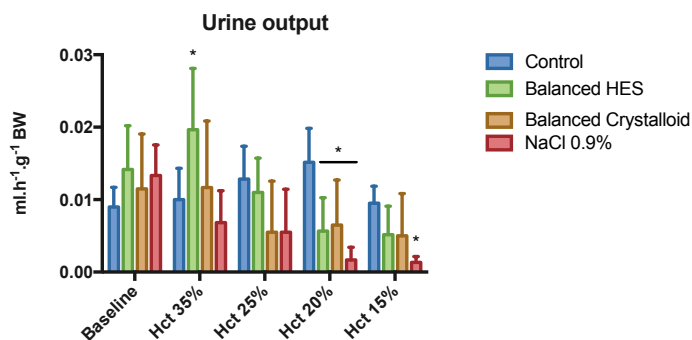
Figure 1. Urine output during acute normovolemic hemodilution

*Repeated measures 2-way ANOVA test used with Bonferroni's correction to adjust for multiple comparisons. * adjusted P<0.01 vs. Control group at the same time point. (n=6/group).*

The total volume of balanced HES during the experiment to achieve each step of ANH, was significantly lesser (10.8±0.9 ml) than in balanced crystalloid (27.5±2.8 ml) and normal saline (29±2.2 ml) groups (*P=0.0001*) (**Supplementary Figure 2**).

Table 1. Hemodynamics, blood hematocrit, hemoglobin, lactate and arterial partial pressure of CO$_2$ levels throughout experiment

	BL	Hct 30%	Hct 25%	Hct 20%	Hct 15%
MAP (mmHg)					
Control	92±14	80±4	80±11	80±10	84±10
Balanced HES	95±10	66±1*	60±1*	58±4*	56±5*
Balanced Crystalloid	87±10	66±11*	54±4*	54±8*	47±7*
NaCl %0.9	90±12	61±5*	56±5*	50±2*	42±5*
CVP (mmHg)					
Control	7±1	7±1	6±2	6.5±1.5	7±1
Balanced HES	6±1	6±1	7±1	6.9±1.3	7±1
Balanced Crystalloid	6±1	7±1	7±2	7±2	7±2
NaCl %0.9	5±1*	5±1*	6±1#	6±1#	6±1*#
Hemoglobin (g/dl)					
Control	14.2±0.5	13.5±1.1	12.9±1	13.6±1.1	12.2±1.3
Balanced HES	14.6±0.8	9.6±0.5*	7.9±0.7*	6.2±0.4*	4.6±0.4*
Balanced Crystalloid	14.9±0.8	9.9±0.9*	7.8±0.6*	6.2±0.3*	4.7±0.4*
NaCl %0.9	14.3±1.4	10.1±0.3*	8±0.4*	6.5±0.5*	4.8±0.2*
Hematocrit (%)					
Control	44±1	41±3	40±3	41±4	37±4
Balanced HES	45±2	30±2*	25±1*	20±1*	15±2*
Balanced Crystalloid	46±3	31±2*	25±2*	20±1*	15±1*
NaCl %0.9	45±4	31±1*	25±1*	21±1*	15±1*
pH					
Control	7.42±0.05	7.40±0.02	7.42±0.03	7.42±0.02	7.41±0.02
Balanced HES	7.45±0.03	7.44±0.03	7.44±0.04	7.40±0.03	7.39±0.03
Balanced Crystalloid	7.44±0.03	7.41±0.02	7.40±0.02	7.40±0.02	7.36±0.02*
NaCl %0.9	7.46±0.03	7.38±0.03	7.34±0.03*#	7.31±0.03*#	7.29±0.05*#
Lactate (mmol/L)					
Control	0.9±0.3	1.2±0.3	1.2±0.6	1.5±0.5	1.5±0.5
Balanced HES	0.9±0.2	1.1±0.3	1.3±0.5	2.1±0.8*	2.7±1*
Balanced Crystalloid	1.3±0.3	1.4±0.6	1.9±0.7*	2.4±0.7*	2.4±0.7*
NaCl %0.9	1.1±0.2	1.1±0.7	1.4±0.3*	1.6±0.4#	2.5±0.5*
PaCO$_2$ (mmHg)					
Control	34±5	33±4	30±1	30±1	33±3
Balanced HES	31±3	35±4	36±4*	39±3*	39±2*
Balanced Crystalloid	31±3	36±5	37±3*	36±3*	41±3*
NaCl %0.9	30±3	35±3	36±4*	38±5*	36±3#

*MAP; mean arterial pressure, FABF; femoral artery blood flow, HES: Hydroxyethyl starch. Data is presented as mean±SD. * Adjusted P <0.05 vs. control group, # adjusted P value vs. balanced HES group*
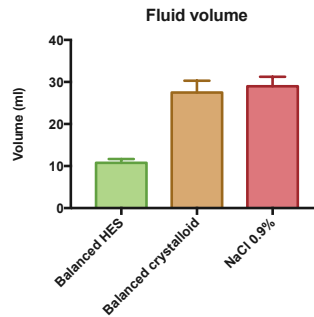
Fluid volume

Supplementary Figure 2. Total fluid volume administered to achieve a hematocrit level of 15% by the end of experiment

Plasma and blood volume

The plasma volume was increased in all groups compared to control ($F_{(3, 20)} = 35.68$, *P<0.0001*) (**Figure 2A**). On the contrary, the total intravascular volume (**Figure 2B**) was only increased in the balanced HES group (18.8±1.1 ml) compared to controls (17.2 ±1.2 ml) (mean diff. -1.6, 95%CI [-3.1 to -0.07], *P=0.039*). Despite similar hematocrit levels in all ANH groups (**Table 1**), hemodilution with balanced HES resulted in an increased intravascular volume.
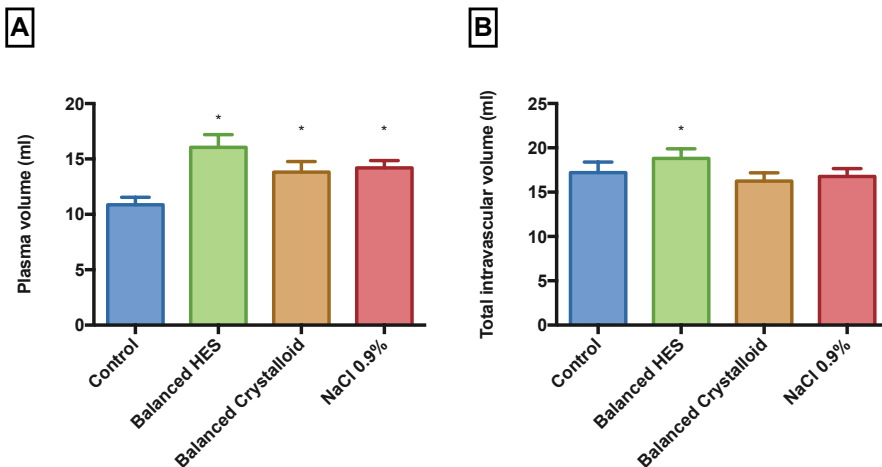
Figure 2. Plasma (panel A) and total intravascular (panel B) volumes at the end of the experiment determined by the measure of albumin Alexa

*Ordinary One-way ANOVA test with Bonferroni's correction to adjust for multiple comparisons. * adjusted P<0.001 vs. Control group (n=6/group)*

Glycocalyx degradation biomarkers

Syndecan-1 was degraded during the time course of experiment in all groups including controls. At the end of the experiment (Hct 15%), syndecan-1 levels were significantly higher than at baseline (F (3, 60) = 23.88, *P<0.0001*) (**Figure 3A**). ANH with normal saline resulted in a significant degradation of the heparan sulfate (**Figure 3B**) and hyaluronan (**Figure 3C**) components compared to control group (mean diff. -1213, 95%CI [-2070 to -356], *P=0.003*, and -66, 95%CI [-115 to -18], *P=0.004* respectively). Similarly, balanced crystalloid altered the hyaluronan component (mean diff. -59, 95%CI [-107.6 to -10.33], *P=0.013*) but without affecting heparan sulfate. ANH using balanced HES produced minimal changes on the various components of the glycocalyx.
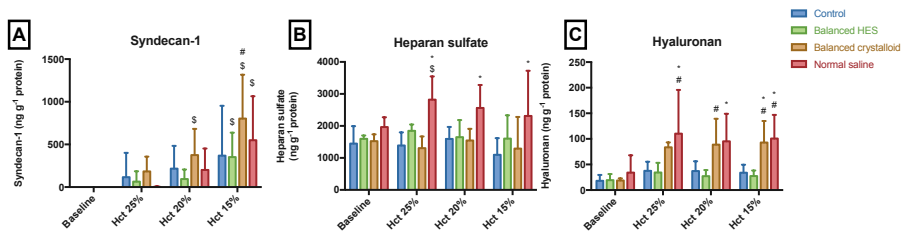
Figure 3. Plasma levels of syndecan-1 (panel A), heparan sulfate (panel B) and hyaluronan (panel C) during the experiment

*Increased glycocalyx shedding persists after fluid resuscitation except for the hyaluronan component, which is decreased with balanced HES resuscitation. Repeated measures 2-way ANOVA test used with Bonferroni's correction to adjust for multiple comparisons. * adjusted P<0.01 vs. Control group at the same time point, # P<0.05 vs. balanced HES group, $ P<0.05 vs. baseline value within the same group. (n=6/group)*

Vascular Barrier permeability

Tissue edema

The water content of each organ using the wet-to-dry weight ratio method is summarized in **Supplementary Figure 3**. Except in the liver, no significant tissue edema was present after ANH regardless of the type of fluid administered.
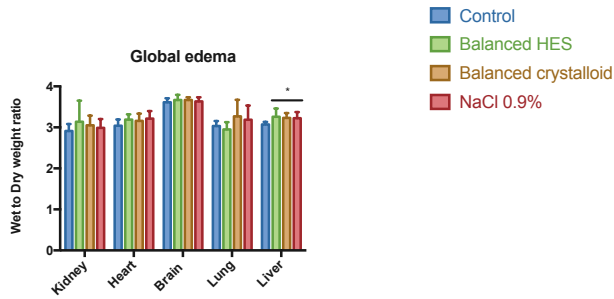
Supplementary Figure 3. Edema in different organs assessed by the wet to dry weight ratio

* adjusted P<0.05 versus control group within the same organ

Fluorescent tracers in the vascular compartment

The retention ratios of the fluorescent dyes injected in the vascular system after the last ANH timepoint (Hct 15%) are presented in **Figure 4**. At 30 minutes after injection, the smallest fluorescent dyes (Texas Red 40kDa) were significantly retained within the vascular system independently of the fluid administered (F (3, 19) = 7.529, *P=0.0016*) as compared to the control group. The balanced HES group showed the highest difference (mean diff. -0.2, 95%CI [-0.32 to -0.08], *P=0.0012*) when compared to the control group. These results bear out the absence of increased vascular leakage in ANH.
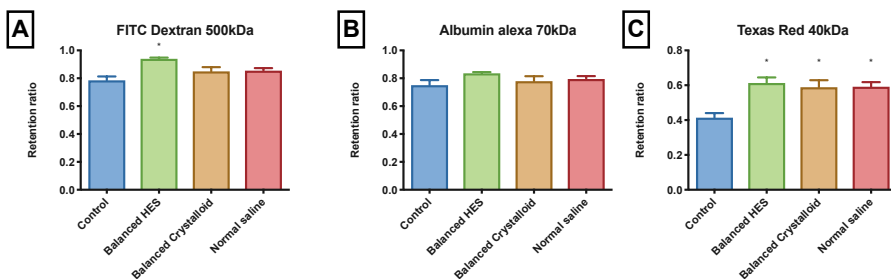
Figure 4. Retention ratios of fluorescent dyes at the end of the experiment

Ordinary One-way ANOVA test with Bonferroni's correction to adjust for multiple comparisons. * adjusted P<0.05 vs. Control group. (n=6/group)

In the **supplementary Figure 4** are presented the decays curves associated with each fluid group according to each fluorescent tracer. Compared to retention ratios, the powers of the exponential decay curves only tended to be different between fluids and control groups with regards to the Texas Red 40kDa dye but without reaching significance.
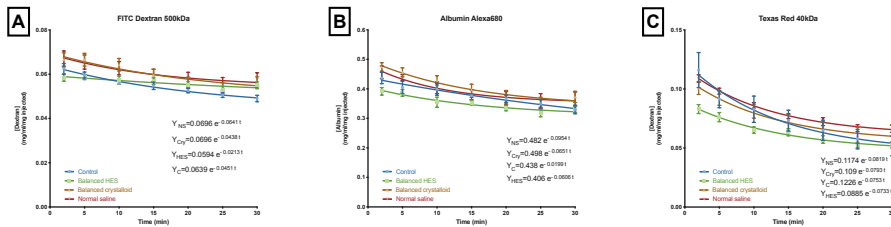
Supplementary figure 2. Decay traces of each fluid group classified by fluorescent tracer

Microcirculation of the muscle during stepwise ANH

Figure 5 depicts the microcirculatory changes occurring during ANH according to the type of fluid used. When compared to baseline values within each group, ANH altered the total vessel density (TVD) and the perfused vessel density (PVD). ANH with balanced colloid demonstrated a lesser degree of microcirculatory parameters alteration especially with regards to PVD. The maximum decrease in TVD and PVD were observed at an Hct level of 15% in the crystalloid groups, with mean differences of 3.1, 95%CI [0.32 to 5.9], *P=0.02* and 4.7, 95%CI [1.9 to 7.5], *P=0.0003* for balanced crystalloid and normal saline groups respectively compared to baseline. No changes were detected in MFI or PPV parameters when compared to baseline values.
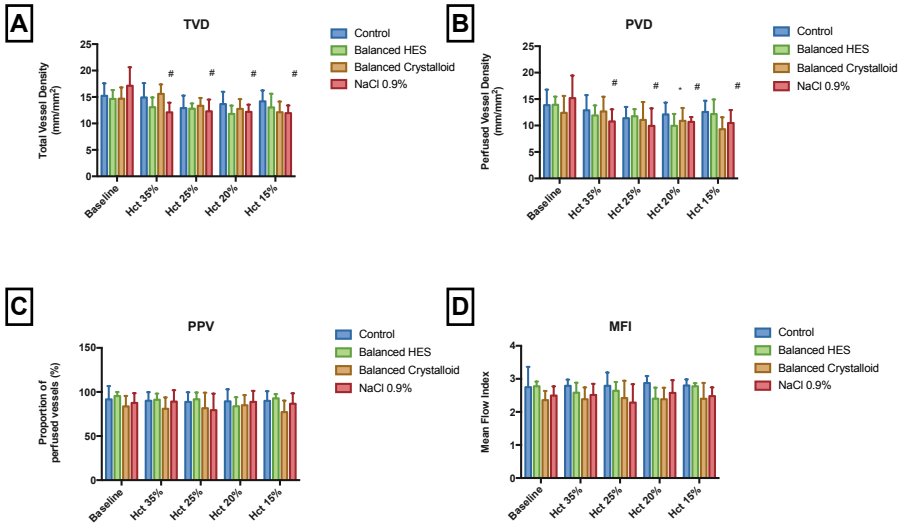
Figure 5. Microcirculatory muscle alterations at each step of acute normovolemic hemodilution. Total vessel density (Panel A), Perfused vessel density (Panel B), Proportion of perfused vessels (Panel C), and Mean Flow Index (Panel D) are presented.

Two-way linear mixed effects model analysis was used. $ P<0.05 compared to baseline within the same group. (n=6/group)

Discussion

In this experimental study, ANH with balanced HES did prevent the shedding of different component of the glycocalyx. On the contrary, crystalloids, either balanced or not, significantly altered the different components of the glycocalyx, namely syndecan-1 and hyaluronan. Only ANH with normal saline produced a degradation of all three main constituents of the glycocalyx (heparan sulfate, syndecan-1, hyaluronan). However, despite glycocalyx degradation following maximum ANH, no increase in VBP was observed, irrespective of the fluid used and its composition. ANH at an Hct level of 15% induced microcirculatory disturbances partially prevented with the use of balanced colloid compared to crystalloids and were associated with impaired macrohemodynamics.

These results are consistent previous studies and are possibly the result of a lower plasma and blood viscosity that dampened the endothelial cell response to shear stress.[13,14] Guerci *et al.* previously demonstrated that plasma and blood viscosity were similarly altered following resuscitation of non-traumatic hemorrhagic shock with either low (Ringer's Lactate) or high (HES) viscosity plasma expanders.[15] In our study, extreme ANH induced microcirculatory disturbances associated with endothelium dysfunction, as previously reported,[13] but did not induce an increase the VBP.

The consequences of hemodilution on the degradation of glycocalyx are not well known because of limited data. Glycocalyx shedding has been confirmed in preclinical models, as well as in human clinical settings, in various conditions such as ischemia/reperfusion injury,[16] trauma,[17,18] sepsis,[19] and even during hyperglycemia[20] or after smoking.[21] In a clinical intraoperative setting, Chappell *et al.* compared the effects of volume loading (top-loading) and ANH on the glycocalyx shed products levels using HES 130/0.4 solely in elective surgery in patients with normal heart function.[7] Volume loading induced a significant release of atrial natriuretic peptide that was associated with increased plasma hyaluronan and syndecan-1 levels whereas ANH did not. These findings are consistent with our results in ANH with balanced HES. In our study however, different fluid composition yielded different profiles of glycocalyx shed products. Although plasma volumes were markedly increased secondary to ANH in all groups compared to controls, the total intravascular volume was increased only in the balanced HES group following ANH. Despite this increase in plasma volume, no significant increase in syndecan-1 nor hyaluronan was observed compared to controls at the same time point in the balanced HES group.

The microcirculatory disturbances observed during ANH with normal saline may have several explanations. First, the macrohemodynamics were severely impaired at the latest stage of ANH with a MAP of 42±4 mmHg in the normal saline group. In this model, the evolution of microcirculation may parallel those of macrocirculation (type II).[22] ANH had a negative impact on blood pressure despite a close to normal intravascular volume. Second, ANH had markedly decreased the viscosity and shear stress which subsequently alters the vascular tone.[13] Indeed, the glycocalyx participates in endothelium shear stress-induced reactivity, by sensing the flow and mediating mechanotransduction signals, through mainly syndecan-1.[14,23] In our study, syndecan-1 was the most shed component by the use of normal saline. However, the alterations observed in the vascular tone and the microcirculatory disturbances did not translate in increased capillary leakage. These results suggest that essential component of the vascular barrier, such as intercellular junctions, withstood despite partial glycocalyx degradation,[24] thus maintaining a normal transendothelial outflux of proteins and water towards the interstitial space. Small molecules (Texas Red Dextran 40kDa) did not escape more rapidly from the vascular compartment as suggested by the similar exponential decay curves fitted to plasma concentration of this dye, irrespective of the fluid used for ANH. Surprisingly, the retention ratios in all ANH groups were higher than the controls emphasizing the absence of vascular barrier disruption during ANH. One would expect a decrease in retention ratios for small molecules with the vascular barrier became more permeable to water and proteins. In this study, the water keeps on escaping the vascular space without being accompanied by small proteins. Water is not retained more than in physiological conditions. These results imply that irrespective of the type of fluid administered, its water content will relentlessly escape from the vasculature either by urine production or by transendothelial outflux. In case of acute kidney injury, the latter is more likely to occur. However, in our study no fluid accumulation with the wet-to-dry weight ratio technique was evidenced.

Although less performed nowadays, ANH remains a well-recognized safe procedure for patient blood management in the perioperative period.[3,4] Unintended ANH may also result from intraoperative fluid administration during surgery. Actually, because of changes in red blood cells transfusion thresholds, more and more patients remain anemic during the postoperative course, secondary to unintentional ANH, without apparent negative outcomes.[25,26] Even if ANH with normal saline or balanced crystalloid may negatively impact the glycocalyx, the consequences of such a degradation remain inconclusive. However, Joosten *et al.* showed that goal-directed administration of balanced HES was associated with fewer postoperative

complications than with balanced crystalloids and was attributed to a lower intraoperative fluid balance.[27]

Finally, balanced HES was less likely to induce shedding of heparan sulfate, hyaluronan and syndecan-1 components compared to crystalloids, making it a more suitable fluid for ANH from a glycocalyx perspective. Although balanced HES did not induce significant microcirculatory disturbances, lactate levels were similar in all ANH groups at an Hct of 15%. Oxygen debt secondary to critical decrease in oxygen delivery but not perfusion is the most likely mechanism behind lactate production in this study. Despite the increase in lactate levels, no alteration in pH values were noted in the balanced HES group. In a previous study in dogs, cardiac function as well as myocardial ultrastructure, were better preserved in animals that underwent ANH with non-balanced HES even at extremely low values of hemoglobin compared to lactated Ringer's.[28] Similarly, lung structure and function were better preserved after ANH with HES than with lactated Ringer's.[29]

Limitations

This study has several limitations. First, the analysis of the VBP was performed with 2 assays. Previously, we demonstrated similar results about the relative contribution of the glycocalyx to the vascular barrier permeability in a non-traumatic hemorrhagic shock model in rodents using 4 different techniques.[9] Second, we did not investigate the glycocalyx ultrastructure by electronic microscopy nor *in vivo* fluorescent microscopy. We relied on surrogates of glycocalyx shedding products that may suffer some limitations. However, this approach allows translation to human clinical research. Third, we did not analyze the consequences of hemodilution on microcirculatory PO_2 in different organs to determine which fluid can provide the best tissue oxygenation. A similar type of study has been performed previously.[30]

Conclusion

In this model of severe ANH, the use of a balanced colloid better preserved the glycocalyx while maintaining microcirculatory parameters, compared to crystalloids either balanced or not. Although the volumes required to achieve similar ANH in all groups were different, no evidence of increased vascular barrier permeability was observed. These results suggest that glycocalyx shedding may induce a loss in vascular motor tone response to shear stress but without

6

subsequent increase in VBP due to intercellular disruption for instance. Normal saline was the fluid having the more deleterious effects during ANH.

Financial disclosures & funding

Conflicts of interest

Dr Can Ince runs an Internet site microcirculationacademy.org which offers services (e.g., training, courses, analysis) related to clinical microcirculation and, has received honoraria and independent research grants from Fresenius-Kabi, Baxter Health Care, and AM-Pharma; has developed SDF imaging; is listed as an inventor on related patents commercialized by MicroVision Medical under a license from the Academic Medical Center; and has been a consultant for MicroVision Medical in the past but has not been involved with this company for more than 5 years. The company that developed the CytoCam-IDF imaging system, Braedius Medical, is owned by a relative of Dr Ince. Dr Ince has no financial relationship with Braedius Medical (i.e., never owned shares or received consultancy or speaker fees). Dr Martin Westphal is the Chief Medical Officer of Fresenius Kabi AG. The remaining authors declare no conflicts of interest.

References

1.   Bampoe S, Odor PM, Dushianthan A, et al. Perioperative administration of buffered versus non-buffered crystalloid intravenous fluid to improve outcomes following adult surgical procedures. *Cochrane Database Syst Rev*. 2017;9:CD004089.

2.   Qureshi SH, Rizvi SI, Patel NN, Murphy GJ. Meta-analysis of colloids versus crystalloids in critically ill, trauma and surgical patients. *Br J Surg*. 2016;103(1):14-26.

3.   Grant MC, Resar LMS, Frank SM. The Efficacy and Utility of Acute Normovolemic Hemodilution. *Anesth Analg*. 2015;121(6):1412-1414.

4.   Zhou X, Zhang C, Wang Y, Yu L, Yan M. Preoperative Acute Normovolemic Hemodilution for Minimizing Allogeneic Blood Transfusion: A Meta-Analysis. *Anesth Analg*. 2015;121(6):1443-1455.

5.   Lipowsky HH. Role of the Glycocalyx as a Barrier to Leukocyte-Endothelium Adhesion. *Adv Exp Med Biol*. 2018;1097:51-68.

6.   Zeng Y, Zhang XF, Fu BM, Tarbell JM. The Role of Endothelial Surface Glycocalyx in Mechanosensing and Transduction. *Adv Exp Med Biol*. 2018;1097:1-27.

7.   Chappell D, Bruegger D, Potzel J, et al. Hypervolemia increases release of atrial natriuretic peptide and shedding of the endothelial glycocalyx. *Crit Care*. 2014;18(5):538.

8.   Makaryus R, Miller TE, Gan TJ. Current concepts of fluid management in enhanced recovery pathways. *Br J Anaesth*. 2018;120(2):376-383.

9.   Guerci P, Ergin B, Uz Z, et al. Glycocalyx Degradation Is Independent of Vascular Barrier Permeability Increase in Nontraumatic Hemorrhagic Shock in Rats. *Anesth Analg*. November 2018.

10.   Walker AM, Xiao Y, Johnston CR, Rival DE. The viscous characterization of hydroxyethyl starch (HES) plasma volume expanders in a non-Newtonian blood analog. *Biorheology*. 2013;50(3-4):177-190.

11.   Aykut G, Veenstra G, Scorcella C, Ince C, Boerma C. Cytocam-IDF (incident dark field illumination) imaging for bedside monitoring of the microcirculation. *Intensive Care Med Exp*. 2015;3(1):40.

12.   Massey MJ, Shapiro NI. A guide to human in vivo microcirculatory flow image analysis. *Crit Care*. 2016;20:35.

13.   Cabrales P, Tsai AG. Plasma viscosity regulates systemic and microvascular perfusion during acute extreme anemic conditions. *Am J Physiol Heart Circ Physiol*. 2006;291(5):H2445-2452.

14.   Martini J, Cabrales P, Tsai AG, Intaglietta M. Mechanotransduction and the homeostatic significance of maintaining blood viscosity in hypotension, hypertension and haemorrhage. *J Intern Med*. 2006;259(4):364-372.

15.   Guerci P, Tran N, Menu P, Losser M-R, Meistelman C, Longrois D. Impact of fluid resuscitation with hypertonic-hydroxyethyl starch versus lactated ringer on hemorheology and microcirculation in hemorrhagic shock. *Clin Hemorheol Microcirc*. 2014;56(4):301-317.

16.   van Golen RF, Reiniers MJ, Vrisekoop N, et al. The mechanisms and physiological relevance of glycocalyx degradation in hepatic ischemia/reperfusion injury. *Antioxid Redox Signal*. 2014;21(7):1098-1118.

17.   Chignalia AZ, Yetimakman F, Christiaans SC, et al. The glycocalyx and trauma: a review. *Shock*. 2016;45(4):338-348.

18.   Tuma M, Canestrini S, Alwahab Z, Marshall J. Trauma and Endothelial Glycocalyx: The Microcirculation Helmet? *Shock*. 2016;46(4):352-357.

19.   Ince C, Mayeux PR, Nguyen T, et al. The endothelium in sepsis. *Shock*. 2016;45(3):259-270.

20.   Zuurbier CJ, Demirci C, Koeman A, Vink H, Ince C. Short-term hyperglycemia increases endothelial glycocalyx permeability and acutely decreases lineal density of capillaries with flowing red blood cells. *J Appl Physiol*. 2005;99(4):1471-1476.

21.   Ikonomidis I, Marinou M, Vlastos D, et al. Effects of varenicline and nicotine replacement therapy on arterial elasticity, endothelial glycocalyx and oxidative stress during a 3-month smoking cessation program. *Atherosclerosis*. 2017;262:123-130.

22.   Ince C, Guerci P. Why and when the microcirculation becomes disassociated from the macrocirculation. *Intensive Care Med*. 2016;42(10):1645-1646.

23.   Weinbaum S, Tarbell JM, Damiano ER. The structure and function of the endothelial glycocalyx layer. *Annu Rev Biomed Eng*. 2007;9:121-167.

24.   Curry FE, Adamson RH. Endothelial glycocalyx: permeability barrier and mechanosensor. *Ann Biomed Eng*. 2012;40(4):828-839.

25.   American Society of Anesthesiologists Task Force on Perioperative Blood Management. Practice guidelines for perioperative blood management: an updated report by the American Society of Anesthesiologists Task Force on Perioperative Blood Management*. *Anesthesiology*. 2015;122(2):241-275.

26.   Carson JL, Guyatt G, Heddle NM, et al. Clinical Practice Guidelines From the AABB: Red Blood Cell Transfusion Thresholds and Storage. *JAMA*. 2016;316(19):2025-2035.

27.   Joosten A, Delaporte A, Ickx B, et al. Crystalloid versus Colloid for Intraoperative Goal-directed Fluid Therapy Using a Closed-loop System: A Randomized, Double-blinded, Controlled Trial in Major Abdominal Surgery. *Anesthesiology*. 2018;128(1):55-66.

28.   Fraga A de O, Fantoni DT, Otsuki DA, Pasqualucci CA, Abduch MCD, Junior JOCA. Evidence for myocardial defects under extreme acute normovolemic hemodilution with hydroxyethyl starch and lactated ringer's solution. *Shock*. 2005;24(4):388-395.

29.   Margarido CB, Margarido NF, Otsuki DA, et al. Pulmonary function is better preserved in pigs when acute normovolemic hemodilution is achieved with hydroxyethyl starch versus lactated Ringer's solution. *Shock*. 2007;27(4):390-396.

30.   Johannes T, Mik EG, Nohé B, Unertl KE, Ince C. Acute decrease in renal microvascular PO2 during acute normovolemic hemodilution. *Am J Physiol Renal Physiol*. 2007;292(2):F796-803.

6

7

A LED-BASED PHOSPHORIMETER FOR MEASUREMENT OF MICROCIRCULATORY OXYGEN PRESSURE

Philippe Guerci,[1,2] Yasin Ince,[1] Paul Heeman,[3] Dirk Faber [4]

Bulent Ergin,[1] and Can Ince[1]

1.   Department of Translational Physiology, Academic Medical Center, Amsterdam, The Netherlands
2.   INSERM U1116, Faculty of Medicine, University of Lorraine, Nancy, France
3.   Department of Medical Technical Innovation & Development (MIO), Academic Medical Center, Amsterdam, The Netherlands
4.   Department of Biomedical Engineering and Physics, Academic Medical Center, Amsterdam, The Netherlands

Abstract

Quantitative measurements of microcirculatory and tissue oxygenation are of prime importance in experimental research. Non-invasive phosphorescence quenching method has given further insight into the fundamental mechanisms of oxygen transport to healthy tissues and in models of disease. Phosphorimeters are devices dedicated to the study of phosphorescence quenching. The experimental applications of phosphorimeters range from measuring a specific oxygen partial pressure (PO_2) in cellular organelles such as mitochondria, finding values of PO_2 distributed over an organ or capillaries, to measuring microcirculatory PO_2 changes simultaneously in several organ systems.

Most of the current phosphorimeters use flash lamps as a light excitation source. However, a major drawback of flash lamps is their inherent plasma glow that persists for tens of microseconds after the primary discharge. This complex distributed excitation pattern generated by the flash lamp can lead to inaccurate PO_2 readings unless a deconvolution analysis is performed. Using light-emitting diode (LED), a rectangular shaped light pulse can be generated that provides a more uniformly distributed excitation signal. This study presents the design and calibration process of an LED-based phosphorimeter (LED-P).

The *in vitro* calibration of the LED-P using Palladium(II)-meso-tetra(4-carboxyphenyl)-porphyrin (Pd-TCCP) as a phosphorescent dye is presented. The pH and temperature were altered to assess whether the decay times of the Pd-TCCP measured by the LED-P were significantly influenced. An *in vivo* validation experiment was undertaken to measure renal cortical PO_2 in a rat subjected to hypoxic ventilation conditions and ischemia/reperfusion. The benefits of using LEDs as a light excitation source are presented.

Introduction

The precise measurement of tissue oxygenation *in vivo* can be considered of major importance for assessing the success of the cardiovascular system in transporting oxygen to the parenchymal cells to sustain their viability in support of organ function. This exchange primarily occurs in the smallest vessels of the microvascular bed.[1,2] Ideally, measurement techniques must be quantitative, non-invasive, and associated with a specific physiological compartment (e.g., capillary, interstitial, or intracellular) as well as allow assessment of the heterogeneity of oxygen pressures in the microcirculation *in vivo*.

Measures of oxygen pressures *in vivo* have been traditionally performed with oxygen electrodes. Initially, polarographic Clark type of electrodes were used, and more recently, quenching of fluorescence optodes is being used.[3-7] However, these electrodes have some limitations, as there is a need to penetrate the tissue when making measurements, which causes microtrauma and a limited sample volume (<1 mm^3). In addition, there is uncertainty about the physiological compartment that is being measured, with probably the most precise definition given by Dyson *et al.* as the measurement of the PO_2 of the interstitial space.[8]

A major advance in the measurement of oxygen pressures *in vivo* was accomplished by Wilson and co-workers when they introduced of the Palladium-porphyrin (Pd-porphyrin) quenching of phosphorescence technique [6] and the subsequent developments of this technique.[9-11] Briefly, phosphorescence occurs as a result of the delayed emission of photons when a molecule is excited by light, and the absorbed energy is excited into a triplet state before returning to the singlet ground state. Pd-porphyrin either emits this energy as photons or transfers this energy to oxygen (the only molecule in a biological system that has this property), which is referred to as oxygen quenching. Oxygen quenching results in a decrease in phosphorescence intensity as well as a decrease in the lifetime of phosphorescence decay. This time dependent process of phosphorescence decay is directly dependent on the concentration of available oxygen and is described by the Stern Volmer relation. Phosphorimeters provide the excitation and measure the kinetics of phosphorescence decay to measure lifetime values with the aim of measuring oxygen pressures in the environment of a phosphor.[6,10] Once calibrated, the phosphorimeter does not require recalibration, which is one of the main advantages of the technique. This time-resolved technique configured in intravital microscopy allowed quantitative measurements with great precision in microvessels and even between red blood cells.[12,13] Oxygen pressure measurements within the mitochondria have also been reported.[14]

Measurements using optical fibers placed on organ surfaces provide the advantage of investigating organs other than muscle and mesentery microcirculation such as the heart, the brain or the kidney without disrupting the tissue architecture or creating trauma that may significantly influence the tissue PO_2 because of local bleeding. It is essential that the measurement be non-destructive and does not introduce artifacts. Thus, phosphorimeter devices provide organ or tissue PO_2 values by placing the tip of the probe on the surface without entering, making the measurement almost non-invasive (surgery is required to expose the organ). The next improvement in the technique arrived with the introduction of Oxyphor R2 and G2.[9] For instance, Oxyphor G2 phosphor may be excited by different wavelengths (440 nm and 632 nm), allowing the measurement of phosphorescence decay times at different depths in the tissue.[15]

Previously, a number of devices were developed for the measurement of the phosphorescence decay times.[6,7,10,14-20] These phosphorimeters commonly used a xenon flash lamp as an the most common excitation light source. A major drawback of flash lamps is the plasma glow that persists for tens of microseconds after the primary discharge. A flash lamp continues to emit light in the red spectrum long after the capacitor has discharged. The decay is exponential with reported associated lifetimes between 18 μs and 19 μs, which set a lower limit for the delay time around 50 μs; during the time after the light pulse, approximately 93% of the glow would have faded (manufacturer data). Thus, phosphor molecules were still being excited during the long afterglow, while some that were those excited during the initial part of the light pulse were deactivated. The flash lamp within the phosphorimeter is also known to produce heat and to saturate the PMT. To address these issues, the PMT was gated [18] and/or the flash lamp was turned off. Because of the design and the narrow-band wavelength of the LEDs, no significant heat is produced during the light pulse. The obtained signal from the flash-lamp phosphorimeter needed to be deconvoluted.[21,22] Additionally, the superposed spectral bands from the flash lamp needed to be removed from the decay signal.

An important feature for a phosphorimeter is that the PO_2 can be measured in every medium and is independent of the dye concentration. To our knowledge only a single phosphorimeter type has been described where this required property has been demonstrated.[18,23] If there is an excitation light dependency of the phosphorescence decay, then false values of oxygen concentrations will be given especially in cases of changing hemodynamic conditions.

With the advent of light-emitting diode (LED) technology, we undertook the development of a new LED-based phosphorimeter (LED-P). LED technology has the advantage of providing short well-defined pulses with a large choice of different LED spectral bands. This paper describes the construction and validation of such an LED-P for *in vitro* and *in vivo* measurements of oxygen pressures using the oxygen dependent quenching of phosphorescence of Pd-porphyrin conjugated to bovine serum albumin (BSA). The accuracy of calibration constants needed to convert phosphorescence decay times to PO_2 in the Stern Volmer equation are crucial to obtain reliable measurements. First, the *in vitro* calibration of the LED-P at fixed human physiological conditions (pH 7.4, temperature 37°C) using Pd-porphyrin as a phosphorescent dye is presented with a stepwise decrease in oxygen concentrations using an enzymatic reaction within a sealed cuvette to obtain calibration constants. Second, the Pd-porphyrin dye has the disadvantage of exhibiting pH and temperature dependencies.[18,24] We aimed to test the dependencies of Pd-porphyrin bound to BSA with the LED-P by altering the pH and temperature at various degrees and determining the equation constants for each value. Finally, we conducted an *in vivo* experiment in a rat subjected to hypoxic ventilation and ischemia/reperfusion where we measured renal cortical microvascular PO_2 with the LED-P.

Theory

The oxygen quenching of phosphorescence is theoretically independent of the concentration of Pd-porphyrin.[6,10] The Stern-Volmer equation describes the relationship between the concentration of O_2 and the measured decay lifetime for a specific phosphor (eq. 1).

$$\frac{\tau_0}{\tau} = 1 + \tau_0 . k_q . [O_2] \qquad\qquad (1)$$

The quenching efficiency/sensitivity of the sensor allows for the calculation of the Stern-Vomer quenching constant k_q. τ_0 is the decay time in the absence of oxygen. τ is oxygen dependent.

A modified form of the Stern-Volmer equation can be used in order to translate the value of the concentration of O_2 into PO_2 using the following relationships (eq. 2 and 3). Decay time τ is inversely proportional to O_2, and therefore long decay times and high phosphorescence intensities are expected with low levels of O_2.

$$\frac{\tau_0}{\tau} = 1 + \tau_0 . k'_q . PO_2 \qquad\qquad (2)$$

$$k'_q = \alpha . k_q \qquad\qquad (3)$$

O_2 concentration ($[O_2]$ in µmol.L^{-1}) can be converted into PO_2 in mmHg using the following relation (eq. 4)

$$PO_2 = \frac{Vm.760}{\alpha} . [O_2] \qquad\qquad (4)$$

where α is the Bunsen solubility coefficient, measured as the number of milliliters of gas dissolved per milliliters of liquid and per atmosphere (760 mmHg) partial pressure of the gas at any given temperature. Both *in vivo* at 37°C and in plasma, the Bunsen coefficient α is 0.0214.[25] V_m is the molar volume at 0°C and 1 atm (22.414 L.mol^{-1}). It is better to express the amount of oxygen *in vivo* in terms of $[O_2]$ because k_q does not depend on α whereas k'_q does.

Material and methods

Phosphorimeter technical specifications

A block diagram of the LED-P we developed is shown in Figure 1 to best illustrate the setup and process as well as and to compare it with the previous flash lamp phosphorimeter (FL-P).[15,18]

The light source consists of four LEDs, each mounted on a fast switching current controlled power source. This LED driver is custom-built with an LED current source. The LED current is real-time monitored and adjusted in hardware and is controlled by the data acquisition device (DAQ NI USB-6259 BNC, National Instruments, Austin, TX, USA), resulting in a rise and fall times of 100 ns. The frequency of the light pulse can be easily changed from 10 Hz to 100 Hz for repetitive measurements. These LEDs can be switched on and off separately according to the phosphorescent dye chosen. The following four LEDs are within the phosphorimeter: LXML-PR02-1100 (Royal Blue 447.5 nm), LXML-PM01-0100 (Green 530 nm), LXML-PL01-0060 (Amber 590 nm) and LXM2-PD01-0050 (Red 627 nm) (LUXEON Rebel, Lumileds, Schiphol, Netherlands). The wavelength values were chosen for Pd-porphyrin (excitation 530 nm), Oxyphor R2

(excitation 415 nm and 524 nm) and Oxyphor G2 (excitation 440 nm and 632 nm). We chose not to embed a 415 nm LED in our setup because of the short penetration distance into the tissue at this wavelength. Each LED with its own LED driver and collimator is one assembly that is inserted into the lid of the container.
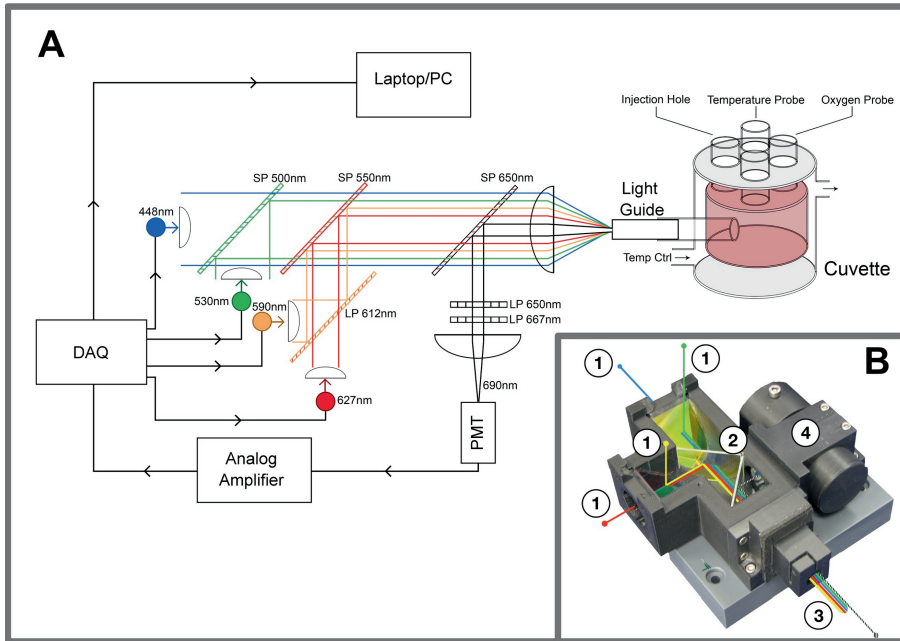

Figure. 1. Block diagram of the LED phosphorimeter and the cuvette setup used for *in vitro* calibration

(A) *Technical schematic drawing of the LED-P. In the LED-P, 4 LEDs are used converging to a single light guide and a non-gated photomultiplier tube. A magnification of the cuvette setup is presented. The calibration cuvette was custom-made out of glass. It is a double jacketed cuvette that allows thermostated water to be circulated around the inner chamber for temperature control of the Pd-porphyrin-albumin containing solution. The injection hole is where the enzymes can be added to the solution. The oxygen and temperature probes are placed in one hole if a bubbling reaction is desired. The cuvette is placed on a magnetic stirrer with a magnet in the chamber to ensure a homogenous solution concentration. The cuvette can be sealed airtight to obtain a zero-oxygen condition when an enzymatic reaction is used to scavenge oxygen. A side view is presented.*
(B) *Picture of the LED-block and dichroic mirror assembly used in the LED-P (LEDs have been removed). To generate a parallel beam, each LED is provided with a collimator. The excitation light pulse produced by an LED (1), is transmitted through the dichroic mirrors (2) and reaches the light guide (3) (removed for convenience) and then hits the medium. This liquid light guide is placed directly in contact with the tissue. The emission light (black and white dashed line) comes back and is reflected to the photomultiplier (4).*

A dichroic mirror acts as an interference filter that selectively passes light from a range of wavelengths while reflecting the others. The dichroic mirror (650 nm, 25.2 x 35.6 mm, Dichroic Shortpass Filter, Edmund Optics Ltd., York, UK) allows wavelengths below 650 nm to pass through. This mirror is selected to reflect light wavelengths from Pd-porphyrin emissions as well as and most generally of most common phosphorescent dyes designed for *in vivo* experimental use.[9,18] The excitation light is focused using a lens (Plastic Aspheric Lens, Edmund Optics Ltd., York, UK), into a liquid light guide (Newport 77637, Newport Spectra-Physics BV, Utrecht, The Netherlands) with a diameter of 5 mm and a tip of the same size. However, this liquid light guide can easily be replaced by another type or different size. A 650 nm long pass filter (FEL0650 Thorlabs Inc, Newton, New Jersey, USA) and a 665 nm long-pass filter (FGL665, 665 nm Longpass, Edmund Optics Ltd., York, UK) are placed in front of the photomultiplier tube (PMT) in this order to effectively block the excitation light wavelengths and pass the wavelengths to be measured in the range of 665 nm to 800 nm to be measured. For this reason, the phosphorimeter does not require a gated PMT. To avoid ghost signals, special attention was required to select non-autoluminescent optical components.

The emitted phosphorescence light is captured by a PMT (R928 PMT, Hamamatsu Photonics, Hamamatsu, Japan) and outputs an analogue current signal. It is voltage converted by a DC to 350 KHz transresistance amplifier (THS4082, Texas Instruments, Dallas, TX, USA) and then converted at 1.25 Msps to a digital signal (DAQ NI USB-6259 BNC, National Instruments, Austin, TX, USA). The signal is processed using a PC laptop through a USB input. The software used for controlling the LED-P and performing the analysis of the signal (fitting curves of decay signals) was written in Lab View (version 2013, National Instruments, Austin TX, USA).

Calculation of decay lifetime and curve fitting method

The decay time τ was estimated by a nonlinear mono-exponential with a least squared fitting method in a software written in LabView 2014 (National Instruments, Austin, TX, USA). *I(t)* is the phosphorescence intensity at time *t*, τ is the decay time, and *B* is the baseline current. For further details see.[18]

$$I(t) = I(0)e^{\frac{-t}{\tau}} + B \qquad (5)$$

The averaged measured PMT signal decay starting from 1 μs after excitation was normalized and fitted with a nonlinear Levenberg–Marquardt algorithm to find the most appropriate mono-exponential amplitude and damping of the decay. To obtain an adequate fit we considered the decay up to the point where the signal gets lost in the noise floor. For the given PMT setup, the PMT signal start amplitude is approximately 100 μA yielding a signal-to-noise ratio (SNR) of approximately 19 dB. Fitting would then be limited to a decay duration of 2τ. The SNR is enhanced to 29 dB by averaging 250 repetitive measurements of 10 ms to be able to fit for more than 3τ decay durations. Prior to the excitation, the averaged root mean square (RMS) noise floor was measured in the absence of a PMT signal. Then, the averaged PMT signal decay measured was truncated where the RMS value of a fragment of 80 μs (100 samples) had decayed below 12 dB above the RMS noise floor level. Pre-fitting was performed with a nonlinear Levenberg–Marquardt algorithm with initial guess coefficients of normalized amplitude 1 and damping -0.01. The measured PMT signal decay was truncated to a maximum of 6 times the course τ value found. Finally, the actual fitting with initial course coefficients was performed where the mean square error (MSE) was used as a fit indicator.

Excitation shape of the LED light pulse

The shape of the light pulse of the LEDs was sampled before entering the light guide, within their respective wavelength range of emission, using a special photodiode probe for very fast laser pulse response (Oxford Lasers Ltd., Oxon, UK) attached to an oscilloscope device (TDS2000C, Tektronix Inc., Bracknell, UK).We compared the excitation shape of the LED-P to the Xenon flash lamp (Hamamatsu, Hamamatsu Photonics, Shizuoka, Japan) used in the FL-P that we owned and that was similar to the one published elsewhere.[15,18] The light pulse was set at 1 μs. The settings were 500 ns/div and 30 mV/div. One hundred light pulses were analyzed and automatically averaged by the oscilloscope. The obtained signals were normalized.

Chemicals

Fifty milligrams of Palladium-porphyrin Pd(II)-meso-tetra(4-carboxyphenyl)porphyrin (Pd-TCPP) (PdT790, Frontier Scientific, Logan, UT, USA) were dissolved in 0.6 ml of dimethyl sulfoxide (13 mg/ml) (DMSO). Then, 0.6 ml of the mixture DMSO-Pd-TCPP were added with 0.6 ml of 1 M 2-Amino-2-(hydroxymethyl)-1,3-propanediol (TRIS) to 10 ml of 4% bovine serum albumin (BSA, Sigma-Aldrich). This resulted in a final concentration of Pd-TCPP of 5 mM. The final pH was

targeted above 8.0 with the addition of TRIS to reduce the pH dependency, as we previously demonstrated.[18] The solution was incubated overnight (> 8 hours) in the refrigerator and protected from the light, to allow the Pd-TCPP to form a complex with albumin. Then, 2 M hydrochloric acid (HCl) was used for pH adjustment to 7.4.

To test the linearity between $1/\tau$ and the PO_2, 500 µL of the Pd-TCPP-albumin (5 mM) complex were added inside a 100 mL cuvette containing phosphate buffer saline (pH 7.4) (fig. 1). The PO_2 was measured with a 2 mm solid-state polymer optical fiber sensor oxygen optode (POF, Oxy-Mini, World Precision Instruments, Sarasota, FL, USA), which was calibrated in pure water with 0% oxygen content by dissolving 1 g of Na_2SO_3 according to the manufacturer's recommendations. Finally, the calibration was completed by using fully air-saturated water at 20°C and 37°C.

Experimental conditions

In vitro calibration

The procedure for obtaining the Stern Volmer constants involved creating a zero-oxygen condition for determining the τ_0 and the corresponding k_q. Due to the production of foam when using nitrogen bubbling with the Pd-TCPP-albumin complex, an enzymatic reaction is the preferred technique to remove oxygen within the solution.[18,26] To achieve a solution with zero oxygen, the oxygen was removed by adding ascorbic acid (0.1 M, Sigma-Aldrich, Zwijndrecht, The Netherlands) in several steps of 100 µL in the reaction chamber catalyzed by 100 U ascorbate oxidase (1000 U Ascorbate oxidase from Cucurbita, Alfa Aesar, Lancashire, United Kingdom) as described elsewhere.[26] One unit is defined as the amount of enzyme that will oxidize 1 mmol of ascorbate per minute at pH 5.6 and 25°C. The 100 mL cuvette was air-sealed and covered with aluminum foil and placed in a dark room. The temperature of the solution was controlled using a thermostatic circulation bath and was monitored using a temperature sensor coupled with the oxygen probe. Since the calibration constants were temperature dependent, we first set the temperature at 37°C.

The temperature and pH dependencies of k_q and τ for the solution Pd-TCPP-albumin were assessed in 2 separate experiments. First, the temperature was altered to 19°C, 25°C, 28°C, 32°C, 34°C, 37°C and 39°C with the pH kept constant at 7.4. Second, the pH was adjusted to

6.8, 7.0, 7.2, 7.4, and 7.6 using sodium hydroxide or HCl while the temperature was kept constant at 37°C. For each value of pH and temperature a new solution was used and replicated 3 times. Values are given as the mean ± SD of 5 measurements.

To assess whether the decay time measured by the LED-P was influenced by changes in intensity of the phosphorescence, we used a lipid emulsion (Intralipid® 10%, Fresenius Kabi, Bad Homburg, Germany) as a non-fluorescent and non-absorbent phantom material as previously reported.[18] The lipid emulsion induces scattering and it modifies the amount of light available for phosphorescence excitation. We continuously recorded τ while increasing the concentration of lipids in the cuvette from 0 g/L to 25 g/l, containing Pd-TCPP-albumin, at 37°C and saturated ambient air.

In vivo validation

The experiment in this study was approved by the Animal Research Committee of the Academic Medical Center of the University of Amsterdam (DFL102964). Care and handling of the animals were in accordance with the guidelines from the Institutional and Animal Care and Use Committees. The experiment was performed on one male Sprague-Dawley rat (Harlan, The Netherlands) with a weight of 327 g. The rat was anesthetized with an intraperitoneal injection of a mixture of 100 mg/kg ketamine (Nimatek®; Eurovet, Bladel, the Netherlands), 0.5 mg/kg medetomidine (Domitor; Pfizer, New York, NY) and 0.05 mg/kg atropine-sulfate (Centrafarm, Etten-Leur, The Netherlands) and was maintained with 50 mg/kg ketamine (dissolved in 0.9% NaCl) at a dose of 5 ml/kg/h. A thermocouple probe was placed in the rectum, and a heating pad under the animal allowed the body temperature to be controlled and maintained at 37 ± 0.5°C. After tracheotomy, the animal was mechanically ventilated with 0.4 FiO_2. The ventilator settings were adjusted to maintain end-tidal PCO_2 between 30 and 35 mmHg and arterial PCO_2 between 35 and 40 mmHg. The right carotid and femoral arteries and jugular and femoral veins were cannulated. The left kidney was exposed and immobilized in a lucite kidney cup (K. Effenberger, Pfaffingen, Germany) via 3 cm incision in the left flank. Renal vessels were carefully separated under preservation of the nerves and the adrenal gland. A perivascular ultrasonic transient time flow probe was placed around the left renal artery (type 0.7 RB Transonic Systems Inc., Ithaca, NY, USA) and connected to a flow meter (T206, Transonic Systems Inc., Ithaca, NY, USA) to continuously measure renal blood flow (RBF). An intravenous bolus of 5 mg/kg of Pd-TCPP-albumin was administered. The probe of the LED-P was stabilized with a holder 1 mm

above the non-decapsulated kidney surface, eliminating any pressure artifacts. The kidney was wrapped in a gauze frequently humidified with warm normal saline (~35°C) to limit desiccation. In addition to performing the measurements in the darkness, the tip of the light guide and the operation field were covered with aluminum foil to avoid residual ambient room light contamination of the phosphorescence decay signals. After a 20-minutes stabilization period, measurements were taken. The cortical renal PO_2, RBF, mean arterial pressure (MAP) and heart rate were continuously monitored and recorded every 15 seconds. We first increased the FiO_2 to 1 and then decreased it every 5 minutes to change the inspired fractions to 0.6, 0.4 and 0.21. Then, we induced a stepwise hypoxic ventilation with predefined FiO_2 of 0.15, 0.08 and 0.04 with the use of nitrogen attached to a modified ventilator (Babylog 8000, Dräger, Zoetermeer, Nederland). At each step (5 min), an arterial blood gas was withdrawn and measured with ABL 80 FLEX CO-OX OSM (Radiometer, Brønshøj, Denmark). Then, after a recovery period, the renal artery was clamped for 3 minutes. The clamp was released, and the reperfusion effects were observed. The renal cortical microvascular PO_2 calculated from the decay measurements using the LED-P were compared to values of previously published experiments.

Statistical analysis

The drawing of the graphs and derivation of the mathematical equations (τ_0 and k_q) and the statistical analysis were performed using Prism for Mac version 6.0h (GraphPad Software Inc., La Jolla, CA, USA). Appropriate curve fitting methods for these constants were applied with the least squared method, and fit equations were obtained. The correlation coefficient (r^2) was determined to assess the strength of the relationship of linear and non-linear regressions regarding the determination of τ and k_q with their respective pH and temperature dependencies. A p-value <0.05 was considered as a significant relationship.

Results

Technical aspects of the excitation light pulse

The comparison between the 2 shapes of the excitation light pulse yielded significant differences (Fig. 2). Although, the light pulse duration was set to 1 µs in both devices, it resulted in a significantly larger full width at the half maximum (FWHM) time for LED-P than FL-P with 700 ns versus 500 ns approximately. The shape of the light pulse was rectangular for the LED-P with a steep fall in light intensity after a duration of 1 µs. This was validated for the 4 LEDs. In contrast, xenon flash lamp exhibited a mono-exponential decrease in light intensity and still emitted a small intensity of light after 4 µs.
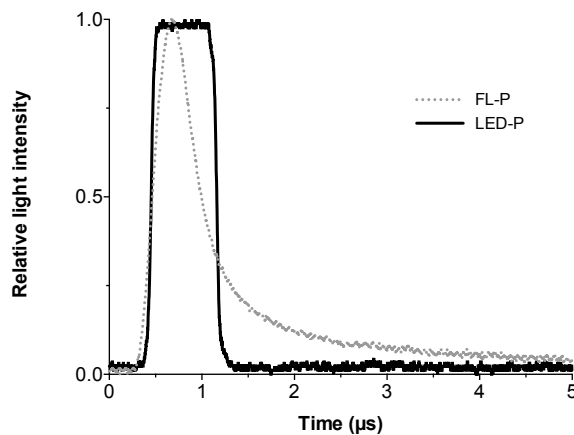
Figure. 2. Typical shapes of LED and xenon flash lamp pulses

An LED pulse is the solid black line and a xenon flash lamp pulse is the dashed black line. The width of the pulses (FWHM) were 700 ns and 500 ns for LED and xenon FL, respectively.

Obtaining of τ_0 and k_q

There was a stepwise decrease in the oxygen concentrations in the solution after titration using ascorbic acid. As predicted by the Stern-Volmer equation, there was a strong linear correlation between the concentration of oxygen measured by the fiber optic sensor and the ratio τ_0/τ at pH 7.4 and temperature 37°C (r^2=0.99) (Fig. 3). The linear regression observed followed the equation: y=0.1852x + 1.473. The solution was deoxygenated by adding several

samples of ascorbate stepwise. Plotting [O$_2$] against τ_0/τ validated the use of the new LED-P. The τ_0 was measured under the same conditions for a total of 5 experiments and these results were averaged. Once the τ_0 was known, the corresponding constant k_q was calculated.
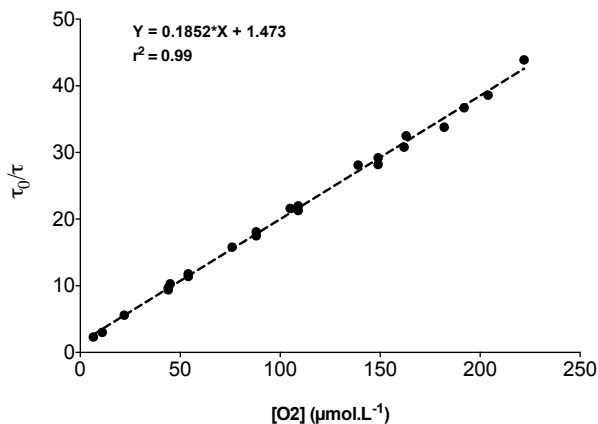

Figure. 3. Plotting τ_0/τ against O$_2$ concentration at 37°C and pH 7.4

To validate the Stern-Volmer equation for describing the quenching of Pd-TCPP by O$_2$ a straight line was fitted on the measured points with a correlation coefficient of r²=0.99.

Temperature dependency. Figures 4A and 4B show τ_0 and k_q as a function of temperature respectively. At higher temperatures the decay time (τ_0) decreased while the k_q increased. τ_0 could then be determined according to the temperature with the following equation *(6)*:

$$\tau_0 \ = \ 637.71 \ - \ 1.1032\,T \ - \ 0.0819\,T^2 \qquad\qquad (6)$$

Once this relation was known, a second order function could be derived for the calculation of k_q, where *T* is the temperature.

A

$$Y = -0.08189*X^2 - 1.013*X + 637.7$$
$$r^2 = 0.99$$

Temperature (°C)

B

$$Y = 0.195*X^2 + 1.1197*X + 60.801$$
$$r^2 = 0.99$$
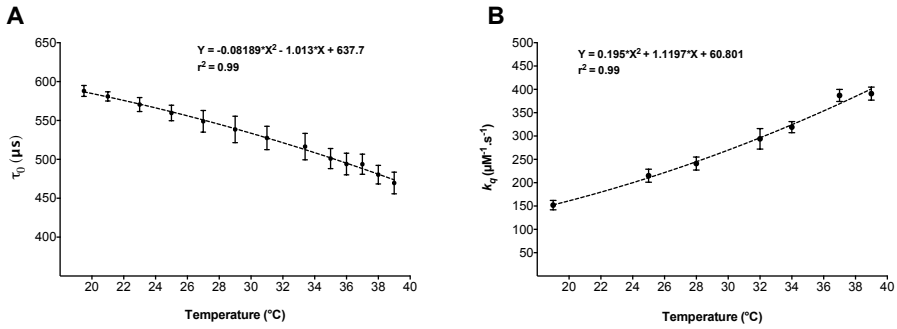
Temperature (°C)

Figure. 4. Temperature dependencies of τ_0 and k_q of the Pd-TCPP-albumin complex maintained at a constant pH of 7.4.

(A) Evolution of τ_0 with different values of temperature ranging from 19°C to 39°C. A second order function was fitted to the data $\tau_0 = 637.71 - 1.1032T - 0.0819T^2$, where T is temperature with a correlation coefficient of $r^2=0.99$. (B) Evolution of k_q at different temperatures. A second order function was fitted to the data $k_q = 0.195\ T^2 + 1.1197\ T + 60.80$

pH dependency. The Figure 5 depicts the significant pH dependency of τ_0 (*p<0.001*). However, its effect was negligible *in vivo*, as there was only a 40 μs difference between the τ_0 for lower and higher pH values; i.e., 6.8 and 7.6 respectively. The k_q was independent of pH.

A

$$Y = -63.50*X + 957.4$$
$$r^2 = 0.897$$

pH

B

$$Y = 8.1*X + 320.9$$
$$r^2 = 0.28$$

pH
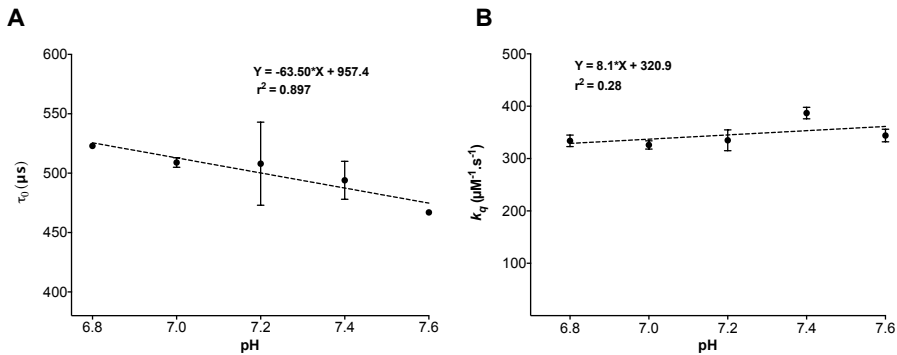
Figure 5. pH dependency of τ_0 and k_q with temperature kept constant at 37°C

(A) For τ_0, a negative linear regression was obtained with a correlation coefficient of 0.897. However, the global pH effect on τ_0 may be neglected in vivo. (B) kq did not exhibit a significant pH dependency.

A

B
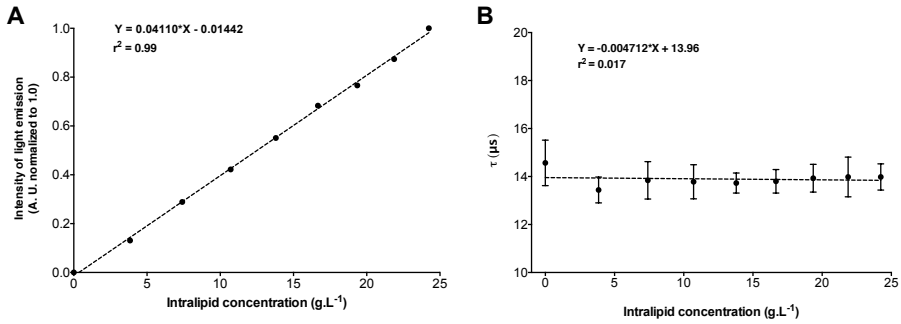
Figure 6. Decay times plotted against lipid emulsion concentrations

(A*) Phosphorescence intensity linearly increased with the increase in lipid emulsion concentrations.* (B) *Plotting of τ against constant increased lipid emulsion concentrations. Measurements were performed at 37°C with saturated ambient air ([O_2] kept constant). Values are mean ± SD of 10 measurements at each point during 2 experiments.*

Intensity of phosphorescence. Altering the intensity of phosphorescence by adding stepwise Intralipid 10% stepwise did not result in significant changes in τ values. There was no correlation between the intensity of phosphorescence and the measured decay times of phosphorescence (Fig. 6). This experiment demonstrated that LED-P was able to measure [O_2] independently of the concentration of the phosphorescence dye and the intensity of phosphorescence.

In vivo validation

As an example of the use of the phosphorimeter, different series of measurements in the kidney were performed in a fully instrumented mechanically ventilated rat. The measurements revealed similar microcirculatory PO_2 values to those published previously during normal and ischemic conditions with 67 ± 1 mmHg and 2.6 ± 0 mmHg respectively.[8,16,27-30] The typical curve for hypoxic/hyperoxic ventilation and ischemia/reperfusion of the kidney is shown in Figure 7. The arterial PO_2 values during different inspired fraction of oxygen are showed on the panel *(A)* of Figure 7. The hemodynamic changes associated with hypoxia and ischemia are presented in panels *(B)* and *(C)* for MAP and RBF. respectively. Because of the major hemodynamic instability at the oxygen fraction of 0.04, the time of hypoxic ventilation was reduced to 2 minutes.
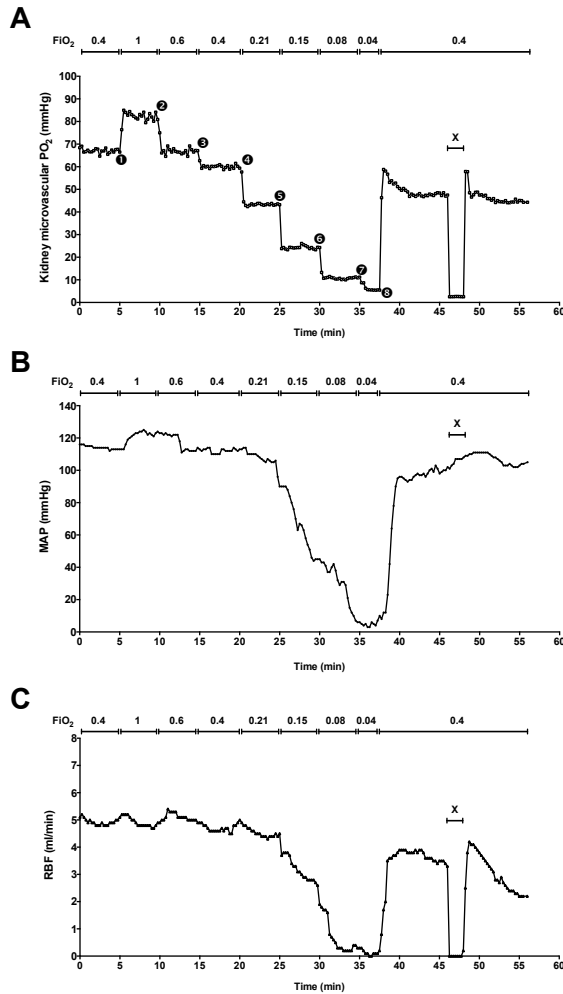
Figure 7. Typical example of renal microvascular PO$_2$ and macrohemodynamic trends during hypoxic ventilation and ischemia.

(A) Microvascular PO$_2$ measured in the kidney, (B) Mean arterial pressure (MAP), and (C) Renal blood flow (RBF). The rat was mechanically ventilated with a Babylog 8000 (Dräger, Zoetermeer, Nederland) in which the oxygen input was changed to nitrogen. The resulting mix between air and nitrogen was varied by stepwise increments of the fraction of nitrogen delivered (former oxygen button) and adequately measured with a calibrated respiratory gas analyzer (CapnoMac, Datex-Ohmeda, Madison, WI, USA). The oxygen fractions used were defined before the experiment was performed. In the first 45 minutes of the experiment, we tested hyperoxic and hypoxic ventilation conditions, and then we clamped the renal artery for 5 minutes to measure the effects of ischemia reperfusion on microvascular PO$_2$. The arterial PO$_2$ values were 204 mmHg, 548 mmHg, 326 mmHg, 226 mmHg, 102 mmHg, 52 mmHg, 39 mmHg, and 28 mmHg at time points 1, 2, 3, 4, 5, 6, 7 and 8, respectively. FiO$_2$: inspired fraction of oxygen, X: renal artery clamping

Discussion

This report presents the design, construction, *in vitro* calibration and *in vivo* validation of a new phosphorimeter using LEDs with different spectral bands as a light source to perform an analysis of quenching by oxygen of the phosphorescence of different phosphors (Pd-TCCP, Oxyphor R2). The use of LEDs as a light source in this LED-P had several advantages over the previous generation of phosphorimeters. LEDs are more cost-effective, with smaller size and simpler electronics which improves their compactness. LEDs are also more energy efficient and have a longer lifetime (20,000 to 25,000 hours compared to the 400 to 5,000 hours reported for Xenon flash lamps). Typically, a xenon flash needs 1,000 to 2,000 times (high voltage) the power of the LED flash to deliver the same light energy, and therefore, LED-based instruments require low voltage to ensure electrical safety. Moreover, LEDs have a narrow spectral band and generate less electromagnetic interference which may influence PMT, amplifier electronics and data acquisition. Despite the fact that the LED-P light pulse has a larger FWHM time than the FL-P, it has a rectangular shape compared to the xenon FL-P (Fig. 2), eliminating a further unwanted time-dependent excitation of the environment containing Pd-porphyrin dye. No afterglow effect was noted with LED-P. Using LEDs avoids the need for deconvolution of the decay signal as there are very limited interference excitations. This is especially important when the concentration in oxygen within the analyzed medium or tissue increases. After the excitation light strikes the dye, the emission of phosphorescence is almost immediate. At high oxygen concentrations, the lifetime of the phosphorescence decay (duration of the total emission decay) is very short and may therefore be significantly influenced in the case of the flash lamp use due to its afterglow tail. Owing to the rectangular shape of the LED light pulse, the earliest part of the phosphorescence decay can be measured after a short suitable delay and does not require being deconvoluted when the decay times are short. Thus, the measurement of oxygen with the LED-P is more accurate and reliable, especially at high concentrations. An additional serious advantage is that LEDs emit light within a narrow-band wavelength, usually within 20 nm. The 4 wavelengths can be used almost simultaneously without having to change filters as was required in the previous FL-P. This allows for the measurement of decay times of several phosphorescent dyes at the same time, e.g. one trapped in the vasculature compared to one that is loaded into the mitochondria. The intensity of LEDs can be modulated to a sine wave that will subsequently provide measurement of PO_2 by the analysis of amplitude or phase responses of the emission signals. Vinogradov *et al.* were the first to develop a phosphorimeter that was operated in a

frequency domain mode using amplitude modulation.[17,31,32] A longer phosphorescence lifetime results in a larger phase shift and lower measured oxygen concentrations. We had designed such phosphorimeters for the measurement of renal venous PO_2 using a laser phase shift detection.[16] Contrary to our previous studies,[15,28] kidney decapsulation was not required to obtain a phosphorescence lifetime decay suggesting a longer sensitivity/efficacy of the device. It should also be noted that the lifetime of LEDs is superior to that of flash lamps, providing a sustained intensity of light pulse for a long period of use or intensive use. Finally, in this device, one liquid light guide was used because all LED spectral bands and emission spectral bands are combined into one optical path (Fig. 1). It can be used not only in small animals but also in large animals such as pigs. Moreover, another liquid light guide diameter can be used, reducing the sampling volume of interest. Classically, the FL-P used one flash lamp for each light excitation source coupled with one filter, followed by a light guide. The different light guides were then gathered into one, but the exact same volume of tissue was not sampled. With the use of one liquid light guide, as in our set up, the measured volume is exactly the same as the one that has been excited.

With this new LED-P, we showed similar results obtained with the FL-P regarding pH and temperature dependencies. As previously reported, the pH effect on the phosphorescence decay times (τ) of the Pd-TCPP-albumin complex was confirmed to be negligible and k_q was independent of pH.[18,26] This is because Pd-TCPP is significantly bound to albumin following incubation at pH 8.0. The lifetime of phosphorescence is however dependent on temperature changes [18,26] and this has to be taken into consideration when changes in temperature occurs during experimental investigations *in vivo*. We also confirmed that the decay times analyzed with this LED-P were not dependent on the intensity of phosphorescence modulated with the use of Intralipid. This experiment is a key validation of the robustness of the LED-P described in this study. This provides a great insight and validation for *in vivo* measurements because the intensity of phosphorescence may change within the tissue. This is key because it shows that the measurement of microcirculatory PO_2 *in vivo* can be made, irrespective of changes in phosphorescence intensity due to variations in dye concentration or with altered hemodynamic conditions.

During the *in vivo* validation, lifetime decays were obtained even in the presence of the renal capsule. In our study, we showed a step-like response of microvascular PO_2 to step-like changes in FiO_2 while there were limited changes in RBF and MAP, emphasizing the reliability of measurement in response to a rapid change in microcirculatory PO_2. Although it has not been

measured, the depth of sampling volume (catchment depth of the excitation light) is estimated to be between 700 μm and 4,000 μm based on the work of Johannes *et al.*.[15] In this study, the authors used 2 lasers with wavelengths of 442 nm and 632 nm to excite Oxyphor G2. Kidney slices were prepared and the phosphorescence intensity was measured to determine the penetration depth. The anatomical region correlated to these wavelengths in the rat kidney were the cortex and outer medulla. The 530 nm green light penetration depth should then lie in these two boundaries and the majority of the emitted phosphorescence should come from the cortex of the kidney.

Limitations

A proposed alternative to flash lamp excitation has been to use a laser pulse as an excitation source.[1,7] A laser-based phosphorimeter can be used to produce light at a single wavelength. However, such phosphorimeters are costly especially if multiple wavelengths are required. In addition, because lasers emit at only one specific wavelength, it can be a challenge to find the perfect match between the laser excitation light pulse that will produce the maximum phosphorescence from the phosphorescent dye. Although the LED has a less precise wavelength (~20 nm), an overlap with the excitation wavelength of the phosphor and the chosen LED can be easier to obtain. Of note, the LEDs should be stable in light output as well as in the color spectrum.

The software developed for PO_2 readings in the current study provides a mono-exponential fit of the decay curves. *In vivo*, however there is a heterogeneity in the distribution of PO_2 that results in multi-exponential decay curves. Extracting the distributions of lifetimes from such multi-exponential decay curves can be accomplished by using suitable algorithms. Previous works reported different methods for recovering the underlying distributions of lifetime and PO_2.[33-36] Several parameters could be set in the algorithms used in these studies, which makes the results difficult to reproduce, inconsistent, and - from our point of view, – not yet ready to implement in practice. Future work needs to be directed at extracting reliable lifetime histograms from the decay curves provided by light pulsed phosphorimeters, as described in this paper.

Conclusion

In this paper, we presented a new LED based phosphorimeter that addresses some of the previous drawbacks of the flash lamp based phosphorimeters. The shape of the light pulse is rectangular with a precise and steep fall in light intensity within a narrow-band wavelength. For this reason, measurement of the phosphorescence signal can simply be made after a suitable delay time without deconvolution of the excitation pulse. Therefore, measurements of PO_2 are more accurate and reliable at high values compared to previous FL-Ps. The temperature dependency of the Pd-TCCP-albumin complex should be taken into account by adjusting the constants of the Stern-Volmer equation when performing measurements to maintain proper and accurate PO_2 readings. During an *in vivo* validation experiment, the LED-P demonstrated reliable and similar measurements of renal cortex microvascular PO_2 during hypoxic ventilation and ischemia reperfusion compared to previous works. We expect that this LED-P will be a useful tool in the investigation of determinants of tissue oxygenation in animal models of health and disease. Finally, this LED-P provides the ability to choose which LED to enable/disable to excite different phosphors within the same measurement.

7

Conflicts of interest:

Acknowledgments

References

1.   Ince C, Mik EG. Microcirculatory and mitochondrial hypoxia in sepsis, shock, and resuscitation. *J Appl Physiol*. 2016;120(2):226–235.

2.   Tsai AG, Johnson PC, Intaglietta M. Oxygen gradients in the microcirculation. *Physiol Rev*. 2003;83(3):933–963.

3.   Vanderkooi JM, Erecińska M, Silver IA. Oxygen in mammalian tissue: methods of measurement and affinities of various reactions. *Am J Physiol*. 1991;260(6 Pt 1):C1131–50.

4.   Springett R, Swartz HM. Measurements of oxygen in vivo: overview and perspectives on methods to measure oxygen within cells and tissues. *Antioxidants & redox signaling*. August 2007:1295–1301.

5.   Swartz HM, Dunn JF. Measurements of oxygen in tissues: overview and perspectives on methods. *Adv Exp Med Biol*. 2003;530:1–12.

6.   Wilson DF, Rumsey WL, Green TJ, Vanderkooi JM. The oxygen dependence of mitochondrial oxidative phosphorylation measured by a new optical method for measuring oxygen concentration. *J Biol Chem*. 1988;263(6):2712–2718.

7.   Mik EG, van Leeuwen TG, Raat NJ, Ince C. Quantitative determination of localized tissue oxygen concentration in vivo by two-photon excitation phosphorescence lifetime measurements. *J Appl Physiol*. 2004;97(5):1962–1969.

8.   Dyson A, Bezemer R, Legrand M, Balestra G, Singer M, Ince C. Microvascular and interstitial oxygen tension in the renal cortex and medulla studied in a 4-h rat model of LPS-induced endotoxemia. *Shock*. 2011;36(1):83–89.

9.   Dunphy I, Vinogradov SA, Wilson DF. Oxyphor R2 and G2: phosphors for measuring oxygen by oxygen-dependent quenching of phosphorescence. *Anal Biochem*. 2002;310(2):191–198.

10.   Vanderkooi JM, Maniara G, Green TJ, Wilson DF. An optical method for measurement of dioxygen concentration based upon quenching of phosphorescence. *J Biol Chem*. 1987;262(12):5476–5482.

11.   Wilson DF, Pastuszko A, DiGiacomo JE, Pawlowski M, Schneiderman R, Delivoria-Papadopoulos M. Effect of hyperventilation on oxygenation of the brain cortex of newborn piglets. *J Appl Physiol*. 1991;70(6):2691–2696.

12.   Golub AS, Pittman RN. PO2 measurements in the microcirculation using phosphorescence quenching microscopy at high magnification. *Am J Physiol Heart Circ Physiol*. 2008;294(6):H2905–16.

13.   Golub AS, Pittman RN. Erythrocyte-associated transients in PO2 revealed in capillaries of rat mesentery. *Am J Physiol Heart Circ Physiol*. 2005;288(6):H2735–43.

14.   Bodmer SIA, Balestra GM, Harms FA, et al. Microvascular and mitochondrial PO(2) simultaneously measured by oxygen-dependent delayed luminescence. *J Biophotonics*. 2012;5(2):140–151.

15.   Johannes T, Mik EG, Ince C. Dual-wavelength phosphorimetry for determination of cortical and subcortical microvascular oxygenation in rat kidney. *J Appl Physiol*. 2006;100(4):1301–1310.

16.   Mik EG, Johannes T, Ince C. Monitoring of renal venous PO2 and kidney oxygen consumption in rats by a near-infrared phosphorescence lifetime technique. *Am J Physiol Renal Physiol*. 2008;294(3):F676–81.

17.   Vinogradov SA, Fernandez-Seara MA, Dupan BW, Wilson DF. A method for measuring oxygen distributions in tissue using frequency domain phosphorometry. *Comp Biochem Physiol, Part A Mol Integr Physiol*. 2002;132(1):147–152.

18.   Sinaasappel M, Ince C. Calibration of Pd-porphyrin phosphorescence for oxygen concentration measurements in vivo. *J Appl Physiol*. 1996;81(5):2297–2303.

19.   Torres Filho IP, Intaglietta M. Microvessel PO2 measurements by phosphorescence decay method. *Am J Physiol*. 1993;265(4 Pt 2):H1434–8.

20.   Shaban S, Marzouqi F, Mansouri Al A, Penefsky HS, Souid A-K. Oxygen measurements via phosphorescence. *Comput Methods Programs Biomed*. 2010;100(3):265–268.

21.   Mik EG, Donkersloot C, Raat NJH, Ince C. Excitation pulse deconvolution in luminescence lifetime analysis for oxygen measurements in vivo. *Photochem Photobiol*. 2002;76(1):12–21.

22.   Golub AS, Popel AS, Zheng L, Pittman RN. Analysis of phosphorescence decay in heterogeneous systems: consequences of finite excitation flash duration. *Photochem Photobiol*. 1999;69(6):624–632.

23.   Sinaasappel M, Ince C, van der Sluijs JP, Bruining HA. A new phosphorimeter for the measurement of oxygen pressures using Pd-porphine phosphorescence. *Adv Exp Med Biol*. 1994;361:75–81.

24.   Pawlowski M, Wilson DF. Monitoring of the oxygen pressure in the blood of live animals using the oxygen dependent quenching of phosphorescence. *Adv Exp Med Biol*. 1992;316:179–185.

25.   Christoforides C, Laasberg LH, Hedley-Whyte J. Effect of temperature on solubility of O2 in human plasma. *J Appl Physiol*. 1969;26(1):56–60.

26.   Lo LW, Koch CJ, Wilson DF. Calibration of oxygen-dependent quenching of the phosphorescence of Pd-meso-tetra (4-carboxyphenyl) porphine: a phosphor with general application for measuring oxygen concentration in biological systems. *Anal Biochem*. 1996;236(1):153–160.

27.   Aksu U, Bezemer R, Yavuz B, Kandil A, Demirci C, Ince C. Balanced vs unbalanced crystalloid resuscitation in a near-fatal model of hemorrhagic shock and the effects on renal oxygenation, oxidative stress, and inflammation. *Resuscitation*. 2012;83(6):767–773.

28.   Legrand M, Legrand M, Mik EG, et al. Fluid resuscitation does not improve renal oxygenation during hemorrhagic shock in rats. *Anesthesiology*. 2010;112(1):119–127.

29.   Johannes T, Mik EG, Nohé B, Unertl KE, Ince C. Acute decrease in renal microvascular PO2 during acute normovolemic hemodilution. *Am J Physiol Renal Physiol*. 2007;292(2):F796–803.

30.   Legrand M, Almac E, Mik EG, et al. L-NIL prevents renal microvascular hypoxia and increase of renal oxygen consumption after ischemia-reperfusion in rats. *Am J Physiol Renal Physiol*. 2009;296(5):F1109–17.

31.   Vinogradov SA, Fernandez-Searra MA. Frequency domain instrument for measuring phosphorescence lifetime distributions in heterogeneous samples. *Rev Sci Instrum*. 2001:3396–3406.

7

32.   Wilson DF, Vinogradov SA, Dugan BW, Biruski D, Waldron L, Evans SA. Measurement of tumor oxygenation using new frequency domain phosphorometers. *Comp Biochem Physiol, Part A Mol Integr Physiol*. 2002;132(1):153–159.

33.   Vinogradov SA, Wilson DF. Phosphorescence lifetime analysis with a quadratic programming algorithm for determining quencher distributions in heterogeneous systems. *Biophys J*. 1994.

34.   James DR, Ware WR. Recovery of underlying distributions of lifetimes from fluorescence decay data. *Chemical physics letters*. 1986;126(1):7–11.

35.   Golub AS, Popel AS, Zheng L, Pittman RN. Analysis of phosphorescence in heterogeneous systems using distributions of quencher concentration. *Biophys J*. 1997;73(1):452–465.

36.   Istratov AA, Vyvenko OF. Exponential analysis in physical phenomena. *Rev Sci Instrum*. 1999;70(2):1233.

7

8

THE ROLE OF BICARBONATE PRECURSORS IN BALANCED FLUIDS DURING HAEMORRHAGIC SHOCK WITH AND WITHOUT COMPROMISED LIVER FUNCTION

Bulent Ergin,[1] Aysegul Kapucu,[2] Philippe Guerci,[1,3,5], Can Ince,[1,4]

1. Department of Translational Physiology, Academic Medical Centre, Amsterdam, The Netherlands
2. Department of Biology, Science Faculty, University of Istanbul, Istanbul, Turkey
3. INSERM U1116, University of Lorraine, Vandoeuvre-Les-Nancy, France
4. Department of Intensive Care Medicine, Erasmus MC, University Medical Centre, Rotterdam, Rotterdam, The Netherlands.
5. Departement of Anaesthesiology and Critical Care Medicine, University Hospital of Nancy, France

Summary

Background: Lactate, acetate and gluconate are anions used in balanced resuscitation fluids of which lactate and acetate are considered bicarbonate precursors. This study investigated the alterations and renal haemodynamics and microvascular oxygenation in a rat model of resuscitated haemorrhagic shock (HS).

Methods: Ringer's Lactate (RL), Ringer's Acetate (RA), Plasma-Lyte (RA-Glu/Mg) or normal saline (NS) were administered following HS in the presence or absence of a 70% partial liver resection (PLR). Renal haemodynamics and microvascular oxygenation (by oxygen-dependent quenching of phosphorescence) were measured as well as concentrations of lactate, gluconate and acetate in plasma and urine. Kidney wet and dry weighing was also assessed.

Results: PLR resulted in increased liver enzymes compared in control and HS groups ($p < 0.01$). HS decreased systemic and renal perfusions and reduced microvascular kidney oxygenation with lactic acidosis ($p < 0.01$). Resuscitation with balanced fluids did not fully restore renal oxygenation ($p < 0.01$). RA and RA-Glu/Mg increased bicarbonate contents and restored pH better than RL or NS in the PLR experiment ($p < 0.01$). PLR caused an increase in plasma gluconate after RA-Glu/Mg resuscitation ($p < 0.05$).

Conclusions: Acetate buffered balanced fluids show superior buffering effects than RL and NS. Gluconate is partially metabolized by the liver although it does not contribute to acid-base control because of large excretion in urine. Acetate is metabolized regardless of liver function and may be the most efficient bicarbonate precursor. Lactate infusion tends to overwhelm the metabolism capacities of the residual liver.

Keywords: microcirculation, haemorrhagic shock, buffered solution, plasma-lyte, gluconate

Introduction

Current evidence suggests that the type of fluid used for resuscitation, particularly colloids, may lead to unfavourable outcomes or have no effect compared to normal saline.[1-5] Several studies have demonstrated that balanced fluids are commonly used for volume expansion of critically ill patients.[6-8] This has led to increased attention on the role of crystalloids and the effects of their different compositions.[9,10] Fluid preparation may be based on a simple, non-buffered salt solution, such as normal saline or, be balanced with anion substitutes, such as maleate, gluconate, lactate or acetate of which the two latter are considered bicarbonate precursors. Plasma-Lyte (Baxter Healthcare, Illinois, US) is a crystalloid fluid encompassing two weak anions, acetate and gluconate and is engineered to closely mimic the plasma electrolyte content while not altering its osmolality.[11] However, the role of gluconate in terms of acid-base control is unknown.

There is a growing body of evidence indicating that balanced fluids improve the acid-base status and preserve strong ion difference.[12] The purpose of using these solutions is based on two principles: (i) reducing the chloride content and its detrimental effects,[13] with providing a plasma-like ionic content, and (ii) increasing bicarbonate content and pH by metabolism of bicarbonate precursors.[14] It is commonly accepted that these precursors are mainly metabolized in the liver.[15,16] To our knowledge there is little information on the role of liver function in acid-base control during fluid balanced resuscitation for haemorrhagic shock. What is unclear and not well described is the metabolic fate of such components during shock states associated with compromised liver function and the degree to which other organ beds are effective in metabolizing these precursors to produce bicarbonate and correct acid-base alterations.[9] Whereas it is generally assumed that lactate is primarily metabolized in the liver in case of shock, the acetate is metabolized in other organs.[17] We hypothesized that acetate-based resuscitation fluids would have superior buffering effect than non-acetate based fluids in case of liver dysfunction.

To this end we assessed the buffering effect of three commonly used balanced fluids, Ringer's Lactate (RL), Ringer's Acetate (RA) and Plasma-Lyte (RA-Glu/Mg) (**supplementary Table 1**), in a relevant model of fixed-pressure haemorrhagic shock. In the first part of the study, we aimed to determine the role of the liver in the metabolism of these buffers. To accomplish this, a ~70% partial liver resection (PLR) was performed to reduce the capacity of the liver to metabolize these precursors. In addition, we studied the fate of gluconate in these models.

8

Secondly, we investigated the extent to which each type of fluid is effective in improving acid-base status, and tissue oxygenation, which can be considered the primary goals fluid resuscitation in states of shock. We focused on the kidney because it is considered to be the organ most at risk during states of shock and fluid overuse.

Supplementary Table 1 Physico-chemical properties of fluids used in the study compared to human plasma

	Plasma	Normal saline (9‰)	Ringer's Lactate (RL)	Ringer's Acetate (RA)	Plasma-Lyte (RA-Glu/Mg)
Sodium (mmol L^{-1})	142	154	131	130	140
Chloride (mmol L^{-1})	103	154	111	110	98
Potassium (mmol L^{-1})	4.5		5	4	5
Calcium (mmol L^{-1})	2.5		2	2	
Magnesium (mmol L^{-1})	1.25			1	1,5
Lactate (mmol L^{-1})	1.5		29		
Acetate (mmol L^{-1})				30	27
Gluconate (mmol L^{-1})					23
HCO$_3$ (mmol L^{-1})	24				
Albumin	30-52				
Proteinate	20				
Effective Strong Ion Difference	24	0	29	27	50
Theoretical osmolarity (mosmol L^{-1})	291	308	276	277	294.5
Water content (%)	94	99.7	99.7	99.7	99.7
Theoretical osmolality (mosmol kg^{-1})	310	308	276	276	294.5
Osmotic coefficient	0.926	0.926	0.926	0.926	0.926
Actual osmolality (mosmol kg^{-1})	287	286	256	256	272.7

Material and methods

Animals

All experiments in this study were approved by the Animal Research Committee of the Academic Medical Centre of the University of Amsterdam (DFL 102919). Care and handling of the animals were in accordance with the guidelines from the Institutional and Animal Care and

Use Committees. A total of 75 rats were needed in these experiments (n=6 per group), including 3 animals for setting up the model of PLR. Experiments were performed on male Sprague-Dawley rats (Harlan, The Netherlands), aged 10±2 weeks with a mean±SD body weight of 330±20g.

Surgical preparation

The rats were anesthetized with an intraperitoneal injection of a mixture of 100 mg kg^{-1} ketamine (Nimatek®; Eurovet, Bladel, the Netherlands), 0.5 mg kg^{-1} medetomidine (Domitor; Pfizer, New York, NY) and 0.05 mg kg^{-1} atropine-sulfate (Centrafarm, Etten-Leur, The Netherlands) and maintained with 50 mg kg^{-1} ketamine at a dose of 5 ml kg^{-1} h^{-1}. After tracheotomy, the animals were mechanically ventilated with 0.4 FiO$_2$. A heating pad under the animal allowed the body temperature to be controlled and maintained at 37±0.5°C. The end-tidal PCO$_2$ was maintained between 4 and 4.7 kPa.

The right carotid (pressure) and femoral (for blood shedding and samples) arteries and jugular anaesthesia) and femoral (fluid resuscitation) veins were cannulated with polyethylene catheters (outer diameter = 0.9 mm; Braun, Melsungen, Germany). For fluid maintenance during surgery, 0.9% NaCl (Baxter, Utrecht, The Netherlands) at a rate of 10 ml kg^{-1} hour^{-1} was administered. For liver resection, a 70% partial liver resection (PLR) was achieved by ligaturing branches of the hepatic artery and portal vein using 3/0 silk thread and resecting 2 lobes of the liver after a midline laparotomy. The left kidney was exposed, de-capsulated and immobilized in a Lucite kidney cup (K. Effenberger, Pfaffingen, Germany) via a 4 cm incision in the left flank. Renal vessels were carefully separated to preserve the nerves and adrenal gland. An ultrasonic flow probe was placed around the left renal artery (type 0.7 RB; Transonic Systems Inc., Ithaca, NY, USA) and connected to a flow meter (T206; Transonic Systems Inc.) to continuously measure renal blood flow (RBF). The left ureter was isolated, ligated and cannulated with a polyethylene catheter for urine collection.

After the surgical procedure (approximately 60 minutes), one optical fibre was placed above the de-capsulated kidney and another one above the renal vein to measure oxygenation using a phosphorescence lifetime technique.[18] A small piece of aluminium foil was placed on the dorsal side of the renal vein to prevent the contribution of the underlying tissue toward the phosphorescence signal in the venous PO$_2$ measurement. Oxyphor G2 (a two-layer glutamate dendrimer of tetra-(4-carboxy-phenyl) benzoporphyrin; Oxygen Enterprises Ltd, Philadelphia,

PA, USA) was subsequently infused (6 mg kg^{-1} IV over 5 min), followed by a 30-minute stabilization period. The surgical field was covered with a humidified gauze compress throughout the experiment to prevent drying of the exposed tissue.

Experimental protocol

After a stabilization period, the animals were bled from the left femoral artery catheter at a rate of 1 ml min^{-1} using a syringe pump (Harvard 33 syringe pump; Harvard apparatus, South Natick, MA) until reaching a MAP of 30 mmHg. This was maintained for 1 hour by re-infusing or withdrawing blood. Coagulation of the shed blood was prevented by adding 200 UI of heparin in the syringe. The animals were then randomized into a total of 12 groups : 4 groups for a 60-min fluid resuscitation process using RL, RA, RA-Glu/Mg or 0.9% NaCl (Saline) until a target MAP of 65 mmHg was reached, 2 haemorrhagic shock (HS) groups, as well as 2 control groups, both with and without PLR, were observed. The fluid infused was prepared in advance and blinded to the technician (B.E). However, only one technician performed the experiments therefore the blinding was only partial. Each group included six animals (n=6). The resuscitation fluid was infused at a rate of 0.5 ml min^{-1}. Measurements were made at baseline (*BL*); 60 minutes after initiation of haemorrhagic shock (*Shock*); and the end of the experiment, which was 60 minutes after starting resuscitation (*R60*). The right kidney, the heart and the brain were harvested to determine their water content using the wet/dry weighing technique (held at 100°C for 24 h) and calculated as follows: [(wet tissue weight-dry tissue weight)/wet tissue weight] /100.

Blood gas measurements, acid-base balance, and osmolality

Arterial blood samples (0.2 ml) were taken at five separate time points. Arterial blood gas parameters were determined using a blood gas analyser (ABL505 Flex, Radiometer, Copenhagen, Denmark), and haemoglobin concentration (Hb), haemoglobin oxygen saturation, base excess (BE) and the concentrations of sodium and chloride were measured. Plasma creatinine, chloride, potassium content, aspartate transaminase (AST) and urine creatinine and urine Na$^+$ (U_{Na}) samples were measured using an automatic analyser (Roche Modular P800 automatic analyser, Roche Diagnostics, Basel, Switzerland) at the end of the experiment. The osmolality of the plasma was determined using the freezing point method with an osmotic pressure meter (OSMOSTATION, OM-6050; Arkray Europe, Amstelveen, The Netherlands) at the end of the experiment.

Measurement of renal microvascular and venous oxygenation

Renal microvascular PO_2 (μPO_2) and renal venous PO_2 ($P_{rv}O_2$) were measured by oxygen-dependent quenching of phosphorescence lifetimes of the systemically infused albumin-targeted (and therefore circulation-confined) phosphorescent dye Oxyphor G2 as described elsewhere.[18] The saturation of renal venous blood ($S_{rv}O_2$) was determined by Hill's equation with an n coefficient of 2.3.

Calculation of oxygenation parameters and vascular resistance

Renal oxygen delivery was calculated as DO_{2ren} (ml minute^{-1}) = RBF×arterial oxygen content (1.31×hemoglobin×S_aO_2)+(0.003×P_aO_2), where S_aO_2 is the arterial oxygen saturation, and P_aO_2 is the arterial partial pressure of oxygen. Renal oxygen consumption was calculated as VO_{2ren} (ml minute^{-1} g^{-1}) = RBF×(arterial–renal venous oxygen content difference). Renal venous oxygen content was calculated as (1.31×hemoglobin×$S_{rv}O_2$)+(0.003×$P_{rv}O_2$).

Assessment of kidney function

The glomerular filtration rate was estimated with the calculation of creatinine clearance (Cl_{crea}): Cl_{ccrea} = (U_{crea}×V)/P_{crea}, where U_{crea} is the concentration of creatinine in urine, V is the urine volume per unit time, and P_{crea} is the concentration of creatinine in plasma. All urine samples were analysed for sodium concentration [Na$^+$]. In addition, the fractional excretion of Na$^+$ [FE_{Na} (%)] was calculated and used as a marker of tubular function using the following formula: FE_{Na} = (U_{Na}×P_{crea})/(P_{Na}×U_{crea})×100, where U_{Na} is the [Na$^+$] in urine, and P_{Na} is the [Na$^+$] in plasma. Cl_{clear} and FE_{Na} were determined at all time points.

Measurements of lactate, gluconate and acetate in plasma and urine

The plasma and urine lactate concentrations were determined by test strips (EDGE™ Handheld Lactate Analyser, Red Med, Poland). The D-Gluconate/D-Glucono-δ-lactone assay kit (detection limit 0.5 mg/L) and acetic acid assay kit (detection limit 0.14 mg/L) (Megazyme

International Ireland, Bray Business Park, Bray, Co. Wicklow, Ireland) were used to determine the plasma, urine gluconate and acetate concentrations. Briefly, this is based on an enzymatic UV (spectrophotometric at 340 nm) method using 2 enzymes, the gluconate kinase and the gluconate-6-phosphate dehydrogenase.

Statistical analysis

Statistical analysis was performed using GraphPad Prism version 6.1 for Windows (GraphPad Software, San Diego, CA). Values are reported as the mean±SD in the tables and are presented with box and whiskers [min – max]. ANOVA for repeated measurements was used for intergroup and intragroup comparisons using *post hoc* analyses with the Bonferroni's post-test where *p*<0.01. One-way variance analyses with parametric or non-parametric tests were used for the biochemical results and *post hoc* analyses with Bonferroni's post-test were conducted when *p*<0.01 was considered significant. We deliberately chose an alpha level of 0.01 to emphasize the significance of the results.

Results

Systemic and renal haemodynamics (**Table 1**) and all the other parameters were similar in the PLR group and the control group at baseline (**Table 2**). The PLR procedure resulted in a significant increase in the liver AST enzyme compared to the control and HS groups (p<0.01) even in the resuscitated groups (**Supplementary Figure 1**).

Haemorrhagic shock in both experiments (with and without PLR) induced significant decreases in MAP, RBF (**Table 1**), pH, base excess, HCO_3^- (**Table 1**), VO_2, DO_2, $C\mu PO_2$, and $M\mu PO_2$ (**Supplementary Figure 2**) (p<0.01). Haemorrhage resulted in increased concentrations of lactate with a higher anion gap (p<0.01) (**Table 2, Figure 1**). The level of lactate was similar at shock between the 2 experiments. During haemorrhage, all rats presented anuria.

Table 1 Systemic and renal haemodynamics during haemorrhagic shock with and without partial liver resection

	Baseline	Shock	R60
MAP (mmHg)			
Control	101 ± 10	106 ± 8	89 ± 11
HS	103 ± 12	31 ± 1 *	27 ± 3 *
HS+RL	101 ± 11	30 ± 1 *	63 ± 7 *+
HS+RA	106 ± 13	30 ± 1 *	66 ± 0 *+
HS+RA-Glu/Mg	99 ± 9	31 ± 1 *	62 ± 4 +
HS+Saline	104 ± 17	30 ± 1 *	66 ± 1 *+
PLR	91 ± 11	92 ± 10 *	71 ± 4 *
PLR+HS	98 ± 7	31 ± 1 *	30 ± 4 *
PLR+HS+RL	102 ± 6	31 ± 1 *	65 ± 1 *+
PLR+HS+RA	99 ± 6	31 ± 1 *	65 ± 1 *+
PLR+HS+RA-Glu/Mg	91 ± 8	30 ± 1 *	60 ± 5 *+
PLR+HS+Saline	99 ± 10	30 ± 1 *	65 ± 1 *+
RBF (mL min^{-1})			
Control	5.5 ± 1.3	4.5 ± 1.0	4.3 ± 1.0
HS	6.2 ± 1.9	0.6 ± 0.5 *	0.3 ± 0.5 *
HS+RL	7.3 ± 1.4	0.0 ± 0.0 *	4.2 ± 1.2 +
HS+RA	6.9 ± 1.8	0.3 ± 0.6 *	4.4 ± 1.6 +
HS+RA-Glu/Mg	4.9 ± 2.2	0.2 ± 0.2 *	3.6 ± 2.2 +
HS+Saline	7.7 ± 1.4 *	0.0 ± 0.0 *	4.2 ± 0.8 +
PLR	5.7 ± 1.5	5.0 ± 1.5	3.7 ± 0.9
PLR+HS	6.5 ± 1.0	0.3 ± 0.4 *	0.6 ± 0.5 *
PLR+HS+RL	6.7 ± 1.3	0.1 ± 0.1 *	3.5 ± 1.2 +
PLR+HS+RA	5.6 ± 0.5	0.0 ± 0.0 *	4.5 ± 1.2 +
PLR+HS+RA-Glu/Mg	6.3 ± 1.3	0.1 ± 0.2 *	4.2 ± 2.2 +
PLR+HS+Saline	5.3 ± 0.9	0.0 ± 0.0 *	3.4 ± 1.4 +

Mean arterial pressure (MAP), renal blood flow (RBF), haemorrhagic shock (HS), partial liver resection (PLR), Ringer's lactate (RL), Ringer's Acetate (RA), PlasmaLyte (RA-Glu/Mg), baseline (BL), after 60 minutes of hemorrhagic shock (Shock), and 60 minutes after starting resuscitation (R60) (*p<0.01 vs. Control, + p< 0.01 vs. HS group). Values are represented as a Mean±SD

8

The targeted MAP of 65 mmHg was achieved in both experiments after fluid resuscitation, regardless of the fluid used. The amounts of fluid required to achieve the targeted MAP were 28.5±5.9 ml for RL, 36.3±5.1 ml for RA, 44.7±10.4 ml for RA-Glu/Mg, and 28.0±8.8 ml for saline in the group without PLR. In the group with PLR, the amounts were 38.2±6.5 ml for RL, 45.9±9.3 ml for RA, 51.5±11.4 ml for RA-Glu/Mg, and 35±10.9 ml for saline. The volume of RA-Glu/Mg infused was significantly greater in both groups compared to the volumes of saline and RL (p<0.01).

Table 2 Acid-base status, anion gap, and chloride levels

	Baseline	Shock	R60
pH			
Control	7.42 ± 0.02	7.36 ± 0.03	7.37 ± 0.04
HS	7.41 ± 0.02	7.12 ± 0.10 *	7.09 ± 0.09 *
HS+RL	7.39 ± 0.03	7.08 ± 0.09 *	7.25 ± 0.05 *+
HS+RA	7.40 ± 0.04	7.06 ± 0.10 *	7.28 ± 0.03 *+
HS+RA-Glu/Mg	7.39 ± 0.05	7.15 ± 0.09 *	7.31 ± 0.05 +
HS+Saline	7.40 ± 0.03	7.13 ± 0.29 *	7.18 ± 0.04 *+$
PLR	7.41 ± 0.03	7.34 ± 0.04	7.35 ± 0.05
PLR+HS	7.39 ± 0.04	7.11 ± 0.07 *	7.06 ± 0.07 *
PLR+HS+RL	7.40 ± 0.04	7.12 ± 0.05 *	7.22 ± 0.12 *+
PLR+HS+RA	7.40 ± 0.02	7.12 ± 0.07 *	7.29 ± 0.09 +
PLR+HS+RA-Glu/Mg	7.40 ± 0.02	7.10 ± 0.06 *	7.30 ± 0.04 +
PLR+HS+Saline	7.40 ± 0.04	7.06 ± 0.10 *	7.14 ± 0.09 *#
HCO_3^- (mmol L^{-1})			
Control	19.6 ± 1.8	17.9 ± 1.9	16.3 ± 2.5
HS	19.6 ± 1.6	10.0 ± 2.0 *	8.6 ± 1.9*
HS+RL	20.3 ± 2.2	9.7 ± 1.9 *	14.6 ± 2.5+
HS+RA	19.6 ± 2.9	8.7 ± 2.1 *	15.0 ± 1.7+
HS+RA-Glu/Mg	20.1 ± 2.0	10.0 ± 1.1 *	15.9 ± 1.7+
HS+Saline	18.3 ± 1.1	9.2 ± 1.2 *	11.5 ± 1.1*+$
PLR	20.3 ± 0.9	18.3 ± 1.3	17.2 ± 1.0
PLR+HS	19.9 ± 2.1	9.20 ± 1.8 *	9.00 ± 1.6*
PLR+HS+RL	20.0 ± 1.4	9.30 ± 1.5 *	13.40 ± 2.0*+#
PLR+HS+RA	19.9 ± 1.8	10.10 ± 0.7 *	15.50 ± 1.1 +
PLR+HS+RA-Glu/Mg	20.6 ± 1.4	9.50 ± 2.2 *	16.40 ± 1.6 +
PLR+HS+Saline	19.7 ± 2.5	8.60 ± 1.8 *	11.50 ± 2.5 *+#
Anion gap (K^+) (mmol L^{-1})			
Control	21.7 ± 2.4	24.5 ± 3.2	24.5 ± 4.0
HS	21.1 ± 2.7	30.4 ± 3.0*	33.8 ± 2.4 *
HS+RL	21.5 ± 2	31.6 ± 2.6*	26.0 ± 1.8 +
HS+RA	22.2 ± 3	34.3 ± 5.5*+	26.6 ± 3.7 +
HS+RA-Glu/Mg	20.4 ± 1.7	30.6 ± 3.1*	25.3 ± 1.9 +
HS+Saline	22.0 ± 2.1	33.0 ± 3.4*	28.1 ± 2.8 *+$
PLR	24.4 ± 1.8	27.4 ± 1.5*	28.8 ± 2.2 *
PLR+HS	21.8 ± 1.3	31.6 ± 2.3*	34.4 ± 1.8 *
PLR+HS+RL	21.9 ± 1.5	32.1 ± 2.2*	29.2 ± 2.2 *+$
PLR+HS+RA	22.0 ± 1.0	33.0 ± 2.6*	26.6 ± 1.0 +
PLR+HS+RA-Glu/Mg	21.3 ± 2.9	33.0 ± 1.5*	27.3 ± 1.6 +
PLR+HS+Saline	22.4 ± 0.7	34.7 ± 2.3*+	29.9 ± 1.3 *+#
Cl^- (mmol L^{-1})			
Control	107.5 ± 0.8	111.5 ± 2.3	115.0 ± 1.4
HS	108.2 ± 2.7	112.5 ± 4.2	114.5 ± 1.4
HS+RL	106.3 ± 1.0	110.0 ± 1.6	112.0 ± 0.9
HS+RA	107.5 ± 3.2	108.8 ± 3.7 +	111.0 ± 1.8 *+
HS+RA-Glu/Mg	108.0 ± 2.5	112.5 ± 2.4	110 ± 2.28 *+
HS+Saline	109.3 ± 2.6	111.5 ± 2.5	119.2 ± 2.3 *+$
PLR	106.6 ± 0.6	110.0 ± 1.0	113.0 ± 1.0
PLR+HS	109.2 ± 1.8	114.2 ± 1.1	116.6 ± 2.0
PLR+HS+RL	108.0 ± 1.3	114.3 ± 1.4	112.3 ± 2.2 #
PLR+HS+RA	108.2 ± 2.8	115.2 ± 1.9 *	112.5 ± 1.8 #
PLR+HS+RA-Glu/Mg	109.5 ± 2.4	116.2 ± 1.8 *+	108.7 ± 1.0 *+
PLR+HS+Saline	108.3 ± 1.4	114.3 ± 1.2	118.7 ± 1.7 *+#

*p<0.01 vs. Control group, + p< 0.01 vs. HS group, $ p<0.01 vs. HS+RA-Glu/Mg for resuscitation fluids within intact liver groups, # p<0.01 vs. PLR+HS+RA-Glu/Mg for resuscitation fluids within liver resection groups. Values are presented as a Mean±SD. Haemorrhagic shock (HS), partial liver resection (PLR), Ringer's lactate (RL), Ringer's Acetate (RA), PlasmaLyte (PL)
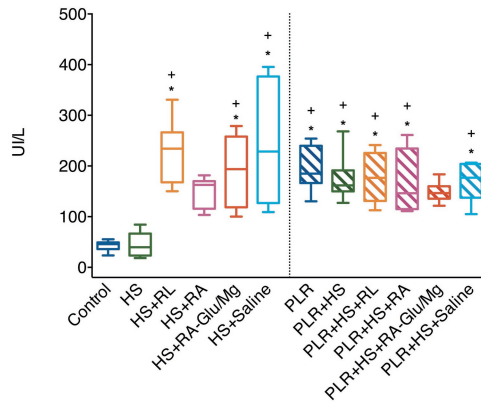
Supplementary Figure 1. Plasma AST levels at the completion of the experiments

*p<0.01 vs. control, + p<0.01 vs. HS. Data is presented in box and whiskers are [min-max].
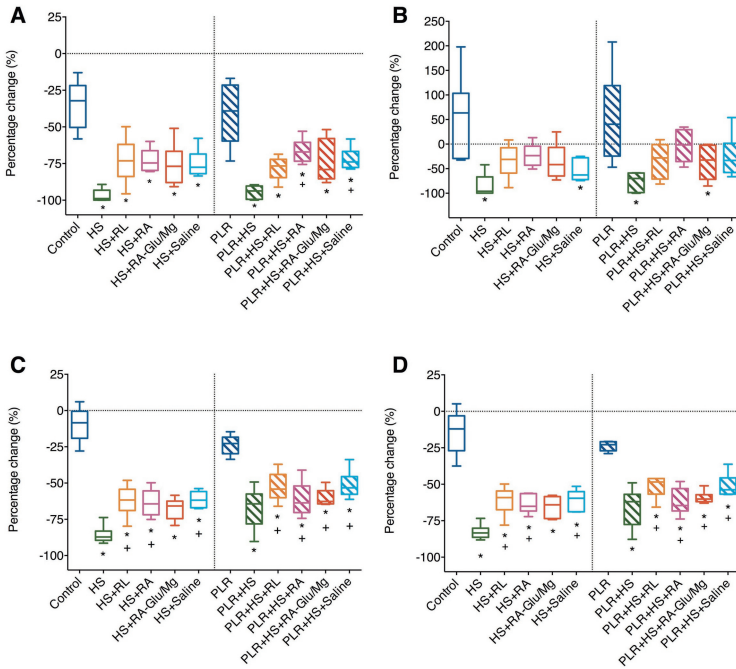
Supplementary Figure 2. Percentage changes in cortical and medullar kidney oxygenation and renal oxygen delivery and consumption from baseline to the end of experiment (R60)

(A) Cortical kidney micro PO$_2$ (CμPO$_2$), (B) medullar kidney micro PO$_2$ (MμPO$_2$), (C) renal oxygen delivery (DO$_{2ren}$), (D) renal oxygen consumption (VO$_{2ren}$). *p<0.01 vs. control, + p<0.01 vs. HS. Data is presented in box and whiskers are [min-max].

Concentrations of bicarbonate precursors and acid-base status after fluid resuscitation

The lactate and gluconate concentrations in plasma at the end of both experiments are shown in **Figure 1 and 2**. The acetate level was not detectable in the plasma because the level was below the threshold. Fluid resuscitation with either RA, RA-Glu/Mg or normal saline was effective in reducing lactate concentrations in experiment without PLR, but such a reduction was not achieved when RL was infused (p<0.01). In the PLR experiment, the level of lactate in urine was higher in the RL group (p<0.01) (**Supplementary Figure 3**). Gluconate was excreted in a similar manner in urine in the 2 experiments (**Figure 3**). However, plasma gluconate level was higher in the PLR group (p=0.03). No significant change was observed in acetate excretion.
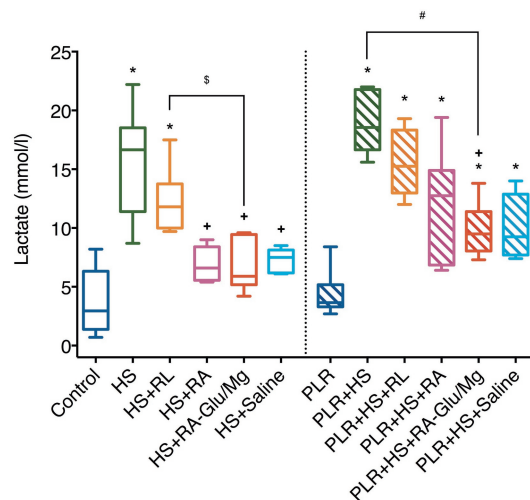
Figure 1. Levels of plasma lactate at the end of both experiments

*p<0.01 vs. control, + p<0.01 vs. HS. $ p<0.01 vs. HS+PL for resuscitation fluids within intact liver groups, # p<0.01 vs. PLR+HS+PL for resuscitation fluids within liver resection groups. Data is presented in box and whiskers are [min-max].

Acetate-based fluids resuscitation led to similar pH and bicarbonate concentrations to control group and increased bicarbonate concentrations more than RL or normal saline did in the PLR experiment (p<0.01) (**Table 2**). Normal saline group in both experiments exhibited the worst acid-base status (p<0.01). $PaCO_2$ did not change across experiments (**Supplementary Table 2**).
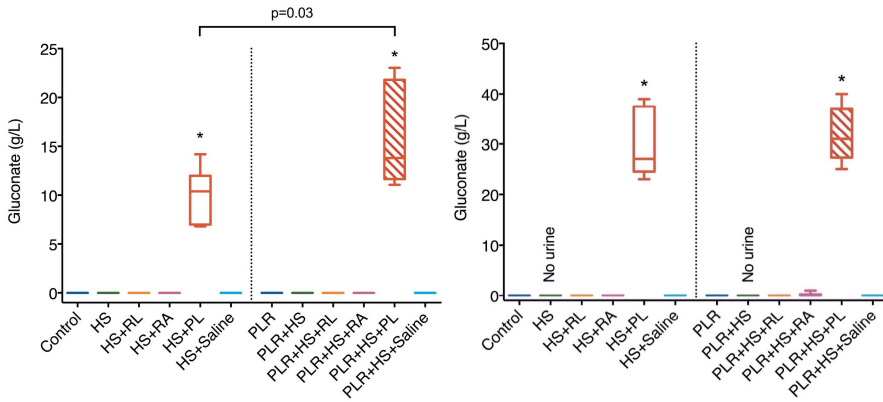
Figure 2 & 3. Levels of plasma gluconate (left panel) and total urine excretion of gluconate (right panel) at the end of both experiments

*p<0.01 vs. control. Data is presented in box and whiskers are [min-max].

Renal oxygenation and function

CμPo2 and MμPo2 decreased during the haemorrhagic phase to ~2.7 and ~1.9 kPa (20 and ~14 mmHg), respectively. Overall, fluid resuscitation did not restore renal oxygenation to baseline (p<0.01) (**Supplementary Figure 2)**. DO_{2ren} remained also significantly lower than the control group (p<0.01) at the end of all experiments.

Renal function, as represented by FE_{Na} and creatinine clearance (Cl_{creat}), is shown in **Table 3**. There was no difference relative to the control group in the PLR experiment. FE_{Na} increased significantly in all groups after fluid resuscitation (p<0.01) by the end of the experiment.

Fluid resuscitation resulted in increases in water content and tissue oedema in the kidney from 78.1±0.4% for the control group to 81.1±0.6%, 81.1±1.2%, 82.1±0.6%, and 82.1±0.7% for the RL, RA, RA-Glu/Mg, and saline groups, respectively, in the experiment without PLR (p<.0.01). The same was observed in rats with liver resection (p<0.01). Finally, the plasma osmolality was higher only in the RA-Glu/Mg group with PLR (p<0.01).

Supplementary Table 2 Base excess and carbon dioxide partial pressure trends

	Baseline	Shock	R60
$PaCO_2$ (mmHg)			
Control	4.3 ± 0.4	4.4 ± 0.3	3.9 ± 0.5
HS	4.3 ± 0.4	4.3 ± 0.8	3.9 ± 0.5
HS+RL	4.7 ± 0.4	4.4 ± 0.5	4.8 ± 0.4
HS+RA	4.4 ± 0.9	4.3 ± 0.9	4.4 ± 0.5
HS+RA-Glu/Mg	4.7 ± 1.1	4.1 ± 0.9	4.4 ± 0.4
HS+Saline	4.1 ± 0.3	4.8 ± 0.5	4.3 ± 0.3
PLR	4.4 ± 0.1	4.7 ± 0.5	4.4 ± 0.7
PLR+HS	4.5 ± 0.4	4 ± 0.5	4.4 ± 0.5
PLR+HS+RL	4.5 ± 0.3	3.9 ± 0.4	4.7 ± 1.7
PLR+HS+RA	4.4 ± 0.5	4.3 ± 0.4	4.5 ± 1.3
PLR+HS+RA-Glu/Mg	4.7 ± 0.3	4.3 ± 0.4	4.7 ± 0.7
PLR+HS+Saline	4.4 ± 0.4	4.1 ± 0.1	4.7 ± 0.7
Base excess (mmol L^{-1})			
Control	-4.2 ± 1.8	-6.6 ± 2.1	-8.1 ± 2.7
HS	-4.3 ± 1.6	-17.5 ± 2.9*	-19.4 ± 2.9*
HS+RL	-3.9 ± 2.4	-18.3 ± 2.9*	-11.3 ± 3.0 +
HS+RA	-4.5 ± 2.5	-19.6 ± 2.9*	-10.5 ± 1.8 +
HS+RA-Glu/Mg	-4.1 ± 1.6	-17.3 ± 1.6*	-9.2 ± 2.1 +
HS+Saline	-5.7 ± 1.3	-19.4 ± 2.0*	-15.2 ± 1.5 *+$
PLR	-3.6 ± 1.3	-6.3 ± 1.5	-7.3 ± 1.0
PLR+HS	-4.2 ± 2.3	-18.4 ± 2.6*	-19.3 ± 2.3 *
PLR+HS+RL	-4.0 ± 1.6	-18.2 ± 2.1*	-12.9 ± 3.0 *+#
PLR+HS+RA	-4.1 ± 1.7	-17.3 ± 1.5*	-10.6 ± 2.5 *
PLR+HS+RA-Glu/Mg	-3.5 ± 1.6	-18.3 ± 3.0*	-8.8 ± 1.7 +
PLR+HS+Saline	-4.3 ± 2.8	-19.6 ± 2.8*	-15.7 ± 3.5 *+#

*$p<0.01$ vs. Control group, + $p< 0.01$ vs. HS group, $ $p<0.01$ vs. HS+RA-Glu/Mg for resuscitation fluids within intact liver groups, # $p<0.01$ vs. PLR+HS+RA-Glu/Mg for resuscitation fluids within liver resection groups. Values are presented as a Mean±SD.

Table 3 Renal function according to different balanced fluid resuscitations in animals with and without partial liver resection

	Baseline	R60
Cl_{creat} (ml min^{-1} g^{-1})		
Control	0.14 ± 0.05	0.16 ± 0.09
HS	0.09 ± 0.08	/
HS+RL	0.16 ± 0.15	0.06 ± 0.05*
HS+RA	0.16 ± 0.04	0.07 ± 0.05
HS+RA-Glu/Mg	0.14 ± 0.03	0.09 ± 0.05
HS+Saline	0.11 ± 0.07	0.08 ± 0.04
PLR	0.10 ± 0.04	0.06 ± 0.04*
PLR+HS	0.09 ± 0.06	/
PLR+HS+RL	0.10 ± 0.04	0.16 ± 0.21
PLR+HS+RA	0.13 ± 0.05	0.13 ± 0.06
PLR+HS+RA-Glu/Mg	0.25 ± 0.37	0.14 ± 0.08
PLR+HS+Saline	0.09 ± 0.03	0.07 ± 0.02
FE_{Na} (%)		
Control	2 ± 0.9	2.9 ± 2
HS	1.6 ± 0.9	/
HS+RL	2.7 ± 3.2	24 ± 8.9*
HS+RA	2.4 ± 1.6	32.5 ± 17.7*
HS+RA-Glu/Mg	2.1 ± 3.2	51 ± 15.6*
HS+Saline	4.6 ± 4.5	35.1 ± 18.8*
PLR	1.5 ± 1.4	2 ± 2

PLR+HS	1.6 ± 0.6	/
PLR+HS+RL	1.5 ± 1	32.9 ± 39*
PLR+HS+RA	1.3 ± 0.6	46 ± 36.3*
PLR+HS+RA-Glu/Mg	2 ± 1.3	45.2 ± 11*
PLR+HS+Saline	1.6 ± 1.5	58.1 ± 28.9*

*The shock time point was removed from the table because almost all animals presented anuria. * p<0.05 vs. control*

Discussion

The main results of our study were that acetate-balanced resuscitation fluids demonstrated a significant improved buffering capacity in the presence or absence of liver impairment. Ringer's lactate was also effective in correcting the acid-base status but to a lesser degree. Normal saline was the less effective fluid regarding acid-base control. Secondly, our study showed an increased plasma level of gluconate in the presence of liver failure (e.g., PLR), suggesting that this portion is actually metabolized by the liver while the other part potentially remains in the vascular system.[19] In this respect, two recent studies have confirmed that gluconate is metabolized through gluconokinase in the human liver into 6-phosphogluconate, which could then be further degraded through the hexose monophosphate shunt via the 6-phosphogluconate dehydrogenase.[20,21] Although our results did not indicate an increase in gluconate excretion by the kidney after PLR, a large amount of gluconate was excreted in urine as previously observed.[22,23] Two separate experimental studies showed no increase in the pH value after an infusion of gluconate. [24,25] These suggest that gluconate is not relevant for the generation of bicarbonate. Therefore, the "anti-acidotic" effect of RA-Glu/Mg might not be due to gluconate, but rather attributed to acetate.

Acetate was metabolized effectively, regardless of liver failure and severe shock in this study. This confirms that acetate is metabolized elsewhere or that limited hepatic function is sufficient to support bicarbonate generation. Acetate can be metabolized in several extra-hepatic tissues, including the muscles, brain, myocardium, and renal cortex, because they all have the required enzymes.[15,17] Therefore, acetate is subject to less accumulation in states of shock with impaired liver function. However, the literature provided inconsistent results regarding the buffering capacity of acetate-balanced fluids. In addition, an in vitro study revealed that the buffering capacity of these fluids was weak compared to human or animal plasma.[26] Fluid resuscitation with RA-Glu/Mg yielded a similar buffering effect to RL but lower survival rate

8

following fatal haemorrhage in swine.[27] In a randomized clinical trial comparing RA-Glu/Mg versus RL during living donor right hepatectomy, a small improvement in base excess was noted without change in pH.[28] Weinberg *et al.* observed less hyperchloremia and hyperlactatemia but also with no change in pH or base excess after infusion of RA-Glu/Mg compared to normal saline in patients with major liver resection.[29] On the contrary, two studies, in trauma patients and in the perioperative setting, provided evidence of an improved acid-base status using RA-Glu/Mg.[12,30]

As expected, lactate concentrations increased during haemorrhagic shock. Measured lactate concentrations were influenced by the additional lactate supplied by resuscitation with RL. In addition, PLR reduced the capacity of lactate to be metabolized as shown by the trend increase in urine lactate. It may have a negative impact on the acid-base balance when it accumulates. Nevertheless, RL was superior to normal saline in terms of correcting acid-base status even in the presence of liver failure. This result was consistent with the literature.[31]

The issue about the choice of anions in resuscitation fluids has been central in the "Great fluid debate" and has mainly focused itself on the choice of chloride as the conventional anion in the routine use of 0.9% NaCl.[13,32] The reason for the controversy has been the result of dilutional acidosis being caused by excessive amounts of chloride administration during fluid resuscitation. The effect of this procedure results in acidosis not being corrected and possibly metabolic acidosis becoming dilutional acidosis causing confusion as to the origin of the acid base disturbance. On the other hand, acidosis in itself can have unwanted effects, such as renal vasoconstriction, and this can cause deleterious effects especially on the kidney. For these reasons balanced salt solutions such based on either acetate or lactate have been advocated also because these anions can function as bicarbonate precursors.[9] Finally, the importance of the ability of clinicians to interpret the origin of acidosis as being metabolic in origin allows its use as a surrogate for tissue oxygenation and is an additional importance for understanding the contribution of various anions to acid base chemistry in a physiological setting such as we chose for this study.

All fluids improved systemic and renal haemodynamics after reaching the targeted MAP but failed to restore renal oxygenation as shown before.[33] The ineffectiveness of the correction of renal oxygenation resides in the fact that these non-oxygen carrying fluids only marginally transport oxygen to the tissues.[33,34] The differences between balanced solutions and normal saline for fluid were found to exist mainly in the acid-base imbalance. Because normal saline

brought a large amount of chloride induced acid-base alteration, it could blunt the benefits of fluid resuscitation, as seen by its lack of efficacy at improving pH levels. While tissue oxygenation might be partially restored with efficient lactate clearance, the existence of a low pH and a low bicarbonate level may invite a further unrequired administration of fluid. This will contribute to increase the plasma level of chloride, prevent metabolic acidosis from being corrected, and increase the fluid load. However, in a large clinical trial including intensive care unit patients, Young *et al.* did not demonstrate beneficial outcomes of RA-Glu/Mg compared to normal saline, especially on the kidney.[5]

Significantly more fluid was required to achieve a MAP of 65 mmHg when using acetate containing fluids. Acetate can cause vasodilation which is presumably mediated by the release of adenosine from tissues,[35,36] and these animals may require additional fluid. Moreover, magnesium present in RA-Glu/Mg may also induce vasodilation[37] and the combined action of both, acetate and magnesium, may decrease systemic resistance. However, it is unknown whether this amount of magnesium (3 mmol/L) can induce such a vasodilation, even though magnesium concentration is increased.[29]

Regarding the limitations, we did not assess true liver function with an indocyanin green test. A 70% PLR might not be sufficient to induce a significant liver failure. However, in a pilot study, the animals did not survive in case of a larger resection. Although unlikely to have a clinical impact, we might have missed a change in plasma acetate concentrations, already low [0.06 to 0.2 mmol L^{-1}],[15] because it remained below the detection threshold of our assay. We chose to administer 0.9% saline for fluid maintenance during liver surgery because we sought to evaluate the effect of anion buffers after PLR and HS and obtain same acid-base status at baseline (after PLR) in all animals. Although the experiment would have been purer, the infusion of normal saline was of similar amount in the different interventions in both experiments. By infusing the study fluid from the start of the surgery, baseline values recorded before haemorrhage might have differed significantly. Finally, although probably low, we cannot precisely state how much the gluconate accounted for the buffering effect during resuscitation.

Conclusion

In cases of haemorrhagic shock with liver failure, the subsequent accumulation of lactate dampened the buffering effect of RL. Acetate and the combination of acetate and gluconate

8

appeared to be metabolized efficiently in this experimental study. Because of the large amount of gluconate excreted in an unchanged form, this anion may not contribute to the buffering effect. Normal saline seemed to be the most unsuitable fluid when compared to balanced fluids, even in cases of liver failure.

Details of Authors contributions

B.E.: Study design, carried out experiments, data analysis and writing up of the first draft and reviewing of manuscript; **A.K:** Study design, carried out experiments, data analysis and writing up of the first draft and reviewing of manuscript; **P.G.:** Data analysis, writing final version and reviewing of manuscript; **C.I.:** study design, writing final version and reviewing of manuscript.

Acknowledgments

Declaration of Interest and funding

.

References

1.   Myburgh JA, Finfer S, Bellomo R, et al. Hydroxyethyl starch or saline for fluid resuscitation in intensive care. *N Engl J Med*. 2012;367(20):1901–1911.

20.   Rolfsson Ó, Paglia G, Magnusdóttir M, Palsson BO, Thiele I. Inferring the metabolism of human orphan metabolites from their metabolic network context affirms human gluconokinase activity. *Biochem J*. 2013;449(2):427–435.

21.   Rohatgi N, Nielsen TK, Bjørn SP, et al. Biochemical characterization of human gluconokinase and the proposed metabolic impact of gluconic acid as determined by constraint based metabolic network analysis. *PLoS ONE*. 2014;9(6):e98760.

22.   Howard PJ, Wilde WS, Malvin RL. Localization of renal calcium transport; effect of calcium loads and of gluconate anion on water, sodium and potassium. *Am J Physiol*. 1959;197:337–341.

23.   Stetten MR, Stetten D. The metabolism of gluconic acid. *J Biol Chem*. 1950;187(1):241–252.

24.   Kirkendol PL, Starrs J, Gonzalez FM. The effects of acetate, lactate, succinate and gluconate on plasma pH and electrolytes in dogs. *Trans Am Soc Artif Intern Organs*. 1980;26:323–327.

25.   Naylor JM, Forsyth GW. The alkalinizing effects of metabolizable bases in the healthy calf. *Can J Vet Res*. 1986;50(4):509–516.

26.   Traverso LW, Medina F, Bolin RB. The buffering capacity of crystalloid and colloid resuscitation solutions. *Resuscitation*. 1985;12(4):265–270.

27.   Traverso LW, Lee WP, Langford MJ. Fluid resuscitation after an otherwise fatal hemorrhage: I. Crystalloid solutions. *J Trauma*. 1986;26(2):168–175.

28.   Shin W-J, Kim Y-K, Bang J-Y, Cho S-K, Han S-M, Hwang G-S. Lactate and liver function tests after living donor right hepatectomy: a comparison of solutions with and without lactate. *Acta Anaesthesiol Scand*. 2011;55(5):558–564.

29.   Weinberg L, Pearce B, Sullivan R, et al. The effects of plasmalyte-148 vs. Hartmann's solution during major liver resection: a multicentre, double-blind, randomized controlled trial. *Minerva Anestesiol*. 2015;81(12):1288–1297.

30.   Young JB, Utter GH, Schermer CR, et al. Saline versus Plasma-Lyte A in initial resuscitation of trauma patients: a randomized trial. *Ann Surg*. 2014;259(2):255–262.

31.   Orbegozo Cortés D, Rayo Bonor A, Vincent JL. Isotonic crystalloid solutions: a structured review of the literature. *Br J Anaesth*. 2014;112(6):968–981.

32.   Ince C, Groeneveld ABJ. The case for 0.9% NaCl: is the undefendable, defensible? *Kidney Int*. 2014;86(6):1087–1095.

33.   Legrand M, Legrand M, Mik EG, et al. Fluid resuscitation does not improve renal oxygenation during hemorrhagic shock in rats. *Anesthesiology*. 2010;112(1):119–127.

34.   Johannes T, Mik EG, Nohé B, Unertl KE, Ince C. Acute decrease in renal microvascular PO_2 during acute normovolemic hemodilution. *Am J Physiol Renal Physiol*. 2007;292(2):F796–803.

35.   Frohlich ED. Vascular Effects of the Krebs Intermediate Metabolites. *Am J Physiol*. 1965;208:149–153.

36.   Nutting CW, Islam S, Ye MH, Batlle DC, Daugirdas JT. The vasorelaxant effects of acetate: role of adenosine, glycolysis, lyotropism, and pHi and Cai2+. *Kidney Int*. 1992;41(1):166–174.

37.   Teragawa H, Matsuura H, Chayama K, Oshima T. Mechanisms responsible for vasodilation upon magnesium infusion in vivo: clinical evidence. *Magnes Res*. 2002;15(3-4):241–246.

8

9

EFFECTS OF N-ACETYLCYSTEINE (NAC) SUPPLEMENTATION IN RESUSCITATION FLUIDS ON RENAL MICROCIRCULATORY OXYGENATION, INFLAMMATION, AND FUNCTION IN A RAT MODEL OF ENDOTOXEMIA

Bulent Ergin,[1,5] Philippe Guerci,[1,2] Lara Zafrani,[1] Frank Nocken,[3] Asli Kandil,[4] Ebru Gurel,[4] Cihan Demirci-Tansel,[4] and Can Ince[1,5]

1. Department of Translational Physiology, Academic Medical Center, Amsterdam, The Netherlands
2. University of Lorraine, Vandoeuvre-Lès-Nancy, France
3. Divisional Medical & Clinical Affairs Generics & Standard Solutions, Volume Therapy, Fresenius Kabi Deutschland GmbH
4. Department of Biology, Faculty of Science, University of Istanbul, Istanbul, Turkey
5. Department of Intensive Care, Erasmus MC, University Medical Center, Rotterdam, the Netherlands

Abstract

Background: Modulation of inflammation and oxidative stress appears to limit sepsis-induced damage in experimental models. The kidney is one of the most sensitive organs to injury during septic shock. In this study, we evaluated the effect of N-acetyl cysteine (NAC) administration in conjunction with fluid resuscitation on renal oxygenation and function. We hypothesized that reducing inflammation would improve the microcirculatory oxygenation in the kidney and limit the onset of acute kidney injury (AKI).

Methods: Rats were randomized into 5 groups (n=8 per group): 1) control group, 2) control + NAC, 3) endotoxemic shock with lipopolysaccharide (LPS) without fluids, 4) LPS + fluid resuscitation and 5) LPS + fluid resuscitation + NAC (150 mg/kg/h). Fluid resuscitation was initiated at 120 min and maintained at fixed volume for 2 hours with hydroxyethyl starch (HES 130/0.4) dissolved in acetate-balanced Ringer's solution (Volulyte) with or without supplementation with NAC (150 mg/kg/h). Oxygen tension in the renal cortex (CμPO$_2$), outer medulla (MμPO$_2$), and renal vein was measured using phosphorimetry. Biomarkers of renal injury, inflammation and oxidative stress were assessed in kidney tissues.

Results: Fluid resuscitation significantly improved the systemic and renal macrohemodynamic parameters after LPS. However, the addition of NAC further improved cortical renal oxygenation, oxygen delivery and oxygen consumption (p<0.05). NAC supplementation dampened the accumulation of NGAL or L-FABP, hyaluronic acid and nitric oxide in kidney tissue (p<0.01).

Discussion: The addition of NAC to fluid resuscitation may improve renal oxygenation and attenuate microvascular dysfunction and AKI. Decreases in renal NO and hyaluronic acid levels may be involved in this beneficial effect. A therapeutic strategy combining initial fluid resuscitation with antioxidant therapies may prevent sepsis-induced AKI.

Keywords: acute kidney injury, sepsis, N-acetyl cysteine, kidney oxygenation, inflammation

Introduction

Inflammation is a key process in the pathophysiology of septic shock.[1] The whole activation of leukocytes, the cascade of inflammation, the associated cytokine storm, and endothelial cell dysfunction collaborate to alter the microcirculation.[2,3] Subsequently, tissue hypoxia and dysoxia due to heterogeneity of the microcirculation will occur.[4] Fluid resuscitation may not only help resolve some of these issues but also lead to the activation of oxidative pathways in itself, resulting in a heterogeneous distribution of blood flow and tissue oxygenation, especially in the renal cortex.[5,6] Because reactive oxygen species (ROS) participate in the pathophysiology of endotoxemic shock, it has been suggested that moderating the oxidative stress and inflammatory reaction would translate into improving the microcirculation and oxygenation of the tissues. Previous studies have demonstrated an interest in the use of antioxidants for preventing sepsis-induced damage in these organs.[7-9] Indeed, the experimental literature is full of studies of drugs that target and are effective at dampening inflammation and oxidative stress. Some trials have reported several anti-inflammatory or antioxidant drugs with discordant effects on major outcomes.[10,11] In fact, antioxidant therapies for specific organs might be of interest. Acute kidney injury (AKI) and acute lung injury are particularly common complications of sepsis, and the development of either increases mortality probably because these organs are more sensitive to inflammation and oxidative stress insults. Thus, the kidney could benefit from antioxidant drugs.

A common approach for the inhibition of oxidant-mediated injury is the use of glutathione-modulating agents such as sulfhydryl or thiol compounds. Among all the drugs used to interact with this pathway, N-acetylcysteine (NAC) is the most studied for its lung and renal protective effects.[12-16] NAC is a thiol compound with antioxidant and vasodilatory properties.[12] NAC is regarded as an important antioxidant as it is a source of sulfhydryl and glutathione groups in cells and, due to its interaction with ROS, is a scavenger of free radicals. In septic patients, the endogenous antioxidant glutathione is depleted.[17] Decreased levels of glutathione may lead to decreased protection of cell membranes against oxygen radicals. NAC serves as a precursor of glutathione and can replenish the intracellular glutathione stores.[12] Moreover, NAC targets kidney microcirculatory blood flow.[18,19] NAC has also been widely studied for its nephroprotective effects in various settings.

Hypoxia and inflammation have an interdependent relationship. Several molecular pathways of cross-talk between hypoxia and inflammation in the kidney have been identified.[20-

22 From a physiological perspective, although hypoxia may lead to inflammation and vice versa, it is unclear whether correcting or modulating either of these states would translate into better tissue oxygenation and improved outcomes. NAC would be interesting for testing whether the modulation of inflammation could correct tissue hypoxia during sepsis.

To date, no study has focused on tissue oxygenation in specific organs such as the kidney but rather demonstrated that either pretreatment or post-treatment with NAC decreased the markers of organ injury. In this study, we assessed kidney tissue oxygenation in an endotoxemic shock model resuscitated with balanced hydroxyethyl starch - Ringer's acetate either with or without supplementation with NAC. We sought to promote blood flow and oxygenation to the organs by the means of reducing inflammation and oxidative stress.

Methods

Animals

All experiments in this study were approved by the institutional Animal Experimentation Committee of the Academic Medical Center of the University of Amsterdam (DFL102538). The care and handling of the animals were in accordance with the guidelines for Institutional Animal Care and Use Committees. The study was conducted in accordance with the Declaration of Helsinki. Experiments were performed on albino Wistar rats (Harlan Netherlands BV, Horst, The Netherlands) with a mean±SD body weight of 325±6 g.

Surgical preparation

All animals were anesthetized with an intraperitoneal injection of a mixture of 90 mg/kg ketamine (Nimatek®, Eurovet, Bladel, The Netherlands), 0.5 mg/kg dexmedetomidine (Dexdomitor, Pfizer Animal Health BV, Capelle aan den IJssel, The Netherlands), and 0.05 mg/kg atropine-sulfate (Centrafarm Pharmaceuticals BV, Etten-Leur, The Netherlands). After a tracheotomy was performed, the animals were mechanically ventilated with a fraction of inspired oxygen (FiO_2) of 0.4. Body temperature was maintained at 37±0.5°C during the entire experiment by an external thermal heating pad. Ventilator settings were adjusted to maintain an arterial partial pressure of carbon dioxide ($PaCO_2$) between 35 and 40 mmHg. For drug and fluid administration as well as hemodynamic monitoring, vessels were cannulated with

polyethylene catheters with an outer diameter of 0.9 mm (Braun, Melsungen, Germany). A catheter in the right carotid artery was connected to a pressure transducer to monitor the mean arterial blood pressure (MAP) and heart rate. The right jugular vein was cannulated for continuous infusion of Ringer's lactate (Baxter, Utrecht, The Netherlands) at a rate of 15 ml/kg/hour and for the maintenance of anesthesia. The right femoral artery was cannulated for drawing blood samples; the right femoral vein, for drug administration. The left kidney was exposed, decapsulated, and immobilized in a Lucite kidney cup (K. Effenberger, Pfaffingen, Germany) via an ~4 cm incision in the left flank in each animal. Renal vessels were carefully separated to preserve the nerves and adrenal gland. A perivascular ultrasonic transient time flow probe was placed around the left renal artery (type 0.7 RB Transonic Systems Inc., Ithaca, NY, USA) and connected to a flow meter (T206, Transonic Systems Inc., Ithaca, NY, USA) to continuously measure renal blood flow (RBF). The left ureter was isolated, ligated, and cannulated with a polyethylene catheter for urine collection. After the surgical preparation, one optical fiber was placed 1 mm above the decapsulated kidney, and another optical fiber was placed 1 mm above the renal vein to measure renal microvascular and venous oxygenation using phosphorimetry. A small piece of aluminum foil was placed on the dorsal side of the renal vein to prevent the underlying tissues from contributing to the phosphorescence signal in the venous PO_2 measurements. The surgical field was covered with a humidified gauze compress throughout the entire experiment to prevent drying of the exposed tissues.

Experimental protocol

After a 30 min stabilization, the rats were randomized into the 5 following groups at baseline: 1) control group, 2) control + NAC, 3) endotoxemic shock with lipopolysaccharide (LPS) without fluid resuscitation, 4) LPS + fluid resuscitation and 5) LPS + fluid resuscitation + NAC (150 mg/kg/h). The groups received either an intravenous bolus of 5 mg/kg LPS (LPS group; *Escherichia coli* 0127:B8, Sigma, Paris, France; 3 groups of 8 rats each) or vehicle (control group, 2 groups of 8 rats each). Animals were observed or kept in shock for over 120 min. Fluid resuscitation (15 ml/kg/h) was then started and maintained for 180 min in the LPS groups with 6% hydroxyethyl starch (HES130/0.4) dissolved in Ringer's acetate (HES-RA; Volulyte® 6%, Fresenius Kabi Deutschland GmbH, Germany) as a balanced colloid solution. NAC was administered to the appropriate groups at a rate of 150 mg/kg/h as previously reported [15]. An LPS group was not resuscitated to serve as a shock control. Time points for the measurements

were baseline (T_0), during shock 120 min after administration of LPS (T_1), 30 min after initiating fluid resuscitation (early reperfusion phase) (T_2) and 120 min after starting fluid resuscitation (late reperfusion phase) (T_3), which was the final endpoint of the experiment (**Figure 1**).
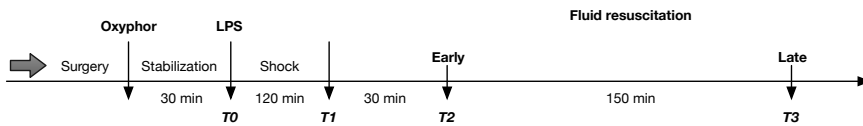

Figure 1. Timeline of the experimental protocol

Blood gas measurements and biochemistry

Arterial blood samples of 0.5 ml were collected from the femoral artery at T_0, T_1, T_2, and T_3. The blood samples were replaced by the same volume of balanced colloid solution. The samples were used to determine blood gas parameters (Radiometer ABL 505 Blood Gas Analyzer, Copenhagen, Denmark). The hematocrit and the levels of potassium, bicarbonate and the anion gap were recorded by the analyzer.

Measurement of renal microvascular oxygenation and venous PO_2

The renal microvascular partial pressure of oxygen (μPO_2) and renal venous PO_2 ($rvPO_2$) were measured by oxygen-dependent quenching of phosphorescence lifetimes of the phosphorescent dye Oxyphor G2 (Oxygen Enterprises Ltd., Philadelphia, PA, USA) as described previously.[23,24] A total of 6 mg/kg IV over 5 min was administered followed by 30 min of stabilization before recording baseline measurements.

Calculation of derivatives of oxygenation parameters and renal vascular resistance

Renal oxygen delivery was calculated using the following formula: DO_{2ren} (ml/min) = RBF × arterial oxygen content (1.31 × hemoglobin × SaO_2) + (0.003 × PaO_2), where SaO_2 is the arterial oxygen saturation and PaO_2 is the arterial partial pressure of oxygen. Renal oxygen consumption

was calculated using the following formula: VO_{2ren} (ml/min/g) = RBF × (CaO_2 – CvO_2), where the renal venous oxygen content (CvO_2) was calculated as (1.31 × hemoglobin × $SrvO_2$) + (0.003 × $rvPO_2$). The $SrvO_{2ren}$ was calculated using the Hill equation with P_{50} = 37 Torr (4.9 kPa) and the Hill coefficient = 2.7. An estimation of the renal vascular resistance (RVR) was defined as RVR (dynes·sec·cm^{-5}) = (MAP/RBF) × 100.

Assessment of kidney function

Creatinine clearance (Cl_{crea} [ml/min]) was assessed as an index of the glomerular filtration rate. Clearance was calculated using the following formula: Cl_{crea} = (U_{crea} × V)/P_{crea}, where U_{crea} is the concentration of creatinine in urine, V is the urine volume per unit time, and P_{crea} is the concentration of creatinine in the plasma. The renal energy efficiency for sodium transport (VO_2/TNa) was assessed using a ratio calculated from the total amount of VO_2 over the total amount of sodium reabsorbed (TNa, mmol/min) according to the following formula: (Cl_{crea} × PNa) – UNa × V.

NO metabolism

The index of total nitric oxide (NO) production is the sum of both nitrite and nitrate accumulated in tissue samples. To determine this index, a saturated solution of vanadium (III) chloride (VCl_3) in 1 mol/l HCl was used as a reducing agent. At a temperature of 90°C, the VCl_3 reagent quantitatively converts nitrite, nitrate, and S-nitroso compounds to NO in a glass reaction vessel. NO was then flushed out of the reaction vessel by the flow of helium gas and was then measured using a Sievers NO analyzer (General Electric Company, GE Water & Process Technologies Analytical Instruments) to detect chemiluminescence as the amount of light from the ozone-NO reaction in the measurement chamber of the analyzer. NO levels were determined in homogenized frozen kidney tissues. A ratio of tissue NO to tissue protein content was used for standardization of NO release per gram of protein.

Glycocalyx component assessments

Hyaluronan is the main component of the endothelial glycocalyx, and alterations in its concentration are attributed to glycocalyx volume loss. Inhibition of tumor necrosis factor-alpha

9

protects against endotoxin-induced endothelial glycocalyx perturbation. Plasma hyaluronan concentrations were determined using a Corgenix hyaluronic acid test kit (Corgenix Inc., Westminster, CO, USA) based on an enzyme-linked hyaluronic acid-binding protein assay.

Measurement of oxidative stress and inflammatory cytokines

All kidneys were homogenized in cold 5 mM sodium phosphate buffer. The homogenates were centrifuged at 12,000 g for 15 min at 4°C, and the supernatants were used to determine TNF-α, IL-6, hyaluronic acid, malondialdehyde (MDA) and protein carbonyl levels. The levels of these markers were expressed as per gram of protein (Bradford assay). To determine the oxidative stress and inflammatory cytokines levels, enzyme-linked immunosorbent assay (ELISA) kits were used. Tumor necrosis factor-α (TNF-α) (DY510, R&D system, Inc. Minneapolis, USA), interleukin-6 (IL-6) (DY506, R&D system, Inc. Minneapolis, USA), tissue MDA and protein carbonyl were determined in homogenized tissue samples.

Immunohistochemical analysis

Kidney tissues were fixed in 4% formalin and embedded in paraffin. After preparation, kidney sections were incubated with a neutrophil gelatinase-associated lipocalin (NGAL) antibody (NGAL antibody 41105, Abcam, Cambridge, UK) and a polyclonal antibody to rat liver-type fatty acid protein (L-FABP) (HP8010, Hycult Biotect, Uden Holland). Antibodies were diluted in a large volume of UltrAb Diluent (TA-125-UD, Thermo Fisher Scientific, Breda, Holland). The slides were counterstained with Mayer's hematoxylin (LabVision TA-125-MH Thermo Fisher Scientific, Breda, Holland) and mounted in a vision mount (LabVision, TA-060-UG, Thermo Fisher Scientific, Breda, Holland) after washing in distilled water. Both the intensity and the distribution of L-FABP and NGAL staining were scored. For each sample, a histological score (HSCORE) value was derived by summing the percentages of cells that were stained at each intensity multiplied by the weighted intensity of the staining: HSCORE = S Pi (i+1), where i is the intensity score and Pi is the corresponding percentage of the cells.

Statistical analyses

The results are expressed as the mean ± SD. Statistical significance was calculated by one-way and two-way analysis of variance (ANOVA) followed by either Tukey's or Bonferroni multiple comparison tests using GraphPad Prism (GraphPad Prism, Version 5, Software Program, San Diego, CA, USA). $p < 0.05$ was considered statistically significant.

Results

Systemic and renal hemodynamic parameters

The evolution of systemic and renal hemodynamics is presented in **Table 1**. Infusion of LPS induced an early drop in the MAP (76.8±9.3 mmHg vs 45.8±7.9 mmHg, $p < 0.001$) and RBF (4.5±1.5 ml/min vs 0.7±0.6 ml/min, $p < 0.001$) in the control group vs the LPS group, respectively, at T_3. Fluid resuscitation with HES-RA both with and without NAC significantly improved RBF compared to the LPS alone group ($p < 0.05$). Both HES-RA and HES-RA+NAC significantly decreased the RVR compared to LPS alone ($p < 0.001$). After LPS, the addition of NAC to the fluid did not result in improved hemodynamic parameters compared to fluid resuscitation alone. The infusion of NAC led to a decrease in the MAP in the absence of LPS (57.3±5.6 mmHg vs 76.8±9.3 mmHg in the control group, $p < 0.001$).

9

Table 1. Evolution of systemic and renal hemodynamics parameters during the experiment

	T_0 (baseline)	T_1 (shock)	T_2 (30 min)	T_3 (120 min)
MAP[mmHg]				
Time control	102±9.0	86±13	80±9	77±9
Control+NAC	88±8	75±11	71±8	57±6[***]
LPS	101±11	57±11[***]	54±9[***]	46±8[***]
LPS+HES-RA	92±9	56±10[***]	66±5[*,+]	52±4[***]
LPS+HES-RA+NAC	99±9	50±9[***]	64±5[**]	53±6[***]
RBF[mL/min]				
Time control	5.4±0.6	4.8±0.8	5.3±0.9	4.5±1.5
Control+NAC	5.7±0.7	4.3±0.9	4.8±1.5	4±1.1
LPS	5.7±1.4	1.3±0.7[***]	1.4±0.5[***]	0.7±0.6[***]
LPS+HES-RA	6.6±0.3	1.9±1.5[***]	5.6±1.8[+++]	5.0±0.4[+++]
LPS+HES-RA+NAC	5.5±0.4	1±0.4[***]	3.5±0.9[*++]	4.8±2.2[+++]
RVR[dyn.s.sec^{-5}]				
Time control	1910±261	1794±227	1524±188	1861±751
Control+NAC	1549±249	1783±369	1607±583	1522±511
LPS	1775±302	5912±3333[***]	4183±830[*]	10372±5182[***]
LPS+HES-RA	1410±152	3293±1979[+]	1130±348[++]	1004±483[+++]
LPS+HES-RA+NAC	1787±236	5796±2517[***]	1910±376	1199±318[+++]

LPS=lipopolysaccharide; HES-RA= Hydroxyethyl starch-ringer acetate; NAC= N-acetyl cysteine. Values are presented as mean ± SD

[*]p<0.05, [**]p<0.01 and [***]p<0.001 Control vs. other groups; [+]p<0.05, [++]p<0.01 and [+++]p<0.001 LPS vs. other groups

Renal microvascular oxygenation

The percentage variations in $C\mu PO_2$, $M\mu PO_2$, DO_{2ren}, and VO_{2ren} between baseline (T_0) and the end of the experiment (T_3) are shown in **Figure 2**. Compared to the control groups, LPS infusion induced a significant decrease in $C\mu PO_2$ (40.6±8.8 mmHg vs 68.2±4.1 mmHg in the control group at T_3, p<0.001) and $M\mu PO_2$ (32.2±7.9 mmHg vs 51.6±3.2 mmHg in the control group, p<0.001). Fluid resuscitation with HES-RA alone did not improve either $C\mu PO_2$ or $M\mu PO_2$. HES-RA combined with NAC significantly improved $C\mu PO_2$ during sepsis (p<0.01). LPS induced a significant decrease in DO_{2ren} and VO_{2ren} (8.3±6.1 ml O_2/min in the LPS group versus 67.2±23.2 ml O_2/min in the control group at T_3 and 7.8±6.5 ml O_2/min in the LPS group versus 32.9 ±10 ml O_2/min in the control group at T_3, p<0.05, respectively). Fluid resuscitation with or without NAC significantly improved VO_{2ren} compared to the LPS alone group (p<0.05). Of note, the addition of NAC to the control group also increased VO_{2ren} compared to the control group alone (p<0.05). The hematocrit values are reported in **Table 3**. A significant decrease in hematocrit occurred after fluid resuscitation in both groups compared to the control and LPS alone groups (p<0.001). The magnitude of hemodilution in both groups was in the same range.

LPS induced a significant increase in ER% O_2 at T_1, T_2 and T_3 compared to the control group (p<0.01, p<0.01 and p<0.001, respectively), and this value was only improved in LPS+HES-RA

group at T_2. In the control group receiving NAC, ER%O_2 was also increased at T_3 compared to control (p<0.001).
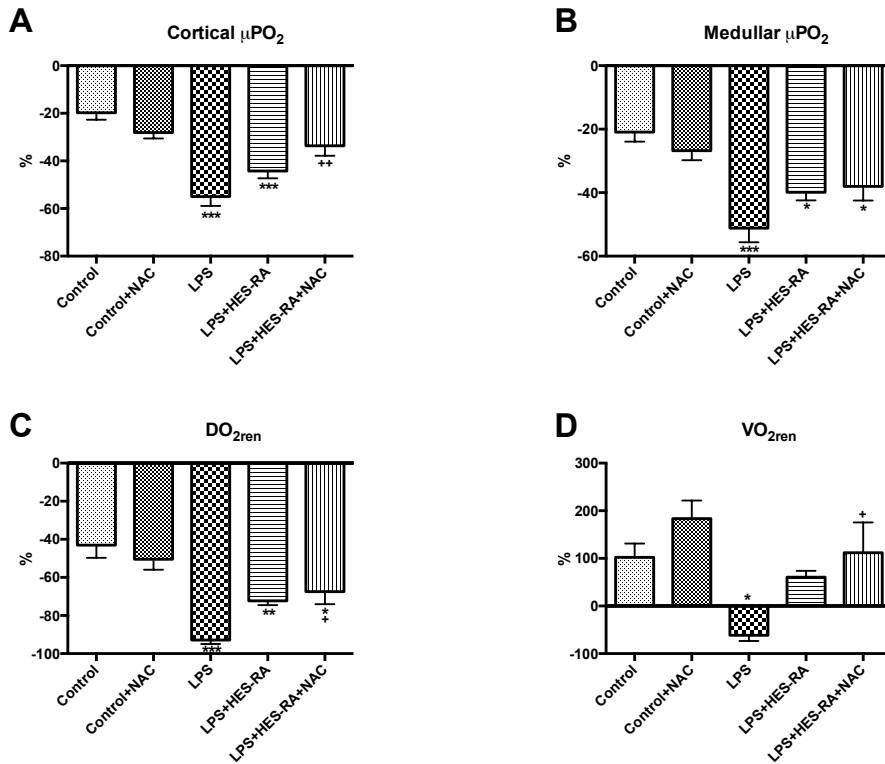

Figure 2. Percentage change of renal microvascular oxygen tension, oxygen delivery and consumption from baseline to T_3

In the renal cortex (CμpO_2) (Panel A), in the medulla (MμpO_2) (Panel B), renal oxygen delivery (DO$_{2ren}$) (Panel C), and renal oxygen consumption (VO$_{2ren}$) (Panel D).

$^*p<0.05$, $^{**}p<0.01$, $^*p<0.001$ vs Control; $^+p<0.05$ LPS vs. LPS group.

Kidney function and biomarkers of kidney injury

The evolution of TNa$^+$, VO$_{2ren}$/TNa$^+$, Cl$_{Crea}$ and EFNa$^+$ at different time points is presented in **Table 2**. TNa$^+$ levels were lower in the LPS, LPS+HES-RA and LPS+HES+RA+NAC groups (p<0.001) than the control group at T_1, T_2, and T_3. Fluid resuscitation did not restore these values. The addition of NAC also decreased the TNa+ in the control+NAC group compared to the control

group (p<0.01). VO_{2ren}/TNa^+ increased in LPS groups receiving HES-RA and HES+RA+NAC at T_3 compared to the control group (p<0.05 and p<0.001, respectively) and the LPS alone group (p<0.05 and p<0.001, respectively). Compared to the control and LPS alone groups, $EFNa^+$ values were increased in the LPS groups treated with HES-RA with and without NAC at T_2 and T_3. NAC administration in the control group tended to decrease TNa^+ and $EFNa^+$ without reaching a significant level. Fluid resuscitation improved urine output regardless of the addition of NAC compared to the LPS group (p<0.001). No effect of NAC on urine output was noted in the control+NAC group compared to the control group, but a significant decrease in Cl_{creat} was observed (p<0.001).

Table 2. Parameters of renal function and excretion at different time points of the experiment

	T0 (baseline)	T1 (shock)	T2 (30 min)	T3 (120 min)
TNa^+[mmol/min^{-1}]				
Time control	15.3±9.6	14.1±7.0	18.8±6.8	19.7±4.7
Control+NAC	15.0±6.4	13.2±6.5	15.9±6.5	9.5±4.3**
LPS	12.3±5.5	0.00±0.00***	0.00±0.00***	0.00±0.00***
LPS+HES-RA	12.0±8.3	0.00±0.00***	5.0±1.12***	2.2±1.3***
LPS+HES-RA+NAC	11.9±5.7	0.00±0.00***	2.8±2.8***	2.2±1.8***
VO_2/TNa^+				
Time control	1.77±1.6	2.19±1.3	1.59±0.6	1.79±0.7
Control+NAC	1.36±0.4	2.19±0.9	1.95±1.18	6.32±3.9
LPS	2.5±1.2	0.00±0.00	0.00±0.00	0.00±0.00
LPS+HES-RA	2.24±1.1	0.00±0.00	6.06±1.7	17.17±7.1*+
LPS+HES-RA+NAC	1.97±1.3	0.00±0.0*	23.36±22.2	28.53±28***+++
Cl_{Crea}[mL/min.]				
Time control	0.11±0.6	0.10±0.04	0.14±0.04	0.14±0.03
Control+NAC	0.11±0.04	0.09±0.04	0.11±0.04	0.06±0.03***
LPS	0.09±0.04	0.00±0.00***	0.00±0.00***	0.00±0.00***
LPS+HES-RA	0.09±0.06	0.00±0.00***	0.05±0.01***+	0.02±0.01***
LPS+HES-RA+NAC	0.09±0.04	0.00±0.00***	0.04±0.01***	0.02±0.01***
$EFNa^+$				
Time control	4.8±4.7	13.2±5.7	11.9±4.9	10.4±2.4
Control+NAC	2.3±0.8	3.22±1.7	2.9±1.7	6.9±6.6
LPS	3.7±1.4	0.00±0.00	0.00±0.00	0.00±0.00
LPS+HES-RA	3.5±2.8	0.00±0.00	35.3±7.3**,+++	17.1±8.1
LPS+HES-RA+NAC	4.4±3.9	0.00±0.00	45.8±36.7***,+++	31.4±28.4***,+++
Urine volume[mL]				
Time control	0.39±0.14	0.53±0.13	0.45±0.13	0.19±0.03
Control+NAC	0.25±0.09	0.34±0.17	0.2±0.04	0.16±0.06
LPS	0.31±0.13	0.06±0.09***	0.04±0.05***	0.02±0.05***
LPS+HES-RA	0.37±0.3	0.12±0.19***	0.6±0.23+++	0.16±0.08+++
LPS+HES-RA+NAC	0.33±0.26	0.04±0.09***	0.65±0.47+++	0.2±0.13+++

TNa+, tubular sodium reabsorption; Cl_{creat}, clearance of creatinine; LPS, lipopolysaccharide; HES-RA, Hydroxyethyl starch-ringer acetate; NAC, N-acetyl cysteine. Values are presented as mean ± SD. *p<0.05, **p<0.01 and ***p<0.001 vs. control; ⁺p<0.05 and ⁺⁺⁺p<0.001 vs. LPS.

Biomarkers of AKI (NGAL and L-FABP) were significantly increased in the kidney after LPS infusion (p<0.05 and p<0.001, respectively, versus the control group) (**Figure 3**). The resuscitation fluid combined with NAC significantly decreased these biomarkers compared to the LPS alone group (p<0.001 and <0.05, respectively). Moreover, L-FABP was lower in the group of septic rats resuscitated with HES-RA+NAC than with HES-RA alone (p<0.001).
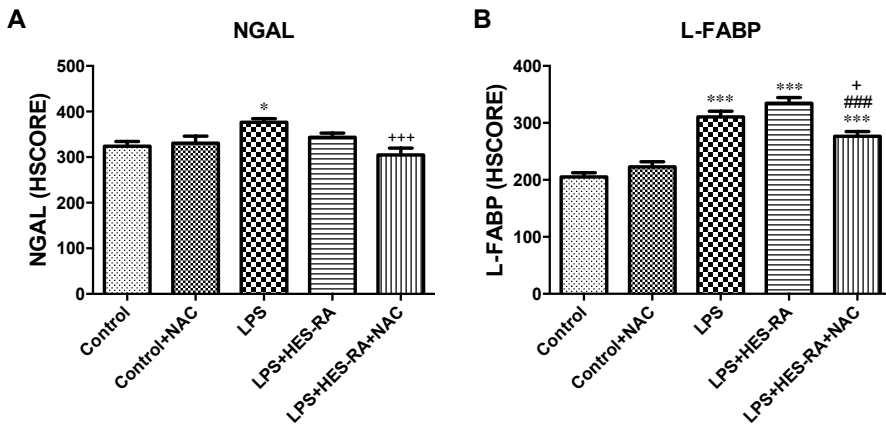
Figure 3. Immunostaining intensity (HSCORE) of NGAL (Panel A) and L-FABP (Panel B) in kidney cortex of all groups.

*p<0.05, ***p<0.001 versus control group; +p<0.05, +++p<0.001 versus LPS group, ###p<0.001 vs. LPS+HES-RA group.

Plasma electrolytes and acid-base status

Bicarbonate and plasma lactate levels, pH, base excess and anion gap with K^+ are shown in **Table 3**. LPS infusion significantly increased the plasma lactate level and anion gap, which could not be corrected by the administration of HES-RA either with or without NAC (p<0.001) compared to the control group. Base excess, pH, and bicarbonate levels were similarly decreased after LPS infusion and were partially corrected by fluid resuscitation. NAC infusion alone in the control group resulted in a significant decrease in pH, base excess and bicarbonate levels compared to the control group (p<0.01). NAC administration worsened the acid-base status in the LPS resuscitated and control groups. The level of bicarbonate and base excess were significantly lower in rats resuscitated with fluid plus NAC than with fluid alone (p<0.01).

Table 3. Time-course of acid-base status, lactate levels and hematocrit resuscitated with and without the addition of NAC

	T0 (baseline)	T1 (shock)	T2 (30 min)	T3 (120 min)
pH				
Time control	7.37±0.03	7.39±0.06	7.42±0.03	7.42±0.04
Control+NAC	7.48±0.12	7.42±0.03	7.38±0.02	7.32±0.05*
LPS	7.36±0.03	7.27±0.06**	7.26±0.07***	7.2±0.07***
LPS+HES-RA	7.36±0.03	7.26±0.07***	7.31±0.07*	7.27±0.05***
LPS+HES-RA+NAC	7.37±0.04	7.26±0.09***	7.27±0.08***	7.20±0.03***
HCO_3^- [mmol/L]				
Time control	20.6±0.9	21±0.6	21.2±1.3	21.6±1.3
Control+NAC	18.8±0.6	18.4±1.5*	19.3±1.2	14.2±3.8***
LPS	20.2±0.7	15±0.9***	15.3±1.2***	12.8±0.5***
LPS+HES-RA	21.6±0.7	14.8±1.5***	18.1±0.9***++	16.7±1.6***+++
LPS+HES-RA+NAC	20.7±0.8	14.7±2.5***	16.6±1.6***	14±1.7***##
Base excess [mmol/L]				
Time control	-3.5±1.2	-2.7±1.6	-1.7±1.3	-1.8±1.5
Control+NAC	-3.5±0.5	-4.4±1.7	-4.5±1.3	-8.9±2.4***
LPS	-4±1.3	-10.8±1.9***	-10.5±1.7***	-14.1±1.3***
LPS+HES-RA	-2.9±1.1	-11.3±2.7***	-7±2***++	-8.9±1.9***+++
LPS+HES-RA+NAC	-3.4±1.5	-11.2±4.1***	-9.1±2.8***	-12.5±1.7***##
Anion Gap K^+ [mmol/L]				
Time control	17.7±0.8	18.0±0.7	16.4±0.5	16.8±1.3
Control+NAC	18.9±2.0	18.5±2.0	17.0±1.2	18.9±4.8
LPS	18.9±2.3	21.8±1.1	21.6±1.8	23.2±1.6***
LPS+HES-RA	17.5±1.3	22.7±1.3	19.2±1.0	20.9±2.5***
LPS+HES-RA+NAC	18.4±1.0	22.5±2.5**	20.6±2.3*	23.1±1.9***
Lactate [mmol/L]				
Time control	2.32±0.52	2.22±0.34	2.08±0.31	1.73±0.27
Control+NAC	3.10±0.64	2.92±0.76	2.17±0.36	2.10±0.33
LPS	2.42±0.32	3.08±0.28	3.08±0.5	4.32±0.6***
LPS+HES-RA	1.92±0.2	3.32±0.55	2.75±0.48	5.08±1.83***
LPS+HES-RA+NAC	2.70±0.21	3.83±1.36**	3.30±1.17*	4.98±1.21***
Hct (%)				
Time control	49.6±1.3	41.6±1.9	39±2.9	33.3±3
Control+NAC	48.8±2.6	42.8±4.4	41.1±4.2	33.8±2.6
LPS	49.3±4.0	39.6±3.0	35.1±2.9	34.0±3.5
LPS+HES-RA	49.3±1.7	43.3±2.5	30.1±4.5***+	17.5±3***+++
LPS+HES-RA+NAC	48.6±0.8	44.1±3.2+	33.0±2.6**	18.0±2.0***+++

LPS, lipopolysaccharide; HES-RA, Hydroxyethyl starch-ringer acetate; NAC, N-acetyl cysteine. Values are presented as mean ± SD, *p<0.05, **p<0.01, ***p<0.001 versus control; ++ p<0.05, +++p<0.001 versus LPS; ##p<0.01 versus LPS+HES-RA.

Oxidative stress and inflammatory cytokines

The levels of biomarkers of oxidative stress, pro-inflammatory cytokines and products of glycocalyx degradation are represented in **Figure 4**. The levels of TNF-α (**4A**) and IL-6 (**4B**) in kidney homogenates from the LPS group were significantly increased compared to the control group (528.1±143.9 pg/mg protein versus 291.8±99.1 pg/mg protein, p<0.05; and 1246±441

pg/mg protein versus 753.8±122 pg/mg protein, p<0.05, respectively). The same results were observed regarding hyaluronic acid (HA) (**4C**), nitric oxide (**4D**) and MDA (**4E**) after LPS infusion (p<0.05). The addition of NAC to HES-RA during fluid resuscitation resulted in a significant lower level of HA and nitric oxide compared to the LPS group (p<0.01). Infusion of HES-RA alone decreased the levels of MDA compared to LPS alone (p<0.01) (**4E**). Protein carbonyl levels were not altered (**4E**).
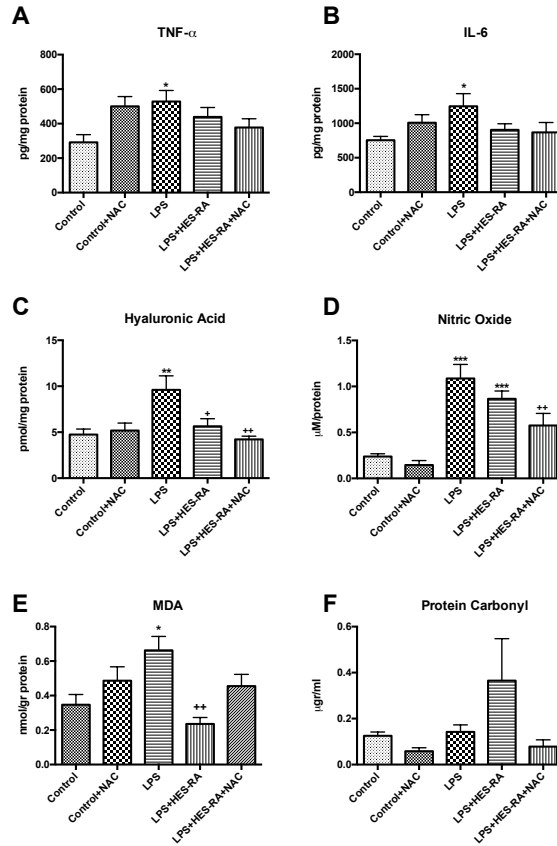
Figure 4. Levels of biomarkers of oxidative stress and pro-inflammatory cytokines in renal tissue

Renal tissue TNF-α (Panel A), IL-6 (Panel B), hyaluronic acid (Panel C), nitric oxide (Panel D), MDA (Panel E) and protein carbonyl (Panel F). *p<0.05, **p<0.01, ***p<0.001 vs. control; +p<0.05, ++p<0.01 vs. LPS group

Discussion

In the present study, we found that fluid supplemented with NAC improved cortical renal oxygenation, oxygen delivery and oxygen consumption compared to the LPS group. Fluid resuscitation alone was partially effective in correcting kidney hypoxia but did not reach a significant level compared to the LPS group. The addition of NAC to the resuscitation fluid did not further improve systemic or renal hemodynamics compared to HES-RA alone. It has been suggested that a specific effect of NAC on microvascular oxygenation exists independent of renal macrovascular perfusion. In an experimental study, Heyman *et al.* showed that NAC induced vasodilation in a pre-constricted renal microvasculature rat model.[18] The vasculature may be similarly constricted after LPS infusion leading to microcirculation heterogeneity.[25] Although creatinine levels did not differ between septic rats receiving fluids either with or without NAC, the fluid resuscitation combined with NAC decreased the levels of renal NO, hyaluronic acid and early markers of acute kidney injury such as NGAL or L-FABP. Previous studies demonstrated a significant decrease in inflammatory biomarkers in specific organs such as lungs and kidneys in models of sepsis.[14-16,26-29] However, none of these studies reported the beneficial effects of NAC on tissue oxygenation during sepsis by decreasing oxidative stress and inflammation.

Several studies using microcirculatory techniques have now questioned the significance of arterial RBF and have focused on the renal microcirculation as the hemodynamic culprit in the pathophysiology of septic AKI.[6,25,30] Microcirculatory dysfunction may contribute to renal hypoxia even in the absence of overt renal hypoperfusion. The microcirculation of the renal cortex has been shown to be severely injured in animal models of sepsis. After LPS infusion in rats, Legrand *et al*. showed that fluid resuscitation could not fully restore renal microcirculatory dysfunction.[6] In dogs, endotoxemia was found to be associated with renal hypoperfusion and hypoxia in the renal cortex but was concomitant with increased renal venous PO_2, supporting the concept that convective shunting of oxygen may contribute to the development of tissue hypoxia.[31] In our study, the LPS-induced renal microvascular heterogeneity and hypoxia appeared to be corrected with the NAC-supplemented fluid.

We also observed negative effects of NAC infusion. Delayed hypotension occurred in the control+NAC group, highlighting the vasodilatory effects of this compound as previously described.[12,32] The mechanism involved in this lowering effect might be mediated by the interaction of sulfhydryl groups with enzymes such as the guanylate cyclase, which is the primary

receptor for NO.[32] This drop in the MAP may contribute to tissue hypoperfusion and hypoxia as well as the lower pH observed in the control+NAC group compared to the control group. However, no significant change was observed in renal blood flow measured in the renal artery. Conflicting data exist between experimental and human clinical studies regarding the effects of NAC on regional blood flow and cardiac output.[19,33-37] First, NAC administration was shown to improve survival in experimental models of peritonitis-induced sepsis.[38,39] In mongrel dogs subjected to endotoxemia, Zhang *et al.* demonstrated the myocardial protective effects of NAC pretreatment (150 mg/kg) with enhanced oxygen delivery but lower systemic and pulmonary pressures.[37] In contrast, in a study involving 20 patients with septic shock, NAC infusion (150 mg/kg for 15 min followed by continuous infusion) that was initiated within 24 hours after the onset of septic shock resulted in a decrease in left ventricular stroke work—revealing myocardial depression—without a significant impact on MAP at 48 hours after treatment initiation.[33] In a similar population, Rank *et al.* demonstrated the exact opposite effect with an improvement in liver blood flow, oxygen delivery and oxygen consumption related to an increase in cardiac index.[34] However, the infusion of NAC lasted less than 2 hours in this latter study. Agustí *et al.* reported an increase in the cardiac index associated with vasodilatation but without improvements in splanchnic microcirculation after NAC infusion in patients presenting with septic shock and multiple organ failure.[35] Clinical studies yielded controversial results with the use of NAC in sepsis.[11] NAC treatment during the first hours of sepsis or septic shock may decrease peroxidative stress,[40] improve hepatic function [34] and enhance tissue oxygenation and cardiac function,[41] whereas delayed administration adversely affected the outcomes of critically ill patients with multiple organ failure.[33,42]

Most published studies have examined the effects of NAC when given as a pretreatment, e.g., before the insult. Here, we evaluated the ability of NAC when administered during the resuscitation process to correct tissue hypoxia and inflammation already present. It seems that the beneficial effects on tissue oxygenation, if any, are not similar if NAC is administered before or after the insult. The effects also depend on the time elapsed since the insult. We showed that NAC-supplemented fluid did not provide additional benefits on the acid status and renal function compared to fluid alone. Only kidney oxygenation was significantly higher in the group receiving fluid supplemented with NAC compared to the LPS alone group, whereas fluid alone did not reach a level of significance. Pretreatment with NAC appeared to be more efficient than post-injury treatment in protecting tissues against oxidative stress and inflammation in models of sepsis and ischemia/reperfusion injury. Due to the mechanisms of

action of NAC, it is conceivable that it would be easier to prevent certain pathways from being activated rather than to modulate already highly activated signals with redundant or alternative pathways.

The effects of NAC on renal oxygenation could be mediated by different mechanisms. First, tissue NO levels were significantly increased after LPS infusion. By decreasing NO levels in the cortex, NAC combined with fluid administration may improve microvascular dysfunction, microvascular delivery of oxygen and cortical oxygenation. Similarly, our group previously demonstrated that the prostaglandin analog iloprost restored kidney function in a rat model of endotoxemia and prevented the occurrence of hypoxic regions.[43] The improvement of renal microvascular oxygenation was mediated in part by inhibition of inducible nitric oxide synthase expression in the kidney. Another major player involved in endothelial dysfunction in sepsis-induced AKI is the widespread damage to the endothelial glycocalyx, which may contribute to microvascular dysfunction via impaired flow-dependent vasodilatation. Hyaluronic acid levels reflect the disruption of the glycocalyx.[44] In the present study, hyaluronic acid levels were significantly increased after LPS infusion. Fluid resuscitation either with or without the addition of NAC significantly dampened these levels. However, the decrease was more prevalent with NAC treatments, but all of the significant benefits were due to the fluids as opposed to NAC. NAC may still further improve microvascular oxygenation by decreasing endothelial glycocalyx damage in addition to fluid resuscitation. In contrast, a clinical study monitored volume loading with HES during elective surgery (20 ml/kg) and observed increased serum glycocalyx biomarkers with HES alone.[45] In our study, fluid resuscitation with HES seemed to be beneficial with regard to these biomarkers levels. One of the main pathways of glycocalyx disruption is thought to be the formation of ROS such as peroxynitrite. As NAC is a well-known scavenger of ROS, we measured the tissue levels of malondialdehyde as a marker of lipid peroxidation. We did not observe a significant decrease when using NAC-supplemented fluid compared to fluid alone. This result can be explained because of the high dose of NAC in our study. Some authors have previously suggested that high doses of NAC may increase MDA levels, whereas lower doses may decrease MDA levels.[46] Additionally, a lack of effect of NAC on lipid peroxidation in cases of established endotoxemia has been shown.[47]

Limitations

In the light of the ongoing debate about the deleterious effects of HES on the kidney, a possible limitation of our study is our use of HES as a resuscitation fluid. However, the present study is a mechanistic study wherein we investigated whether we could ameliorate the inflammatory effects of fluid administration in a sepsis model. In our experience, all fluids cause inflammation,[48] and it is the fluid volume that determined the extent of injury. It could be argued that we should have chosen a balanced crystalloid solution instead of a colloid-based solution. However, crystalloid solutions have issues as well. For example, Ringer's lactate causes even more inflammation than HES,[49,50] and we would also have had to administer a larger volume to maintain blood pressure causing more hemodilution. We chose a colloid solution to keep the amount of fluid required to correct blood pressure to a minimum. We could have used albumin, but even albumin can promote renal failure, as has been shown in a recent study in cardiac surgery.[51] In conclusion, arguably, all fluids have deleterious effects on the kidney to a greater or lesser extent. However, in this proof of concept study, we hope to have introduced the idea that controlling the inflammatory component imposed by fluids such as HES can be implemented by co-administration of an anti-inflammatory drug such as NAC. Our results suggest that such an approach could be used for other fluids, but this approach would require testing in subsequent studies.

Conclusion

In conclusion, the addition of NAC to fluid resuscitation may improve renal oxygenation and attenuate microvascular dysfunction and AKI. Decreases of renal NO levels and hyaluronic acid levels may be involved in this beneficial effect. A therapeutic strategy combining the macrovascular effects of fluids and the microvascular effects of NAC may be critical to preventing sepsis-induced AKI. This study sets forth a new concept for changing the procedure of fluid resuscitation by the addition of antioxidant therapy during the initial phase of resuscitation.

9

Competing interests

Funding

Acknowledgments

References

1.   Angus DC, van der Poll T. Severe sepsis and septic shock. *N Engl J Med*. 2013;369(9):840–851.

2.   Ait-Oufella H, Maury E, Lehoux S, Guidet B, Offenstadt G. The endothelium: physiological functions and role in microcirculatory failure during severe sepsis. *Intensive Care Med*. 2010;36(8):1286–1298.

3.   Ince C, Mayeux PR, Nguyen T, et al. The endothelium in sepsis. *Shock*. 2016;45(3):259–270.

4.   Ince C. The microcirculation is the motor of sepsis. *Crit Care*. 2005;9 Suppl 4(Suppl 4):S13–9.

5.   Legrand M, Mik EG, Johannes T, Payen D, Ince C. Renal hypoxia and dysoxia after reperfusion of the ischemic kidney. *Mol Med*. 2008;14(7-8):502–516.

6.   Legrand M, Bezemer R, Kandil A, Demirci C, Payen D, Ince C. The role of renal hypoperfusion in development of renal microcirculatory dysfunction in endotoxemic rats. *Intensive Care Med*. 2011;37(9):1534–1542.

7.   Oudemans-van Straaten HM, Spoelstra-de Man AM, de Waard MC. Vitamin C revisited. *Crit Care*. 2014;18(4):460.

8.   Galley HF, DiMatteo MA, Webster NR. Immunomodulation by anaesthetic, sedative and analgesic agents: does it matter? *Intensive Care Med*. 2000;26(3):267–274.

9.   Berger MM, Chioléro RL. Antioxidant supplementation in sepsis and systemic inflammatory response syndrome. *Crit Care Med*. 2007;35(9 Suppl):S584–90.

10.   Angstwurm MWA, Engelmann L, Zimmermann T, et al. Selenium in Intensive Care (SIC): results of a prospective randomized, placebo-controlled, multiple-center study in patients with severe systemic inflammatory response syndrome, sepsis, and septic shock. *Crit Care Med*. 2007;35(1):118–126.

11.   Szakmany T, Hauser B. N-acetylcysteine for sepsis and systemic inflammatory response in adults. *The Cochrane Library*. 2012.

12.   Zafarullah M, Li WQ, Sylvester J, Ahmad M. Molecular mechanisms of N-acetylcysteine actions. *Cell Mol Life Sci*. 2003;60(1):6–20.

13.   Sehirli AO, Sener G, Satiroglu H, Ayanoğlu-Dülger G. Protective effect of N-acetylcysteine on renal ischemia/reperfusion injury in the rat. *J Nephrol*. 2003;16(1):75–80.

14.   Ozdulger A, Cinel I, Koksel O, et al. The protective effect of N-acetylcysteine on apoptotic lung injury in cecal ligation and puncture-induced sepsis model. *Shock*. 2003;19(4):366–372.

15.   Hsu B-G, Lee R-P, Yang F-L, Harn H-J, Chen HI. Post-treatment with N-acetylcysteine ameliorates endotoxin shock-induced organ damage in conscious rats. *Life Sci*. 2006;79(21):2010–2016.

16.   Carbonell LF, Díaz J, Hernández I, et al. N-acetylcysteine exerts protective effects and prevents lung redox imbalance and peroxynitrite generation in endotoxemic rats. *Med Chem*. 2007;3(1):29–34.

17.   Huet O, Cherreau C, Nicco C, et al. Pivotal role of glutathione depletion in plasma-induced endothelial oxidative stress during sepsis. *Crit Care Med*. 2008;36(8):2328–2334.

9

18.   Heyman SN, Goldfarb M, Shina A, Karmeli F, Rosen S. N-acetylcysteine ameliorates renal microcirculation: studies in rats. *Kidney Int*. 2003;63(2):634–641.

19.   Schaller G, Pleiner J, Mittermayer F, Posch M, Kapiotis S, Wolzt M. Effects of N-acetylcysteine against systemic and renal hemodynamic effects of endotoxin in healthy humans. *Crit Care Med*. 2007;35(8):1869–1875.

20.   Eltzschig HK, Carmeliet P. Hypoxia and inflammation. *N Engl J Med*. 2011;364(7):656–665.

21.   Bartels K, Grenz A, Eltzschig HK. Hypoxia and inflammation are two sides of the same coin. *Proc Natl Acad Sci USA*. 2013;110(46):18351–18352.

22.   Haase VH. Inflammation and hypoxia in the kidney: friends or foes? *Kidney Int*. 2015;88(2):213–215.

23.   Johannes T, Mik EG, Ince C. Dual-wavelength phosphorimetry for determination of cortical and subcortical microvascular oxygenation in rat kidney. *J Appl Physiol*. 2006;100(4):1301–1310.

24.   Mik EG, Johannes T, Ince C. Monitoring of renal venous PO2 and kidney oxygen consumption in rats by a near-infrared phosphorescence lifetime technique. *Am J Physiol Renal Physiol*. 2008;294(3):F676–81.

25.   Ergin B, Kapucu A, Demirci-Tansel C, Ince C. The renal microcirculation in sepsis. *Nephrol Dial Transplant*. 2015;30(2):169–177.

26.   Hsu B-G, Yang F-L, Lee R-P, Peng TC, Harn H-J, Chen HI. N-acetylcysteine ameliorates lipopolysaccharide-induced organ damage in conscious rats. *J Biomed Sci*. 2004;11(2):152–162.

27.   Andrades M, Ritter C, de Oliveira MR, Streck EL, Fonseca Moreira JC, Dal-Pizzol F. Antioxidant treatment reverses organ failure in rat model of sepsis: role of antioxidant enzymes imbalance, neutrophil infiltration, and oxidative stress. *J Surg Res*. 2011;167(2):e307–13.

28.   Campos R, Shimizu MHM, Volpini RA, et al. N-acetylcysteine prevents pulmonary edema and acute kidney injury in rats with sepsis submitted to mechanical ventilation. *Am J Physiol Lung Cell Mol Physiol*. 2012;302(7):L640–50.

29.   Lee JH, Jo YH, Kim K, et al. Effect of N-acetylcysteine (NAC) on acute lung injury and acute kidney injury in hemorrhagic shock. *Resuscitation*. 2013;84(1):121–127.

30.   Zafrani L, Payen D, Azoulay E, Ince C. The microcirculation of the septic kidney. *Semin Nephrol*. 2015;35(1):75–84.

31.   Gullichsen E, Nelimarkka O, Halkola L, Niinikoski J. Renal oxygenation in endotoxin shock in dogs. *Crit Care Med*. 1989;17(6):547–550.

32.   Girouard H, Chulak C, Wu L, Lejossec M, de Champlain J. N-acetylcysteine improves nitric oxide and alpha-adrenergic pathways in mesenteric beds of spontaneously hypertensive rats. *Am J Hypertens*. 2003;16(7):577–584.

33.   Peake SL, Moran JL, Leppard PI. N-acetyl-L-cysteine depresses cardiac performance in patients with septic shock. *Crit Care Med*. 1996;24(8):1302–1310.

34.   Rank N, Michel C, Haertel C, et al. N-acetylcysteine increases liver blood flow and improves liver function in septic shock patients: results of a prospective, randomized, double-blind study. *Crit Care Med*. 2000;28(12):3799–3807.

35.   Agustí AGN, Togores B, Ibañez J, et al. Effects of N-acetylcysteine on tissue oxygenation in patients with multiple organ failure and evidence of tissue hypoxia. *European Respiratory Journal*. 1997;10(9):1962–1966.

36.   Zhang H, Spapen H, Nguyen DN, Rogiers P, Bakker J, Vincent JL. Effects of N-acetyl-L-cysteine on regional blood flow during endotoxic shock. *Eur Surg Res*. 1995;27(5):292–300.

37.   Zhang H, Spapen H, Nguyen DN, Benlabed M, Buurman WA, Vincent JL. Protective effects of N-acetyl-L-cysteine in endotoxemia. *Am J Physiol*. 1994;266(5 Pt 2):H1746–54.

38.   Ritter C, Andrades ME, Reinke A, Menna-Barreto S, Moreira JCF, Dal-Pizzol F. Treatment with N-acetylcysteine plus deferoxamine protects rats against oxidative stress and improves survival in sepsis. *Crit Care Med*. 2004;32(2):342–349.

39.   de Mello RO, Lunardelli A, Caberlon E, et al. Effect of N-acetylcysteine and fructose-1,6-bisphosphate in the treatment of experimental sepsis. *Inflammation*. 2011;34(6):539–550.

40.   Ortolani O, Conti A, De Gaudio AR, Moraldi E, Cantini Q, Novelli G. The effect of glutathione and N-acetylcysteine on lipoperoxidative damage in patients with early septic shock. *Am J Respir Crit Care Med*. 2000;161(6):1907–1911.

41.   Spies CD, Reinhart K, Witt I, et al. Influence of N-acetylcysteine on indirect indicators of tissue oxygenation in septic shock patients: results from a prospective, randomized, double-blind study. *Crit Care Med*. 1994;22(11):1738–1746.

42.   Molnár Z, Shearer E, Lowe D. N-Acetylcysteine treatment to prevent the progression of multisystem organ failure: a prospective, randomized, placebo-controlled study. *Crit Care Med*. 1999;27(6):1100–1104.

43.   Johannes T, Ince C, Klingel K, Unertl KE, Mik EG. Iloprost preserves renal oxygenation and restores kidney function in endotoxemia-related acute renal failure in the rat. *Crit Care Med*. 2009;37(4):1423–1432.

44.   Dane MJC, van den Berg BM, Lee DH, et al. A microscopic view on the renal endothelial glycocalyx. *Am J Physiol Renal Physiol*. 2015;308(9):F956–66.

45.   Chappell D, Bruegger D, Potzel J, et al. Hypervolemia increases release of atrial natriuretic peptide and shedding of the endothelial glycocalyx. *Crit Care*. 2014;18(5):538.

46.   Fitri LE, Sardjono TW, Simamora D, Sumarno RP, Setyawati SK. High dose of N-acetylcysteine increase H_2O_2 and MDA levels and decrease GSH level of HUVECs exposed with malaria serum. *Trop Biomed*. 2011;28(1):7–15.

47.   Caglikulekci M, Dirlik M, Pata C, et al. Effect of N-acetylcysteine on blood and tissue lipid peroxidation in lipopolysaccharide-induced obstructive jaundice. *J Invest Surg*. 2006;19(3):175–184.

48.   Aksu U, Bezemer R, Yavuz B, Kandil A, Demirci C, Ince C. Balanced vs unbalanced crystalloid resuscitation in a near-fatal model of hemorrhagic shock and the effects on renal oxygenation, oxidative stress, and inflammation. *Resuscitation*. 2012;83(6):767–773.

49.   Hussmann B, Lendemans S, de Groot H, Rohrig R. Volume replacement with Ringer-lactate is detrimental in severe hemorrhagic shock but protective in moderate hemorrhagic shock: studies in a rat model. *Crit Care*. 2014;18(1):R5.

50.   Rohrig R, Rönn T, Lendemans S, Feldkamp T, de Groot H, Petrat F. Adverse effects of resuscitation with lactated ringer compared with ringer solution after severe hemorrhagic shock in rats. *Shock*. 2012;38(2):137–145.

9

51.   Frenette AJ, Bouchard J, Bernier P, et al. Albumin administration is associated with acute kidney injury in cardiac surgery: a propensity score analysis. *Crit Care*. 2014;18(6):602.

9

10

Effect of PEGylated-Carboxyhemoglobin on Renal Microcirculation in a Rat Model of Hemorrhagic Shock

Philippe Guerci,[1,2,3] Bulent Ergin,[1,4] Aysegul Kapucu,[5]

Matthias P. Hilty,[1] Ronald Jubin,[6] Jan Bakker,[4,7,8] Can Ince,[1,4]

1. Department of Translational Physiology, Academic Medical Center, University of Amsterdam, Amsterdam, The Netherlands
2. INSERM U1116, University of Lorraine, Vandoeuvre-Les-Nancy, France
3. Department of Anesthesiology and Critical Care Medicine, University Hospital of Nancy, France
4. Department of Intensive Care Adults, Erasmus MC, University Medical Center, Rotterdam, Rotterdam, The Netherlands
5. Department of Biology, Faculty of Science, University of Istanbul, Istanbul, Turkey
6. Prolong Pharmaceuticals, South Plainfield, NJ, USA
7. Department of Pulmonology & Critical Care, Columbia University Medical Center, New York. USA
8. Department of Intensive Care, Pontificia Universidad Católica de Chile, Santiago, Chile

What We Already Know About This Topic

- Acute kidney injury is a frequent complication following hemorrhagic shock resuscitation.
- Low concentrations of carbon monoxide produce vasodilation via a direct action on vascular smooth muscle and anti-inflammatory effects.
- Data on the effects of polyethylene glycolated (PEGylated)-carboxyhemoglobin on the kidney are scarce

What This Article Tells Us That Is New

- PEGylated-carboxyhemoglobin may be used as a low volume resuscitation fluid
- PEGylated-carboxyhemoglobin sustains urine output and may protect against acute kidney injury following resuscitation of hemorrhagic shock
- Increase in oxygen-carrying capacity and delivery may not be the primary mechanism involved in protecting the kidney from injury

Abstract

Background: Primary resuscitation fluid to treat hemorrhagic shock remains controversial. Use of hydroxyethyl starches raised concerns of acute kidney injury. Polyethylene glycolated (PEGylated)-carboxyhemoglobin, which has CO-releasing molecules and oxygen-carrying properties was hypothesized to sustain cortical renal microcirculatory PO_2 following hemorrhagic shock and reduce kidney injury.

Methods: Anesthetized and ventilated rats (n=42) were subjected to pressure-controlled hemorrhagic shock for 1 hour. Renal cortical Po_2 was measured in exposed kidneys using a phosphorescence quenching method. Rats were randomly assigned to 6 groups: PEGylated-carboxyhemoglobin 320 $mg.kg^{-1}$, 6% hydroxyethyl starch-(130/0.4) in Ringer's acetate, blood retransfusion, diluted blood retransfusion (~4 $g.dl^{-1}$), nonresuscitated animals and time control. NO and heme-oxygenase-1 levels were determined in plasma. Kidney immunohistochemistry (histological scores of Neutrophil Gelatinase-Associated Lipocalin and Tumor Necrosis Factor-α) and tubular histological damages analyses were performed.

Results: Blood and diluted blood restored renal Po_2 to 51±5 mmHg (mean diff. -18, 95%CI[-26 to -11], *P<0.0001*) and 47±5 mmHg (mean diff. -23, 95%CI [-31 to -15], *P<0.0001*) respectively compared to 29±8 mmHg for hydroxyethyl starch. No differences between PEGylated-carboxyhemoglobin and hydroxyethyl starch were observed (33±7 mmHg versus 29±8 mmHg, mean diff. -5, 95%CI[-12 to 3], *P=0.387*), but significantly less volume was administered (4.5[3.3-6.2] versus 8.5[7.7-11.4] ml, mean rank diff. 11.98, *P=0.387*). Blood and diluted blood increased the plasma bioavailability of NO compared to hydroxyethyl starch (mean rank diff. -20.97, *P=0.004* and -17.13, *P=0.029* respectively). No changes in heme-oxygenase-1 levels were observed. PEGylated-carboxyhemoglobin limited tubular histological damages compared to hydroxyethyl starch (mean rank diff. 60.12, *P=0.0012*) with reduced neutrophil gelatinase-associated lipocalin (mean rank diff. 84.43, *P<0.0001*) and tumor necrosis factor-α (mean rank diff. 49.67, *P=0.026*) histological scores.

Conclusions: PEGylated-carboxyhemoglobin resuscitation did not improve renal PO_2 but limited tubular histological damages and neutrophil gelatinase-associated lipocalin upregulation following hemorrhage compared to hydroxyethyl starch, while a lower volume was required to sustain macrocirculation.

Keywords: Low volume resuscitation, PEGylated carboxyhemoglobin, acute kidney injury, hemorrhage

10

Introduction

Fluid administration is the first step of rescue therapy during severe hemorrhage or hypovolemic shock before blood products become available.[1] However, aggressive volume fluid resuscitation may lead to secondary severe tissue edema and clinical signs of volume overload, which result in unfavorable outcomes.[2,3] Colloidal solutions are used to sustain intravascular oncotic pressure and to shorten the circulatory stabilization time while limiting fluid administration. Hydroxyethyl starch solutions remain the most used synthetic colloids for volume replacement. However, no definitive evidence exists for outcome advantage of starches over crystalloids in various settings, and concerns were raised for kidney function. Therefore, the European Medicines Agency (EMA) restricts the use of hydroxyethyl starch solutions across the European Union.[4,5] Hyperosmotic and hypertonic saline fluids are also considered alternatives, but the fluids produce uncertain outcomes and possible harm.[6] Therefore, crystalloids remain the sole resuscitation fluid for the treatment of hemorrhage and severe hypovolemia prior to blood product transfusion. Current resuscitation fluids of crystalloids or synthetic colloids possess no oxygen-carrying capacity and may promote inflammation.

Acute kidney injury is one of the most frequent organ failures in perioperative and critically ill patients.[7] The pathophysiology of acute kidney injury is not fully understood to date, but major contributors were identified, such as renal microcirculatory hypoxemia, tissue inflammation and fluid overload.[8–10] The early reestablishment of oxygenation and kidney perfusion during hemorrhage is essential to limit the subsequent development of acute kidney injury.[9,10]

Polyethylene glycolated (PEGylated)-carboxyhemoglobin (Sanguinate™, Prolong Pharmaceuticals, South Plainfield, NJ, USA) is a novel agent that exhibits a dual action of carbon monoxide (CO)-release and O_2 carrying and transfer.[11] CO is poisonous at high concentrations because it inhibits cellular respiration and interacts tightly with hemoglobin to limit oxygen delivery, but it also produces beneficial effects at low concentrations. CO's homeostatic effects occur via multiple cellular and molecular mechanisms of action, including redox control, anti-apoptosis and anti-inflammation, modulation of vasoactive responses (vasodilation) and modulation of the innate immune response.[12,13] There is compelling preclinical data on the use of CO as a therapeutic agent via CO-releasing molecules in models of acute lung injury,[14] sepsis,[15] hemorrhagic shock,[16] and ischemia/reperfusion injury.[17] CO mitigated the inflammatory response and ischemic damage in all of these settings.

The present study hypothesized that a molecule with the ability to release CO molecules to injured tissues and carry oxygen to hypoxic tissue would sustain kidney function by increasing renal microcirculatory oxygen tension and limiting the damage of ischemia and hypoxia following resuscitation from hemorrhagic shock while providing a low volume of resuscitation fluid. The primary outcome of our study was improvement of cortical renal microcirculatory oxygen tension. Secondary outcomes included the volume of fluid resuscitation, macrohemodynamics, renal immunohistochemistry and histological damages, acid-base status, and levels of plasma biomarkers of injury.

We sought to compare the renal microcirculatory impact of PEGylated-carboxyhemoglobin, 6% hydroxyethyl starch balanced in Ringer's acetate, and blood transfusion as resuscitation strategies in a blood pressure-targeted resuscitation model of hemorrhagic shock in the rat.

Material and methods

Animals

The Animal Research Committee of the Academic Medical Centre of the University of Amsterdam approved all experiments in this study (DFL 103073). Care and handling of the animals were performed in accordance with the guidelines from the Institutional and Animal Care and Use Committees. This study and the following reporting adhere to the applicable ARRIVE guidelines.[18] All experiments were performed on male Wistar-Albinos rats (Charles River, The Netherlands), aged 10 ± 3 weeks with a mean±SD body weight of 320 ± 26 g, at 09:30AM (weekdays) at the Department of Experimental Surgery, University Medical Center, Amsterdam, The Netherlands.

10

Surgical preparation

Rats were anesthetized using an intraperitoneal injection of a mixture of 100 mg.kg^{-1} ketamine (Nimatek; Eurovet, Bladel, the Netherlands), 0.5 mg.kg^{-1} dexmedetomidine (Dexdomitor; Orion Group, Espoo, Finland) and 0.05 mg.kg^{-1} atropine-sulfate (Centrafarm, Etten-Leur, The Netherlands). Anesthesia was maintained with 50 mg·kg·h^{-1} ketamine. A tracheotomy was performed. The animals were connected to a ventilator (Babylog 8000, Dräger, The Netherlands) and ventilated with tidal volumes of 6 ml.kg^{-1} with a positive end-expiratory

pressure of 3 cmH$_2$O and an FiO$_2$ of 0.4. A heating pad under the animal allowed the body temperature to be controlled and maintained at 37±0.5°C. The end-tidal CO$_2$ was maintained between 35 and 42 mmHg by adjusting respiratory rate (CapnoMac, Datex-Ohmeda, USA).

The carotid (pressure) and femoral (for blood shedding and samples) arteries and jugular (anesthesia) and femoral (fluid resuscitation) veins were cannulated using polyethylene catheters (outer diameter = 0.9 mm; Braun, Melsungen, Germany). Fluid maintenance during surgery was sustained using Ringer's acetate (Baxter, Utrecht, The Netherlands) administration at a rate of 10 ml.kg^{-1}.h^{-1}. The left kidney was exposed without decapsulation and immobilized in a Lucite kidney cup (K. Effenberger, Pfaffingen, Germany) via a 3-cm incision in the left flank. Renal vessels were carefully separated to preserve the nerves and adrenal gland. An ultrasonic flow probe was placed around the left renal artery (type 0.7 RB; Transonic Systems Inc., Ithaca, NY, USA) and connected to a flow meter (T206; Transonic Systems Inc.) to continuously measure renal blood flow (RBF). The left ureter was isolated, ligated and cannulated using a polyethylene catheter for urine collection. The animals rested for 30 min after completion of surgery (~1 h).

Experimental protocol

Animals were randomized according to a unique code that was generated by an internet website (Sealed Envelope Ltd. 2016. Simple randomization service. [Online] Available from https://www.sealedenvelope.com/simple-randomiser/v1/) and placed in sealed envelopes. A technician prepared the resuscitation fluid according to the generated code on the day of the experiment. The investigator performing the experiments was partially blinded to group assignment or treatment. Control and hemorrhage groups received no fluids. Another investigator who was blinded to the type of randomization performed the data analyses.

Animals underwent stabilization period (30 min) and were bled from the left femoral artery catheter at a rate of 1 ml.min^{-1} using a syringe pump (Harvard 33 syringe pump; Harvard apparatus, South Natick, MA) until reaching a mean arterial pressure (MAP) of ~30 mmHg. This pressure was maintained for 1 h via reinfusing or withdrawing blood. Coagulation of the shed blood was prevented with the addition of 200 IU of heparin in the syringe. The animals were randomized into 6 groups: (1) PEGylated-carboxyhemoglobin with a max. dosage of 320 mg.kg^{-1}, (2) 6% hydroxyethyl starch (130/0.4) balanced with Ringer's acetate (Volulyte®, Fresenius Kabi, Germany), (3) diluted blood with PEGylated-carboxyhemoglobin's buffer (to the same hemoglobin content as PEGylated-carboxyhemoglobin: 4 g.dl^{-1}) (Diluted blood), (4) blood

transfusion (Blood), (5) nonresuscitated animals and (6) control, in which surgery was performed without hemorrhage. Fluid resuscitation was divided into 2 periods of time: a rescue therapy period of 30 min (rescue period, 30 min after resuscitation), where the fluid tested was administered alone until reaching MAP of 80 mmHg and stopped, and a maintenance period of 30 min (60 min after resuscitation), where the resuscitated groups were all received 6% hydroxyethyl starch. This design allowed comparisons between groups with a similar target (**Figure 1**).
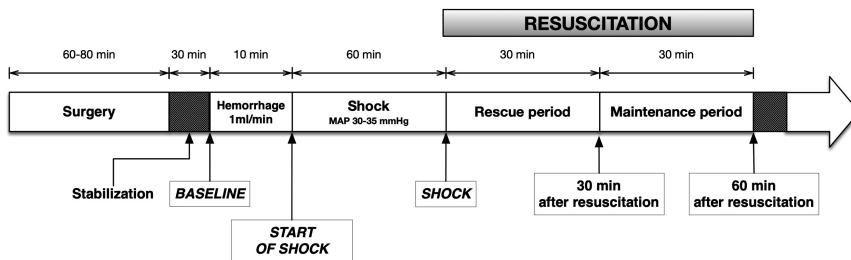

Figure 1. Design and timeline of the experiment

Control rats were subjected to the same surgery but did not undergo the hemorrhage protocol. Non-resuscitated hemorrhagic shock rats were observed during the same time of observation.

Measurement of renal cortical microcirculatory PO$_2$

An optical fiber with a tip diameter of 5 mm was placed ~1 mm above the exposed kidney to measure oxygenation using a phosphorescence lifetime technique described elsewhere.[19] Palladium(II)-meso-tetra(4-carboxyphenyl)-porphyrin (Pd-TCCP) at a concentration of ~5 mg.ml^{-1} was used as a phosphorescent dye, injected at a dose of 1.5 ml.kg^{-1} and excited at 530 nm. The phosphorescent decay time signal corresponds to the microcirculatory PO$_2$ in the kidney, and it was continuously recorded and processed using software developed in LabView 2014 (National Instruments, Austin, TX, USA) as described previously.[19] The depth of penetration of green light and catchment depth were estimated to be within the renal cortex. We excluded any interference between Pd-TCCP and PEGylated-carboxyhemoglobin (*in vitro*) prior to the *in vivo* experiment.

10

Determination of oxygen carrying capacity of PEGylated-carboxyhemoglobin and spectrophotometric analyses of its derivatives

As PEGylated-carboxyhemoglobin is bound with CO molecules, and its oxygen carrying-capacity is reduced. The release of CO likely increases the oxygen-carrying capacity of the molecule. The oxygen-binding/carrying capacity of PEGylated-carboxyhemoglobin was determined at 37°C under normal atmospheric conditions using similar previously described methods (**supplementary document 1**). A second set of experiments determined the oxygen-binding/carrying capacity of the molecule after full saturation of PEGylated-carboxyhemoglobin in 100% oxygen (for 2 h) to induce CO-release. However, complete CO release was not achieved.

The unknown spectrum was determined spectrophotometrically in UV-Vis ranging from 500 to 650 nm with 1 nm increment at 37°C (Synergy HTX, BioTek, Germany) to determine the concentration of each derivative (carboxyhemoglobin, oxy and deoxy-hemoglobin) of PEGylated-carboxyhemoglobin in the plasma. The observed total absorption spectrum of each plasma sample was then compared to the known spectra of the different derivatives of bovine hemoglobin[20] with their absorption values. With the use of the classical least squares' method (mixture of 3 components with 150 wavelengths, **see supplementary document 1**), the different concentrations of each component were recovered.

The concentration of PEGylated-carboxyhemoglobin in the plasma was obtained after the addition of 5 µl of both 2% KCN and 2% $K_3Fe(CN)_6$ to 40 µl of plasma to convert all PEGylated-carboxyhemoglobin derivatives to hemiglobincyanide (HiCN). The endpoint absorbance was read at 540 nm against a calibration curve.

Measurements of arterial blood gas and biochemistry

Arterial blood samples (250 µl) were collected at four time points (**Figure 1**). Arterial blood gas parameters were determined using a blood gas analyzer (ABL80 Flex, Radiometer, Copenhagen, Denmark), and total hemoglobin concentration (Hb), hemoglobin oxygen saturation, base excess (BE) and lactate levels were measured. The arterial oxygen content (C_aO_2) (ml $O_2.dl^{-1}$) was calculated considering the oxygen carrying capacity of PEGylated-carboxyhemoglobin in the plasma: $CaO_2=(SaO_2 \times Hb_{RBC} \times \gamma_{Hb})+ (S_{PEGylated-carboxyhemoglobin}O_2 \times Hb_{PEGylated-carboxyhemoglobin} \times \gamma_{PEGylated-carboxyhemoglobin})+ PaO_2 \times 0.0031$ where Hb_{RBC} is the hemoglobin

concentration in red blood cells (g.dl^{-1}), S is the arterial oxygen saturation of Hb$_{RBC}$ or PEGylated-carboxyhemoglobin, and γ is the oxygen carrying capacity of Hb$_{RBC}$ (1.34 ml O$_2$.g^{-1} Hb for rat blood) or PEGylated-carboxyhemoglobin, as previously determined. Renal delivery of O$_2$ (DO$_2$) (ml O$_2$.min^{-1}) was determined at the end of the experiment as follows: Renal DO$_2$= CaO$_2$ x RBF

Plasma creatinine and urine creatinine were measured using an automatic analyzer (c702 Roche Diagnostics, Roche Diagnostics, Basel, Switzerland). We established a calibration curve for creatinine levels prior to measurements to correct for a significant interference due to the presence of PEGylated-carboxyhemoglobin. Plasma osmolarity was determined using the freezing point method with an osmotic pressure meter (OSMOstation OM-6050, Menarini, Benelux B.V.). The glomerular filtration rate was estimated at the end of the experiment using the measurement of creatinine clearance (Cl$_{crea}$): Cl$_{crea}$=(U$_{Crea}$ x V)/(time x P$_{Crea}$) where U$_{Crea}$ is the concentration of creatinine in urine (mmol.l^{-1}), V is the urine volume (ml) per unit time of urine collection and P$_{Crea}$ is the concentration of creatinine in plasma (mmol.l^{-1}).

Plasma nitric oxide and heme-oxygenase 1 levels

The samples were placed in the reducing agent vanadium (III) chloride (VCl3) in 1 mol.l^{-1} HCl at 90 °C to reduce the nitrate and nitrite in the plasma samples to NO. The VCl3 reagent converts nitrite, nitrate, and S-nitroso compounds to NO gas which is guided towards an NO chemiluminescence signal analyzer (Sievers 280i analyzer, GE Analytical Instruments) to allow the direct detection of NO.[21] NO within the reaction vessel reacts with ozone to generate oxygen and excited-state NO species, and the decay is associated with the emission of weak near-infrared chemiluminescence. A sensitive photodetector detects this signal and converts it to millivolts (mV). The area under the curve of the detected chemiluminescence (mV.s) represents the amount of NO-ozone reactions in real time and thus the amount of bioavailable NO in the tested samples.

Heme-oxygenase 1 (HO-1) constitutes an essential cytoprotective component that ameliorates hemorrhagic shock-induced oxidative tissue injuries.[22] Plasma HO-1 levels were measured at the end of the experiment using an ELISA kit based on the sandwich assay principle (Rat HMOX1 / HO-1 ELISA Kit (Sandwich ELISA) - LS-F4085, LSBio LifeSpan BioSciences Inc., Seattle, WA, USA).

10

Immunohistochemical analysis and histology

Animals were euthanized at the end of the experiment using 40% Euthasol (Produlab Pharma BV, Raamsdonksveer, the Netherlands). Kidneys were harvested, fixed in 4% formalin and embedded in paraffin. Ten tubular areas (n=10) on each slice per animal were analyzed. The complete description of immunohistochemical analyses and histology are detailed in **Supplementary document 1.** A histological score (H-Score) value for Neutrophil Gelatinase-Associated Lipocalin (NGAL) and Tumor Necrosis Factor-α (TNF-α) was derived for each sample via summing the percentages of cells that stained at each intensity multiplied by the weighted intensity of the staining [H-Score = S Pi (i+1), where i is the intensity score and Pi is the corresponding percentage of the cells] under a light microscope at x400 magnification. Histological changes (brush border, vacuolar degeneration, cast formation, and invagination) in the cortex were assessed using quantitative measurements of tissue damage.

Statistical Analysis

Values are expressed as mean±SD when normally distributed (Kolmogorov-Smirnov test), or as median [interquartile range] otherwise. Repeated measures 2-way analysis of variance (RM-ANOVA) (2 factors: time as a related within-animal factor and group as a between-animal factor) and *post hoc* Bonferroni's correction test for multiple analyses were used to determine intergroup and/or intragroup differences in hemodynamics, cortical renal PO_2, and biochemical data. We reported the simple main effects of group (type of fluid) compared to the control and to the hydroxyethyl starch groups at each time point when a significant interaction was observed between time and group, and the simple main effect of time versus baseline within the same group. Ordinary one-way ANOVA with Bonferroni's correction was used for the analyses of the oxygen binding capacity of PEGylated-carboxyhemoglobin, renal oxygen delivery, ELISA heme-oxygenase-1 and volume of blood withdrawn. Analyses of creatinine clearance, total fluid volume, plasma NO, histological damages to the kidney and tumor necrosis factor-α and Neutrophil Gelatinase-Associated Lipocalin H-Scores were performed using a Kruskal-Wallis test with Dunn's correction test because of their non-Gaussian distribution. Outliers were evaluated but no action was necessary. Statistical analyses were performed using GraphPad Prism version 7.0a for Mac (GraphPad Software, La Jolla, USA). The overall significance level for each hypothesis was 0.05. Adjusted P-values are reported throughout the manuscript in *post hoc* tests.

We assumed that the microcirculatory PO_2 in the kidney would be of 26±3 mmHg (mean ± SD) at 30 min after resuscitation of hemorrhagic shock using 6% balanced hydroxyethyl starch based on previous experiments lead by our group. Therefore, a sample size of n = 6/group was needed to detect a 20% increase in kidney microcirculatory PO_2 (estimated to be 31 mmHg, delta of 5 mmHg) associated with the administration of PEGylated-carboxyhemoglobin (compared to balanced hydroxyethyl starch) and provide a power (1-β) of 80% with a type I error rate (α) of 5% using a 2-group Satterthwaite two-sided *t* test.

Results

A total of 42 animals were included in the present study (n=6-8/group). Eight animals were included in the PEGylated-carboxyhemoglobin group, and 4 served to established reliability in the protocol. No animal died during the experiment. The volume of blood withdrawn to induce hemorrhagic shock at T1 (6.7 ± 0.8 ml) was similar in all groups. The withdrawn volume represented 32.2 ± 4.4% of the total blood volume. The hemorrhagic shock produced similar alterations in hemodynamics (MAP and renal blood flow) and similar reductions in kidney microcirculatory PO_2 associated with a metabolic acidosis and hyperlactatemia in all groups compared to controls (*P <0.0001*). The hemodynamic data throughout the experiment are presented in **Table 1**. MAP was restored to ~80 mmHg in all animals that underwent resuscitation after hemorrhagic shock, according to the protocol. At the end of experiment, the renal blood flow recovered similarly to controls except for the blood transfusion group, which was lower than in the hydroxyethyl starch group (*P=0.015*). The changes acid-base status and lactate levels differed according to the resuscitation fluid administered (**Table 2**). Balanced hydroxyethyl starch was the most efficient fluid at restoring the acid-base status at the end of the rescue phase compared to other therapies. PEGylated-carboxyhemoglobin corrected the pH, but base excess, bicarbonate levels, and lactate levels remained significantly higher than controls (mean diff. -1.5, 95%CI [-2.6 to -0.4], *P=0.0018*) (**Table 2**).

10

Table 1. Systemic and renal hemodynamics and urine excretion

	Baseline	Shock	Rescue phase (30 min after resuscitation)	Maintenance (60 min after resuscitation)
MAP (mmHg)				
Control	94 ± 10	81 ± 5	84 ± 6	90 ± 6
Non-resuscitated	92 ± 5	32 ± 2*	32 ± 1*	30 ± 1*
6% balanced hydroxyethyl starch	92 ± 10	32 ± 1*	81 ± 4	83 ± 6
PEGylated-carboxyhemoglobin	91 ± 7	32 ± 2*	76 ± 11	81 ± 3
Blood transfusion	89 ± 4	32 ± 2*	86 ± 8	87 ± 10
Diluted blood transfusion	90 ± 6	33 ± 2 *	81 ± 1	79 ± 4*
Renal blood flow (ml.min^{-1})				
Control	9.8 ± 2.3	7.9 ± 2.6	7.4 ± 2.4	7 ± 2.4
Non-resuscitated	10.5 ± 3.2	3.0 ± 1*	3.2 ± 1.1*	3.0 ± 1*
6% balanced hydroxyethyl starch	9.7 ± 1.3	3.9± 2.4*	7.4 ± 2.4	8.4 ± 2.9
PEGylated-carboxyhemoglobin	11.6 ± 2	2.8 ± 0.5*	6.3 ± 1.2	8.3 ± 1.6
Blood transfusion	10.0 ± 1.7	2.3 ± 0.3*	5.0 ± 0.3	5.4 ± 0.5#
Diluted blood transfusion	11.6 ± 1.2	3.1 ± 1.5*	7.0 ± 1.7	7.3 ± 1.6
Urine output (ml.h^{-1})				
Control	2.80 ± 0.73	2.2 ± 1.42	2.46 ± 0.94	1.87 ± 0.53
Non-resuscitated	4.68 ± 1.8	0 ± 0 $	0 ± 0$	0 ± 0$
6% balanced hydroxyethyl starch	2.77 ± 0.91	0 ± 0 $	2.55 ± 0.75	3.93 ± 2.35
PEGylated-carboxyhemoglobin	4.01 ± 2.3	0 ± 0 $	0.76 ± 0.55$	3.97 ± 1.43
Blood transfusion	3.29 ± 1.94	0 ± 0 $	0.85 ± 0.52$	2.2 ± 1.43
Diluted blood transfusion	4.04 ± 1.31	0 ± 0 $	1.63 ± 1.20$	3.63 ± 1.75

MAP: Mean Arterial Pressure, PEGylated: polyethylene glycolated.

Repeated measures 2-way ANOVA test used with Bonferroni's correction to adjust for multiple comparisons. * adjusted *P<0.01* vs. Control group at the same time point, # adjusted *P<0.05* vs. 6% balanced hydroxyethyl starch group at the same time point, *$ P<0.01* vs. baseline value within the same group.

Significant differences in urine output at baseline were observed between groups. Therefore, only intragroup comparisons were performed. Notably, urine output after the rescue phase in the blood transfusion group was lower than at baseline (mean diff. 2.44, 95%CI [0.93 to 3.95], *P=0.0006*), and urine output was readily restored 30 min after resuscitation in the hydroxyethyl starch group (mean diff. 0.23, 95%CI [-1.28 to 1.74], *P=0.969*) (**Table 1**).

Table 2. Acid-base balance and arterial lactate levels during experiment

	Baseline	Shock	Rescue phase (30 min after resuscitation)	Maintenance (60 min after resuscitation)
pH				
Control	7.41 ± 0.04	7.38 ± 0.04	7.38 ± 0.02	7.37 ± 0.01
Non-resuscitated	7.39 ± 0.02	7.23 ± 0.02 *	7.16 ± 0.05 *	7.13 ± 0.05 *
6% balanced hydroxyethyl starch	7.40 ± 0.04	7.22 ± 0.05 *	7.36 ± 0.03 *	7.40 ± 0.04
PEGylated-carboxyhemoglobin	7.38 ± 0.02	7.20 ± 0.06 *	7.29 ± 0.04 *#	7.35 ± 0.02
Blood transfusion	7.40 ± 0.03	7.22 ± 0.03 *	7.26 ± 0.04 *#	7.33 ± 0.06
Diluted blood transfusion	7.39 ± 0.04	7.22 ± 0.06 *	7.28 ± 0.05 *#	7.32 ± 0.05 #
Base excess (mmol.l^{-1})				
Control	-4.5 ± 2	-4.6 ± 1	-4.4 ± 0.9	-3.3 ± 0.6
Non-resuscitated	-2.4 ± 1.3	-12.5 ± 1.9 *	-15 ± 3.0 *	-16.6 ± 2.7 *
6% balanced hydroxyethyl starch	-3.5 ± 2.0	-13.6 ± 0.8 *	-5.6 ± 1.4 *	-2.2 ± 1.4
PEGylated-carboxyhemoglobin	-3.7 ± 0.8	-13.4 ± 2.3 *	-9.3 ± 2.0 *#	-4.5 ± 0.8
Blood transfusion	-2.5 ± 1.7	-13.2 ± 1.4 *	-9.5 ± 1.3 *#	-6.6 ± 1.6
Diluted blood transfusion	-1.7 ± 1.9	-12.2 ± 3.8 *	-8.7 ± 3.1 *	-6.9 ± 2.5 *
HCO$_3^-$ (mmol.l^{-1})				
Control	19.3 ± 1.1	19.5 ± 0.5	19.8 ± 1.1	20.8 ± 0.8
Non-resuscitated	21.6 ± 1.8	13.8 ± 1.9 *	12.7 ± 2.4*#	11.4 ± 2.2 *
6% balanced hydroxyethyl starch	20.0 ± 1.9	12.9 ± 1.1 *	18.5 ± 1.4	22.1 ± 1.3
PEGylated-carboxyhemoglobin	20.1 ± 1.2	13.6 ± 1.2 *	16.3 ± 1.9 *	20.2 ± 0.9 #
Blood transfusion	21.1 ± 1.9	13.2 ± 1.8 *	16.6 ± 1 *	18.3 ± 0.9 #
Diluted blood transfusion	22.4 ± 1.4	14.2 ± 2.8 *	16.9 ± 2.6	18.0 ± 2.5 #
Lactate$^-$ (mmol.l^{-1})				
Control	0.9 ± 0.2	1.4 ± 0.3	1.9 ± 0.4	2.1 ± 0.5
Non-resuscitated	0.8 ± 0.2	5.1 ± 0.5 *	5.8 ± 0.6 *	7.2 ± 1.1 *
6% balanced hydroxyethyl starch	1.1 ± 0.4	5.3 ± 1.3 *	3.3 ± 0.6 *	2.7 ± 0.5
PEGylated-carboxyhemoglobin	0.8 ± 0.2	4.5 ± 0.7 *	3.9 ± 0.8 *	3.6 ± 0.8 *
Blood transfusion	0.8 ± 0.1	5.1 ± 0.5 *	3.0 ± 0.2	2.3 ± 0.3
Diluted blood transfusion	0.7 ± 0.1	5.0 ± 1.4 *	3.0 ± 0.8	1.9 ± 0.4

Values are presented as mean±SD. PEGylated: polyethylene glycolated.

Repeated measures 2-way ANOVA test used with Bonferroni's correction to adjust for multiple comparisons. * adjusted *P<0.01* vs. Control group at the same time point, # adjusted *P<0.01* vs. 6% balanced hydroxyethyl starch group at the same time point, *$ P<0.05* vs. baseline value within the same group.

Kidney microcirculatory PO$_2$ and renal function

Figure 2 shows that hemorrhagic shock significantly reduced baseline renal cortical PO$_2$ in all groups compared to baseline and controls. The mean renal cortical PO$_2$ was 13±5 mmHg 60 minutes after hemorrhagic shock induction. Similar MAP and renal blood flow were observed between groups, but none of the fluid therapies restored renal cortical PO$_2$ to levels similar to controls 30 or 60 min after resuscitation. Whole blood transfusion and diluted blood transfusion outperformed 6% balanced hydroxyethyl starch in increasing renal cortical PO$_2$ at the end of experiment to 51±5 mmHg (mean diff. -19, 95%CI [-26 to -11], *P<0.0001*) and 47±5 mmHg (mean diff. -23, 95%CI [-31 to -15], *P<0.0001*) versus 29±8 mmHg respectively. However, there were no differences between PEGylated-carboxyhemoglobin and balanced hydroxyethyl starch in renal

10

cortical PO$_2$ in the early rescue phase (32±7 mmHg versus 27±4 mmHg, mean diff. -6, 95%CI [-13 to 2], *P=0.209*) or at the end of the experiment (33±7 mmHg versus 29±8 mmHg, mean diff. -5, 95%CI [-12 to 3], *P=0.387*).
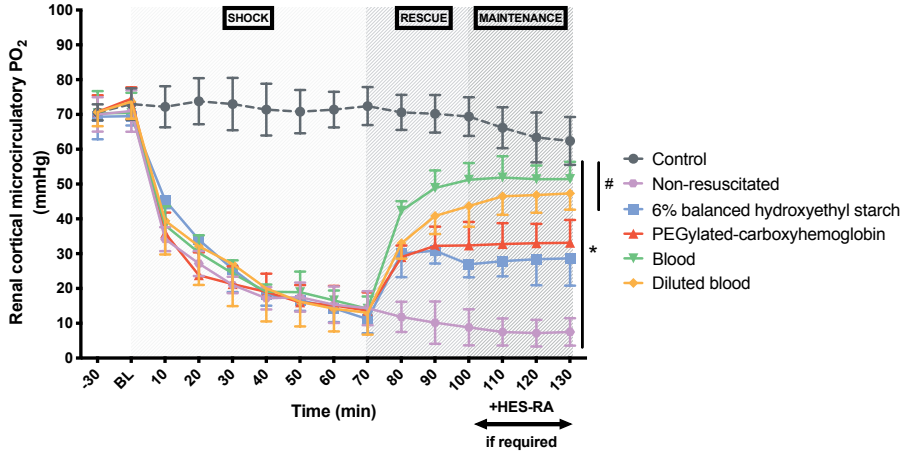

Figure 2. Renal cortical microcirculatory PO$_2$ during the experiment

*For the sake of clarity only significant differences were shown at the end of the experiment. Repeated measures 2-way ANOVA test used with Bonferroni's correction to adjust for multiple comparisons. * adjusted P<0.005 vs. Control group, # adjusted P<0.05 compared to 6% balanced hydroxyethyl starch at the same time point. Data is presented as mean±SD. (n=8 for PEG-carboxyhemoglobin group and n=6/group for other groups).*

Hemorrhagic shock induced acute kidney injury with a significant increase in plasma creatinine levels (greater than two-fold increase of baseline values) (**Figure 3A**) compared to controls (*P<0.0001*). Creatinine levels remained higher 60 min after resuscitation compared to the control rats, regardless of the therapy used (*P<0.0001*). There were no differences regarding plasma creatinine between hydroxyethyl starch and PEGylated-carboxyhemoglobin 60 min after resuscitation (44.0 ± 6.7 µmol/l versus 49.9 ± 6.4 µmol/l, respectively, mean diff. 5.9, 95%CI [-3.0 to 14.8], *P=0.230*). Conversely, the measured creatinine clearance (**Figure 3B**) was not different at 60 min between groups.

The CaO$_2$ (**Table 3**) was calculated for all time points. However, the contribution of PEGylated-carboxyhemoglobin's hemoglobin to arterial oxygen content was only considered at the last time point of the experiment (60 min after resuscitation) for technical reasons. Therefore, we did not investigate the contribution of PEGylated-carboxyhemoglobin's hemoglobin to CaO$_2$ 30 min after resuscitation. Blood and diluted blood transfusions produced

CaO_2 values similar to controls. The CaO_2 was superior in the PEGylated-carboxyhemoglobin group compared to balanced hydroxyethyl starch only after the rescue period (30 min) (12.5 ± 1.3 g.dl^{-1} versus 9.4 ± 1.1 g.dl^{-1}, mean diff. -3.0, 95%CI [-5.4 to -0.6], *P=0.005*). This difference was offset at the end of the experiment.

The renal oxygen delivery was significantly lower in all groups at the end of experiment compared to controls except in the diluted blood transfusion group (**Supplementary Figure 1**).
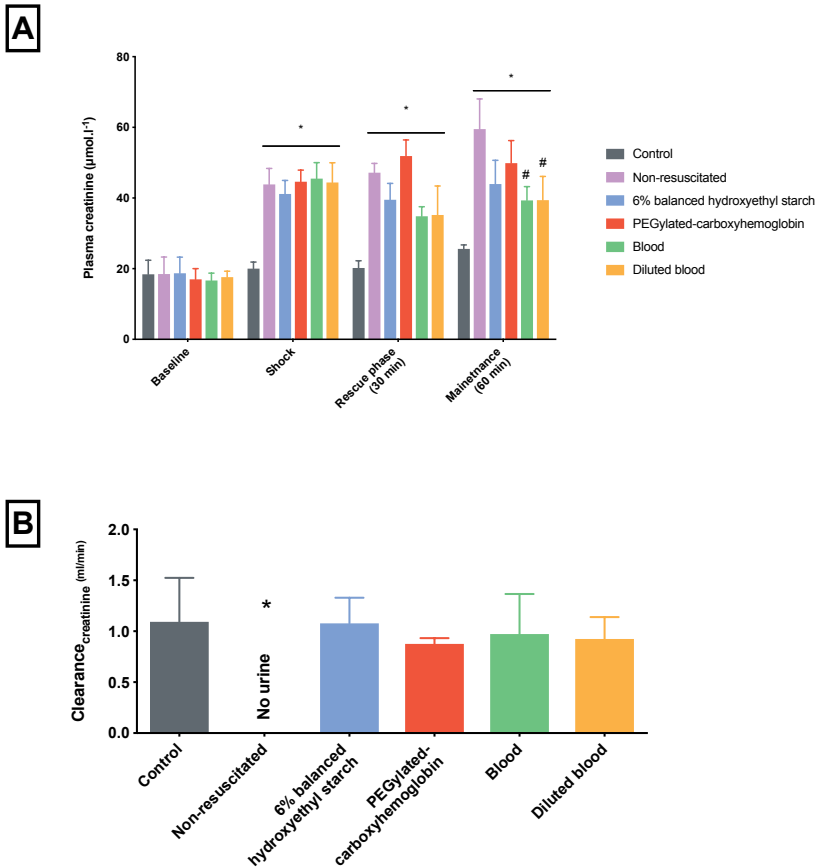
Figure 3. Time course of changes in plasma creatinine (A) and creatinine clearance at the end of the experiment (B)

*(A) Repeated measures 2-way ANOVA test used with Bonferroni's correction to adjust for multiple comparisons. * adjusted P<0.001 vs. Control group, # adjusted P<0.05 compared to 6% balanced hydroxyethyl starch at the same time point.. Data is presented as mean±SD. (B) Kurskal-Wallis test with Dunn's posttest was used. * adjusted P<0.0001 compared to control group. Data is presented as median [interquartile range]. (n=8 for PEG-carboxyhemoglobin group and n=6/group for other groups)*

10
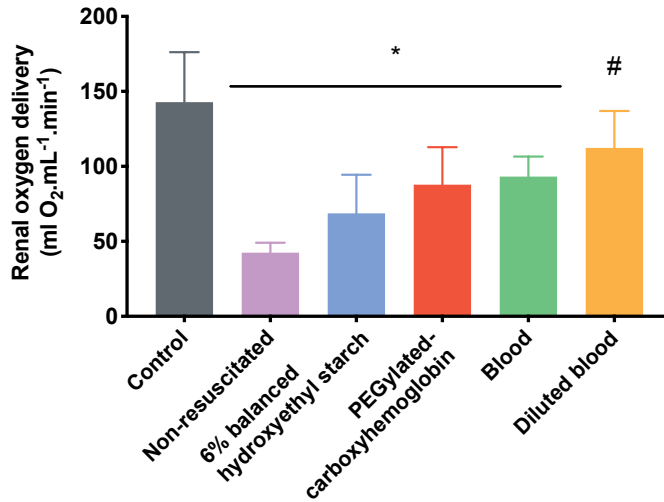
Supplementary Figure 1. Renal oxygen delivery at the end of the experiment

* adjusted P<0.01 compared to control group, # adjusted P<0.05 compared to 6% balanced hydroxyethyl starch.

Ordinary one-way ANOVA with Bonferroni's multiple comparisons test used. (n=8 for PEG-carboxyhemoglobin group and n=6/group for other groups). Data is presented as mean±SD.

Fluid volume

The stacked (total) fluid volume and separate volumes of each therapy plus balanced hydroxyethyl starch are presented in **Figure 4**. The fluid volumes needed to achieve similar MAP targets varied significantly between groups, 8.5 [7.7 to 11.4] ml, 4.5 [3.3 to 6.2] ml, 7.3 [6.4 to 7.8] ml and 13.2 [11.9 to 15.35] ml, for balanced hydroxyethyl starch, PEGylated-carboxyhemoglobin, blood transfusion and diluted blood transfusion groups respectively (*P<0.0002*). The PEGylated-carboxyhemoglobin group required significantly less volume than balanced hydroxyethyl starch (mean rank diff. -11.98, *P=0.011*) to achieve similar MAP and renal cortical PO$_2$. No additional volume of balanced hydroxyethyl starch was required in the diluted blood transfusion group to maintain MAP over the time of observation time of the experiment. However, this latter group required the largest amount of fluid administration.
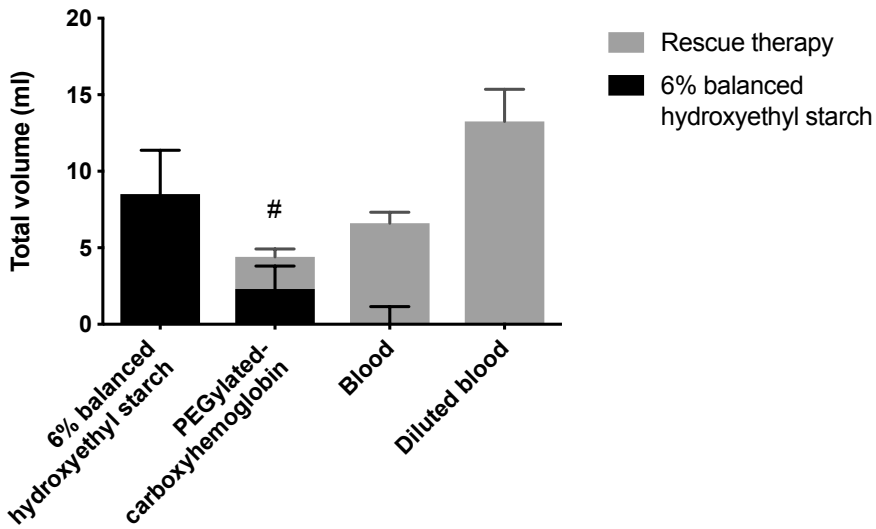
Figure 4. Total volume of fluid administered in each group

The volumes are stacked for the sake of clarity. The height of the stacked bins represents the total volume administered. The total volumes (rescue therapy + maintenance) were compared between groups. # adjusted P<0.05 compared to 6% balanced hydroxyethyl starch. Kurskal-Wallis test with Dunn's posttest was used. Data is presented as median [interquartile range]. (n=8 for PEG-carboxyhemoglobin group and n=6/group for other groups).

Fate of PEGylated-carboxyhemoglobin

PEGylated-carboxyhemoglobin partially released its CO molecules after injection in the cardiovascular system (**Table 3**). The percentage of carboxyhemoglobin decreased from ~85% measured *in vitro* (manufacturer data) to 23.6 ± 9% (*P<0.0001*) (as determined in the **Supplementary document 1**).

The oxygen biding capacity of PEGylated-carboxyhemoglobin *in vitro* was determined to be 0.29 ± 0.09 ml $O_2.g^{-1}$ of hemoglobin (7 measurements) in its original form. This OBC increased significantly after full oxygenation of the molecule to induce CO release, reaching 0.92 ± 0.02 ml $O_2.g^{-1}$ of hemoglobin (*P<0.0001*).

10

Table 3. Hemoglogin levels, arterial oxygen content and fractions of PEGylated-carboxyhemoglobin's derivatives

	Baseline	Shock	Rescue phase (30 min after resuscitation)	Maintenance (60 min after resuscitation)
Total hemoglobin concentration (g.dl^{-1})				
Control	14.4 ± 0.9	14.5 ± 0.5	14.3 ± 0.8	13.0 ± 0.3
Non-resuscitated	15.1 ± 0.9	10.5 ± 2.0*	10.3 ± 1.2*#	9.3 ± 0.7*#
6% balanced hydroxyethyl starch	14.8 ± 1.5	9.7 ± 1.0*	6.6 ± 0.8*	5.5 ± 0.5*
PEGylated-carboxyhemoglobin	15.6 ± 0.9	11.2 ± 1.0	8.6 ± 0.9	7 ± 1
Blood transfusion	15.3 ± 0.5	9.9 ± 0.8	13.5 ± 1.3	12.4 ± 0.9
Diluted blood transfusion	14.8 ± 0.2	10.1 ± 0.7	11.0 ± 0.6	10.9 ± 0.2
Hematocrit (%)				
Control	44 ± 3	45 ± 1	43 ± 3	40 ± 1
Non-resuscitated	46 ± 3	32 ± 6*	32 ± 4*#	29 ± 2*#
6% balanced hydroxyethyl starch	45 ± 5	30 ± 3*	21 ± 2*	17 ± 2*
PEGylated-carboxyhemoglobin	48 ± 3	35 ± 3	28 ± 3	22 ± 3
Blood transfusion	47 ± 1	31 ± 3	41 ±4	38 ± 3
Diluted blood transfusion	45 ± 0.5	31 ± 2	34 ± 1.7	34 ± 0.7
PEGylated-carboxyhemoglobin and derivatives				
Plasma PEGylated-carboxyhemoglobin concentration (g.dl^{-1})	-	-	N/D	0.6 ± 0.1
PEGylated-carboxyhemoglobin fraction (%)	-	-	N/D	23.6 ± 9
CaO$_2$ (ml O$_2$.dl^{-1})				
Control	19.8 ± 1.2	20.1 ± 0.6	19.8 ± 1	18.1 ± 0.4
Non-resuscitated	20.8 ± 1.2	14.7 ± 2.7*	14.5 ± 1.6*#	13.1 ± 0.9*#
6% balanced hydroxyethyl starch	20.4 ± 2.10	13.6 ± 1.40*	9.5 ± 1.10*	8.0 ± 0.7*
PEGylated-carboxyhemoglobin	21.6 ± 1.1	15.7 ± 1.2	13 ± 1.3	10.4 ± 1.5
Blood transfusion	21.1 ± 0.6	13.9 ± 1.1	18.7 ± 1.7	17.2 ± 1.2
Diluted blood transfusion	20.4 ± 0.2	14.2 ± 1	15.3 ± 0.8	15.3 ± 0.3

*Values are presented as mean±SD. CaO$_2$: Arterial oxygen content, PEGylated: polyethylene glycolated*

Repeated measures 2-way ANOVA test used with Bonferroni's correction to adjust for multiple comparisons. * adjusted P<0.01 vs. Control group at the same time point, # adjusted P<0.01 vs. 6% balanced hydroxyethyl starch group at the same time point, $ P<0.05 vs. baseline value within the same group.

Nitric oxide and Heme-oxygenase-1 in plasma

The administration of PEGylated-carboxyhemoglobin did not result in a decrease in plasma NO concentrations, excluding a NO-scavenging effect. Plasma NO levels were higher in the blood transfusion, diluted blood transfusion and nonresuscitated hemorrhagic shock groups compared to balanced hydroxyethyl starch (*P<0.05*). However, there was no significant difference between the control and balanced hydroxyethyl starch or PEGylated-carboxyhemoglobin groups (**Supplementary Figure 2A**). Blood and diluted blood increased the

bioavailability of NO in the plasma compared to balanced hydroxyethyl starch (mean rank diff. -20.97, *P=0.004* and -17.13, *P=0.029* respectively).

CO is produced via the heme-oxygenase-1 pathway. Therefore, we investigated the levels of HO-1 in the plasma. We were unable to detect any significant changes in plasma HO-1 between groups, but there was a trend towards higher HO-1 levels in the blood transfusion group (**Supplementary Figure 2B**).
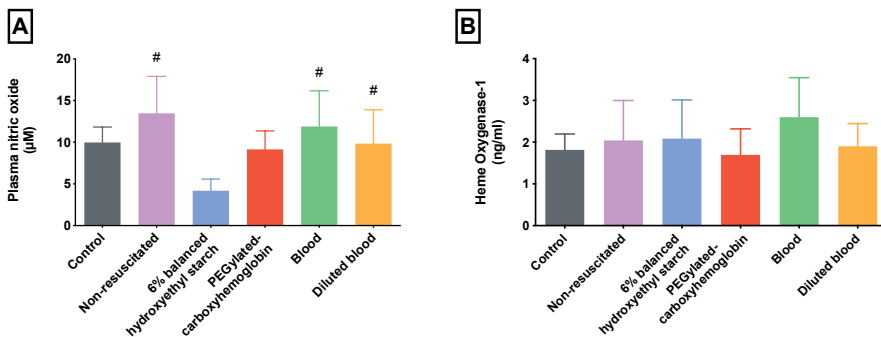
Supplementary Figure 2. Plasma nitric oxide (A) and heme oxygenase-1 (B) levels

(Panel A) Kurskal-Wallis test with Dunn's posttest was used for plasma NO. Data is presented as median [interquartile range]. Panel (B) Ordinary one-way ANOVA with Bonferroni's multiple comparisons test used for heme-oxygenase-1. (n=8 for PEG-carboxyhemoglobin group and n=6/group for other groups). Data is presented as mean±SD. * adjusted P<0.01 compared to control group, # adjusted P<0.05 compared to 6% balanced hydroxyethyl starch.

Kidney immunohistochemistry and histology

Figure 5 depicts the Tumor Necrosis Factor-α (**5A**) and Neutrophil Gelatinase-Associated Lipocalin (**5B**) histological scores in the kidney. Hemorrhagic shock produced a significant increase in Neutrophil Gelatinase-Associated Lipocalin histological score compared to control rats (270 [210 to 300] versus 225 [197.5 to 251], mean rank diff. -46, *P=0.006*, respectively). Only PEGylated-carboxyhemoglobin and blood transfusion prevented the alterations in Neutrophil Gelatinase-Associated Lipocalin histological score after hemorrhagic shock and outperformed fluid resuscitation with balanced hydroxyethyl starch (*P<0.0005*). Consistently, the damage scores in kidney (brush border loss, vacuolization and luminal casts) were markedly decreased in the PEGylated-carboxyhemoglobin, diluted blood transfusion and blood transfusion groups (4 [3.3 to 4.3], 4 [3.7 to 4.7] and 3.7 [3.3 to 4], respectively) compared to balanced hydroxyethyl starch (5 [4.7 to 5]) (*P<0.001*), but remained significantly higher than the controls (*P<0.001*) (**Figure 5C**).
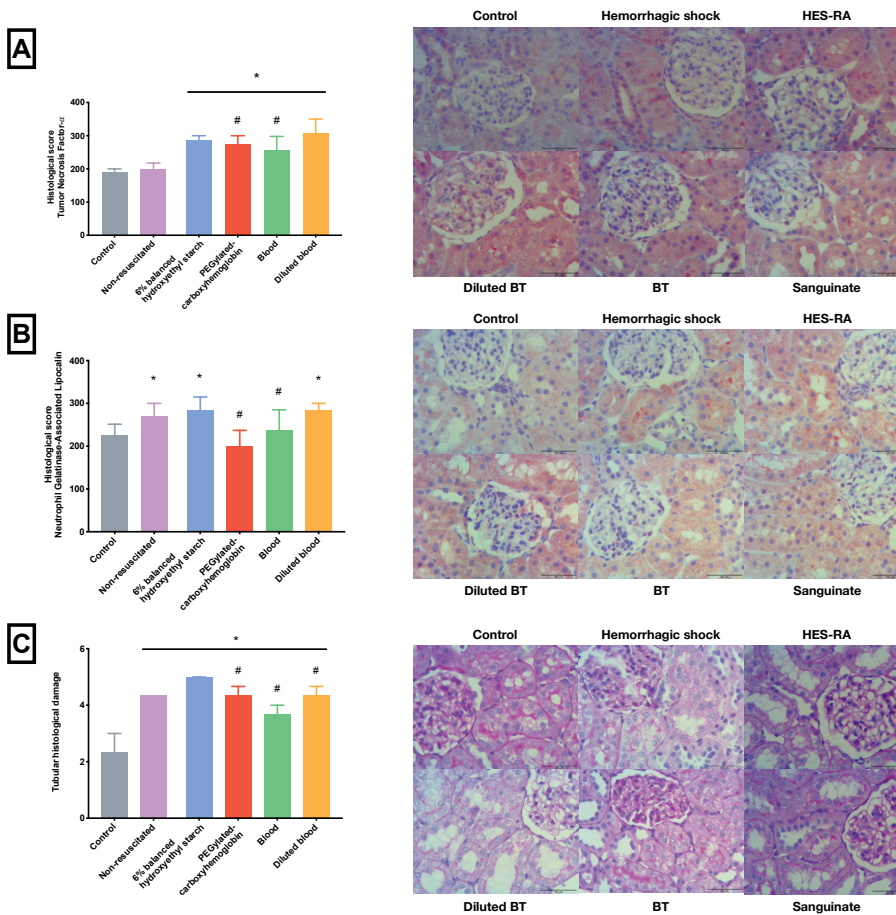
10

Figure 5. Kidney immunochemistry and tubular histological damage scores

*Left panel. The histological scores of Tumor Necrosis Factor-α (A), and Neutrophil Gelatinase-Associated Lipocalin (B) are presented (see supplementary document 1 for additional information). Tubular histological damage graph (C) was drawn by calculating mean of damages of tubular brush border loss, presence of luminal cast and vacuoles. **Right panel.** Observation of the corresponding histological images are shown at magnification x400. The scale bar is 50 μm.*

(A) Kidney sections were incubated overnight at 4°C with rabbit polyclonal TNF-α (1:100) (abcam 6671) or (B) incubated for 1 hour at room temperature with Lipocalin 2 antibody (NGAL, 1/150) (abcam 41105). (C) The kidney sections were stained with periodic acid-schiff reagent (PAS) and hematoxyline to depict tubular damage defined as loss of brush border, vacuolar degeneration, and cast formation.

* adjusted P<0.05 compared to control group, # adjusted P<0.05 compared to 6% balanced hydroxyethyl starch. Kurskal-Wallis test with Dunn's posttest was used. A minimum of 40 tubules were examined per group, with n=6/kidney per animal minimum. Data is presented as median [interquartile range].

Discussion

The present study demonstrated that low volume rescue therapy with PEGylated-carboxyhemoglobin provided efficient restoration of the macrohemodynamics and maintained a similar kidney microcirculatory PO_2 compared to synthetic balanced hydroxyethyl starch following resuscitation of pressure-controlled hemorrhagic shock in a rodent model. PEGylated-carboxyhemoglobin also modulated tubular damages in the kidney, which was associated with a mitigated expression of Neutrophil Gelatinase-Associated Lipocalin, because of its embedded CO molecules. PEGylated-carboxyhemoglobin may blunt the risk for acute kidney injury in this setting. The small increase in oxygen-carrying capacity provided by this molecule did not affect kidney tissue oxygenation of improve lactate or creatinine clearance, but the low volume administered sustained urine output and produced very stable hemodynamic conditions for 60 min after hemorrhagic shock. We also demonstrated that diluted blood transfusion at the same level as PEGylated-carboxyhemoglobin provided significantly higher renal cortical Po_2 in the kidney but required markedly more volume to reach the targeted MAP.

Low volume strategies were considered for decades to limit aggressive fluid resuscitation using large uncontrolled fluid boluses that increased bleeding, hemodilution, coagulopathy, hemodynamic decompensation, fluid overload and excess in mortality.[1,2,23] Our group already published several studies on fluid resuscitation following hemorrhagic shock comparing crystalloids to colloids, balanced or unbalanced and their consequences on renal cortical Po_2.[24–26] Balanced hydroxyethyl starch solution was found more efficient at restoring macrohemodynamics and renal cortical Po_2 than crystalloids. In the present study, we sought to evaluate an alternative colloid in the context of ongoing controversies about hydroxyethyl starch use. The European Medicines Agency recently issued several restrictions on the use of hydroxyethyl starch solutions in different clinical settings across the European Union.[5] Hydroxyethyl starch solutions are contraindicated in patients with renal impairment and should be administered to manage hemorrhage only when crystalloids alone are not considered sufficient. Therefore, new fluid therapies that outperform crystalloids and compete with the latest synthetic colloid solutions are desired to improve and sustain volume status to promptly restore blood pressure and flow in the context of hemorrhage. However, blood product transfusions remain the gold standard treatment of hemorrhage, but this treatment is not always readily available. Transfusion thresholds during the last decade with the implementation

10

of restrictive transfusion strategies,[27,28] and fewer patients are likely to receive blood transfusions in the perioperative setting.

Previous generations of hemoglobin-based oxygen carriers failed in clinical practice primarily due to major side effects such as hypertension and myocardial injury, that were overlooked in preclinical models.[29,30] These effects were presumably related to the extravasation of tetrameric hemoglobin and NO-scavenging effects. The formulation of hemoglobin-based oxygen carriers has changed to comply with more physiological prerequisites. PEGylated-carboxyhemoglobin provides a larger expansion volume than balanced hydroxyethyl starch partially because of its oncotic effect.[11] The increase in MAP was likely due to the PEGylation process of the carboxyhemoglobin rather than an NO-scavenging effect. PEGylated-carboxyhemoglobin infusion produced similar plasma NO levels as blood transfusion in our experiment. However, the administration of hydroxyethyl starch alone as a resuscitation fluid significantly decreased the bioavailability of NO. This result suggests a decreased shear-stress mediated NO release from the endothelium.[31]

Our group previously demonstrated that a low volume of diaspirin-crosslinked hemoglobin (DCLHb), restored epicardial and gut serosal and mucosal microvascular oxygenation.[32,33] Similarly, diaspirin-crosslinked hemoglobin restored pancreatic functional capillary density in a rodent model of hemorrhagic shock.[34] However, increasing the dose of diaspirin-crosslinked hemoglobin produced to two main consequences: hyperoxia in the gut serosa and mucosae and severe hypertension. The latter effect was caused by vasoconstriction via the inhibition of NO. Similarly, the extensive literature on bovine hemoglobin-based oxygen carrier (HBOC-201, Hemopure, HbO_2 Therapeutics LLC) reported improvements in tissue oxygenation and macrohemodynamics with induced vasoconstriction.[35] Little data on hemoglobin-based oxygen carriers and kidney oxygenation and function are available. PEGylated-carboxyhemoglobin should not be regarded as a hemoglobin-based oxygen carrier *per se*, but more as a colloid with additional beneficial effects. Our experiment highlighted that PEGylated-carboxyhemoglobin cannot compete with blood transfusion (even diluted at the same hemoglobin concentration) in terms of quality of oxygen carrying capacity and delivery to hypoxic tissue. In contrast, PEGylated-carboxyhemoglobin may be an interesting alternative when blood is not an option or in cases of delayed blood transfusion. First, the P_{50} is lower than the one of whole blood (8 to 16 mmHg versus 26 to 30 mmHg respectively),[11] which impedes oxygen release to moderately hypoxic tissue. Second, we demonstrated that (i) the oxygen binding capacity of native PEGylated-carboxyhemoglobin was significantly lower than rat (or human) hemoglobin oxygen

binding capacity even after CO release and (ii) the concentration of PEGylated-carboxyhemoglobin in the plasma was too low to expect any significant increase in oxygen delivery compared to whole blood. To test whether PEGylated-carboxyhemoglobin can release more oxygen, its P_{50} could be theoretically altered by the use of RSR13 (2-[4-[[(3, 5-dimethylanilino)carbonyl]methyl]phenoxyl]-2-methylproprionic acid),[36] a synthetic allosteric modifier of O_2-hemoglobin affinity that increases O_2 release (rightward shift of oxygen-hemoglobin dissociation curve) to tissue by allosterically stabilizing deoxyhemoglobin. However, two limits have to be considered: (i) RSR13 will also alter the P_{50} of native hemoglobin and (ii) it could exacerbate acute renal dysfunction.[36,37]

The renal damage was mitigated with the use of PEGylated-carboxyhemoglobin compared to the administration of hydroxyethyl starch alone. These effects may be attributed to CO release. Previous studies demonstrated possible anti-inflammatory effects of carbon monoxide mediated via HO-1 activation.[38] Nassour *et al.* demonstrated that CO-releasing molecules protected against hemorrhagic shock and resuscitation-induced organ injury and inflammation in a similar rodent model of hemorrhagic shock.[16] However, the CO-releasing molecules used could not carry oxygen, which highlights the central role of CO and heme-oxygenase-1 in ischemia/reperfusion injury following hemorrhage.

The off-loading of CO molecules from PEGylated-carboxyhemoglobin is not instantaneous. Approximately 23% of PEGylated-carboxyhemoglobin remained saturated with CO 60 min after the start of resuscitation in our study. Vandegriff *et al.* demonstrated that the percentage of carboxyhemoglobin of CO-MP4 (another PEGylated-carboxyhemoglobin) decreased to 20-25% 30 min after mixing CO-MP4 with red blood cells *in vitro* which is similar to our observations.[39] In contrast, Zhang *et al.* observed different results in an *in vivo* top-load rodent model.[40] Whole blood and plasma gas analyses revealed a low percentage (5-7%) of carboxyhemoglobin 1 and 3 minutes after PEGylated-carboxyhemoglobin injection, which suggests a rapid exchange of CO between PEGylated-carboxyhemoglobin and native red blood cells.[40] Overall, these results demonstrated a disassociation of CO molecules from PEGylated-carboxyhemoglobin, which subsequently re-equilibrates with native red blood cells. The remaining Pegylated- hemoglobin (without CO) binds oxygen or may be oxidized in the context of hemorrhagic shock. However, whether this chemical process persists after 60 min is not known.

Parrish *et al.* previously brought evidence that the cell impermeant PEG-20 kDa significantly affected colloid pressure and improved survival in low volume resuscitation hemorrhagic shock models.[41] However, the effects of the administration of this PEG-20 kDa on the kidney were not

10

assessed. PEGylated-carboxyhemoglobin provides additional benefits with its ability to release CO molecules and oxygen binding capacity.

Limitations

First, we focused only on the golden hour after resuscitation following hemorrhagic shock and long-term results on the use of PEGylated-carboxyhemoglobin therefore cannot be anticipated. Second, lactate and creatinine levels were higher in the PEGylated-carboxyhemoglobin group after 1 h due to low volume resuscitation even when the preset target of resuscitation, namely, MAP, was reached. The changes in creatinine clearance may not be reflected at 1 h. However, there is evidence that low volume resuscitation may improve survival, although it may delay the correction of biological parameters.[42] The delay in correction of biological parameters is unlikely to be related to CO toxicity because of the very small amount released. However, we cannot exclude a direct toxicity of PEGylated-hemoglobin. Third, it may be difficult to distinguish the cytoprotective effects of CO from the colloidal effect of PEGylated-carboxyhemoglobin that restores blood flood and pressure. Nevertheless, previous works demonstrated that the administration of hemoglobin-based oxygen carrier in the carboxy state protected against focal ischemia.[39,40] Fourth, 6% balanced hydroxyethyl starch was used in each group to maintain the targeted MAP after the rescue phase, and it may be considered a bias. However, this study design provided a more realistic approach. The use of a crystalloid or colloid to maintain blood volume in a context of hemorrhage occurs daily in clinical practice. Fifth, the observation time was set at 1 h after resuscitation, which may be short. However, the present study sought to specifically assess the effects of PEGylated-carboxyhemoglobin on renal oxygenation and function in the early phase of resuscitation following hemorrhagic shock. A survival benefit of PEGylated-carboxyhemoglobin was demonstrated previously.[43] Further research is warranted to determine the mid- to long-term effects on the kidney. An observation period of 3 to 7 days of recovery after resuscitation of hemorrhagic shock with PEGylated-carboxyhemoglobin would be relevant in this context.

Conclusions

PEGylated-carboxyhemoglobin exhibited interesting properties for the resuscitation of hemorrhagic shock, especially because of the limited volume administered. Biomarkers of shock were not corrected as quickly as expected, but there is evidence that PEGylated-carboxyhemoglobin's dual action protects the kidney against ischemia/reperfusion damages following resuscitation through its CO molecules and sustained urine output, which partially contribute to an increase in the oxygen delivery to tissues during the first hour of resuscitation. Further research on colloidal solutions should be intensified to provide the anesthesiologists and intensive care unit physicians an interesting option for meeting unmet clinical needs. Finally, whether PEGylated-carboxyhemoglobin exhibits long-term protective effects on the kidney without adverse effects on the other organs should be determined in future studies.

Acknowledgments

Funding statement

Conflicts of Interest

Prof. Dr Can Ince runs an Internet site microcirculationacademy.org which offers services (e.g., training, courses, analysis) related to clinical microcirculation and, has received honoraria

10

Authors contribution

References

1.   Cannon JW. Hemorrhagic Shock. *N Engl J Med*. 2018;378(19):1852-1853.

2.   Cantle PM, Cotton BA. Balanced Resuscitation in Trauma Management. *Surg Clin North Am*. 2017;97(5):999-1014.

3.   Feinman M, Cotton BA, Haut ER. Optimal fluid resuscitation in trauma: type, timing, and total. *Curr Opin Crit Care*. 2014;20(4):366-372.

4.   Wiedermann CJ, Eisendle K. Comparison of hydroxyethyl starch regulatory summaries from the Food and Drug Administration and the European Medicines Agency. *J Pharm Policy Pract*. 2017;10:12.

5.   European Medicines Agency - Human medicines - Hydroxyethyl starch (HES) containing medicinal products.

6.   Dubick MA, Bruttig SP, Wade CE. Issues of concern regarding the use of hypertonic/hyperoncotic fluid resuscitation of hemorrhagic hypotension. *Shock*. 2006;25(4):321-328.

7.   Hoste EAJ, Bagshaw SM, Bellomo R, et al. Epidemiology of acute kidney injury in critically ill patients: the multinational AKI-EPI study. *Intensive Care Med*. 2015;41(8):1411-1423.

8.   Basile DP, Anderson MD, Sutton TA. Pathophysiology of Acute Kidney Injury. *Compr Physiol*. 2012;2(2):1303-1353.

9.   Prowle JR, Kirwan CJ, Bellomo R. Fluid management for the prevention and attenuation of acute kidney injury. *Nat Rev Nephrol*. 2014;10(1):37-47.

10.   Evans RG, Ince C, Joles JA, et al. Haemodynamic influences on kidney oxygenation: clinical implications of integrative physiology. *Clin Exp Pharmacol Physiol*. 2013;40(2):106-122.

11.   Abuchowski A. SANGUINATE (PEGylated Carboxyhemoglobin Bovine): Mechanism of Action and Clinical Update. *Artif Organs*. 2017;41(4):346-350.

12.   Motterlini R, Otterbein LE. The therapeutic potential of carbon monoxide. *Nat Rev Drug Discov*. 2010;9(9):728-743.

13.   Wegiel B, Hanto DW, Otterbein LE. The social network of carbon monoxide in medicine. *Trends Mol Med*. 2013;19(1):3-11.

14.   Faller S, Hoetzel A. Carbon monoxide in acute lung injury. *Curr Pharm Biotechnol*. 2012;13(6):777-786.

15.   Nakahira K, Choi AMK. Carbon monoxide in the treatment of sepsis. *Am J Physiol Lung Cell Mol Physiol*. 2015;309(12):1387-1393.

16.   Nassour I, Kautza B, Rubin M, et al. Carbon monoxide protects against hemorrhagic shock and resuscitation-induced microcirculatory injury and tissue injury. *Shock*. 2015;43(2):166-171.

17.   Ananthakrishnan R, Li Q, O'Shea KM, et al. Carbon monoxide form of PEGylated hemoglobin protects myocardium against ischemia/reperfusion injury in diabetic and normal mice. *Artif Cells Nanomed Biotechnol*. 2013;41(6):428-436.

18.   Kilkenny C, Browne WJ, Cuthill IC, Emerson M, Altman DG. Improving bioscience research reporting: the ARRIVE guidelines for reporting animal research. *PLoS Biol*. 2010;8(6):e1000412.

10

19.   Guerci P, Ince Y, Heeman P, Faber D, Ergin B, Ince C. A LED-based phosphorimeter for measurement of microcirculatory oxygen pressure. *J Appl Physiol*. 2017;122(2):307-316.

20.   Zijlstra WG, Buursma A. Spectrophotometry of Hemoglobin: Absorption Spectra of Bovine Oxyhemoglobin, Deoxyhemoglobin, Carboxyhemoglobin, and Methemoglobin. *Comparative Biochemistry and Physiology Part B: Biochemistry and Molecular Biology*. 1997;118(4):743-749.

21.   Michelakis ED, Archer SL. The measurement of NO in biological systems using chemiluminescence. *Methods Mol Biol*. 1998;100:111-127.

22.   Takahashi T, Shimizu H, Morimatsu H, et al. Heme Oxygenase-1 is an Essential Cytoprotective Component in Oxidative Tissue Injury Induced by Hemorrhagic Shock. *J Clin Biochem Nutr*. 2009;44(1):28-40.

23.   Stern SA. Low-volume fluid resuscitation for presumed hemorrhagic shock: helpful or harmful? *Curr Opin Crit Care*. 2001;7(6):422-430.

24.   Legrand M, Mik EG, Balestra GM, et al. Fluid resuscitation does not improve renal oxygenation during hemorrhagic shock in rats. *Anesthesiology*. 2010;112(1):119-127.

25.   Aksu U, Bezemer R, Yavuz B, Kandil A, Demirci C, Ince C. Balanced vs unbalanced crystalloid resuscitation in a near-fatal model of hemorrhagic shock and the effects on renal oxygenation, oxidative stress, and inflammation. *Resuscitation*. 2012;83(6):767-773.

26.   Almac E, Aksu U, Bezemer R, et al. The acute effects of acetate-balanced colloid and crystalloid resuscitation on renal oxygenation in a rat model of hemorrhagic shock. *Resuscitation*. 2012;83(9):1166-1172.

27.   Practice guidelines for perioperative blood management: an updated report by the American Society of Anesthesiologists Task Force on Perioperative Blood Management. *Anesthesiology*. 2015;122(2):241-275.

28.   Kozek-Langenecker SA, Ahmed AB, Afshari A, et al. Management of severe perioperative bleeding: guidelines from the European Society of Anaesthesiology: First update 2016. *Eur J Anaesthesiol*. 2017;34(6):332-395.

29.   Silverman TA, Weiskopf RB, Planning Committee and the Speakers. Hemoglobin-based oxygen carriers: current status and future directions. *Anesthesiology*. 2009;111(5):946-963.

30.   Weiskopf RB. Hemoglobin-based oxygen carriers: disclosed history and the way ahead: the relativity of safety. *Anesth Analg*. 2014;119(4):758-760.

31.   Intaglietta M, Cabrales P, Tsai AG. Microvascular perspective of oxygen-carrying and -noncarrying blood substitutes. *Annu Rev Biomed Eng*. 2006;8:289-321.

32.   van Iterson M, Siegemund M, Burhop K, Ince C. Hemoglobin-based oxygen carrier provides heterogeneous microvascular oxygenation in heart and gut after hemorrhage in pigs. *J Trauma*. 2003;55(6):1111-1124.

33.   van Iterson M, Sinaasappel M, Burhop K, Trouwborst A, Ince C. Low-volume resuscitation with a hemoglobin-based oxygen carrier after hemorrhage improves gut microvascular oxygenation in swine. *J Lab Clin Med*. 1998;132(5):421-431.

34.   von Dobschuetz E, Hoffmann T, Messmer K. Diaspirin cross-linked hemoglobin effectively restores pancreatic microcirculatory failure in hemorrhagic shock. *Anesthesiology*. 1999;91(6):1754-1762.

35.   Mackenzie CF, Dubé GP, Pitman A, Zafirelis M. Users Guide to Pitfalls and Lessons Learned about HBOC-201 During Clinical Trials, Expanded Access, and Clinical use in 1,701 Patients. *Shock*. October 2017.

36.   Wahr JA, Gerber M, Venitz J, Baliga N. Allosteric modification of oxygen delivery by hemoglobin. *Anesth Analg*. 2001;92(3):615-620.

37.   Burke TJ, Malhotra D, Shapiro JI. Effects of enhanced oxygen release from hemoglobin by RSR13 in an acute renal failure model. *Kidney Int*. 2001;60(4):1407-1414.

38.   Bolisetty S, Zarjou A, Agarwal A. Heme Oxygenase 1 as a Therapeutic Target in Acute Kidney Injury. *Am J Kidney Dis*. 2017;69(4):531-545.

39.   Vandegriff KD, Young MA, Lohman J, et al. CO-MP4, a polyethylene glycol-conjugated haemoglobin derivative and carbon monoxide carrier that reduces myocardial infarct size in rats. *Br J Pharmacol*. 2008;154(8):1649-1661.

40.   Zhang J, Cao S, Kwansa H, Crafa D, Kibler KK, Koehler RC. Transfusion of hemoglobin-based oxygen carriers in the carboxy state is beneficial during transient focal cerebral ischemia. *J Appl Physiol*. 2012;113(11):1709-1717.

41.   Parrish D, Plant V, Lindell SL, et al. New low-volume resuscitation solutions containing PEG-20k. *J Trauma Acute Care Surg*. 2015;79(1):22-29.

42.   Tran A, Yates J, Lau A, Lampron J, Matar M. Permissive hypotension versus conventional resuscitation strategies in adult trauma patients with hemorrhagic shock: A systematic review and meta-analysis of randomized controlled trials. *J Trauma Acute Care Surg*. 2018;84(5):802.

43.   Nugent WH, Cestero RF, Ward K, Jubin R, Abuchowski A, Song BK. Effects of Sanguinate® on Systemic and Microcirculatory Variables in a Model of Prolonged Hemorrhagic Shock. *Shock*. December 2017.

Supplementary data

Oxygen binding capacity

10

The oxygen binding/carrying capacity of polyethylene glycolated (PEGylated)-carboxyhemoglobin was determined at 37°C under normal atmosphere similarly to the methodology described elsewhere.[1,2] Briefly, PEGylated-carboxyhemoglobin (40 mg.ml^{-1}) was diluted in its own buffer (pH 7.38 - 7.40) for a final concentration of 4.0 mg.ml^{-1}. A fiber optic oxygen micro sensor using luminescence lifetime (MiniTip, Oxy Micro, World Precision Instruments, FL, USA) was used for the determination of oxygen concentration and was calibrated by a simple two-point calibration, 100% air-saturation and 0% air saturation (dithionite) with barometric pressure and temperature adjustment according to the manufacturer's recommendations. The fiber optic was placed in a double jacked thermostated

(37°C) small cuvette through a dedicated hole (side) and sealed with a rubber. Two milliliters and a half (2.5 ml) of the solution were placed in the cuvette, continuously stirred with a magnetic bar and allowed to equilibrate to room air before being hermetically sealed. The concentration of oxygen (μmol.l^{-1}) in the medium was continuously recorded. After stabilization of the oxygen concentration in the cuvette, 10 μL $K_3Fe(CN)_6$ 1M (kept at 37°C in a thermostated bath and equilibrated at room air) was added through the rubber with a precise syringe. The release of bound-oxygen due to the conversion of oxy- to met-Hb was monitored.

The oxygen binding/carrying capacity was calculated as follows:

$$\Delta n_{O_2 released} = n_{O_2\ initial} - n_{O_2\ final} = C_{O_2\ initial}\ x\ V_{initial} - C_{O_2\ final}\ x\ V_{final} \qquad \text{Eq. 1}$$

where n is the number of moles of O_2 (mol), C is the concentration of O_2 provided by the fiber optic sensor (mol.L-1) and V is the volume in the cuvette before (initial) and after (final) adding $K_3Fe(CN)_6$.

$$V_{O_2} = \Delta n_{O_2 released}\ x\ V_m \qquad \text{Eq. 2}$$

where V_{O_2} (L) represents the volume of oxygen released in the cuvette and V_m the molar volume (L.mol^{-1}) which is 25.45 L.mol^{-1} at 37°C (310.15°K) and under 1 atm (ideal gas law).

$$Oxygen\ content\ concentration = \frac{V_{O_2}}{V_{final}}\ x\ 10^3 \qquad \text{Eq. 3}$$

where the oxygen content concentration (ml O_2.L^{-1}) represents the volume of oxygen dissolved in the cuvette

$$Measured\ oxyen\ carrying\ capacity = \frac{oxygen\ content\ concentration}{C_{Hb\ final}} \qquad \text{Eq. 4}$$

where oxygen carrying capacity is expressed in mL O_2.g^{-1} Hb and $C_{Hb\ final}$ is the final concentration of hemoglobin/HBOC (g.L^{-1}) in the cuvette.

The difference between the solubility coefficients of oxygen in PEGylated-carboxyhemoglobin +buffer and $K_3Fe(CN)_6$ has been neglected.

Spectrophotometric analysis of PEGylated-carboxyhemoglobin and derivatives

The observed total absorption spectrum of each plasma sample was then compared to the known spectra of the different derivatives of bovine hemoglobin with their absorptivities.[3] With the use of the classical least squares method (mixture of 4 components and at 150 wavelengths), the different concentrations of each component were recovered. We used the methodology proposed by Prof. Tom O'Haver (https://terpconnect.umd.edu/~toh/spectrum), to recover the concentration of each component after entering the 4 known spectra of bovine hemoglobin: oxy-Hb, deoxy-Hb, met-Hb and carboxy-Hb. However, the met-Hb could not be accurately determined due to a possible interference with Pd-TCCP. The original spectra of PEGylated-carboxyhemoglobin were provided by Prolong Pharmaceuticals and were found to perfectly match with the bovine hemoglobin spectra found in the publication of Zijlstra *et al.*[3]

The oxygen saturation of PEGylated-carboxyhemoglobin was determined as follows:

$$S_{\text{PEGylated-carboxyhemoglobin}}O_2(\%) = \frac{C_{oxy-\text{PEGylated-carboxyhemoglobin}}}{(C_{oxy-\text{PEGylated-carboxyhemoglobin}} + C_{deoxy-\text{PEGylated-carboxyhemoglobin}})}$$

Immunohistochemical analysis and histology

Kidney sections (4 µm) were deparaffinized with xylene and rehydrated with decreasing percentages of ethanol and finally with water. Antigen retrieval was accomplished by microwaving slides in citrate buffer (pH 6.0) (Thermo Scientific, AP-9003-500) for 10 min. Slides were left to cool for 20 min at room temperature and then rinsed with distilled water. Surroundings of the sections were marked with a PAP pen. The endogenous peroxidase activity was blocked with 3% H_2O_2 for 10 min at room temperature and later rinsed with distilled water and PBS. Blocking reagent (Lab Vision, TA-125-UB) was applied to each slide followed by 10 min incubation at room temperature in a humid chamber. Kidney sections were incubated for overnight at 4°C with rabbit polyclonal Tumor Necrosis Factor-α (1:100) (abcam 6671) and incubated for 1 h at room temperature with Lipocalin 2 antibody (Neutrophil Gelatinase-Associated Lipocalin, 1/150) (abcam 41105). Antibodies were diluted in a large volume of UltrAb Diluent (Thermo Scientific, TA-125-UD). The sections were washed in PBS three times for 5 min each time and then incubated for 30 min at room temperature with biotinylated goat anti-rabbit antibodies (LabVision, TP-125-BN). After slides were washed in PBS, the streptavidin peroxidase label reagent (LabVision, TS-125-HR) was applied for 30 min at room temperature in a humid

chamber. The colored product was developed by incubation with AEC. The slides were counterstained with Mayer's hematoxylin (LabVision, TA-125-MH) and mounted in vision mount (LabVision, TA-060-UG) after being washed in distilled water. Both the intensity and the distribution of specific Tumor Necrosis Factor-α and Neutrophil Gelatinase-Associated Lipocalin staining were scored. For each sample, a histological score (H-Score) value was derived by summing the percentages of cells that stained at each intensity multiplied by the weighted intensity of the staining [H-Score = S Pi (i+1), where i is the intensity score and Pi is the corresponding percentage of the cells] (Birman et al, 2012) under a light microscope at x400 magnification. Kidney sections were photographed using Leica Qwin microscope.

The kidney sections were stained with periodic acid-schiff reagent (PAS) and hematoxyline. Histologic changes in the cortex were assessed by quantitative measurements of tissue damage. Tubular damage was defined as loss of brush border, vacuolar degeneration, cast formation, and invagination. The degree of kidney damage was estimated at 400x magnification using 10 randomly selected fields for each animal by the following criteria: 0, normal; 1, areas of damage <10% of tubules; 2, damage involving 10% to 25% of tubules; 3, damage involving 25% to 50% of tubules; 4, damage involving 50% to 75% of tubules; 5, damage more than 75% of tubules. A minimum of 40 tubules were examined per group, with n=6/kidney per animal minimum.

References

1.   Tucker VA: Method for oxygen content and dissociation curves on microliter blood samples. J Appl Physiol 1967; 23:410–4
2.   Dijkhuizen P, Buursma A, Fongers TM, Gerding AM, Oeseburg B, Zijlstra WG: The oxygen binding capacity of human haemoglobin. Hüfner's factor redetermined. Pflugers Arch 1977; 369:223–31
3.   Zijlstra WG, Buursma A: Spectrophotometry of Hemoglobin: Absorption Spectra of Bovine Oxyhemoglobin, Deoxyhemoglobin, Carboxyhemoglobin, and Methemoglobin. Comparative Biochemistry and Physiology Part B: Biochemistry and Molecular Biology 1997; 118:743–9

10

11

Resuscitation with pegylated-carboxyhemoglobin preserves the renal function and tissue oxygenation during endotoxemia

Philippe Guerci*,[1,2,3] Bulent Ergin*,[1,5] Aysegul Kapucu,[4]

Yasin Ince,[1,5] Matthias Hilty,[1] Jan Bakker,[5] Can Ince,[1,5]

1. Department of Translational Physiology, Academic Medical Center, University of Amsterdam, Amsterdam, The Netherlands
2. INSERM U1116, University of Lorraine, Vandoeuvre-Les-Nancy, France
3. Department of Anesthesiology and Critical Care Medicine, University Hospital of Nancy, France
4. Department of Biology, Faculty of Science, University of Istanbul, Istanbul, Turkey
5. Department of Intensive Care Medicine, Erasmus MC, University Medical Center, Rotterdam, Rotterdam, The Netherlands

*Guerci P and Ergin B contributed equally to this manuscript

Abstract

Background: Options for fluid therapy in septic shock are limited and hemoglobin-based oxygen carriers have been barely investigated. We hypothesized that PEGylated-carboxyhemoglobin (PEGHbCO), which has carbon monoxide-releasing molecules, plasma expansion and oxygen-carrying properties, would improve both renal cortical microcirculatory PO_2 ($C\mu PO_2$) and skeletal microcirculatory flow thereby limiting sepsis-induced acute kidney injury (AKI) in a rat model of endotoxemia.

Methods: Anesthetized and ventilated rats (n=44) were subjected to an endotoxemic shock following lipopolysaccharide (LPS) infusion. $C\mu PO_2$ was measured in exposed kidneys using a phosphorescence-quenching method. Rats were randomly assigned to 5 groups: (1) unresuscitated LPS, (2) ringer's acetate (LPS+RA), (3) LPS+RA+norepinephrine (NE) ($0.5\mu g.kg^{-1}min^{-1}$), (4) LPS+RA+PEGHbCO ($320mg.kg^{-1}$), (5) LPS+RA+PEGHbCO+NE. The total volume of resuscitation administered was $30ml.kg^{-1}$ in each group. Animals were compared to a time control group. Skeletal muscle microcirculation was assessed by handheld intravital microscopy. Kidney immunohistochemistry (NGAL, TNF-α, IL-6, iNOS, eNOS), and myeloperoxidase-stained leukocytes in glomerulus and peritubular areas were analyzed. Sepsis-induced histological damages were assessed. Finally, plasma levels of IL-6, heme oxygenase-1, malondialdehyde, and syndecan-1 were assessed by ELISA.

Results: $C\mu PO_2$ was higher in groups resuscitated with PEGHbCO, 36±6 mmHg (mean diff. -13.53, 95%CI[-26.35; -0.7156], P=0.035) and 37±10 mmHg (-14.3, 95%CI[-27.12; -1.482], P=0.023), for LPS+RA+PEGHbCO and LPS+RA+PEGHbCO+NE respectively, compared to 23±12mmHg for LPS+RA. PEGHbCO, reduced the number of non-flowing, intermittent or sluggish capillaries compared to resuscitation with RA alone (P<0.05) while increasing the number of normally perfused vessels (P<0.05). Sepsis-induced kidney immunohistochemistry and histological alterations were not mitigated by PEGHbCO 1h after resuscitation. Renal leukocyte infiltration and plasma levels of IL-6, heme oxygenase-1, malondialdehyde, and syndecan-1 were similar across groups.

Conclusions: PEGHbCO enhanced renal $C\mu PO_2$ while restoring skeletal muscle microcirculatory flow in previously non-flowing capillaries in an endotoxemia model. The addition of NE did not further improve renal $C\mu PO_2$. PEGHbCO did not mitigate short term sepsis-induced AKI.

Keywords: acute kidney injury, PEGylated carboxyhemoglobin, carbon monoxide, hemoglobin-based oxygen carrier, renal injury, sepsis

Introduction

Sepsis and septic shock induce major microcirculatory disorders that are not appropriately corrected by fluid resuscitation.[1–3] Previous studies demonstrated that endotoxemia has also been associated with impaired ability to increase oxygen extraction, even in the presence of normal or elevated cardiac output and systemic oxygen delivery.[4] This is mainly attributed to heterogeneity in the microcirculation with the presence of plugged vessels (Type I) and/or increase in the diffusive distance (Type II) and reduced ability of the oxygen to reach the tissue cells.[3]

The beneficial effects of blood transfusion in a murine model of endotoxemia in restoring oxygen pressures in the kidney – which is one of the most sensitive organ to injury during sepsis – have been previously demonstrated.[5] However, blood transfusion may not be readily available during fluid resuscitation and it is possible that a small increase in the local delivery of oxygen would maintain the microvascular oxygen tension. Furthermore, pragmatic human clinical trial failed to demonstrate a benefit of red blood cell transfusion in septic shock.[6] Therefore, the concept of a "pink fluid resuscitation" emerged, combining the effects of fluid resuscitation to improve systemic hemodynamics associated to increased O_2 carrying capacity in the aim of delivering more oxygen locally and anti-inflammatory modulation activity.

PEGylated-carboxyhemoglobin (PEGHbCO, Sanguinate®, Prolong Pharmaceuticals, NJ, USA) is an novel hemoglobin-based oxygen carrier (HBOC).[1] The interest of this molecule resides in the carbon monoxide (CO) molecules it embeds. CO is believed to have two main effects at a low concentration in the blood: (i) an anti-inflammatory modulation function,[2] and (ii) a vasoactive, namely vasodilation function in the microcirculation.[3] These characteristics may be of utmost importance to restore an altered microcirculatory flow such as it occurs in septic shock. While using PEGHbCO the arterial oxygen content and delivery to tissue should increase, and especially where only plasma can flow because of plugged red blood cells in vessels.

We hypothesized that PEGHbCO would: (i) decrease the risk of sepsis-induced acute kidney injury (AKI), by sustaining renal cortical microcirculatory PO_2 (CµPO2) and downregulating

11

inflammatory biomarkers in the kidney, and (ii) mitigate sepsis-induced skeletal muscle microcirculatory alterations. We sought to compare different resuscitation strategies in a rat model of endotoxemia-induced septic shock using balanced crystalloid, PEGHbCO with and without additional infusion of norepinephrine. The primary outcome measure was the $C\mu PO_2$. Secondary outcomes were the percentage of flowing capillaries, the biomarkers of inflammation and the histopathological damages of acute kidney injury.

Material and methods

Animals

The Animal Research Committee of the Academic Medical Centre of the University of Amsterdam approved all experiments in this study (DFL103073). Care and handling of the animals were performed in accordance with the guidelines from the Institutional and Animal Care and Use Committees. This study and the following reporting adhere to the applicable ARRIVE guidelines. All experiments were performed at 09:00am (weekdays) at the Department of Experimental Surgery, University Medical Center, Amsterdam, The Netherlands. Male Wistar-Albinos rats (Charles River, The Netherlands), aged 12±3 weeks with a mean±SD body weight of 384±41 g were included.

Surgical intervention and experimental model of endotoxemia

The complete anesthesia protocol, surgical intervention with cannulas insertion, and exposition of the left kidney are described in detail in the **supplemental document**. Our group previously published several articles using these techniques.[5,7,8] The right biceps femoris was exposed. To prevent muscle desiccation, the exposed area was protected with a humidified gauze with warm 0.9% NaCl. The animals rested for 30 min after completion of surgery (~1 h).

The experimental protocol is presented in **Figure 1**. Following surgery, the rats underwent a stabilization period (*Baseline*). Endotoxemia was induced by lipopolysaccharide (LPS) (serotype 0127:B8) (Sigma-Aldrich Corporation, St Louis, MO, USA); 25 mg.kg⁻1 intravenously over 30 min followed by a cessation period until mean arterial pressure (MAP) of 40 mmHg is reached (~2 to 3h) (*Shock*).
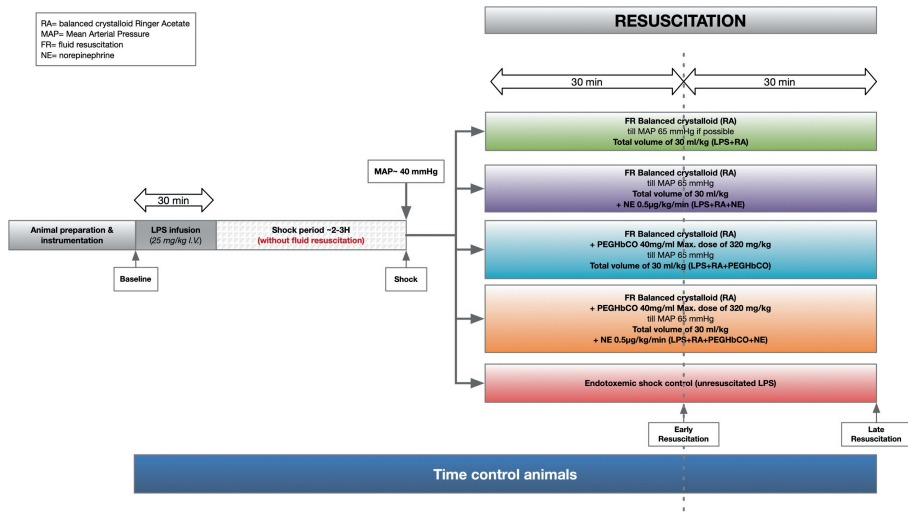
Figure 1. Time course of the endotoxemia experiment

FR: fluid resuscitation, MAP: mean arterial blood pressure, NE: norepinephrine, PEGHbCO: PEGylated-carboxyhemoglobin, RA: ringer's acetate

The animals were randomized, according to a unique code that was generated by an internet website (Sealed Envelope Ltd. 2016. Simple randomization service. [Online] Available from https://www.sealedenvelope.com/simple-randomiser/v1/), into 6 groups: balanced crystalloid solution (Ringer's acetate (RA); Fresenius Kabi., Schelle, Belgium) (max. volume of 30 ml.kg^{-1}) (LPS+RA), (2) RA 30 ml.kg^{-1} plus a fixed infusion of norepinephrine (NE) of 0.5 µg.kg^{-1}.min^{-1} (LPS+RA+NE), (3) PEGHbCO (40mg.ml^{-1}) with a maximum dosage of 320 mg.kg^{-1} in addition to RA for total volume of 30 ml.kg^{-1} (LPS+RA+PEGHbCO), (4) PEGHbCO (40mg.ml^{-1}) with a maximum dosage of 320 mg.kg^{-1} in addition to RA for total volume of 30 ml.kg^{-1} plus NE at a dosage of 0.5 µg.kg^{-1}.min^{-1} (LPS+RA+PEGHbCO+NE), (5) time-control group (surgery only), and (6) non-resuscitated endotoxemia shock group (LPS). A MAP (greater than 65 mmHg) was targeted in accordance with the Surviving Sepsis Campaign guidelines. A fixed dose of NE could however overshoot the targeted MAP.

A technician prepared the resuscitation fluid according to the generated code on the day of the experiment. The investigator performing the experiments was partially blinded to group assignment or treatment. Control and non-resuscitated endotoxemia groups received no

11

additional fluids except anesthesia maintenance. Another investigator who was blinded to the type of randomization performed the data analyses.

Microcirculatory renal cortical oxygen tension (CμPO$_2$)

An optical fiber with a tip diameter of 5 mm was placed ~1 mm above the exposed kidney to measure microcirculatory oxygenation using a phosphorescence lifetime technique as described elsewhere.[7] We excluded any interference between Palladium(II)-meso-tetra(4-carboxyphenyl)-porphyrin (Pd-TCCP) and PEGHbCO (*in vitro*) prior to the *in vivo* experiment.

Kidney function

Plasma creatinine and urine creatinine were measured using an automatic analyzer (c702 Roche Diagnostics, Roche Diagnostics, Basel, Switzerland). We established a calibration curve for creatinine levels prior to measurements to correct for a significant interference due to the presence of PEGylated-carboxyhemoglobin. The glomerular filtration rate was estimated at the end of the experiment using the measurement of creatinine clearance (Cl$_{crea}$): Cl$_{crea}$=(U$_{Crea}$ x V)/(time x P$_{Crea}$) where UCrea is the concentration of creatinine in urine (mmol.l-1), V is the urine volume (ml) per unit time of urine collection and PCrea is the concentration of creatinine in plasma (mmol.l-1). The renal oxygen delivery (DO$_2$) and consumption (VO$_2$) were determined as explained in the **supplemental document**.

Skeletal muscle microcirculation analysis

A hand-held in vivo microscope using incident dark-field (IDF) imaging, CytoCam™ (Braedius Scientific, Huizen, The Netherlands) was placed on the surface of the exposed biceps femoris to continuously monitor the same microcirculatory spot with the help of a micromanipulator. One hundred frames clips (100 sec) were recorded at every time point. All clips obtained were randomly anonymized and analyzed in a blinded fashion (group and time point). Only vessels with a diameter <20μm were considered. The analysis of the microvasculature was performed at baseline and at each timepoint of sepsis with AVA 3.2 (Microvision Medical, Amsterdam, The Netherlands) for the percentage of non-, intermittent, sluggish and continuously flowing capillaries of the total vessel length by 3 trained operators and experts (Y.I, P.G and M. H.).

Immunohistochemical analysis and histology of the kidney

The complete methods of immunohistochemistry and histology analyses is provided in the **supplemental document**. Briefly, a histological score (HSCORE) value was derived by summing the percentages of cells that stained at each intensity multiplied by the weighted intensity of the staining [HSCORE = S Pi (i+1), where i is the intensity score and Pi is the corresponding percentage of the cells]. We evaluated myeloperoxidase (MPO) reaction in the glomerulus from 300 selected glomeruli and in 300 selected peritubular areas under a light microscope at a magnification X400. We scored 1 if leukocytes could be seen in the glomerulus and 0 if not.

Kidney histological damages were assessed by kidney injury scores defined in the **supplemental document** and graded on a scale of 0 to 3. The degree of damage was defined as follows: 0-normal (0-5%); 1-Mild (5-25%); 2-Moderate (25–75%); 3-Severe (>75%).

Plasma nitric oxide, heme oxygenase-1 and biomarkers of inflammation

Plasma NO levels were measured by chemiluminescence as previously described.[9] Heme-oxygenase 1 (HO-1) constitutes an essential cytoprotective component that ameliorates hemorrhagic shock-induced oxidative tissue injuries. Plasma HO-1 levels were measured at the end of the experiment using an ELISA kit based on the sandwich assay principle (Rat HMOX1 / HO-1 ELISA Kit (Sandwich ELISA) - LS-F4085, LSBio LifeSpan BioSciences Inc., Seattle, WA, USA).

Plasma IL-6 (Rat IL-6 Elisa, R&D systems, Mineapolis, MN, USA), malondialdehyde (MDA Elisa Kit, MyBiosource, Bio-Connect B.V., The Netherlands) and syndecan-1 (Rat Syndecan-1/CD138(SDC1) ELISA Kit Cusabio, Bio Connect, The Netherlands) were measured in the plasma.

Statistical analysis

Values are expressed as mean±SD when normally distributed (Kolmogorov-Smirnov test), or as median [IQR] otherwise. Repeated measures 2-way analysis of variance (RM-ANOVA) (2 factors: time as a related within-animal factor and group as a between-animal factor) with post hoc Bonferroni's correction test for multiple analysis were used to determine intergroup and/or intragroup differences of hemodynamics, CµPO2, and biochemical data. When significant interaction was observed between time and group, we reported simple main effects of group (type of fluid) compared to the control and to the RA groups at each timepoint and the simple

11

main effect of time versus baseline within the same group. Ordinary one-way ANOVA with Bonferroni's correction was used for renal DO_2 or VO_2, plasma biomarkers (IL-6, Heme-oxygenase-1, NO, MDA). Because of their non-gaussian distribution, the analyses of creatinine clearance, urine output, immunohistochemistry (NGAL, TNF-α, iNOS, eNOS, MPO) were performed using a Kruskal-Wallis test with Dunn's correction test. For comparison of microcirculatory parameters between baseline, septic shock and resuscitation time-points, as well as between different resuscitation solutions, two-way linear mixed effects model analysis was used. As independent variable fixed effects induction of septic shock and resuscitation, as well as type of resuscitation solution, were entered into the model without interaction terms. As random effects, intercepts for subjects as well as per-subject random slopes for the effect on dependent variables were employed. P values for individual fixed effects were obtained by two-sided Satterthwaite approximation. For subgroups analysis, where a statistically significant effect was detected, a one-way linear mixed effect model was applied. The overall significance level for each hypothesis was 0.05. Adjusted P-values were reported throughout the manuscript in post hoc tests. Statistical analysis was performed using GraphPad Prism version 8.1.0 for Mac (GraphPad Software, La Jolla, USA).

Based on previous results obtained in a similar model,[5,8] we assumed that microcirculatory PO_2 in the kidney would be of 25±6 mmHg at 1h after establishment of the septic shock. Thus, to detect a 40% increase in kidney microcirculatory PO_2 associated with the administration of PEGHbCO, a sample size of n=7/group will provide a power (1-β) of 90% with a type I error rate (α) of 5%.

Results

A total of 44 animals were included in the present study (n=6-8/group). The groups resuscitated with PEGHbCO included 8 animals. Four extra animals helped to determine the dosage for LPS infusion. No animal died during the experiment. The time course of the macrohemodynamics changes throughout the experiment are presented in **Table 1**. Infusion of LPS induced endotoxemia with associated septic shock (MAP ~40 mmHg with a significant increase in lactate levels (**Table 1**)). Septic shock induced a metabolic acidosis (P<0.001) parallel to a decrease in MAP and RBF.

Table 1. Systemic and renal hemodynamics, acid-base balance and arterial lactate levels during experiment

|	BL	Shock	Early Res.	Late Res.
MAP (mmHg)				
Control	93±8	94±20	88±15	79±9
Unresuscitated LPS	87±5	42±4*	39±5*	38±8*
LPS+RA	93±6	40±2*	43±9*	45±7*
LPS+RA+NE	88±5	41±2*	86±15#	76±13#
LPS+RA+PEGHbCO	90±9	42±5*	61±13*#	65±13#
LPS+RA+PEGHbCO+NE	87±5	39±1*	98±17#	97±21*#
CVP (mmHg)				
Control	6±1	8±1	8±1	8±1
Unresuscitated LPS	6±1	9±1	9±1	9±2
LPS+RA	6±1	8±1	9±1	9±1
LPS+RA+NE	6±1	8±1	8±1	8±1
LPS+RA+PEGHbCO	7±1	9±1	10±1*	11±2*#
LPS+RA+PEGHbCO+NE	6±1	8±1	9±1	9±1
RBF (mL.min^{-1})				
Control	10±2	9±1	9±1	8±1
Unresuscitated LPS	11±1	4±2*	3±1*	3±1*
LPS+RA	11±3	3±1*	4±1*	3±0*
LPS+RA+NE	9±3	3±2*	4±2*	4±2*
LPS+RA+PEGHbCO	9±2	2±1*	3±1*	4±1*
LPS+RA+PEGHbCO+NE	10±1	3±0*	5±1*	6±2
pH				
Control	7.43±0.02	7.38±0.05	7.38±0.02	7.40±0.03
Unresuscitated LPS	7.44±0.04	7.21±0.04*	7.20±0.02*	7.22±0.03*
LPS+RA	7.43±0.02	7.23±0.04*	7.21±0.04*	7.24±0.03*
LPS+RA+NE	7.41±0.03	7.24±0.04*	7.25±0.05*	7.27±0.05*
LPS+RA+PEGHbCO	7.45±0.02	7.23±0.02*	7.25±0.03*	7.30±0.04*
LPS+RA+PEGHbCO+NE	7.46±0.02	7.24±0.05*	7.27±0.06*#	7.33±0.06*#
HCO$_3^-$ (mmol.l^{-1})				
Control	20.0±0.6	21.0±1.9	21.5±2.1	20.2±2.3
Unresuscitated LPS	19.6±0.5	13.3±1.2*	14.1±1.3*	12.8±1.2*
LPS+RA	21.5±1.5	12.1±2.0*	13.9±1.4*	13.5±1.8*
LPS+RA+NE	20.6±2.0	13.3±1.3*	15.0±1.9*	14.7±2.1*
LPS+RA+PEGHbCO	20.0±1.4	13.1±1.5*	15.1±0.8*	16.9±0.7*#
LPS+RA+PEGHbCO+NE	21.4±1.2	13.6±0.8*	16.2±1.4*#	16.5±1.3*#
Lactate$^-$ (mmol.l^{-1})				
Control	0.9±0.1	1.4±0.4	1.4±0.3	1.6±0.3
Unresuscitated LPS	1.0±0.3	2.3±0.3*	2.6±0.6*	3.0±0.2*
LPS+RA	0.9±0.2	3.5±1.0*	4.1±1.6*	4.0±1.7*
LPS+RA+NE	1.0±0.2	2.4±0.4*#	2.0±0.3#	2.4±0.7#
LPS+RA+PEGHbCO	1.1±0.2	3.2±0.8*	3.2±0.6*	2.6±0.3*#
LPS+RA+PEGHbCO+NE	1.1±0.1	3.0±0.7*	2.0±0.4#	2.3±0.7#

MAP: Mean Arterial Pressure, RBF: Renal Blood Flow, CVP: Central Venous Pressure, NE: norepinephrine. Repeated measures 2-way ANOVA test used with Bonferroni's correction to adjust for multiple comparisons. * adjusted P<0.01 vs. Control group at the same time point, # adjusted P<0.05# vs. LPS+RA group at the same time point.

During the resuscitation period, the MAP was restored to 65 mmHg or above in the LPS+RA+PEGHbCO, LPS+RA+NE, LPS+RA+PEGHbCO+NE groups but not in the LPS+RA group (P<0.001). Similarly, the LPS+RA group presented the highest lactate level at the end of the

experiment (P<0.05) (**Table 1**). Interestingly, the addition of NE did not improve further pH, HCO_3^- or lactate levels compared to LPS+RS alone.

Renal function and urine output (**Supplemental Figure 1**)

The plasma creatinine was markedly increased in the non-resuscitated LPS group compared to control (101 [94-103] vs. 42 [23-75] $\mu mol.l^{-1}$, mean rank diff. -27.08, P<0.0001). Creatine clearance was significantly lower in the LPS+RA and LPS+RA+PEGHbCO+NE groups, 0 [0-0.03] and 0.22 [0.07-0.36] $ml.min^{-1}$ respectively, than in controls, 0.74 [0.55-1.80] $ml.min^{-1}$ (mean rank diff. 21.21, P<0.0001 and 14.33, P=0.025 respectively). Although MAP was greater in groups where NE was infused, creatinine clearance was not different than in the LPS+RA+PEGHbCO group.
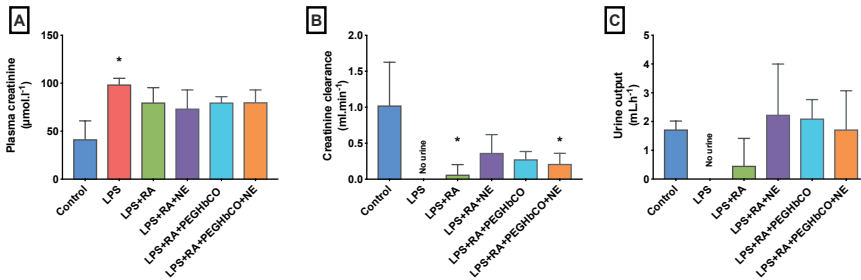
Supplemental Figure 1. Renal function and urine output at the end of endotoxemia. Panel A, Plasma creatinine levels. Panel B, Creatinine clearance measured using urine output during the last hour after start of resuscitation. Panel C, Urine output measured 15 minutes before the end of experiment

*Values are presented as mean±SD. Kruskal-Wallis test used with Dunn's correction to adjust for multiple comparisons. * adjusted P<0.05 vs. Control group*

Renal cortical microcirculatory PO2 and renal oxygen delivery and consumption

Figure 2 depicts the time course of $C\mu PO_2$ in the kidney throughout the experiment. The $C\mu PO_2$ decreased after induction of septic shock in all groups (P<0.0001). At the early phase of fluid resuscitation, only the LPS+RA+PEGHbCO+NE group exhibited a significantly higher $C\mu PO_2$

compared to LPS+RA alone (P=0.02). At a later timepoint, CμPO$_2$ was higher in groups resuscitated with PEGHbCO, 36±6 mmHg (mean diff. -13.53, 95%CI[-26.35; -0.7156], P=0.035) and 37±10 mmHg (-14.3, 95%CI[-27.12; -1.482], P=0.023), for LPS+RA+PEGHbCO and LPS+RA+PEGHbCO+NE respectively, compared to 23±12mmHg for LPS+RA.
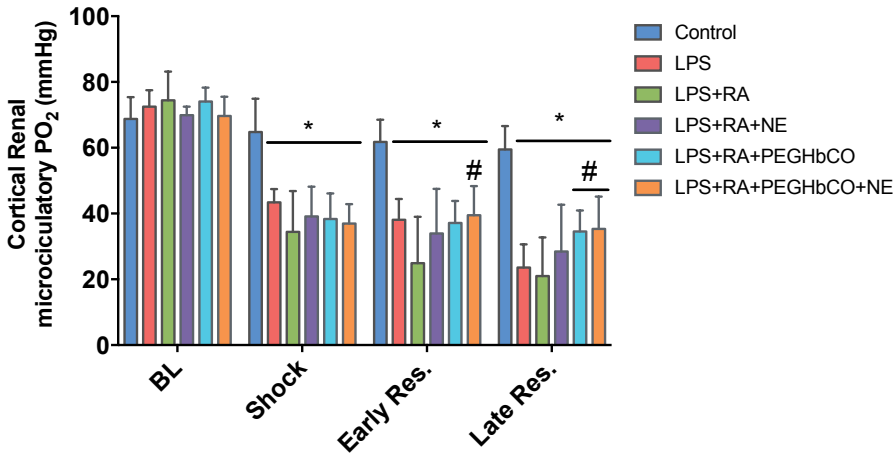

Figure 2. Time course of renal cortical microcirculatory PO$_2$

LPS: non-resuscitated LPS infused group, LPS+RA: resuscitated with ringer's acetate (total volume of 30 ml.kg^{-1}), LPS+RA+NE: resuscitated with ringer's acetate (total volume of 30 ml.kg^{-1}) plus norepinephrine at a fixed dose of 0.5 µg.kg.$^{-1}$min^{-1}, LPS+RA+S: resuscitated with ringer's acetate + PEGHbCO (max 320 mg.kg^{-1}) for a total volume of 30 ml.kg^{-1}, LPS+RA+S+NE: resuscitated with ringer's acetate + PEGHbCO (max 320 mg.kg^{-1}) for a total volume of 30 ml.kg^{-1} plus norepinephrine at a fixed dose of 0.5 µg.kg.$^{-1}$min^{-1}. Repeated measures 2-way ANOVA test used with Bonferroni's correction to adjust for multiple comparisons. * denotes adjusted P<0.05 compared to control group, # adjusted P<0.05 compared to LPS+RA group

The renal oxygen delivery (Renal DO$_2$), consumption (Renal VO$_2$) and the renal energy efficiency for sodium transport (VO$_2$/TNa$^+$) at the end of the experiment are presented in **Supplemental Figure 2**. Renal VO$_2$ was significantly higher in non-resuscitated LPS and LPS+RA groups compared to controls (mean diff. -0.501 95% CI [-0.750 to -0.252], P=0.0001 and -0.345 95% CI [-0.59 to -0.096], P=0.004 respectively). However, the renal DO$_2$ was similarly decreased in all groups compared to the time control group (F(5, 34) = 9.045, P<0.0001). Fluid resuscitation with either PEGHbCO or RA combined or not to NE infusion did not improve renal DO$_2$.

11
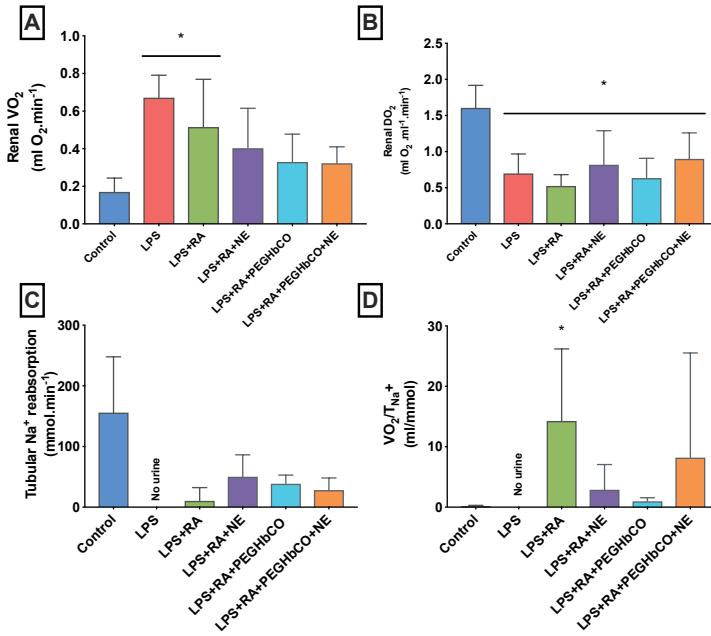
Supplemental Figure 2. Renal oxygen delivery and consumption

*One-way ANOVA test was used with Bonferroni's correction to adjust for multiple comparisons. * adjusted P<0.05 vs. Control group*

LPS: lipopolysaccharide, RA: ringer's acetate, PEGHbCO: pegylated-carboxyhemoglobin, NE: norepinephrine

Effects of fluid resuscitation on the muscle microcirculation

The **Figure 3** depicts the time course of the muscle microcirculation before and after fluid resuscitation. At shock, the number of continuously perfused vessels markedly decreased (P<.0001) whereas there was a proportional increase in the proportion of non-flowing, intermittent or sluggish capillaries (P<.001).

In non-resuscitated LPS animals, there was an increased number of non-flowing capillaries at the late time point (P<0.01) compared to controls. Resuscitation with PEGHbCO, significantly reduced the number of non-flowing, intermittent or sluggish capillaries compared to resuscitation with RA alone (P<0.05) while increasing the number of normally perfused vessels (P<0.05). However, addition of NE to PEGHbCO did not provide an overall better microcirculatory

flow. These results suggest that resuscitation with PEGHbCO can help sparing norepinephrine use while maintaining an adequate microcirculatory flow.
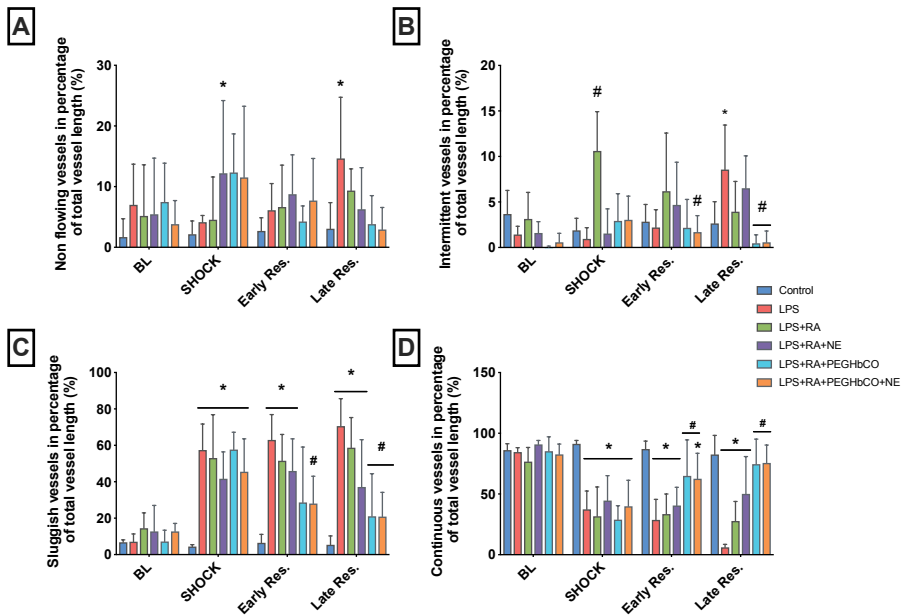

Figure 3. Representative proportion of capillaries graded (per vessel) according to their microvascular flow index (MFI)

* denotes adjusted P<0.05 compared to control group, # P<0.05 compared to LPS+RA grou

Biomarkers of injury

Figure 4 depicts the different plasma biomarkers of injury. Endotoxemia induced an increase in IL-6 ($F_{(6, 33)}$ = 53.34, P<0.0001) and plasma nitric oxide ($F_{(6, 92)}$ = 4.181, P=0.0009) compared to controls. No differences were noted between the different strategies of fluid resuscitation. None dampened the inflammation nor limited the production of nitric oxide. Syndecan-1 levels were increased in all groups at the end of the experiment irrespective of the fluid used compared to the control group ($F_{(5, 29)}$ = 22.12, P<0.0001). Although PEGHbCO can interfere in the metabolism of HO-1, its plasma level was not altered.

11
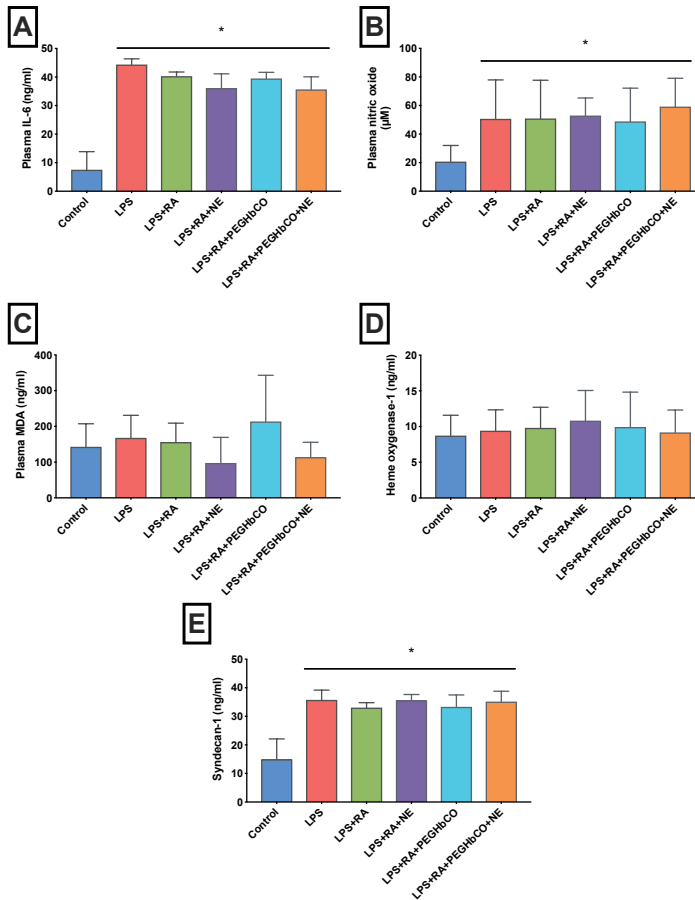
Figure 4. Plasma biomarkers of injury at the end of resuscitation following endotoxemia. Panel A, plasma interleukin-6 (IL-6). Panel B, plasma heme oxygenase-1. Panel C, plasma malondialdehyde. Panel D, total nitric oxide content released in the plasma. Panel E, plasma syndecan-1 levels reflecting injury to glycocalyx and vascular endothelial barrier.

*One-way ANOVA test was used with Bonferroni's correction to adjust for multiple comparisons. * adjusted P<0.05 vs. Control group.*

Immunohistochemical markers of damage to the kidney

The immunostaining intensities (HSCORE) of iNOS, eNOS, NGAL, IL-6, and TNF-α in the kidney cortex are presented in the **Figure 5**. NGAL, iNOS, TNF-α, and IL-6 were significantly upregulated in the LPS-treated and LPS resuscitated groups compared to control group (p<0.001). On the contrary, eNOS reaction was downregulated in the non-resuscitated LPS group only compared to controls (mean diff. 54.76, 95%CI [16.61 to 92.91], P=0.0014). The reaction was seen mostly in the proximal tubules and endothelial cells in the kidney cortex. The damages to the kidney were not mitigated by PEGHbCO nor by the addition of NE at least one hour after the start of resuscitation.
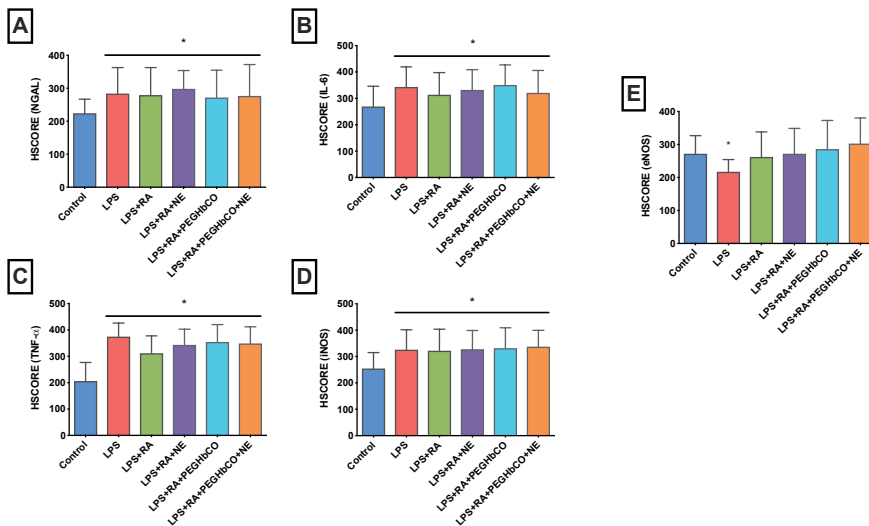
Figure 5. Immunohistochemical markers of renal tissue damage at the end of experiment

*One-way ANOVA test was used with Bonferroni's correction to adjust for multiple comparisons. * adjusted P<0.0001 vs. Control group.*

MPO-stained leukocytes increased both in the glomerulus and in peritubular areas after LPS stimulation compared to controls (mean rank diff. -159, P<0.0001 and -216, P<0.0001 respectively). Similarly, the number of MPO-stained leukocytes increased in LPS resuscitated groups irrespective of the strategy of resuscitation used (**Supplemental Figure 3**).
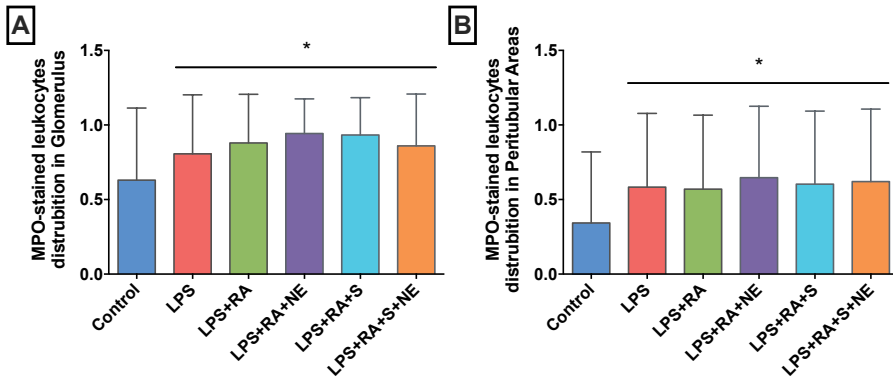
Supplemental Figure 3. Myeloperoxidase (MPO)-stained leukocytes in the glomerulus (A) and in peritubular areas (B)

*Kruskal-Wallis test was used with Dunn's correction to adjust for multiple comparisons. * adjusted P<0.01 vs. Control group (n=300/group)*

Histological alterations following sepsis-induced acute kidney injury

Histological signs of acute kidney injury (**Supplemental Figure 4**) were markedly present in the LPS group in comparison to control group (mean rank diff. -168.4, P<0.0004). Interestingly, the groups resuscitated with additional NE, exhibited also a higher kidney injury score than groups that did not compared to controls.
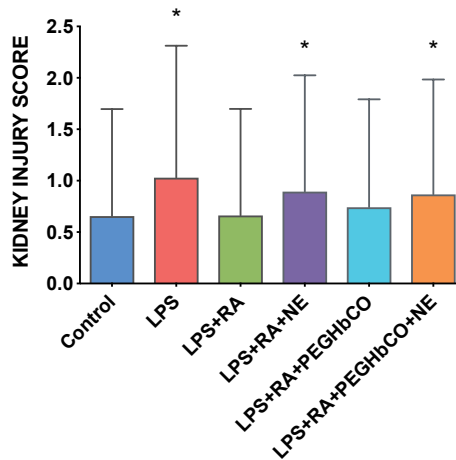
Supplemental Figure 4. Histological damages assessed by the kidney injury score

*Kruskal-Wallis test was used with Dunn's correction to adjust for multiple comparisons. * adjusted P<0.01 vs. Control group,*
 # adjusted P<0.01 vs LPS+RA group (n=384/group).

Discussion

In this rat model of endotoxemia, fluid resuscitation with PEGHbCO improved renal CµPO$_2$ while in parallel, decreased the number of sepsis-induced microcirculatory flow abnormalities, such as plugged capillaries. The addition of NE in the process of resuscitation using PEGHbCo did neither confer additional benefits in terms of renal tissue oxygenation nor skeletal microcirculatory flow although it increased significantly the MAP. In this short-term model, PEGHbCO did not mitigate sepsis-induced inflammation within the kidney. However, the infusion of this molecule did not cause harm to the kidney compared to the other strategies of resuscitation.

Contrary to hemorrhagic shock experimental models, few studies focused on the use of HBOCs during sepsis.[10–13] Some of these studies have been performed with diaspirin cross-linked hemoglobin (DCLHb) and showed a similar improvement in the microcirculatory perfusion of the ileum or other vital organs of septic rats as compared to pentastarch but with additional vasopressor properties.[10,11] However, it induced pulmonary hypertension while no improvement in oxygen utilization nor in survival was observed in a swine model of endotoxemia.[13] DCLHb and other HBOCs were latter known to induced severe hypertension

11

through NO-scavenging mechanisms and caused plasma nitrosyl hemoglobin formation, resulting in peripheral vasoconstriction.[14–16] Similarly to our study, a novel cross-linked hemoglobin-based oxygen carrier (YQ23) at a concentration of 0.15 g.kg^{-1} showed an increase in tissue oxygen delivery and consumption, with improved mitochondrial function of heart, liver, kidney and intestine, and improved animal survival in a cecal, ligation and puncture rat model of septic shock.[17]

The specific NO-scavenging effect of HBOCs was used to design trials where excessive NO release was believed to play a pivotal role in the pathophysiology of the disease, namely in septic shock. In a human multicenter randomized controlled trial, Vincent *et al.* infused pyridoxalated hemoglobin polyoxyethylene (PHP) in the idea of counteracting vasoplegia in patients with vasopressor-dependent distributive shock.[18] However, this clinical trial was terminated prematurely after interim analysis showed higher mortality with use of PHP whereas it decreased the need for vasopressors in survivors.[18] Further development of HBOCs dedicated to fluid resuscitation of septic shock was severely hampered.

Although still subjected to debate, large clinical trials have not demonstrated that colloids provide additional advantage over crystalloids as resuscitation fluid in critically ill patients with septic shock.[19,20] Some even highlighted an increased risk for AKI or death,[21] and the European Medicine Agency suspended the use of hydroxyethyl starches for fluid resuscitation in sepsis and septic shock. For now, options for fluid therapy resuscitation in patients with sepsis and septic shock remain very limited. Alternative fluids with different physico-chemical and antioxidant properties are desirable. PEGHbCO offers dual properties of (i) fluid resuscitation and (ii) antioxidant and hemoglobin oxygen carrying capacities. It has been previously shown that PEGHbCO improves microvascular flow without inducing vasoconstriction.[22] The PEGylation process helps retaining the hemoglobin from escaping the vasculature, and preventing from NO-scavenging effect while being a volume expander. Although, polyethylene glycol solutions have previously been regarded as resuscitation fluids for hemorrhage,[23,24] no preclinical data is available in model of sepsis using PEGylated molecules yet. In the present study, whether the benefits observed in terms of microcirculatory flow and renal cortical oxygenation are related to a better volume expansion due to the PEGylation of HbCO or whether CO release in the microcirculation plays a pivotal role remain to be determined. Indeed, previous experimental studies using CO-releasing molecules in models of sepsis showed a dampening of inflammation with an inhibition of different inflammasome pathways.[25–28] The beneficial effects of CO during a septic insult combining cytoprotective functions, mainly anti-apoptotic, inflammation

modulation and bacterial killing have been reported.[29,30] It should be noted that histopathological markers of AKI were not significantly altered in PEGHbCO-resuscitated animals compared to other groups in this short term model of endotoxemia.

Microcirculatory flow abnormalities occur during sepsis. Hemodynamic coherence may be jeopardized, making resuscitation of septic shock more challenging especially due to plugged capillaries.[3] Very few therapies demonstrated a significant improvement in reestablishing normal microcirculatory flow within these plugged capillaries. Administration of PEGHbCO in this model of endotoxemia not only restored the macrohemodynamics but improved disturbed microcirculatory flow with an increased number of flowing capillaries compared to animals resuscitated with RA with the addition of NE. Interestingly, the restoration of skeletal muscle microcirculatory flow was accompanied with an increase in $C\mu PO_2$ suggesting an improvement in other organs. Besides, the addition of NE to PEGHbCO did neither further improve $C\mu PO_2$ nor microcirculatory flow. Thus, resuscitation with PEGHbCO outperformed RA alone for fluid resuscitation of sepsis and should be further investigated as a valuable colloid alternative in this context.

Limitations

First, endotoxemia model of sepsis may cause different tissue injuries and dysfunctions compared to the cecal, ligation and puncture model. Second, this is a rather short-term model of sepsis. Further research is warranted to investigate mid- to long-term (> 14 days) effects of PEGHbCO on renal function. Third, the different isoforms of PEGHb (deoxy-, oxy- or met-) and the effectiveness of CO release were not investigated at the end of the experiment.

Conclusion

In a model of sepsis-induced AKI, fluid resuscitation with PEGHbCO in addition with RA not only restored macrohemodynamics without the need of additional vasopressors but enhanced renal $C\mu PO_2$ while restoring skeletal muscle microcirculatory flow in previously plugged capillaries. This study was not able to demonstrate a significant modulation of inflammation in the kidney, however PEGHbCO did not cause harm on the overall parameters of the renal function.

11

Summary

- PEGHbCO+RA in comparison to RA alone resuscitation improves the microcirculation and restores flow in previously sepsis-induced plugged capillaries with a significant decreased number of sluggish ad/or intermittent flow capillaries

- Increased microcirculatory oxygen availability in the renal cortex parallels the improved skeletal microcirculatory capillary blood flow

- The infusion of NE did not further improve microcirculation in the muscle nor the renal cortical renal microcirculatory PO2 levels. PEGHbCO+RA resuscitation performed similarly to RA+NE resuscitation in this model of endotoxemia.

- There were no significant effects on renal function or inflammatory parameters although there was a slight increase across the board on all parameters in favor of PEGHbCO. In any case, PEGHbCO did not cause harm on the overall parameters of kidney function and inflammation.

Financial disclosures & funding

Conflicts of interest

Prof. Dr Can Ince runs an Internet site microcirculationacademy.org which offers services (e.g., training, courses, analysis) related to clinical microcirculation and, has received honoraria and independent research grants from Fresenius-Kabi, Baxter Health Care, Prolog and AM-Pharma; has developed SDF imaging; is listed as an inventor on related patents commercialized by MicroVision Medical under a license from the Academic Medical Center; and has been a consultant for MicroVision Medical in the past but has not been involved with this company for more than 5 years. The company that developed the CytoCam-IDF imaging system, Braedius

Authors contribution

P.G. and B.E.: study design, carried out experiments, data analysis, writing of the first draft and of the final version, and review of the manuscript. C.I.: study design, writing of the final version, and review of the manuscript. A.K: performing the immunochemistry and histological analyses on kidney slices, data analysis, and writing of methodology part and review the manuscript. M.H: data analysis, statistical analysis, review of the manuscript. J.B: study design, data analysis, review of the manuscript.

11

References

1.   Ince C. The microcirculation is the motor of sepsis. *Crit Care*. 2005;9 Suppl 4:S13-19.

2.   Kanoore Edul VS, Ince C, Dubin A. What is microcirculatory shock? *Curr Opin Crit Care*. 2015;21(3):245-252.

3.   Ince C. Hemodynamic coherence and the rationale for monitoring the microcirculation. *Crit Care*. 2015;19 Suppl 3:S8.

4.   Ince C, Mik EG. Microcirculatory and mitochondrial hypoxia in sepsis, shock, and resuscitation. *J Appl Physiol*. 2016;120(2):226-235.

5.   Zafrani L, Ergin B, Kapucu A, Ince C. Blood transfusion improves renal oxygenation and renal function in sepsis-induced acute kidney injury in rats. *Crit Care*. 2016;20(1):406.

6.   Holst LB, Haase N, Wetterslev J, et al. Lower versus higher hemoglobin threshold for transfusion in septic shock. *N Engl J Med*. 2014;371(15):1381-1391.

7.   Guerci P, Ince Y, Heeman P, Faber D, Ergin B, Ince C. A LED-based phosphorimeter for measurement of microcirculatory oxygen pressure. *J Appl Physiol*. 2017;122(2):307-316.

8.   Ergin B, Zafrani L, Kandil A, et al. Fully Balanced Fluids do not Improve Microvascular Oxygenation, Acidosis and Renal Function in a Rat Model of Endotoxemia. *Shock*. 2016;46(1):83-91.

9.   Michelakis ED, Archer SL. The measurement of NO in biological systems using chemiluminescence. *Methods Mol Biol*. 1998;100:111-127.

10.   Sielenkämper AW, Eichelbrönner O, Martin CM, Madorin SW, Chin-Yee IH, Sibbald WJ. Diaspirin cross-linked hemoglobin improves mucosal perfusion in the ileum of septic rats. *Crit Care Med*. 2000;28(3):782-787.

11.   Mourelatos MG, Enzer N, Ferguson JL, Rypins EB, Burhop KE, Law WR. The effects of diaspirin cross-linked hemoglobin in sepsis. *Shock*. 1996;5(2):141-148.

12.   Creteur J, Zhang H, De Backer D, Sun Q, Vincent JL. Diaspirin cross-linked hemoglobin improves oxygen extraction capabilities in endotoxic shock. *J Appl Physiol*. 2000;89(4):1437-1444.

13.   Freilich E, Freilich D, Hacker M, Leach L, Patel S, Hebert J. The hemodynamic effects of diaspirin cross-linked hemoglobin in dopamine-resistant endotoxic shock in swine. *Artif Cells Blood Substit Immobil Biotechnol*. 2002;30(2):83-98.

14.   Alayash AI. Mechanisms of Toxicity and Modulation of Hemoglobin-Based Oxygen Carriers (HBOCs). *Shock*. November 2017.

15.   Tsai AG, Cabrales P, Manjula BN, Acharya SA, Winslow RM, Intaglietta M. Dissociation of local nitric oxide concentration and vasoconstriction in the presence of cell-free hemoglobin oxygen carriers. *Blood*. 2006;108(10):3603-3610.

16.   Greenburg AG, Kim HW. Nitrosyl Hemoglobin Formation In-Vivo After Intravenous Administration of A Hemoglobin-Based Oxygen Carrier in Endotoxemic Rats. *Artificial Cells, Blood Substitutes, and Biotechnology*. 1995;23(3):271-276.

17.   Kuang L, Zhu Y, Zhang J, et al. A novel cross-linked haemoglobin-based oxygen carrier is beneficial to sepsis in rats. *Artif Cells Nanomed Biotechnol*. 2019;47(1):1496-1504.

18.   Vincent J-L, Privalle CT, Singer M, et al. Multicenter, Randomized, Placebo-Controlled Phase III Study of Pyridoxalated Hemoglobin Polyoxyethylene in Distributive Shock (PHOENIX)*. *Crit Care Med*. 2015;43(1):57.

19.   Lewis SR, Pritchard MW, Evans DJ, et al. Colloids versus crystalloids for fluid resuscitation in critically ill people. *Cochrane Database Syst Rev*. 2018;8:CD000567.

20.   A Comparison of Albumin and Saline for Fluid Resuscitation in the Intensive Care Unit. *New England Journal of Medicine*. 2004;350(22):2247-2256.

21.   Perner A, Haase N, Guttormsen AB, et al. Hydroxyethyl Starch 130/0.42 versus Ringer's Acetate in Severe Sepsis. *N Engl J Med*. 2012;367(2):124-134.

22.   Abuchowski A. SANGUINATE (PEGylated Carboxyhemoglobin Bovine): Mechanism of Action and Clinical Update. *Artif Organs*. 2017;41(4):346-350.

23.   Parrish D, Plant V, Lindell SL, et al. New low-volume resuscitation solutions containing PEG-20k. *J Trauma Acute Care Surg*. 2015;79(1):22-29.

24.   Plant V, Parrish DW, Limkemann A, Ferrada P, Aboutanos M, Mangino MJ. Low-Volume Resuscitation for Hemorrhagic Shock: Understanding the Mechanism of PEG-20k. *J Pharmacol Exp Ther*. 2017;361(2):334-340.

25.   Jiang L, Fei D, Gong R, et al. CORM-2 inhibits TXNIP/NLRP3 inflammasome pathway in LPS-induced acute lung injury. *Inflamm Res*. 2016;65(11):905-915.

26.   Mizuguchi S, Stephen J, Bihari R, et al. CORM-3-derived CO modulates polymorphonuclear leukocyte migration across the vascular endothelium by reducing levels of cell surface-bound elastase. *Am J Physiol Heart Circ Physiol*. 2009;297(3):H920-929.

27.   Tsoyi K, Lee TY, Lee YS, et al. Heme-oxygenase-1 induction and carbon monoxide-releasing molecule inhibit lipopolysaccharide (LPS)-induced high-mobility group box 1 release in vitro and improve survival of mice in LPS- and cecal ligation and puncture-induced sepsis model in vivo. *Mol Pharmacol*. 2009;76(1):173-182.

28.   Zhang W, Tao A, Lan T, et al. Carbon monoxide releasing molecule-3 improves myocardial function in mice with sepsis by inhibiting NLRP3 inflammasome activation in cardiac fibroblasts. *Basic Res Cardiol*. 2017;112(2):16.

29.   Motterlini R, Otterbein LE. The therapeutic potential of carbon monoxide. *Nat Rev Drug Discov*. 2010;9(9):728-743.

30.   Nakahira K, Choi AMK. Carbon monoxide in the treatment of sepsis. *Am J Physiol Lung Cell Mol Physiol*. 2015;309(12):1387-1393.

11

Supplemental document

Anesthesia, surgical intervention, catheters insertion and left kidney exposure

The rats were anesthetized with an intraperitoneal injection of a mixture of 100 mg.kg^{-1} ketamine (Nimatek®; Eurovet, Bladel, the Netherlands), 0.5 mg.kg^{-1} dexmedetomidine (Dexdomitor; Orion Group, Espoo, Finland) and 0.05 mg.kg^{-1} atropine-sulfate (Centrafarm, Etten-Leur, The Netherlands) and maintained with 50 mg.kg^{-1} ketamine at an infusion rate of 5 ml.kg^{-1}.h^{-1}. Following tracheotomy, the animals were mechanically ventilated with 0.4 FiO$_2$. A heating pad under the animal allowed the body temperature to be controlled and maintained at 37±0.5°C. The end-tidal PCO$_2$ was adjusted between 32 and 42 mmHg with changes in ventilator settings.

The right carotid (pressure) artery and jugular (anesthesia) and femoral (lipopolysaccharide infusion, fluid resuscitation) veins were cannulated using polyethylene catheters (outer diameter = 0.9 mm; Braun, Melsungen, Germany). Fluid maintenance during surgery was sustained using Ringer's acetate (Baxter, Utrecht, The Netherlands) administration at a rate of 10 ml.kg^{-1}.h^{-1} and stopped. The left kidney was exposed without decapsulation and immobilized in a Lucite kidney cup (K. Effenberger, Pfaffingen, Germany) via a 3-cm incision in the left flank. Renal vessels were carefully separated to preserve the nerves and adrenal gland. An ultrasonic flow probe was placed around the left renal artery (type 0.7 RB; Transonic Systems Inc., Ithaca, NY, USA) and connected to a flow meter (T206; Transonic Systems Inc.) to continuously measure renal blood flow (RBF). The left ureter was isolated, ligated and cannulated using a polyethylene catheter for urine collection.

Renal oxygen delivery and consumption

The arterial oxygen content (C$_a$O$_2$) (ml O$_2$.dl^{-1}) was calculated considering the oxygen carrying capacity of PEGHbCO in the plasma: CaO$_2$=(SaO$_2$ x Hb$_{RBC}$ x γ$_{Hb}$)+ (S$_{PEGHbCO}$O$_2$ x Hb$_{PEGHbCO}$ x γ$_{PEGHbCO}$)+ PaO$_2$ x 0.0031 where Hb$_{RBC}$ is the hemoglobin concentration in red blood cells (g.dl^{-1}), S is the arterial oxygen saturation of Hb$_{RBC}$ or PEGHbCO, and γ is the oxygen carrying capacity of Hb$_{RBC}$ (1.34 mlO$_2$.g^{-1} Hb for rat blood) or PEGHbCO, as previously determined. Renal delivery

of O_2 (DO_2) (ml O_2.min^{-1}) was determined at the end of the experiment as follows: Renal DO_2= CaO_2 x RBF. Venous oxygen content (CvO_2) was determined by analysis of a blood gas of the renal vein.

Renal oxygen consumption (VO_{2ren}, in ml O_2.min^{-1}) was determined as follows: VO_{2ren} = C(a-v)O_2 x RBF. The renal energy efficiency for sodium transport (VO_2ren/TNa$^+$) was assessed using the ratio of the total amount of VO_{2ren} over the total amount of sodium reabsorbed (TNa$^+$, millimolar per minute).

Immunohistochemical analysis and histology of the kidney

Animals were euthanized at the end of the experiment using 40% Euthasol (Produlab Pharma BV, Raamsdonksveer, the Netherlands). Kidneys were harvested, fixed in 4% formalin and embedded in paraffin.

For immunohistochemical analysis, kidney sections (5 µm) were deparaffinized with xylene and rehydrated with decreasing percentages of ethanol and finally with water. Antigen retrieval was accomplished by microwaving slides in citrate buffer (pH 6.0) (Lab Vision, AP-9003-500) for 10 min. Slides were left to cool for 20 min at room temperature and then rinsed with distilled water. Surroundings of the sections were marked with a PAP pen. The endogenous peroxidase activity was blocked with H_2O_2 for 10 min at room temperature and later rinsed with distilled water and PBS. Blocking reagent (Lab Vision, TA-125-UB) was applied to each slide followed by 5 min incubation at room temperature in a humid chamber. Kidney sections were incubated for overnight at +4°C with inducible NO synthase (iNOS) (Thermo Fisher Scientific, B-1605-P), tumor necrosis factor-α (TNF-α) (Abcam ab66579) and IL-6 (Abcam, 6672), and incubated for 1 hour at room temperature with myeloperoxidase (MPO) (Thermo Fisher Scientific, RB-373-A), endothelial NO synthase (eNOS) (Thermo Fisher Scientific, RB-9279-P) and neutrophil gelatinase-associated lipocalin (NGAL) (Abcam, 41105) antibodies. Antibodies were diluted in a large volume of UltrAb Diluent (Lab Vision, TA-125-UD). The sections were washed in PBS three times for 5 min each time and then incubated for 30 min at room temperature with biotinylated goat anti-rabbit antibodies (LabVision, TP-125-BN). After slides were washed in PBS, the streptavidin peroxidase label reagent (LabVision, TS-125-HR) was applied for 30 min at room temperature in a humid chamber. The colored product was developed by incubation with AEC. The slides were counterstained with Mayer's hematoxylin (LabVision, TA-125-MH) and mounted in vision mount (LabVision, TA-060-UG) after being washed in distilled water. Both the intensity

11

and the distribution of specific the antibodies staining were scored. Ten tubular areas (n=10) on each slice per animal were analyzed. For each sample, a histological score (HSCORE) value was derived by summing the percentages of cells that stained at each intensity multiplied by the weighted intensity of the staining [HSCORE = S Pi (i+1), where i is the intensity score and Pi is the corresponding percentage of the cells]. We evaluated MPO reaction in the glomerulus from 300 selected glomeruli and in 300 selected peritubular areas under a light microscope at a magnification X400. We scored 1 if leukocytes could be seen in the glomerulus and 0 if not.

The kidney tissues were fixed in 10% neutral buffer formaldehyde solution and embedded in paraffin. Kidney sections (4 μm) stained with hematoxylin (H) and periodic acid Schiff (PAS). Histopathology changes in kidney cortex were examined under a light microscope at X200 magnification. Sections were scored using semi-quantitate scale and evaluated the degree of kidney injury. Kidney injury scores were defined as swelling and clear vacuolation of tubular epithelium, separation/detachment of tubular epithelium from underlying tubular baseline membrane, loss/attenuation of PAS-positive brush border of proximal tubular epithelial cells, simplification with thinning of tubular epithelium, sloughing of apical cytoplasm into the tubular lumen, and flattening of the epithelial cells with resultant widening of the tubular lumen, dilatation of the tubular lumina, casts in tubule lumens (hyaline, cellular, granular, cellular debris, pigmented), glomeruli lesions, Interstitial edema (clear widening of the normally sparse cortical interstitium), and graded on a scale of 0 to 3. The degree of damage was defined as fallow: 0-normal (0-5%); 1-Mild (5-25%); 2-Moderate (25–75%); 3-Severe (>75%). The ten eight were analysed in each section were selected at random. Kidney sections were photographed using Image Pro-Plus.

12

SUMMARY
& CONCLUSIONS

English summary

The architecture of the microcirculation differs significantly across organs. The microcirculation of the kidney is unique, highly heterogenous and presents one of the richest densities while embedding different types of endothelial cells with various specialized functions. Thus, the observations of microcirculation performed in other organs cannot strictly be extrapolated to this singular structure. Although, the kidney is very sensitive to ischemia/reperfusion injury, hypoxemia, or anemia that induce acute kidney injury, its microcirculation is however one of the hardest to apprehend at bedside. In experimental preclinical studies, the assessment of renal microcirculation depends on semi- to very invasive techniques to explore several aspects of the different constituents of the microcirculation but requires advanced and/or costly techniques. Translation of experimental research to the beside regarding the analysis of renal microcirculation remains a challenging project. To date, only surrogates of the well-being of the microcirculation are available; namely biomarkers of acute kidney injury (AKI) assessed either in the plasma or in the urine. However, these measurements do not grant a continuous monitoring. To obtain a continuous monitoring of this specific organ function, such as what is available for the heart, will be the challenge for the next upcoming years.

This dissertation focuses on the analysis of the different constituents of the microcirculation and the response to different therapeutics employed to resuscitate the critically injured microcirculation with a special focus on the renal microcirculatory oxygenation.

First, we reviewed the essential determinants of the microcirculation in the kidney. AKI is driven by three main components: (i) imbalance between oxygen demand and consumption, (ii) renal inflammation with the generation of radical oxygen species and (iii) vascular barrier and endothelial alterations with associated microcirculatory flow disturbances. This helped us to outline the main axes of our research. Although triggers of injury may differ, there is a large body of evidence supporting that common pathways lead to AKI in a critical setting (*chapters 2 and 3*).

In the past decades, the role of plasma viscosity in the regulation of microcirculatory perfusion was emphasized in dorsal skinfold chamber rodent models. We evaluated in a pig model of hemorrhagic shock whether low volume resuscitation associated with hydroxyethyl starch (with a higher viscosity than Ringer's lactate) was able to maintain plasma viscosity close to a physiologic range. We demonstrated that commercially available volume expanders had

similar effects on rheological and microcirculatory variables (partial oxygen tissue pressure), irrespective of their viscosity, compared to Ringer's lactate (*chapter 4*).

It has been reportedly suggested that the glycocalyx plays a fundamental role in the regulation of vascular barrier permeability. In these experimental models however, nonphysiological insults were used to degrade the various components of the glycocalyx, such as enzymatic degradation. The causal relationship between glycocalyx degradation and vascular barrier breakdown has not been clearly demonstrated yet. We assessed vascular barrier permeability with 4 different techniques in models of nontraumatic hemorrhagic shock and hemodilution, to determine the role of the glycocalyx in contributing to increase vascular permeability (*chapters 5 and 6*). Interestingly, when considering the various components of the vascular barrier, these results suggest that glycocalyx shedding may occur independently of an increase in vascular barrier permeability. Thus, we concluded that a gradation in vascular barrier injury should be considered, to determine to which extent the increase in permeability will occur and how microcirculation is affected.

The measurement of microcirculatory oxygen pressure is of utmost importance to assess how changes in kidney function and occurrence of AKI are related to a decrease in oxygen availability in the kidney. Thus, we designed a modern LED-based phosphorimeter that is able to combine 4 different LEDs to measure microcirculatory PO_2 within different range of depth and in multiple organs. The design of this device addressed previous drawbacks related to the use of flashlamps. We demonstrated that phosphorescence decay times were independent of the concentration of the dye within the medium under analysis. The details provided in our study offered opportunity for other research teams working in the field of microcirculation to build a similar device (*chapter 7*).

In all of our models of shock; hemorrhage, endotoxemia, hemodilution or ischemia/reperfusion injury, we consistently observed a significant decrease in microcirculatory oxygen pressure. Interestingly, none of the therapies used could restore the renal cortical microcirculatory PO_2 to the baseline or control values. Anions in balanced crystalloids fluids, used in everyday practice, are considered bicarbonate precursors. Thus, these fluids exhibit buffering effects, that may be interesting during AKI. We demonstrated that acetate-balanced fluids had preserved buffering effects irrespective of the liver function. Although, acid-bae status was improved, no significant effect on renal oxygenation was observed (*chapter 8*).

We further focused on the means to increase microcirculatory oxygenation in the kidney. We investigated the links between inflammation and hypoxia in the kidney in a model of

12

endotoxemia. We found that fluid supplemented with N-acetylcysteine (NAC) improved cortical renal oxygenation, oxygen delivery and oxygen consumption compared to non-supplemented fluid. It suggested that NAC provide beneficial effect on renal microcirculatory PO_2, mediated through possible antioxidant effect, independently of renal macrohemodynamics (*chapter 9*).

In the quest for holy grail of fluid resuscitation, the development of a compound combining oxygen carrying capacities, plasma expansion with high viscosity properties, and embedded antioxidant/anti-inflammatory molecules targeting the microcirculation, appears necessary. Fluid resuscitation with PEGylated carboxyhemoglobin during hemorrhage sustained urine output and may protect against acute kidney injury without a significant increase in renal cortical PO_2 (*chapter 10*). During endotoxemia, PEGylated carboxyhemoglobin improved the microcirculation and restored flow in previously sepsis-induced plugged capillaries while increasing microcirculatory oxygen availability in the renal cortex (*chapter 11*). Considered together, these results suggest that this compound may be an interesting fluid meeting previously unmet needs and require further evaluation.

To conclude, microcirculatory disturbances observed during circulatory shock states require a multifaceted approach. In the hope of limiting AKI, the resuscitation of the microcirculation should not only consider the volume expander effect of the fluids but also anti-inflammatory or antioxidant aspects targeting ischemia/reperfusion injuries and oxygen carrying properties to sustain microcirculatory oxygen pressure. It is yet to be demonstrated by clinical trials that such a fluid might improve the outcome of patients with critically injured microcirculation.

NEDERLANDSE SAMENVATTING

De architectuur van de microcirculatie verschilt aanzienlijk tussen de organen. De microcirculatie van de nier is uniek, zeer heterogeen en vertoont een van de rijkste microvasculaire dichtheden, terwijl verschillende typen endotheelcellen worden ingebed met verschillende gespecialiseerde functies. Aldus, kunnen de waarnemingen van microcirculatie uitgevoerd in andere organen niet strikt worden geëxtrapoleerd naar deze enkelvoudige structuur. Hoewel de nier erg gevoelig is voor ischemie/reperfusie-schade, hypoxemie en bloedarmoede wat acuut nierbeschadiging kan induceren, is de microcirculatie van de nier echter moeilijk te begrijpen aan het bed van de patiënt. In experimentele preklinische onderzoeken is de beoordeling van de microcirculatie van de nier afhankelijk van semi- tot zeer invasieve technieken om verschillende aspecten van de verschillende bestanddelen van de microcirculatie te onderzoeken, maar dit vereist geavanceerde en/of dure technieken. Translatie van experimenteel onderzoek naar de kliniek met betrekking tot de analyse van de microcirculatie van de nieren blijft een uitdagend project. Tot op heden zijn alleen surrogaten van het goed functioneren van de microcirculatie beschikbaar; namelijk biomarkers van de acute nierbeschadiging (AKI), beoordeeld in het plasma of in de urine. Deze metingen bieden echter geen continue monitoring. Een voortdurende monitoring van deze specifieke orgaanfunctie, zoals wat beschikbaar is voor het hart, is de uitdaging voor de komende jaren.

Dit proefschrift richt zich op de analyse van de verschillende bestanddelen van de microcirculatie en de respons op verschillende therapeutische middelen die worden gebruikt om de ernstig beschadigde microcirculatie te reanimeren met een speciale focus op de renale microcirculatoire oxygenatie.

Eerst hebben we de essentiële determinanten van de microcirculatie in de nier beoordeeld. AKI wordt aangedreven door drie hoofdcomponenten: (i) disbalans tussen zuurstofbehoefte en -consumptie, (ii) nierontsteking met het genereren van radicale zuurstofsoorten en (iii) vasculaire barrière en endotheel veranderingen met bijbehorende microcirculatoire flow afwijkingen. Dit hielp ons om de hoofdlijnen van ons onderzoek te schetsen. Hoewel triggers van schade kunnen verschillen, is er een groot aantal aanwijzingen dat gemeenschappelijke paden naar AKI leiden in een kritieke setting (*hoofdstukken 2 en 3*).

In de afgelopen decennia werd de rol van plasmaviscositeit in de regulatie van microcirculatoire perfusie benadrukt in knaagdiermodellen met dorsale huidplooien. We

12

evalueerden in een varkensmodel, met hemorragische shock, of een laag volume resuscitatie met hydroxyethylzetmeel (met een hogere viscositeit dan Ringer's lactaat) in staat was om plasmaviscositeit te bereiken dat dicht bij de fysiologische waarden zat. We hebben aangetoond dat in de handel verkrijgbare volume-expanders vergelijkbare effecten hebben op reologische en microcirculatie variabelen (gedeeltelijke zuurstofweefseldruk), ongeacht hun viscositeit, in vergelijking met Ringer's lactaat *(hoofdstuk 4)*.

Bij vele experimenten is er gesuggereerd dat de glycocalyx een fundamentele rol speelt bij de regulatie van de permeabiliteit van de vaat barrière. In deze experimentele modellen werden echter niet-fysiologische insulten gebruikt om de verschillende componenten van de glycocalyx af te breken, zoals enzymatische afbraak. Het causale verband tussen glycocalyx afbraak en afbraak van vasculaire barrière is nog niet duidelijk aangetoond. We hebben de permeabiliteit van de vasculaire barrière beoordeeld met 4 verschillende technieken in modellen van niet-traumatische hemorragische shock en hemodilutie, om de rol van de glycocalyx te identificeren bij het bijdragen aan het verhogen van de vasculaire permeabiliteit (*hoofdstuk 5 en 6*). Interessant is dat, uitgaande van de verschillende componenten waaruit de vaatbarrière bestaat, de resultaten suggereren dat glycocalyx afbraak onafhankelijk van een toename van de permeabiliteit van de vaatbarrière kan optreden. We concludeerden daarom dat een gradatie van schade aan de vaatbarrière moet worden overwogen om te bepalen in welke mate de toename van de permeabiliteit zal optreden en hoe de microcirculatie wordt beïnvloed.

De meting van de zuurstof in de microcirculatie is van het grootste belang om te beoordelen hoe veranderingen in de nierfunctie en het optreden van AKI verband houden met een afname van de beschikbaarheid van zuurstof in de nier. Daarom hebben we een moderne LED-gebaseerde fosforimeter ontworpen die in staat is om 4 verschillende LED's te combineren om de microcirculatoire zuurstof spanning te meten, binnen verschillende dieptebereiken en in meerdere organen. Het ontwerp van dit apparaat loste eerdere nadelen op met betrekking tot het gebruik van flitslampen. We hebben aangetoond dat fosforescentie vervaltijden onafhankelijk waren van de concentratie van de kleurstof in het te analyseren medium. De details in ons onderzoek boden andere onderzoeksteams die op het gebied van microcirculatie werken de mogelijkheid om een soortgelijk apparaat te bouwen (*hoofdstuk 7*).

In al onze schokmodellen; bloeding, endotoxemie, hemodilutie of ischemie/reperfusie-schade, hebben we consistent een significante afname van de microcirculatoire zuurstofspanning waargenomen. Interessant is dat geen van de toegepaste therapieën de

renale corticale microcirculatoire zuurstof spanning naar de basislijn of controlewaarden kon herstellen.

Anionen in gebalanceerde kristalloïdenvloeistoffen, gebruikt in de dagelijkse praktijk, worden beschouwd als bicarbonaatprecursoren. Deze vloeistoffen vertonen dus bufferende effecten, die interessant kunnen zijn tijdens AKI. We toonden aan dat acetaat-gebalanceerde vloeistoffen bufferende effecten hadden behouden, ongeacht de leverfunctie. Hoewel de zuur-base status was verbeterd, werd geen significant effect op renale oxygenatie waargenomen (*hoofdstuk 8*).

We hebben ons verder gericht op de middelen om de zuurstof in de microcirculatie van de nier te verhogen. We onderzochten het verband tussen ontsteking en hypoxie in de nier in een endotoxemie model. We vonden dat vloeistof aangevuld met N-acetylcysteïne (NAC) de corticale renale oxygenatie, zuurstofafgifte en zuurstofverbruik verbeterde in vergelijking met niet-gesupplementeerde vloeistof. Het suggereerde dat NAC een gunstig effect heeft op de microcirculatie van de nier zuurstofspanning, gemedieerd door een mogelijk antioxidant effect, onafhankelijk van de renale macrohemodynamiek (*hoofdstuk 9*).

In de zoektocht naar de heilige graal van de vloeibare resuscitatie lijkt de ontwikkeling van een verbinding, die zuurstofdragende capaciteiten combineert met plasma-expansie met hoge viscositeitseigenschappen en ingebedde antioxiderende/ontstekingsremmende moleculen bevat die gericht zijn op de microcirculatie, noodzakelijk. Vochtresuscitatie met gePEGyleerd carboxyhemoglobine tijdens bloeding leidde tot het behouden van urineproductie en kan dus protectief zijn tegen acute nierschade, zonder dat er een significante toename van de nier cortex zuurstofspanning zal ontstaan (*hoofdstuk 10*). Tijdens endotoxemie verbeterde gepegyleerde carboxyhemoglobine de microcirculatie en herstelde de microvasculaire flows in eerder, door sepsis, verstopte capillairen terwijl de beschikbaarheid van microcirculatoire zuurstof in de niercortex werd verhoogd (*hoofdstuk 11*). Samenvattend, suggereren deze resultaten dat deze verbinding een interessante vloeistof kan zijn die eerder onvervulde behoeften vervult en verdere evaluatie vereist.

Concluderend vereisen microcirculatiestoornissen waargenomen tijdens shock van de bloedsomloop een veelzijdige aanpak. In de hoop AKI te beperken moet bij de resuscitatie van de microcirculatie niet alleen rekening worden gehouden met het volume-expansie-effect van de vloeistoffen, maar ook met ontstekingsremmende of antioxiderende aspecten gericht op ischemie reperfusie-schade en zuurstofdragende eigenschappen, om de microcirculatoire zuurstofspanning te behouden. Uit klinische onderzoeken moet nog worden aangetoond dat

12

een dergelijke vloeistof de uitkomst van patiënten met ernstig beschadigde microcirculatie zou kunnen verbeteren.

12

A

APPENDICES

A

Acknowledgments

Writing the acknowledgments part is always harder than it looks, not because there is nothing to say, but rather too much wanted to say. Back in 2014, Prof. Marie-Reine Losser played the role of the matchmaker at the ESICM congress in Barcelona to meet Prof. Can Ince. Marie-Reine I couldn't have done all of this without your unwavering support, your mentorship and your goodwill. I owe you eternal gratitude and respect.

When I was first introduced to Prof. Can Ince, I already knew it was a good match. He offered me to spend a year or more abroad in Amsterdam in the Netherlands. I read so much about his research and it is always very pleasant to work with someone you admire. It definitely turned out to be a win-win situation. Since I was a child, I always wanted to live abroad to experience how life could be outside of France. By the end of 2015, I stepped in the Netherlands and it was the beginning of one of the best journeys of my life. Leaving my family and especially my son Paul, was heartbreaking at the beginning, but Can definitely knows how to make people comfortable and confident. Can, you turned this experience into something special. Along the months in the lab, I discovered not only talented researchers and scientists, but I found a second family. Can, you are one these very inspirational persons, very committed to his work and his passion, and you are undoubtedly the "pope" of the microcirculation. Everyone is welcomed in your lab and you created what people should envy, a very international network of scientists delighted to work with you. During these years in Amsterdam, I had the opportunity to meet your family: Janet your lovely wife, Yasin and Yilmaz your sons, who I like very much. They align with you. I honestly considered you, somehow, as my second father. I am so grateful to you Can, for being my mentor, my friend, and a part of a dad that I never had.

I would like to thank all the scientists in the Department of Translational Physiology, that I had the chance to meet and to work with over the years. I would start with Bulent. Bro, without you it clearly would not have been possible. Your skills in experimental surgery are outstanding. You basically taught me everything in this field. Thank you for all these funny moments in the lab, for listening to radio Veronica, for the gym lessons, for being so resilient like nothing can hit you. I wish you all the best for you and your family in Erasmus MC and I hope we will pursue our European collaboration and develop our research network on microcirculation. Yasin, so many times you made my day. You are a "behind-the-scenes worker", always around to help. I really appreciated all these meaningful and in-depth conversations about everything. I really enjoyed

some of our nights and dinners that I will never forget. Matthias, you came in Amsterdam when I was almost leaving. During that period of time, we had so many conversations about anything and everything. So inspirational and meaningful. I sometimes believe you are the most advanced brain-computer interface ever made. I was really impressed working at your side. I wish long life to Mathilda and hope I will dramatically transform the way we currently analyze the microcirculation. Zehra, you have been the shinning lady of the department over these months. I wish you and to your family all the best.

Last but not least, I would like to thank my family for their unwavering support. I have been through really hard times regarding my personal life during these past years and you were always there standing by. I would like to dedicate this thesis to my love, Fanny, you kept on supporting me and helped me to carry out all these projects, even though some appeared truly unattainable. Now, we are sharing and building our life together and I could not be happier. On November 23rd 2019, you offered me the most unevaluable gift a man can dream of: our son Louis. Louis, Paul, you and I will go on building the family we always dreamt of and withstand unparalleled to the challenges of life. I LOVE YOU to the moon and back my sweethearts.

"Give the ones you love wings to fly, roots to come back, and reasons to stay."

Dalai Lama

A word for posterity. By the end of 2019, Humanity has been struck by a pandemic named COVID-19. This disease has unprecedented impacted the modern world, the health care system, the economy, travels but also younger generations. #stayathome was the new normal.

For these reasons, the defense of this Thesis could not be held in Amsterdam, as it was previously scheduled. After 5 years of hard working, it is a bit of a disappointment but that did not take away the pride I feel while writing these last words.

A

PhD PORTFOLIO

Name PhD student: Philippe Guerci

Place and date of birth: Nancy, France, December 16th 1982

PhD period: 2016-2019

Affiliation: Department of Translational Physiology

                           Amsterdam University Medical Center, AMC location, Amsterdam, The Netherlands

                           Ecole doctorale BioSE, INSERM U1116, Faculty of Medicine, University of Lorraine, Nancy, France

Name supervisors   Prof. dr. C. Ince, Prof. dr. B. Lévy, Prof dr. M.R. Losser

PhD Training

Graduate School Courses	Year	Workload (ECTS)
Master of Science (MSc): Bioengineering, Medications and Targets (BIMC), University of Lorraine	2010	30
Courses on Laboratory Animal Science, University of Utrecht	2016	2
Advanced course on microcirculation analysis, Academic Medical Center	2016	1
Digital education tools for teachers and learners (Fi4 282), University of Lorraine	2018	0.5
Digital solutions for collaborative work (Fi4 283), University of Lorraine	2018	0.5
Doctoral School Day, University of Lorraine	2018	2
Advanced university degree in medical education and teaching, University of Lorraine	2018	8
(Inter)national conferences		
2nd International Scientific Symposium: Functional Renal imaging The Parenchima Initiative - COST - Charité - Max Delbruck Communication Center - Berlin - Germany	2017	8
Annual congress – French Society of Anesthesiology and Critical Care Medicine (SFAR), Paris, France	2016-19	5
Annual congress – European Society of Intensive Care Medicine, ESICM, Vienna, Milano, Paris, Berlin	2016-19	5

Oral presentations	Year	Workload (ECTS)
The role of bicarbonate precursors in balanced fluids during haemorrhagic shock with and without compromised liver function, ESICM, Milano, Italy	2016	0.5
An LED-based phosphorimeter for measurement of microcirculatory oxygen concentrations in vivo in the kidney, ESICM, Milano, Italy	2016	0.5
Glycocalyx degradation is independent of vascular barrier permeability in non-traumatic hemorrhagic shock – SFAR, Paris, France	2017	0.5
Renal optical methods: Phosphorimetric pO2 measurement - Max Delbruck Communication Center - Berlin - Germany	2017	0.5
Glycocalyx shedding during stepwise hemodilution and microvascular permeability, ESICM, Vienna, Austria	2017	0.5
Evaluation of high oxygen affinity of bovine PEGylated Carboxyhemoglobin (PEG-COHb) on the renal oxygenation and function in septic rats, ESICM, Paris, France	2018	0.5

Teaching, Tutoring and mentoring

	Year	
Degree of associate Professor in Anesthesiology and Critical Care Medicine	2018	
Tutoring four physician residents in Anesthesiology and Critical Care Medicine for their medical degree, University hospital of Nancy, university of Lorraine	2016-19	
Tutoring one junior doctor for his master thesis	2019	
Lecturing at the University of Lorraine	2013-19	

Parameters of Esteem

	Year	
Grant from the Dutch Kidney Foundation (DKF)	2017	
Grant from the French Society of Anesthesiology and Critical Care Medicine (SFAR)	2016	

A

CURRICULUM VITAE

Philippe Guerci was born on the 16th of December 1982 in Nancy, France where he grew up and spent most of his life. He is the eldest of two children. Both of his parents were medical doctors with a PhD degree. Although, his primary aim was to become a pilot, he decided to pursue a career in the medical field after an eye trauma revealed his sight was not good enough. He graduated high-school in 2000 and enrolled in Medicine at the University of Lorraine, Nancy, France. He obtained his Medical degree in 2007. Very early in his student life, he was attracted to emergent situations as well as by the environment of the operating room. He naturally chose Anesthesiology and Critical Care Medicine as a specialty. During his studies, he was introduced to research science in 2009 in Immunology where he studied the expression of Fc-γ receptor RI (CD64) in patients with HIV infection under the supervision of prof. dr. M.C Béné. While pursuing clinical practice, it became obvious to him that experimental and fundamental research was essential for meaningful translational research at the bedside. He obtained a master's degree in research in 2010. He participated in several scientific projects, most notably on microcirculation and anesthesia. Paul, his first son was born in 2012 while in the last year of his residency. In 2013, he started his fellowship in Anesthesiology and Critical care Medicine. Introduced by his mentor and supervisor prof. dr. M.R. Losser, he met prof. dr C. Ince at the European Congress of Intensive Care Medicine on 2014 in Barcelona. He offered him a joint doctorate (PhD) between University of Amsterdam and University of Lorraine to extensively study the relations between microcirculation alterations and acute kidney injury. He moved and settled in Amsterdam, the Netherlands by the end of 2015 and started to work as a PhD student for 14 months at the Department of Translational Research, University Medical Center. There, he developed skills in the study of microcirculation, measurement of oxygenation and assessment of vascular barrier permeability in rodent models. Eventually he returned to his hometown Nancy to become a staff physician in the surgical ICU of the university hospital of Nancy. In the meantime, he kept on doing experimental and clinical research and developed a collaborative network with prof. dr. C. Ince research team. His studies evolved into the current PhD dissertation.

List of publications

1. Novy E, Scala-Bertola J, Roger C, **Guerci P.** Preliminary Therapeutic Drug Monitoring Data of β-Lactams in Critically Ill Patients With SARS-CoV-2 Infection. Anaesth Crit Care Pain Med. 2020 Apr 18:S2352-5568(20)30071-0. doi: 10.1016/j.accpm.2020.04.005

2. Barnes BJ, Adrover JM, Baxter-Stoltzfus A, Borczuk A, Cools-Lartigue J, Crawford JM, Daßler-Plenker J, **Guerci P**, Huynh C, Knight JS, Loda M, Looney MR, McAllister F, Rayes R, Renaud S, Rousseau S, Salvatore S, Schwartz RE, Spicer JD, Yost CC, Weber A, Zuo Y, Egeblad M. Targeting Potential Drivers of COVID-19: Neutrophil Extracellular Traps. J Exp Med. 2020 Jun 1;217(6):e20200652. doi: 10.1084/jem.20200652.

3. **Guerci P**, Ergin B, Kandil A, Ince Y, Heeman P, Hilty MP, Bakker J, Ince C. Resuscitation with pegylated-carboxyhemoglobin preserves renal cortical oxygenation and improves skeletal muscle microcirculatory flow during endotoxemia. Am J Physiol Renal Physiol. 2020 Apr 13. doi: 10.1152/ajprenal.00513.2019.

4. Esposito M, Rocq PL, Novy E, Remen T, Losser MR, **Guerci P**; ICURTASK study. Smartphone to-do list application to improve workflow in an intensive care unit: A superiority quasi-experimental study. Int J Med Inform. 2020;136:104085. doi: 10.1016/j.ijmedinf.2020.104085.

5. **Guerci P**, Bellut H, Mokhtari M, Gaudefroy J, Mongardon N, Charpentier C, Louis G, Tashk P, Dubost C, Ledochowski S, Kimmoun A, Godet T, Pottecher J, Lalot JM, Novy E, Hajage D, Bouglé A; AZUREA research network. Outcomes of Stenotrophomonas maltophilia hospital-acquired pneumonia in intensive care unit: a nationwide retrospective study. Crit Care. 2019;23(1):371. doi: 10.1186/s13054-019-2649-5.

6. Leon L, **Guerci P**, Pape E, Thilly N, Luc A, Germain A, Butin-Druoton AL, Losser MR, Birckener J, Scala-Bertola J, Novy E. Serum and peritoneal exudate concentrations after high doses of β-lactams in critically ill patients with severe intra-abdominal infections: an observational prospective study. J Antimicrob Chemother. 2019 Oct 10. pii: dkz407. doi: 10.1093/jac/dkz407.

7. Belveyre T, **Guerci P**, Pape E, Thilly N, Hosseini K, Brunaud L, Gambier N, Meistelman C, Losser MR, Birckener J, Scala-Bertola J, Novy E. Antibiotic prophylaxis with high-dose cefoxitin in bariatric surgery: an observational prospective single center study. Antimicrob Agents Chemother. 2019 Oct 7. pii: AAC.01613-19. doi: 10.1128/AAC.01613-19.

8. **Guerci P**, Ergin B, Kapucu A, Hilty MP, Jubin R, Bakker J, Ince C. Effect of Polyethylene-glycolated Carboxyhemoglobin on Renal Microcirculation in a Rat Model of Hemorrhagic Shock. Anesthesiology. 2019;131(5):1110-1124. doi: 10.1097/ALN.0000000000002932.

9. Rimbert S, Schmartz D, Bougrain L, Meistelman C, Baumann C, **Guerci P**. MOTANA: study protocol to investigate motor cerebral activity during a propofol sedation. Trials. 2019;20(1):534. doi: 10.1186/s13063-019-3596-9.

10. Mongardon N, Bouglé A, Sola C, Bouroche G, Verdonk F, Le Gall A, Bataille A, Beylacq L, Bourgeois E, Charbit J, **Guerci P**, Chousterman BG; "Groupe jeune de la Société

A

Française d'Anesthésie-Réanimation (SFAR)". Publication outcome of abstracts presented at an Anesthesiology and Critical Care Medicine meeting: Does being a junior presenter matter? J Clin Anesth. 2019;60:49-50. doi: 10.1016/j.jclinane.2019.08.019.

11. Hilty MP, **Guerci P**, Ince Y, Toraman F, Ince C. MicroTools enables automated quantification of capillary density and red blood cell velocity in handheld vital microscopy. Commun Biol. 2019;2:217. doi:10.1038/s42003-019-0473-8.

12. **Guerci P**, Ergin B, Ince C. In Response. Anesth Analg. 2019;129(3):e102-e103. doi: 10.1213/ANE.0000000000004182.

13. Garnier M, Gallah S, Vimont S, Benzerara Y, Labbe V, Constant A-L, Siami S, Guerot E, Compain F, Mainardi J-L, Montil M, Quesnel C, BLUE-CarbA study group. Multicentre randomised controlled trial to investigate usefulness of the rapid diagnostic βLACTA test performed directly on bacterial cell pellets from respiratory, urinary or blood samples for the early de-escalation of carbapenems in septic intensive care unit patients: the BLUE-CarbA protocol. BMJ Open. 2019;9(2):e024561. doi:10.1136/bmjopen-2018-024561.

14. Uz Z, van Gulik TM, Aydemirli MD, **Guerci P**, Ince Y, Cuppen D, Ergin B, Aksu U, de Mol BA, Ince C. Identification and quantification of human microcirculatory leukocytes using handheld video microscopes at the bedside. J Appl Physiol. 2018;124(6):1550-1557. doi:10.1152/japplphysiol.00962.2017.

15. Uz Z, Ince C, **Guerci P**, Ince Y, P Araujo R, Ergin B, Hilty MP, van Gulik TM, de Mol BA. Recruitment of sublingual microcirculation using handheld incident dark field imaging as a routine measurement tool during the postoperative de-escalation phase-a pilot study in post ICU cardiac surgery patients. Perioper Med (Lond). 2018;7:18. doi:10.1186/s13741-018-0091-x.

16. Novy E, Laithier F-X, Machouart M-C, Albuisson E, **Guerci P**, Losser M-R. Determination of 1,3-β-D-glucan in the peritoneal fluid for the diagnosis of intra-abdominal candidiasis in critically ill patients: a pilot study. Minerva Anestesiol. 2018;84(12):1369-1376. doi:10.23736/S0375-9393.18.12619-8.

17. Jabaudon M, Belhadj-Tahar N, Rimmelé T, Joannes-Boyau O, Bulyez S, Lefrant J-Y, Malledant Y, Leone M, Abback P-S, Tamion F, Dupont H, Lortat-Jacob B, **Guerci P**, Kerforne T, Cinotti R, Jacob L, Verdier P, Dugernier T, Pereira B, Constantin J-M, Azurea Network. Thoracic Epidural Analgesia and Mortality in Acute Pancreatitis: A Multicenter Propensity Analysis. Crit Care Med. 2018;46(3):e198-e205. doi:10.1097/CCM.0000000000002874.

18. **Guerci P**, Ergin B, Uz Z, Ince Y, Westphal M, Heger M, Ince C. Glycocalyx Degradation Is Independent of Vascular Barrier Permeability Increase in Nontraumatic Hemorrhagic Shock in Rats. Anesth Analg. 2019;129(2):598-607. doi: 10.1213/ANE.0000000000003918.

19. **Guerci P**, Claudot J-L, Novy E, Settembre N, Lalot J-M, Losser M-R. Immediate postoperative plasma neutrophil gelatinase-associated lipocalin to predict acute kidney injury after major open abdominal aortic surgery: A prospective observational

study. Anaesth Crit Care Pain Med. 2018;37(4):327-334. doi:10.1016/j.accpm.2017.09.006.

20.   Bonnassieux M, Duclos A, Schneider AG, Schmidt A, Bénard S, Cancalon C, Joannes-Boyau O, Ichai C, Constantin J-M, Lefrant J-Y, Kellum JA, Rimmelé T, AzuRéa Group. Renal Replacement Therapy Modality in the ICU and Renal Recovery at Hospital Discharge. Crit Care Med. 2018;46(2):e102-e110. doi:10.1097/CCM.0000000000002796.

21.   Vial F, Hime N, Feugeas J, Thilly N, **Guerci P**, Bouaziz H. Ultrasound assessment of gastric content in the immediate postpartum period: a prospective observational descriptive study. Acta Anaesthesiol Scand. 2017;61(7):730-739. doi:10.1111/aas.12930.

22.   **Guerci P**, Ince Y, Heeman P, Faber D, Ergin B, Ince C. A LED-based phosphorimeter for measurement of microcirculatory oxygen pressure. J Appl Physiol. 2017;122(2):307-316. doi:10.1152/japplphysiol.00316.2016.

23.   **Guerci P**, Ergin B, Ince C. The macro- and microcirculation of the kidney. Best Pract Res Clin Anaesthesiol. 2017;31(3):315-329. doi:10.1016/j.bpa.2017.10.002.

24.   Bulyez S, Pereira B, Caumon E, Imhoff E, Roszyk L, Bernard L, Bühler L, Heidegger C, Jaber S, Lefrant J-Y, Chabanne R, Bertrand P-M, Laterre P-F, **Guerci P**, Danin P-E, Escudier E, Sossou A, Morand D, Sapin V, Constantin J-M, Jabaudon M, EPIPAN Study Group, AzuRea network. Epidural analgesia in critically ill patients with acute pancreatitis: the multicentre randomised controlled EPIPAN study protocol. BMJ Open. 2017;7(5):e015280. doi:10.1136/bmjopen-2016-015280.

25.   Baka NE, Vial F, Iohom G, **Guerci P**, Hubert C, Rouabah M, Bouaziz H. The effect of nefopam on lactation after caesarean section: a single-blind randomised trial. Int J Obstet Anesth. 2017;31:84-90. doi:10.1016/j.ijoa.2017.02.005.

26.   Avercenc-Léger L, **Guerci P**, Virion J-M, Cauchois G, Hupont S, Rahouadj R, Magdalou J, Stoltz J-F, Bensoussan D, Huselstein C, Reppel L. Umbilical cord-derived mesenchymal stromal cells: predictive obstetric factors for cell proliferation and chondrogenic differentiation. Stem Cell Res Ther. 2017;8(1):161. doi:10.1186/s13287-017-0609-z.

27.   Legrand M, Le Cam B, Perbet S, Roger C, Darmon M, **Guerci P**, Ferry A, Maurel V, Soussi S, Constantin J-M, Gayat E, Lefrant J-Y, Leone M, support of the AZUREA network. Urine sodium concentration to predict fluid responsiveness in oliguric ICU patients: a prospective multicenter observational study. Crit Care. 2016;20(1):165. doi:10.1186/s13054-016-1343-0.

28.   Ince C, **Guerci P**. Why and when the microcirculation becomes disassociated from the macrocirculation. Intensive Care Med. 2016;42(10):1645-1646. doi:10.1007/s00134-016-4494-1.

29.   Ergin B, **Guerci P**, Zafrani L, Nocken F, Kandil A, Gurel-Gurevin E, Demirci-Tansel C, Ince C. Effects of N-acetylcysteine (NAC) supplementation in resuscitation fluids on renal microcirculatory oxygenation, inflammation, and function in a rat model of endotoxemia. Intensive Care Med Exp. 2016;4(1):29. doi:10.1186/s40635-016-0106-1.

30.   Ergin B, Kapucu A, **Guerci P**, Ince C. The role of bicarbonate precursors in balanced fluids during haemorrhagic shock with and without compromised liver function. Br J Anaesth. 2016;117(4):521-528. doi:10.1093/bja/aew277.

A

31.   Vial F, Mory S, **Guerci P**, Grandjean B, Petry L, Perrein A, Bouaziz H. [Evaluating the learning curve for the transversus abdominal plane block: a prospective observational study]. Can J Anaesth. 2015;62(6):627-633. doi:10.1007/s12630-015-0338-7.

32.   Raft J, **Guerci P**, Harter V, Fuchs-Buder T, Meistelman C. Biological evaluation of the effect of sugammadex on hemostasis and bleeding. Korean J Anesthesiol. 2015;68(1):17-21. doi:10.4097/kjae.2015.68.1.17.

33.   Poussel M, **Guerci P**, Kaminsky P, Heymonet M, Roux-Buisson N, Faure J, Fronzaroli E, Chenuel B. Exertional Heat Stroke and Susceptibility to Malignant Hyperthermia in an Athlete: Evidence for a Link? J Athl Train. 2015;50(11):1212-1214. doi:10.4085/1062-6050-50.12.01.

34.   **Guerci P**, Vial F, Feugeas J, Pop M, Baka N-E, Bouaziz H, Losser M-R. Cerebral oximetry assessed by near-infrared spectrometry during preeclampsia: an observational study: impact of magnesium sulfate administration. Crit Care Med. 2014;42(11):2379-2386. doi:10.1097/CCM.0000000000000519.

35.   **Guerci P**, Tran N, Menu P, Losser M-R, Meistelman C, Longrois D. Impact of fluid resuscitation with hypertonic-hydroxyethyl starch versus lactated ringer on hemorheology and microcirculation in hemorrhagic shock. Clin Hemorheol Microcirc. 2014;56(4):301-317. doi:10.3233/CH-141663.

36.   **Guerci P**, Vial F, Mcnelis U, Losser MR, Raft J, Klein O, Iohom G, Audibert G, Bouaziz H. Neuraxial anesthesia in patients with intracranial hypertension or cerebrospinal fluid shunting systems: what should the anesthetist know? Minerva Anestesiol. 2014;80(9):1030-1045.

37.   Christ B, **Guerci P**, Baumann C, Meistelman C, Schmartz D. Influence of neuromuscular block and reversal on bispectral index and NeuroSense values. Eur J Anaesthesiol. 2014;31(8):437-439. doi:10.1097/EJA.0b013e32836394df.

38.   Breton O, Vial F, Feugeas J, Podrez K, Hosseini K, Boileau S, **Guerci P**, Bouaziz H, Les membres du bureau de l'Institut lorrain d'anesthésie-réanimation (Ilar), Aubert F, Audibert G, Borgo J, Chalot Y, Didelot F, Fuchs-Buder T, Hotton J, Junke E, Lalot J-M, Losser M-R, Pierron A. [Risks acceptability related to obstetrical epidural analgesia]. Ann Fr Anesth Reanim. 2014;33(11):581-586. doi:10.1016/j.annfar.2014.06.004.

39.   Schmartz D, **Guerci P**, Fuchs-Buder T. Sugammadex dosing in bariatric patients. Anesthesiology. 2013;118(3):754. doi:10.1097/ALN.0b013e31827bd335.

40.   Novy E, Charpentier C, **Guerci P**, Settembre N, Malikov S, Audibert G. [Traumatic injuries of the descending thoracic aorta apart from the isthmus: diagnosis and therapeutic approach]. Ann Fr Anesth Reanim. 2013;32(11):799-802. doi:10.1016/j.annfar.2013.08.006.

41.   Nepo Karangwa J, Vial F, Uwambazimana J, **Guerci P**, Ndoli J, Raft J, Bouaziz H. [Postoperative pain management after caesarean section in Kigali University Medical Center: first use of intrathecal morphine]. Ann Fr Anesth Reanim. 2013;32(9):631-632. doi:10.1016/j.annfar.2013.07.801.

42.   Kimmoun A, **Guerci P**, Bridey C, Ducrocq N, Vanhuyse F, Levy B. Prone positioning use to hasten veno-venous ECMO weaning in ARDS. Intensive Care Med. 2013;39(10):1877-1879. doi:10.1007/s00134-013-3007-8.

43.   **Guerci P**, Novy E, Vial F, Lecointe B, Geffroy-Bellan M, Longrois D, Bouaziz H. Sulprostone for postpartum hemorrhage in a parturient with a history of Tako-tsubo cardiomyopathy. J Clin Anesth. 2013;25(4):327-330. doi:10.1016/j.jclinane.2012.11.011.

44.   **Guerci P**, Vial F, Raft J, Nelis UM, Mory S, Morel O, Bouaziz H. [Medical termination of pregnancy in a patient with severe cystic fibrosis. Possible effect of the antiglucocorticoid action of mifepristone on the respiratory disease]. Ann Fr Anesth Reanim. 2013;32(2):115-117. doi:10.1016/j.annfar.2012.11.011.

45.   **Guerci P**, Novy E, Guibert J, Vial F, Malinovsky J-M, Bouaziz H. [Inadvertent peripheral nerve catheter shearing occurring during ultrasound guidance]. Ann Fr Anesth Reanim. 2013;32(5):364-367. doi:10.1016/j.annfar.2013.02.016.

46.   Grandjean B, **Guerci P**, F Vial null, Raft J, Fuchs-Buder T, Bouaziz H. [Sugammadex and profound rocuronium neuromuscular blockade induced by magnesium sulphate]. Ann Fr Anesth Reanim. 2013;32(5):378-379. doi:10.1016/j.annfar.2013.03.008.

47.   Fuchs-Buder T, Baumann C, De Guis J, **Guerci P**, Meistelman C. Low-dose neostigmine to antagonise shallow atracurium neuromuscular block during inhalational anaesthesia: A randomised controlled trial. Eur J Anaesthesiol. 2013;30(10):594-598. doi:10.1097/EJA.0b013e3283631652.

48.   Jacques V, **Guerci P**, Vial F, Abel F, Bouaziz H. [Dissection of the descending aorta complicated by preeclampsia at 30 weeks of gestation: medical treatment and caesarean delivery]. Ann Fr Anesth Reanim. 2012;31(1):67-71. doi:10.1016/j.annfar.2011.09.010.

49.   Hime N, Auchet T, **Guerci P**, Vial F, McNelis U, Bouaziz H. Vaginal delivery in a parturient excessively anticoagulated with fondaparinux. Int J Obstet Anesth. 2012;21(4):385-387. doi:10.1016/j.ijoa.2012.06.007.

50.   **Guerci P**, Vial F, Bouaziz H. [Single-use and reusable laryngoscope blades: a randomized controlled trial in elective surgery]. Can J Anaesth. 2012;59(1):114-115. doi:10.1007/s12630-011-9603-6.

51.   **Guerci P**, Vial F, Raft J, Meistelman C, Bouaziz H. [Prolonged residual paralysis after a single intubating dose of rocuronium: an unexpected cause]. Ann Fr Anesth Reanim. 2012;31(7-8):632-634. doi:10.1016/j.annfar.2012.02.019.

52.   **Guerci P**, Vial F, Raft J, Jurkolow G, Bouaziz H. [Postoperative brachial neuropathy, a rare aetiology: the Parsonage-Turner syndrome]. Ann Fr Anesth Reanim. 2012;31(5):485-486. doi:10.1016/j.annfar.2012.02.001.

A

Doctorat d'Université

—

Current And New Therapies For The Critically Injured Microcirculation

Effets des thérapies actuelles et nouvelles sur la microcirculation sévèrement endommagée

—

Dr Philippe Guerci

Thèse soutenue le 16 Juin 2020

Co-Tutelle de Thèse entre
l' Université d'Amsterdam (UvA), Pays-Bas
et l' Université de Lorraine (UL), France

Résumé Français

La microcirculation est un élément fondamental de la composition du système vasculaire de l'Homme et des mammifères terrestres. La microcirculation est un réseau complexe et hétérogène comprenant des artérioles, des capillaires, des veinules mais aussi des lymphatiques. Les principales fonctions de la microcirculation sont d'assurer l'apport d'oxygène aux tissus et aux cellules tout en fournissant des nutriments et en éliminant le dioxyde de carbone produit par le métabolisme cellulaire, afin de répondre aux demandes métaboliques.

Les mécanismes de régulation contrôlant le débit microcirculatoire et la perfusion sont divers, redondants et élaborés. La régulation du débit vers et dans la microcirculation est déterminée par : (i) au niveau général, la pression de perfusion des organes, le débit de la pompe cardiaque, et (ii) à l'échelle microscopique par les réponses myogéniques au débit (tension et stress), la demande métabolique et l'équilibre acido-basique (niveau loco-régional d'O_2, CO_2, d'ions H^+ et de lactate) et les différentes réponses neurohormonales. Le débit sanguin microcirculatoire est régulé à l'aide d'interactions autocrines et paracrines pour répondre à la demande métabolique, principalement par les besoins en oxygène des cellules tissulaires. Ainsi, le niveau d'oxygène microcirculatoire est d'une importance critique.

D'un point de vue pragmatique, la structure de la microcirculation comprend trois composants principaux : (i) le contenant défini par les différentes couches de la paroi vasculaire, (ii) le contenu représentant le flux plasmatique qui irrigue les capillaires avec ses éléments figurés (globules

rouges, leucocytes) et (iii) le tissu extraluminal environnant. En cas de pathologie, chacun de ces composants peut être altéré séparément ou simultanément. Les cellules endothéliales forment l'interface entre le contenu de la lumière interne des vaisseaux et le tissu environnant. L'endothélium est remarquablement hétérogène dans sa structure et sa fonction et diffère d'un organe à l'autre. Il joue un rôle crucial dans la régulation du trafic macromoléculaire, du tonus vasomoteur, de l'hémostase, des fonctions immunologiques et de la sécrétion de molécules par détection via des mécanotransducteurs, qui déclenchent ensuite la signalisation et l'activation transcellulaires et intracellulaires. Les cellules endothéliales sont reliées entre elles par des composants transcellulaires, y compris des jonctions lacunaires pour la communication électrique pour la régulation vasculaire en amont et des jonctions serrées intercellulaires pour maintenir les barrières vasculaires. Le glycocalyx est une couche mince tapissant la membrane luminale et contribue à la perméabilité microvasculaire de la paroi vasculaire. Il s'agit d'un échafaudage hautement interactif capable de détecter le flux sanguin et abrite de nombreux récepteurs endothéliaux qui interagissent avec les leucocytes et d'autres éléments figurés du sang. Bien que le glycocalyx participe à la perméabilité de la barrière vasculaire, sa contribution relative au passage transcapillaire des macromolécules et des fluides est incomplètement élucidée. En ce qui concerne les éléments figurés du sang circulant dans la microcirculation, les globules rouges et les leucocytes sont parmi les plus étudiés, principalement parce que leur taille permet une identification aisée à l'aide d'un microscope intravital portable. Cependant, la quantité d'oxygène produite par les

globules rouges et libérée dans la microcirculation ne peut pas être évaluée par cette technique.

Dans de nombreuses situations, la microcirculation peut être altérée ou même compromise et particulièrement chez les patients en état critique. Le rein reste l'un des organes les plus sensibles au dysfonctionnement de la microcirculation, en particulier en cas d'état de choc ou de phénomènes d'ischémie / reperfusion qui entraînent des lésions rénales aiguës. Ces lésions rénales sont l'une des principales causes de mortalité et de morbidité chez les patients de réanimation. Par conséquent, nos recherches se sont principalement axées sur l'étude de la microcirculation rénale, de l'oxygénation et de la fonction rénale.

Les objectifs de cette thèse étaient de: (i) fournir un aperçu des dommages des différents composants de la microcirculation dans divers contextes tels que le choc hémorragique, l'endotoxémie, les lésion d'ischémie / reperfusion, (ii) décrire les effets des thérapies passées et actuelles sur ces constituants et (iii) évaluer de nouvelles molécules ayant des capacités de transport d'oxygène et des actions anti-inflammatoires.

Les chapitres 2 et 3 de cette thèse examinent les mécanismes structurels et fonctionnels de la microcirculation rénale en condition physiologique et pathologique (infection). Une revue complète des mécanismes de régulation complexes régissant la microcirculation est présentée.

Les altérations des différents composants structuraux considérés comme jouant un rôle central dans la régulation du débit sanguin microcapillaire et de la perméabilité de la barrière vasculaire ont été étudiées dans les chapitres suivants. La viscosité du plasma est l'un des

principaux modulateurs faisant varier les contraintes de cisaillement de l'endothélium est de ce fait est un des déterminants essentiels de la densité capillaire fonctionnelle. Dans le chapitre 4, les conséquences de 2 stratégies de réanimation liquidienne (en dehors de la transfusion) sur la viscosité plasmatique ont été investiguées lors d'un état de choc hémorragique chez le porc. Dans cette étude, nous avons démontré que la viscosité plasmatique diminuait quelle que soit la stratégie utilisée pour la réanimation liquidienne (faible volume et colloïdes hypertoniques par rapport à l'administration de Ringer lactate). De plus, aucune différence n'a été trouvée entre les groupes pour d'autres variables hémorhéologiques, le débit microcirculatoire ou encore sur la pression partielle en oxygène tissulaire.

Dans les chapitres 5 et 6, nous avons entrepris une évaluation intégrative, physiologique du rôle contributif du glycocalyx dans la perméabilité de la barrière vasculaire dans un modèle de choc hémorragique réanimé et d'hémodilution sévère chez le rongeur, respectivement. Les résultats observés ont remis en question l'importance contributive du glycocalyx dans la perméabilité de la barrière vasculaire. En effet, bien que le glycocalyx puisse être endommagé dans ces conditions, il n'a pas altéré la compétence de la barrière vasculaire mais a plutôt provoqué des perturbations microcirculatoires et des altérations du tonus vasculaire probablement lié à un phénomène de mécanotransduction et d'effet de cisaillement diminué. Ces résultats soulignent la complexité de la régulation de la perméabilité de la barrière vasculaire dans le contexte du choc hémorragique et identifient une gradation des lésions vasculaires.

Afin de déterminer avec précision la pression en oxygène microcirculatoire dans la structure corticale rénale, un nouvel appareillage utilisant un système de Light Emitting Diodes (LEDs) et reposant sur la méthode d'extinction de la phosphorescence (phosphorescence quenching) en résolution temporelle a été développé et est présenté dans le chapitre 7. Ce dispositif présente plusieurs avantages par rapport aux précédents dispositifs construits de lampes à décharge (« flash lamp »), qui ont comme principal défaut de produire une lueur de plasma persistant pendant des dizaines de microsecondes après la décharge primaire. Les avantages de l'utilisation des LEDs comme source d'excitation lumineuse sont présentés. Ce dispositif a par la suite été utilisé dans plusieurs autres travaux du doctorant.

Divers traitements ont été envisagés pour guérir la microcirculation lésée ou compromise en raison d'une condition critique. La réanimation liquidienne reste la pierre angulaire de la gestion des états de choc. Les études sur les effets microcirculatoires comparatifs en ce qui concerne la pression d'oxygène microcirculatoire rénale sont limitées. Dans le chapitre 8, nous avons étudié le rôle de précurseurs de bicarbonate dans les solutés balancés, utilisés en pratique quotidienne, pendant la réanimation de choc hémorragique avec et sans dysfonction hépatique dans un modèle animal murin (rat). Pour cela, une résection hépatique partielle de 70% a été réalisée afin de créer une dysfonction hépatique. Bien que les solutés balancés soient largement utilisés, aucune donnée n'était disponible sur le sort des anions (précurseurs de bicarbonate) les composant. Fait intéressant, les solutés balancés à l'acétate ont montré un effet de tamponnement acido-basique du pH sanguin bien supérieur par rapport à

des solutés balancés avec du lactate ou au sérum salé isotonique. Le gluconate lui ne semble pas contribuer au contrôle acido-basique.

Les thérapies antioxydantes ont été largement évaluées en tant que stratégies de réanimation microcirculatoire. De nombreuses preuves précliniques sont disponibles dans la littérature concernant l'utilisation de la N-acétylcystéine (NAC) et ses effets protecteurs antioxydants, vasodilatateurs et rénaux. Dans le chapitre 9, nous avons étudié l'effet de l'administration de NAC en conjonction avec la réanimation liquidienne sur l'oxygénation et la fonction rénale dans un modèle d'endotoxémie chez le rat, en faisant l'hypothèse que l'atténuation de l'inflammation dans le rein améliorerait l'oxygénation microcirculatoire rénale et limiterait l'apparition de lésions rénales aiguës. Nous avons montré que l'ajout de NAC améliorait l'oxygénation rénale et atténuait la dysfonction microvasculaire et les lésions rénales aiguës. Ces effets bénéfiques seraient partiellement médiés par une diminution des niveaux d'oxyde nitrique rénal et d'acide hyaluronique.

Au cours de ces différents travaux et ces différents modèles, il a été montré que la pression d'oxygène microcirculatoire rénale ne peut pas être entièrement restaurée à un niveau identique à celui du contrôle (sans agression aigue). Ainsi, il existe encore des besoins non satisfaits en matière de réanimation de la microcirculation. Le soi-disant concept de «pink fluid resuscitation» a émergé sur la base de thérapies qui devraient allier un effet d'expansion volémique avec des capacités de transport d'oxygène et d'effet d'antioxydant. Suivant cette idée, une nouvelle génération de transporteur d'oxygène à base d'hémoglobine (HBOC) avec des propriétés antioxydantes supplémentaires, telles que la carboxyhémoglobine PEGylée (PEGHbCO), nous est apparu comme une option intéressante à étudier. Dans le chapitre

10, nous avons étudié l'efficacité du PEGHbCO sur la pression d'oxygène microcirculatoire corticale rénale et le rôle de sa molécule de monoxyde de carbone incorporé sur l'atténuation des lésions rénales aiguës lors de la réanimation à faible volume du choc hémorragique. Bien qu'il ne puisse pas rivaliser avec la transfusion sanguine en termes d'oxygénation corticale rénale, ce composé limite les dommages tubulaires avec volume de liquide nécessaire inférieur pour maintenir une stabilité hémodynamique macrocirculatoire.

Au contraire, dans chapitre 11, la réanimation avec de la carboxyhémoglobine PEGylée a amélioré l'oxygénation corticale rénale tout en rétablissant le flux microcirculatoire des muscles squelettiques dans des capillaires auparavant non perméables (sans flux) dans un modèle murin d'endotoxémie mais sans pour autant atténuer la lésion rénale aiguë induite par la septicémie du moins dans ce modèle à court terme.

En conclusion, les altérations microcirculatoires observées lors des états de choc nécessitent une approche multiparamétrique. Dans l'espoir de limiter les lésions rénales aigues, la réanimation de la microcirculation devrait non seulement prendre en compte l'effet d'expansion du volume des fluides mais aussi les aspects anti-inflammatoires ou antioxydants ciblant les lésions d'ischémie / reperfusion tout en possédant des propriétés de transport d'oxygène pour maintenir une pression d'oxygène microcirculatoire. Il n'a pas encore été démontré par des essais cliniques qu'un tel fluide pourrait améliorer le devenir de patients présentant une microcirculation sévèrement altérée.